

ADA 038248

12
20000726094

R-1066

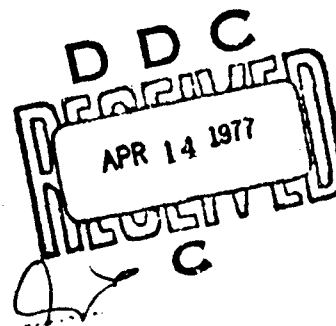
MOORING MECHANICS
A COMPREHENSIVE COMPUTER STUDY

Volume II

Three Dimensional Dynamic Analysis of
Moored and Drifting Buoy Systems

by
Narendar K. Chhabra

December 1976



AD NO.
DDC FILE COPY



The Charles Stark Draper Laboratory, Inc.

Cambridge, Massachusetts 02139

Key No.
Ref ID:
buoy :
dimens:
simula:
oses

Reproduced From
Best Available Copy

Approved for public release; distribution unlimited.

SECURITY CLASSIFICATION OF THIS PAGE (When Data Entered)

REPORT DOCUMENTATION PAGE

READ INSTRUCTIONS
BEFORE COMPLETING FORM.

1. REPORT NUMBER R-1066-Y&I-2		2. GOVT ACCESSION NO. 9	3. RECIPIENT'S DATA FILE NUMBER Firsl + Ropel								
4. TITLE (and Subtitle) MOORING MECHANICS - A Comprehensive Computer Study - Three Dimensional Dynamic Analysis of Moored and Drifting Buoy Systems.		5. TYPE OF REPORT & PERIOD COVERED FINAL									
6. AUTHOR(s) Narendar K. Chabda		7. PERFORMING ORG. REPORT NUMBER NOD014-75-C-1065									
8. CONTRACT OR GRANT NUMBER(s)		9. PERFORMING ORGANIZATION NAME AND ADDRESS The Charles Stark Draper Laboratory, Inc. Cambridge, Massachusetts 02139									
10. PROGRAM ELEMENT, PROJECT, TASK AREA & WORK UNIT NUMBERS		11. CONTROLLING OFFICE NAME AND ADDRESS NORDA National Space Technology Laboratories Bay St. Louis, Mississippi 39520									
12. REPORT DATE December 1976		13. NUMBER OF PAGES 287									
14. MONITORING AGENCY NAME & ADDRESS (if different from Controlling Office) 15 278P.		15. SECURITY CLASS. (of this report) Unclassified									
16. DISTRIBUTION STATEMENT (of this Report) Approved for public release; distribution unlimited		17. DISTRIBUTION STATEMENT (of the abstract entered in Block 20, if different from Report) D D C DRAFTED APR 11 1977 DISTRIBUTED APR 11 1977 C									
18. SUPPLEMENTARY NOTES											
19. KEY WORDS (Continue on reverse side if necessary and identify by block number) <table> <tr><td>1. Oceanographic Systems Simulations</td><td>5. Drogued Buoys</td></tr> <tr><td>2. Mooring Systems</td><td>6. Mathematical Modelling</td></tr> <tr><td>3. Cable Dynamics</td><td>7. Computer Simulations</td></tr> <tr><td>4. Buoy Dynamics</td><td></td></tr> </table>				1. Oceanographic Systems Simulations	5. Drogued Buoys	2. Mooring Systems	6. Mathematical Modelling	3. Cable Dynamics	7. Computer Simulations	4. Buoy Dynamics	
1. Oceanographic Systems Simulations	5. Drogued Buoys										
2. Mooring Systems	6. Mathematical Modelling										
3. Cable Dynamics	7. Computer Simulations										
4. Buoy Dynamics											
20. ABSTRACT (Continue on reverse side if necessary and identify by block number) <p>Ocean currents and surface waves may induce serious errors in oceanographic measurements obtained from moored and drifting buoy systems. A general, computationally efficient solution for the dynamics of moored buoy systems, free drifting buoys, and drogued buoy systems in three-dimensional space is described in this report. Time-domain computer simulations of four specific configurations in various environments are presented. The mathematical model of one of these configurations, a</p>											

DD FORM 1 JAN 73 EDITION OF 1 NOV 65 IS OBSOLETE

SECURITY CLASSIFICATION OF THIS PAGE (When Data Entered)

408386

HP

SECURITY CLASSIFICATION OF THIS PAGE(When Data Entered)

subsurface mooring, was evaluated and improved using full scale ocean test data. The modal of the surface mooring configuration studied will soon also be evaluated using recent test data.

SECURITY CLASSIFICATION OF THIS PAGE(When Data Entered)

R-1066

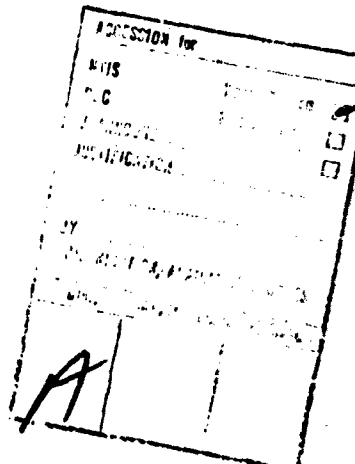
MOORING MECHANICS
A COMPREHENSIVE COMPUTER STUDY

Volume II

Three Dimensional Dynamic Analysis of
Moored and Drifting Buoy Systems

by
Narend : K. Chhabra

December 1976



Approved:

Philip N. Bowditch

Philip N. Bowditch
Head, Scientific
Research Department

The Charles Stark Draper Laboratory, Inc.
Cambridge, Massachusetts 02139

ACKNOWLEDGMENT

The author welcomes this opportunity to thank all those at the Charles Stark Draper Laboratory, Inc. who had valuable contributions to the work described. Special thanks are due to Mr. John Dahlen for his helpful guidance and comments during preparation of this report. To Dr. Jeffrey Loew for his help during mathematical model formulations; Mr. James Scholten for his help during computer simulations; and Mr. William Vachon for his comments during the preparation of this report. Finally, the author wishes to thank Miss Cheryl Gibson and Mrs. Catherine Hall for doing such an excellent job in typing this report.

This report was prepared under CSDL Project 53-68800, sponsored by the Ocean Science and Technology Division of the Office of Naval Research, Department of the Navy, through contract N00014-75-C-1065.

The publication of this report does not constitute approval by the U.S. Navy of the findings or the conclusions herein. It is published only for the exchange and stimulation of ideas.

ABSTRACT

Ocean currents and surface waves may induce serious errors in oceanographic measurements obtained from moored and drifting buoy systems. A general, computationally efficient solution for the dynamics of moored buoy systems, free drifting buoys, and drogued buoy systems in three-dimensional space is described in this report. Time-domain computer simulations of four specific configurations in various environments are presented. The mathematical model of one of these configurations, a subsurface mooring, was evaluated and improved using full scale ocean test data. The model of the surface mooring configuration studied will soon also be evaluated using recent test data.

TABLE OF CONTENTS

<u>Section</u>		<u>Page</u>
1.0	INTRODUCTION	1
1.1	Background	3
1.2	Assumptions, Capabilities, and Limitations	5
2.0	THEORETICAL ANALYSIS - MATHEMATICAL MODELS	9
2.1	Surface Buoys	9
2.1.1	Spar Buoy	22
2.1.2	Other Shapes	38
2.2	Mooring Line	39
2.2.1	Continuous Line Formulation	41
2.2.2	Lumped Parameter Formulation	51
2.3	Attachment Between Surface Buoy and a Mooring Line	61
2.4	Window Shade Drogue	65
3.0	METHOD OF SOLUTION	65
3.1	Moored System Analysis	68
3.2	Initial Conditions for the Steady- State Analysis of a Spar Buoy	75
3.3	Drifting Drogued Spar Buoy	79

TABLE OF CONTENTS (Cont.)

<u>Section</u>		<u>Page</u>
4.0	COMPUTER PROGRAM DETAILS	82
4.1	Surface Moored/Drifting Systems	82
4.2	Subsurface Moored Systems	91
5.0	CASE STUDIES/SIMULATIONS	97
5.1	Spar Buoy	97
5.1.1	Cylindrical Spar	97
5.1.2	Tuned Spar	121
5.2	Subsurface Moored System	143
5.3	Surface Moored System	162
5.4	Drifting Drogued Spar Buoy	184
6.0	SUMMARY	193
 <u>Appendix</u>		
A	COMPUTER PROGRAM LISTINGS	196
REFERENCES		271

NOMENCLATURE

\bar{A}	Acceleration vector.
A_D	Area used in drag calculations.
\bar{A}_{Ec}	Acceleration of point c in the E frame.
A_N, A_T	Normal and Tangential areas for a cylindrical body.
\bar{A}_R	Relative acceleration vector.
a	Point of attachment between the surface buoy and the mooring line.
\bar{AM}	Added mass force vector.
c, x', y', z'	Body coordinate system, Frame B.
c	Mid point of the mooring line element.
{CF}	Array of constant nodal forces.
C_D	Drag coefficient.
C_N, C_T	Added mass coefficients, normal and tangential directions, surface buoy.
C_{DN}, C_{DT}	Normal and tangential drag coefficients for a cylindrical body.
C_{DP}	Pressure drag coefficient for the end plate of a spar buoy.
CDIN, CDIT, CDIA	Appropriate drag constants corresponding to DN, DT, and DA.
\bar{D}^A	Viscous drag force on a body inserted in a mooring line.
\bar{DF}	Viscous drag force vector.
\bar{DM}	Moment vector due to viscous drag force.
\bar{DN}, \bar{DT}	Normal and tangential drag forces per unit stretched length of the mooring line.

\overline{DN}_n , \overline{DT}_n , \overline{DA}_n	Viscous drag forces acting on the n^{th} node of the mooring line.
d_B	Mass of water displaced by a differential disk of the surface buoy, $\int_{\Omega} dz'$.
d_M	Mass of a differential disk of the surface buoy.
\overline{F}	Total force vector acting on the body.
{ F_A }	Array of additional forces and moments.
{ F_D }	Array of wave exciting forces and moments.
\overline{FF}	Froude Krylov exciting force vector.
{ F_G }	Array of hydrostatic and gravitational forces and moments.
\overline{FH}	Hydrostatic pressure force acting on the mooring line, per unit stretched length.
g	Acceleration due to gravity.
H	Length of the surface buoy.
h_o	Instantaneous draft of the surface buoy, measured up to the mean free surface.
h_1	Spar buoy drum height.
h_2	Spar buoy mast height.
h_i	h_o plus the wave elevation component.
\overline{IF}	Inertia force per unit stretched length of the mooring line.
\overline{IF}_b	Inertia force vector of the inserted body.
I_{xx}, I_{yy}	Moments of inertia of the spar buoy in roll and pitch about c.
$\hat{i}_x, \hat{i}_y, \hat{i}_z$	Unit vectors of o,x,y,z.
$\hat{i}_{x'}, \hat{i}_{y'}, \hat{i}_{z'}$	Unit vectors of c,x',y',z'.

\bar{k}	Wave number vector.
k_x	Wave number component, $ \bar{k} \cos \theta$.
k_y	Wave number component, $ \bar{k} \sin \theta$.
k_n	Stiffness coefficient of the n^{th} segment.
ℓ, u_1, u_2, u_3	Integration limits as defined.
M	Total mass of the spar buoy.
[M]	Matrix of tensors of inertia and added inertia.
m_a	Added mass of the inserted body, shape other than cylindrical.
m	Mass of the inserted body.
m_{dn}	Mass of water displaced by the n^{th} mass.
m_n, m_t	Added mass components (normal and tangential) due to cylindrical bodies.
N	Number of nodes or segments of a mooring line.
\bar{N}_B	Net buoyancy of the inserted body.
n	Arbitrary line segment, or lumped mass.
\circ, x, y, z	Fixed coordinate system, frame E.
P	Hydrostatic pressure of the fluid.
P_i	$= \int_{\ell}^{u_2} dB(z_p')^i$
p	Location of the centroid of the differential disk of a surface buoy.
Q_i	$= \int_{\ell}^{u_2} dBe^{Kz_w(z_p')}^i$
\bar{R}	Displacement vector.
\bar{R}_{oc}	Displacement vector from point \circ to point c.

r	Radius of the spar buoy or the reduced radius of the mooring line.
r_1, r_2	Radius of the tuned spar buoy.
\vec{s}	Spatial vector in the x-y (horizontal) plane, describing propagation of the surface wave.
s_o	Cross-sectional area of the surface buoy.
s_{o1}, s_{o2}	Cross-sectional areas of the tuned spar buoy.
s	spatial coordinate of the mooring line.
\vec{T}	The tension vector.
T_e	Effective tension variable along the mooring line.
$\overline{\vec{T}}$	Moment of the tension force \vec{T} .
$\overline{\vec{T}F}$	Tension force vector on a mooring line node.
t	Time variable.
\vec{v}	Fluid velocity vector.
\overline{UR}	Relative fluid velocity vector.
$\overline{UNR}, \overline{UTR}$	Normal and tangential components of \overline{UR} .
\vec{v}	Velocity vector.
\hat{v}	Unit vector along the mooring line.
(V)	Array of translation and rotation rates.
v_{BW}	Velocity of water particle w in frame B.
v_b	Tangential relative fluid velocity at bottom of the tuned spar.
v_{ox}, v_{oy}, v_{oz}	Components of surface current.
v_s	Tangential relative fluid velocity at step of the tuned spar, also static velocity of the drogued drifting buoy system.

\bar{w}	Gravitational force on a fluid element of unit surface density, and angular velocity of the wave.
W_d	Weight in air per unit length of the mooring line.
W_w	Weight in water, at the right end of segment of mooring line at the free surface.
\bar{w}_n, \bar{w}_t	Normal and tangential components of \bar{w} .
w	Location of the particle of water.
\bar{y}	Displacement vector of the floating body.
\bar{x}_n, \bar{x}_t	Normal and tangential directions of the mooring line element.
r_c	Distance between c and the center of the buoy.
ψ	Velocity potential function.
ω	Wave frequency.
θ	Angle between wave direction and the x-axis.
a_0	Wave amplitude.
ζ	Wave surface elevation.
β	Roll angle of the surface buoy, measured for mooring line orientation.
ρ	Pitch angle of the surface buoy.
ϕ	Yaw angle of the surface buoy.
ρ	Water density.
ΔL_n	Change in length of the n th segment.
α	Added mass coefficient for the mass of the spar buoy.

1.0 INTRODUCTION

Oceanographic measurements from moored buoy systems are contaminated by mooring motion. Numerous articles have been published in the last three years pointing out quantitatively the errors introduced by the surface wave field. Large vertical excursions have been experienced at great depths by instruments located on the synthetic rope portions of surface-buoyed mooring lines (WUNSCH and DAHLEN, 1974). Observations during the POLYMODE experiment showed subsurface mooring lines to have undergone hundreds of meters of vertical excursions. For any operational moored instrument system we need two models whose accuracy can be established with known confidence: a mooring system model from which the motion environment of instruments can be predicted, and a model of the instrument motion response characteristics from which the measurement error can be estimated. Possession of these models is required for more effective mooring systems design and for optimum interpretation of oceanographic measurements obtained from moored systems. The first of these two models is the main subject of this report.

An alternative to the moored approach is the use of surface-trackable drogued drifting buoys. Such a

buoy system employs a high drag device (or drogue) at some depth, tethered to a trackable buoy at the surface. The major impediments in the widespread use of this approach have been inadequate component and system design. Both of these impediments can be removed by the development of dynamic modeling of drogued buoys. A part of this report deals with the dynamic modeling of drogued buoys.

Dynamic models of drogued buoys do not exist except in primitive form, while such models of moored buoys and free-drifting buoys are further along. This difference stems from the fact that drogued buoy systems are dynamically very complex, and they have only recently been considered essential to major programs. Even though many dynamic mathematical models for moored buoys and free-drifting buoys are available, not much has been done toward the evaluation of these models using full-scale ocean test data. It is the purpose of this report to present a general, computationally efficient approach for analyzing moored buoy systems, free drifting buoys, and drogued buoy systems and to simulate this analysis on the computer so that these models can then be readily evaluated with full scale ocean test data.

This report constitutes parts 3 and 4 of a four part report. Parts 1 and 2 were published in

volume 1 and dealt with the "Three Dimensional Static Analysis and Design of Single Point Taut and Slack Moored Buoy Systems" (CHHABRA, 1973).

1.1 Background

We at Charles Stark Draper Laboratory Inc. have evaluated one of the mathematical models presented in this report. The mathematical model of a subsurface mooring system (Section 2.2.1 and simulation 5.2 in this report) has been shown previously to predict the mooring motion forced by ocean currents of periods greater than 15 min. (CHHABRA, DAHLEN and FROIDEVAUX, 1974). The model was evaluated in a full scale ocean test that provided experimental data on mooring response and ocean current forces. The ocean test was conducted jointly with Woods Hole Oceanographic Institution on R. V. Chain cruise 107. We obtained a record of the motion of an acoustic transceiver near the top of the subsurface mooring line at the 500-m depth. The transceiver sent out a sound pulse every minute and recorded the four return times of replies from four near-bottom acoustic transponders at 5460m. By comparison with this and other data from precision pressure recorders, tensiometers, and inclinometers, the mooring model had been found to predict well the observed motions. The r.m.s. difference

between the experimental and predicted trajectory of the acoustic transceiver was 11.8m, about 10% of the mean excursion. This mathematical model was evaluated a second time by data from the central mooring (Mooring No. 1, Station 481) of the Mid-Ocean Dynamics Experiment (MODE). In that study (CHIABRA, 1976), the current record from the topmost vector-averaging current meter on the central mooring of the MODE experiment was corrected for the effects of mooring motion, and power spectra of the uncorrected and corrected signals were compared. The correction was $\leq 1 \text{ cm s}^{-1}$, for that mooring line (vertical excursion $< 12 \text{ m}$). Creep in the synthetic portion of the mooring line was also identified.

In addition, we are planning to evaluate a second mathematical model presented in this report. The mathematical model is of a tuned spar buoy (35 ft. long, 1 ft. dia. at W.L.) tethered to a subsurface mooring line by a stiff buoyant line. An instrument line is hanging from the base of the spar (Sections 2.1.1, 2.2.2, 2.3 and simulation 5.3). This configuration was recently tested in the ocean during the October 1976 ONR/NDBO Mooring Dynamics Experiment. A total of fifteen motion sensing instruments (4 Force Vector Recorders, 6 Temperature/Pressure Recorders, 1 POPMIP, and 4 Acoustic

Beacons) were attached along this mooring system. The evaluation and improvement of this mathematical model would be done by comparing measured responses with those computed by the computer simulation for the measured/observed environment.

The above mentioned evaluation and improvement is planned to be completed in CY77. If such an evaluation and improvement is done, the only mathematical model to be evaluated and improved from the analysis presented in this report would be the drifting drogued buoys. We plan to do that task in the near future.

1.2 Assumptions, Capabilities, and Limitations

Surface gravity waves treated in this report have a single frequency and amplitude, propagating in a single direction. It is assumed that the surface buoy is oscillating in the path of small (i.e. amplitude of wave train much less than its wavelength) incident surface waves which are long in relation to the body dimension in the direction of wave propagation. Wave direction has been generalized to include any arbitrary direction in the horizontal plane. For the three-dimensional analysis of surface buoys, we also assume small displacements of buoy when compared to vertical dimension of the buoy. Hence only the first powers of

small quantities are retained for the three-dimensional surface buoy analysis. Moments of inertia about all axes in a horizontal plane are taken equal. Even though moment of inertia about the longitudinal axis of the spar buoy is negligible, it is included for numerical computational purposes.

In all mathematical models an earth fixed frame is assumed to be the valid inertial frame. Viscous drag forces are computed based on the square drag law. For cylindrical shapes these forces are assumed to act in directions normal and tangential to the longitudinal axis; and for any other shape they act in the direction of the relative flow. For the case of a tuned spar viscous drag forces and 'added mass' due to the bottom base and the step are also included. The ideal fluid damping (wave-damping) as derived by Newman (1963) for a spar buoy was found to be negligible and hence is neglected.

All mooring lines are considered elastic. In the continuous line formulation of mooring lines, nonlinear elasticity dependent on the prior loading history as explained in volume 1 (CHHABRA, 1973) is considered. For the lumped parameter formulation; a linear stress-strain curve is derived from the nonlinear curves for the range of stresses in study. Dynamic effects on these stress-

strain curves are neglected. Internal damping forces in the mooring lines are assumed negligible when compared with viscous drag and stiffness forces. The hydrostatic pressure forces are treated more rigorously than they are in the traditional method employed in most previous studies. As it turned out this new method changed only the stress distribution along the mooring system, while the configuration of the mooring system remained essentially unchanged. Instruments or buoyancy packages attached along the mooring lines are treated as concentrated forces which have length and give rise to forces as explained in Section 2.2. A time varying current profile of any nature and shape can be inputted to the computer programs. A list of current profiles used in various simulations is given in volume 1 (CHHABRA, 1973). In its present form no allowance for shrinkage or creep of the synthetic ropes is taken into account, but creep was identified in CHHABRA (1976). Elongations due to rotation of non-torque balanced cables is also not considered. In the mooring line models viscous drag forces due to the velocity field generated by the surface waves are included. Wave-damping forces are neglected. In the continuous line formulation of the mooring line, exciting forces exerted on the line by the wave system are neglected; whereas in the lumped

parameter formulation, exciting forces are taken equal to the 'Froude-Krylov' forces as it is assumed that the presence of the mooring line does not disturb the wave particle motion. For added mass purposes, it is assumed for the continuous line formulation that the body (continuous cylindrical line) motion accelerates fluid only in the direction normal to its longitudinal axis.

2.0 THEORETICAL ANALYSIS - MATHEMATICAL MODELS

This section derives all the equations of motion pertinent to the analysis presented in this report.

Surface floats are analyzed in Subsection 2.1, mooring line in 2.2, their attachment in Section 2.3, and a window shade drogue in Section 2.4. The mooring line analysis includes all subsurface floats, instruments etc. attached to the mooring line.

2.1 Surface Buoys

As is well known, the analysis of the wave induced response of floating bodies is, in general, a most formidable task. Initially the action of the fluid must be decomposed into real (viscous) and ideal (inviscid) effects. Each effect then must be modeled as to its interaction with the floating body. Further, it is convenient to assume that the ocean waves are "gentle" enough so as to permit first order linear surface wave theory to serve as a foundation for the calculation of the wave exciting forces.

The ideal fluid problem is still so difficult in general that only the simplest body shapes are amenable to rigorous analytical solution (potential flow theory). This solution involves the determination of the (velocity) potential function $\phi(\bar{s}, t)$ which must

satisfy: 1) Laplace's equation, 2) the kinematic boundary condition on the moving body surface, 3) the free surface (and bottom) boundary condition(s) and 4) the radiation condition at great distance from the body.

Assuming this potential, $\psi(\bar{S}, t)$, has been determined by some means, the next step is to substitute it into the Bernoulli's expression for fluid pressure which in turn is integrated over the immersed portion of the body to yield the instantaneous force and moment vectors. In principle this is a straight-forward procedure. In practice it is hardly ever possible to find a tractable potential function which satisfies the above four conditions. In a few notable cases, however, for simple geometries and small body motions, rigorous solutions have been worked out. In particular Newman (1963) has derived the linearized equations of motion for a vertical, cylindrical air buoy responding to the influence of a unidirectional wave train. The axisymmetry of the buoy as well as its postulated slenderness was greatly exploited in the work to yield manageable results. In Newman's work as well as in others of comparable rigor, the computed potential is the result of an intricate distribution of singularities (sources, sinks, dipoles, etc.) within or over the wetted body surface.

From these studies, it turns out that the linearized

hydrodynamic forces and moments in general body geometries may be decomposed into constituents proportional to body acceleration, body velocity, displaced fluid acceleration, and the displaced fluid velocity. In general, rigorous integration of the fluid pressure, both hydrostatic and wave, over the body surface yields:

1) the 'Froude-Krylov" force from the pressure distribution due to the undisturbed wave system; 2) the "diffraction" force from disturbance of the waves by the presence of the body; 3) the force due to the motion of the body; and 4) the hydrostatic pressure force. The Froude-Krylov force and the diffraction force in combination are also known as the exciting forces exerted on the body by the wave system. The Froude-Krylov force equals in value to the product of the mass of the displaced fluid times the acceleration of the local undisturbed fluid particles. The diffraction force and the force due to the motion of the body both yield "added mass" coefficients proportional to accelerations and wave-damping coefficients proportional to velocities of the fluid and the body respectively. As shown in Chung (1976), the added mass coefficients are same (opposite signs) for both the fluid and body accelerations. Also the two wave-damping coefficients have the same (opposite signs) value.

Hence, these two forces may be combined to represent an "added mass" force proportional to the relative acceleration (fluid acceleration minus the body acceleration), and a wave-damping force proportional to the relative velocity. Other forces (apart from the fluid pressure forces) acting on the body are: 1) the weight of the body; and 2) the actual unbalanced force which accelerates the body. In the real (viscous) fluid another force, the viscous drag force, acts on the submerged portion of the body.

Analysis in this section includes all the above mentioned forces, as derived from the potential flow theory, except the following deviations: 1) the ideal fluid damping (wave-damping) is omitted; 2) the added mass force is treated slightly differently, and 3) the viscous drag forces are added on to the general equations of motion.

The ideal fluid damping is omitted here for expediency. Later analysis of specific problem addressed in this report showed the wave damping force, as derived by Newman (1963) for a spar buoy, to be negligible compared to the viscous drag force on the submerged body. The added mass force, which is proportional to the relative acceleration is separated into two terms; an added mass force proportional to the longitudinal component

of the relative acceleration, and an added mass force proportional to the transverse component of the relative acceleration. Each of these two terms is multiplied by a different constant coefficient, depending on the shape of the floating body. These coefficients and the coefficients used to derive the viscous drag force are experimentally determined hydrodynamic coefficients.

As will be shown below, our general equations of motion reduce to the ones given in Rudnick (1967) for a particular value of these coefficients. Rudnick in his analysis used the reasoning of Lamb (1945) who treats a uniform two-dimensional flow across a long circular cylinder.

Formulation of the General Equations of Motion:

Derivation of the equations of motion for surface piercing buoys in a train of regular harmonic ocean waves is given. In addition a surface current (not due to surface waves) is present. Surface buoys are considered as rigid bodies with six degrees of freedom. The problem under consideration is represented schematically in Figure 2.1. An earth fixed cartesian coordinate system (z positive upwards) is situated at the undisturbed level of the free surface. Call it the frame E with origin at o;

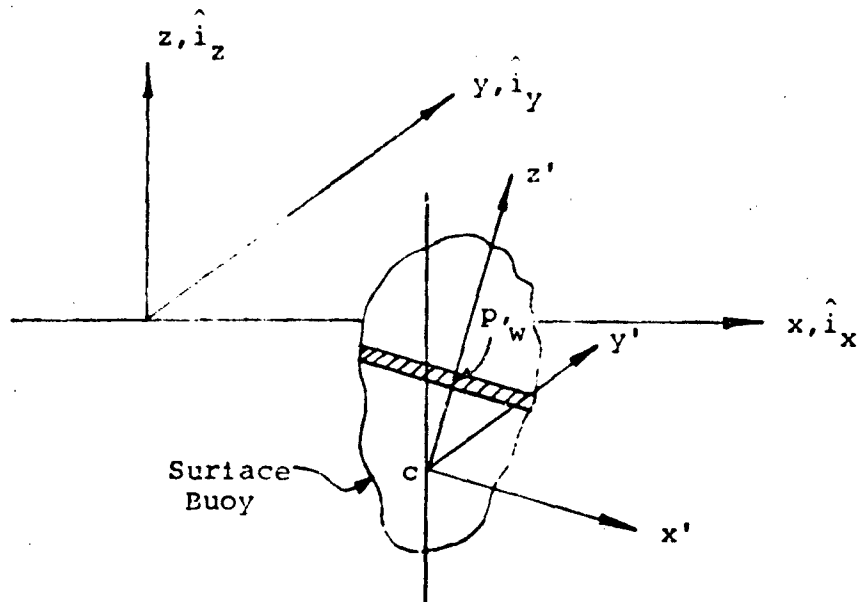


Figure 2.1 Coordinate System for Surface Piercing Buoys

and \hat{i}_x, \hat{i}_y , and \hat{i}_z the unit vectors along x, y , and z respectively. Frame B is a body (surface buoy) fixed cartesian coordinate system with its origin at the centroid (c) of the surface buoy, and x', y', z' being parallel to x, y, z respectively when the buoy is in the upright and non-rotating position. In this analysis \bar{R} represents a displacement vector; \bar{v} , a velocity vector, and \bar{A} , an acceleration vector. It is assumed that the surface buoy is oscillating in the path of small (i.e., amplitude of wave train much less than its wavelength) incident surface waves which are long in relation to the body dimensions in the direction of wave propagation. Point

p is the location of the centroid of a differential disk (height = dz') of the surface buoy (Figure 2.1).

First, the wave direction will be generalized to include any arbitrary direction in the x - y plane. To this end let the wavenumber vector \bar{K} specify the direction of propagation (Figure 2.2) where:

$$\bar{K} = \frac{\omega^2}{g} (\cos\theta \hat{i}_x + \sin\theta \hat{i}_y)$$

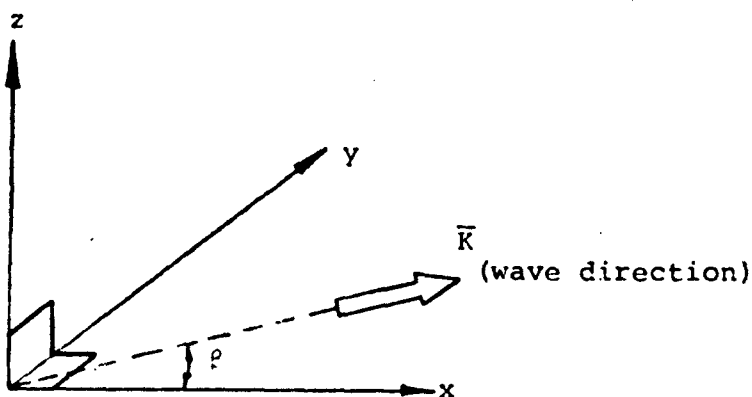


Figure 2.2 - Generalized Wave Direction

The generalized velocity potential field of the incident wave system may now be written:

$$\phi = \frac{g\xi_0}{\omega} e^{|\bar{K}|z} \cos(\bar{K} \cdot \bar{S} - \omega t)$$

where; $\bar{S} = \hat{i}_x x + \hat{i}_y y$; and the wave surface elevation ξ is

given by:

$$\xi = -\xi_0 \sin(\bar{K} \cdot \bar{S} - \omega t)$$

Here, g is the acceleration due to gravity, and ξ_0 is the amplitude of the incident wave of frequency ω . In the earth fixed frame (frame E), assumed to be a valid inertial frame for this problem, we define the fluid particle acceleration vector:

$$\bar{A}_{Ew} = \hat{i}_x \dot{\phi}_x + \hat{i}_y \dot{\phi}_y + \hat{i}_z \dot{\phi}_z$$

where w is the particle of water next to the differential disk of centroid p . It is assumed that A_{Ew} is constant over the entire differential disk. Components of A_{Ew} at point p are given by:

$$\dot{\phi}_x = \frac{d}{dt} \frac{\partial \phi}{\partial x} = g K_x \xi_0 e^{|\bar{K}| z_w} \cos(\bar{K} \cdot \bar{S} - \omega t)$$

$$\dot{\phi}_y = \frac{d}{dt} \frac{\partial \phi}{\partial y} = g K_y \xi_0 e^{|\bar{K}| z_w} \cos(\bar{K} \cdot \bar{S} - \omega t)$$

and $\dot{\phi}_z = \frac{d}{dt} \frac{\partial \phi}{\partial z} = g |\bar{K}| \xi_0 e^{|\bar{K}| z_w} \sin(\bar{K} \cdot \bar{S} - \omega t)$

where; $K_x = |\bar{K}| \cos\beta$; $K_y = |\bar{K}| \sin\beta$, and the higher order terms in $\dot{\phi}_z$ have been neglected.

$$\text{Now; } \bar{R}_{op} = \bar{R}_{oc} + \bar{R}_{cp}$$

$$\therefore \dot{\bar{v}}_{Ep} = [\dot{\bar{R}}_{op}]_E = [\dot{\bar{R}}_{oc}]_E + \bar{w}_{EB} \times \bar{R}_{cp}$$

$$\text{and } \ddot{\bar{A}}_{Ep} = [\ddot{\bar{R}}_{oc}]_E + [\dot{\bar{w}}_{EB}]_E \times \bar{R}_{cp} + \bar{w}_{EB} \times (\bar{w}_{EB} \times \bar{R}_{cp})$$

where; \bar{w}_{EB} is the angular velocity of the buoy.

Let us also define the relative acceleration vector of the fluid particles with respect to the buoy (\bar{A}_R), at the location of point p as:

$$\bar{A}_R = \bar{A}_{EW} - \bar{A}_{Ep}$$

$$\text{also let, } \bar{A}_{RT} = (\bar{A}_R \cdot \hat{i}_z) \hat{i}_z,$$

$$\text{and } \bar{A}_{RN} = \bar{A}_R - \bar{A}_{RT}$$

The vector force equations of motion may now be written as:

$$\int_l^{u_1} dM \bar{A}_{Ep} = \int_l^{u_2} dB \bar{A}_{EW} + C_N \int_l^{u_2} dB \bar{A}_{RN} + \\ C_T \int_l^{u_2} dB \bar{A}_{RT} - \int_l^{u_3} dB \bar{g} + \int_l^{u_1} dM \bar{g} \quad (2.1)$$

where the viscous drag forces and the tension forces (due to the attached mooring lines) are left out for later introduction.

Here; $l = -z_c$, $u_1 = H - z_c$, $u_2 = h_o - z_c$, and $u_3 = h_i - z_c$. z_c is the distance between c and the bottom of the buoy. H is the length of the buoy, h_o is the instantaneous draft of the buoy measured up to the mean free surface, and h_i is h_o plus the wave elevation component. Distances z_c , H, h_o and h_i are measured along \hat{i}_z . dM is the mass of the differential disk (Figure 2.1) of height dz' and dB is the mass of water displaced by this disk. C_N AND C_T are the appropriate hydrodynamic constants.

In equation (2.1) the integrals in order of their appearance represent: 1) the actual unbalanced force which accelerates the buoy; 2) the Froude-Krylov force; 3) the normal component of the added mass force; 4) the tangential component of the added mass force; 5) the hydrostatic pressure force; and 6) the weight of the buoy. This equation reduces to the equation in Rudnick (1967), which was derived for a spar buoy, for $C_N = 1.0$, and $C_T = 0.0$.

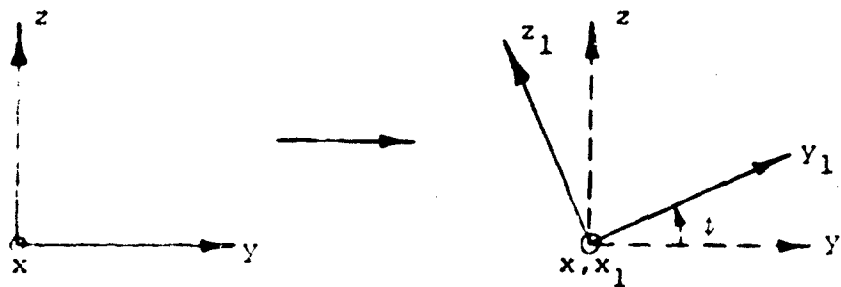
The vector moment equation can now be written similarly as: (moments about C.G.)

$$\begin{aligned}
 \int dM(\bar{R}_{cp} \times \bar{\Lambda}_{Ep}) &= \int dB(\bar{R}_{cp} \times \bar{\Lambda}_{EW}) + \\
 &+ C_N \int dB(\bar{R}_{cp} \times \bar{\Lambda}_{RN}) + \\
 &+ C_T \int dB(\bar{R}_{cp} \times \bar{\Lambda}_{RT}) - \\
 &- \int dB(\bar{R}_{cp} \times \bar{g}) + \int dM(\bar{R}_{cp} \times \bar{g})
 \end{aligned} \tag{2.2}$$

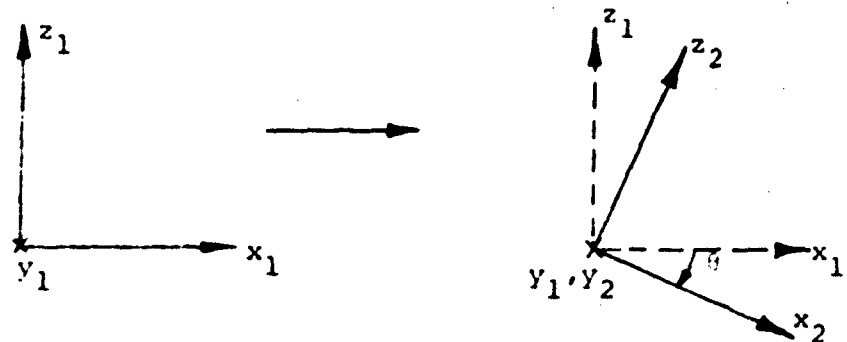
It is also necessary to determine an appropriate transformation scheme to relate vectors in the E frame to vectors in the B frame. A sequence of rotations (Figure 2.3) about the body x' , y' , z' axes (roll = ϕ , pitch = θ , and yaw = ψ) respectively yield the following transformation.

$$\begin{pmatrix} \hat{i}_x' \\ \hat{i}_y' \\ \hat{i}_z' \end{pmatrix} = \begin{bmatrix} \cos\phi \cos\psi & \sin\psi \cos\phi & \sin\phi \sin\psi \\ \sin\phi \cos\psi & \cos\psi \cos\phi & -\cos\phi \sin\psi \\ \sin\psi & -\cos\phi \sin\psi & \cos\phi \cos\psi \end{bmatrix} \begin{pmatrix} \hat{i}_x \\ \hat{i}_y \\ \hat{i}_z \end{pmatrix}$$

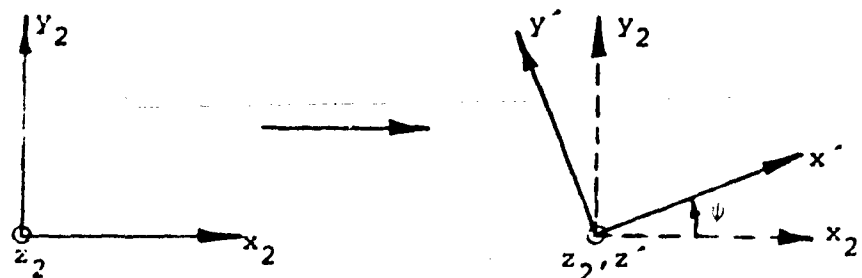
The inverse of this transformation matrix is given by its transpose. The force and moment equations (2.1) and (2.2) may be combined and written in matrix form as:



Step 1 - Roll (θ): Rotate y, z about x to obtain x_1, y_1, z_1



Step 2 - Pitch (ϕ): Rotate x_1, z_1 about y_1 to obtain x_2, y_2, z_2



Step 3 - Yaw (ψ): Rotate x_2, y_2 about z_2 to obtain x', y', z'

Figure 2.3 Transformation Matrix Rotations

$$[M] \cdot \frac{d}{dt} \{V\} = \{F_D\} + \{F_G\} + \{F_A\} \quad (2.3)$$

Here the matrix $[M]$ is composed of the tensors of inertia and added inertia. The $\{V\}$ column vector has three translation rates and three angular rates. The vector $\{F_D\}$ contains the wave exciting forces and moments. The vector $\{F_G\}$ comprises the hydrostatic pressure and weight restoring forces and moments (i.e. gravitational and buoyancy effects); and $\{F_A\}$ is any additional forces and moments including viscous drag forces and moments introduced next and tension forces/moment from attached mooring lines introduced in Section 2.3.

Viscous drag forces and moments. A square drag law, where viscous drag forces are proportional to the square of the relative fluid velocity is used. In Figure 2.1

$$\bar{R}_{ow} = \bar{R}_{oc} + \bar{R}_{cp} + \bar{R}_{pw}$$

$$\therefore \bar{v}_{ew} = \bar{v}_{ec} + \bar{w}_{eb} \times \bar{r}_{cp} + [\dot{\bar{r}}_{pw}]_E$$

If point p and w are overlapping then:

$$[\dot{\bar{r}}_{pw}]_E = [\dot{\bar{r}}_{pw}]_B = \bar{v}_{bw} = \bar{v}_{ew} - \bar{v}_{ec} - \bar{w}_{eb} \times \bar{r}_{cp}$$

Here; $\bar{v}_{Ew} = \hat{i}_x (v_{ox} + \hat{v}_x) + \hat{i}_y (v_{oy} + \hat{v}_y) + \hat{i}_z (v_{oz} + \hat{v}_z)$ and \bar{v}_{Bw} is the relative velocity of water seen by the buoy at the local point p. Hence the viscous drag force on the submerged portion of the buoy is given by:

$$\overline{DF} = \frac{1}{2} \rho C_D \int_l^u dA_D |\bar{v}_{Bw}| |\bar{v}_{dw}| \quad (2.4)$$

where, ρ is the water density, C_D the drag coefficient, and dA_D the appropriate differential area. The viscous drag moment can similarly be written as:

$$\overline{DM} = \frac{1}{2} \rho C_D \int_l^u dA_D |\bar{v}_{Bw}| (\bar{R}_{cp} \times \bar{v}_{Bw}) \quad (2.5)$$

Limits of integration for both (2.4) and (2.5) are the entire submerged depth of the buoy.

In the remainder of Section 2.1 the equations (2.1), (2.2), (2.4), and (2.5) presented above will be specialized to the specific problems at hand. The matrices of equation (2.3) will then be derived and presented for these specific problems.

2.1.1 Spar Buoy

A tuned spar buoy (Figure 2.4) will be analyzed in this section to obtain general spar buoy equations.

Note: Shown for zero rotation and translation.

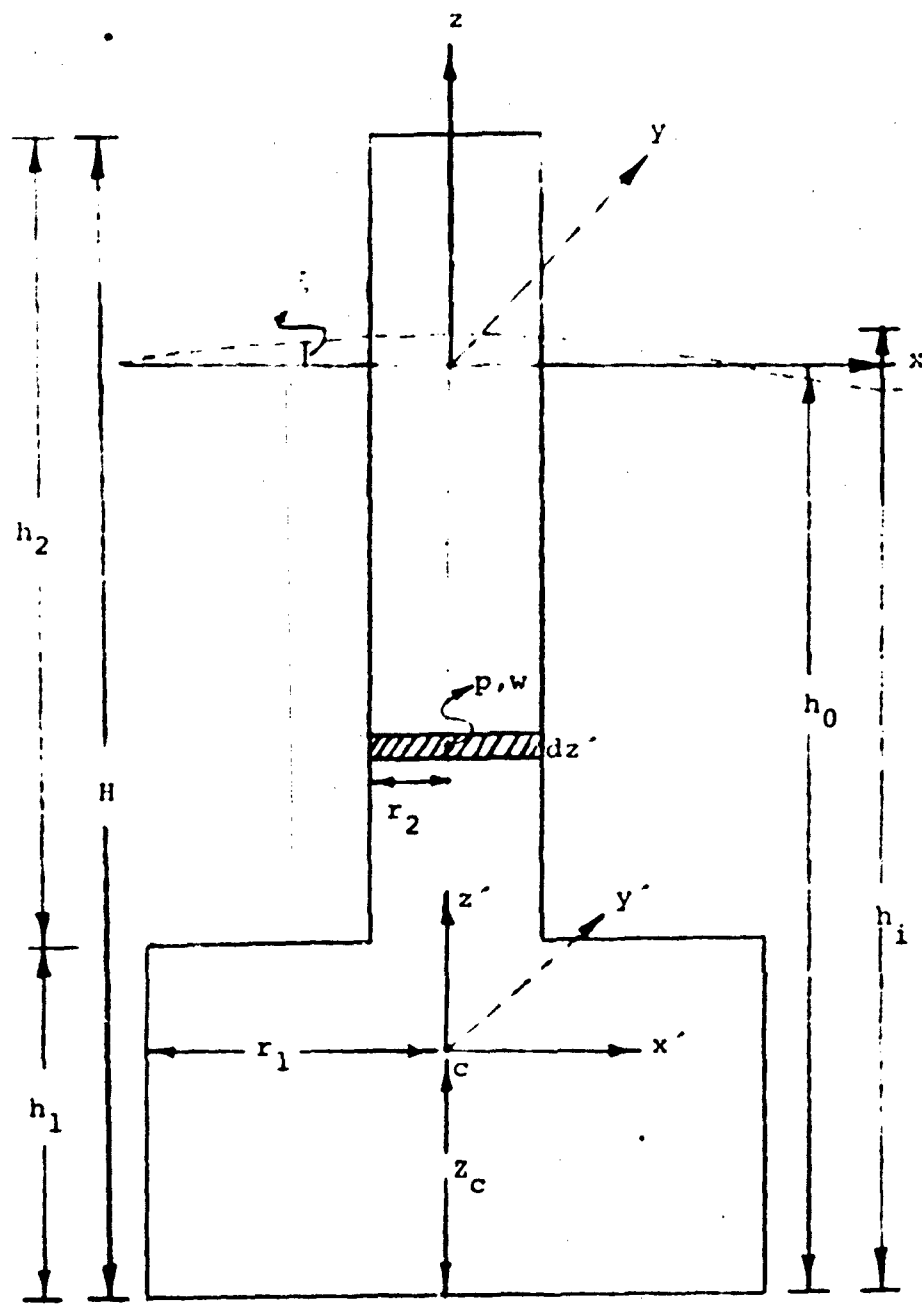


Figure 2.4 - A Tuned Spar Buoy

Cylindrical spar buoy equations can then be obtained as a special case of the tuned spar buoy. Both two-dimensional and three-dimensional analysis will be presented. We will find the equations of motion of its response for a train of surface gravity waves having a single frequency and amplitude, propagating in any single direction.

Variation in wave acceleration and velocity over the horizontal buoy dimensions are neglected. In addition in the three-dimensional analysis, all rotational angles (roll, pitch, and yaw) are restricted to be small.

Two-Dimensional Analysis: In this analysis \bar{K} is a scalar with $\phi = 0$; and \bar{S} is replaced by the scalar x which is the direction of propagation. Also, $\bar{A}_{EW} = i_x \dot{i}_x + i_z \dot{i}_z$.

$$\bar{A}_{RN} = (\bar{A}_E \cdot i_x) i_x,$$

and the appropriate transformation with $\phi = 0$, and $\psi = 0$ becomes

$$\begin{Bmatrix} \dot{i}_x \\ \dot{i}_z \end{Bmatrix} = \begin{bmatrix} \cos\theta & -\sin\theta \\ \sin\theta & \cos\theta \end{bmatrix} \begin{Bmatrix} \dot{i}_x \\ \dot{i}_z \end{Bmatrix}$$

Now let, $[\ddot{R}_{oc}]_E = \hat{i}_x \ddot{x}_c + \hat{i}_z \ddot{z}_c$

$$\bar{w}_{EB} = \hat{i}_y \dot{a}$$

and $\bar{R}_{cp} = z'_p \hat{i}_z$

$$\begin{aligned}\therefore \bar{A}_{Ep} &= i_x [\ddot{x}_c + z'_p (\theta \cos\theta - \dot{\theta}^2 \sin\theta)] \\ &\quad + \hat{i}_z [\ddot{z}_c + z'_p (-\dot{\theta} \sin\theta - \dot{\theta}^2 \cos\theta)]\end{aligned}$$

Also, $\bar{A}_{EW} = \frac{2}{\rho_o} e^{Kz_w} [i_x \cos(Kx_c - \omega t) + i_z \sin(Kx_c - \omega t)]$

Define: $P_i = \int_{-l}^{u_2} dB (z'_p)^i \quad i = 0, 1, 2$

and $Q_i = \int_{-l}^{u_2} dB e^{Kz_w} (z'_p)^i \quad i = 0, 1$

Integrals of equation (2.1) can now be written as:

1. $\int dM \bar{A}_{Ep} = M[\hat{i}_x \ddot{x}_c + \hat{i}_z \ddot{z}_c]$

Where M is the total mass of the buoy.

2. $\int dB A_{EW} = \frac{2}{\rho_o} Q_0 [i_x \cos(Kx_c - \omega t) + i_z \sin(Kx_c - \omega t)]$

$$3. C_N \int dB \bar{A}_{RN} = C_N \hat{i}_x \{\omega^2 \xi_o Q_o [\cos(Kx_c - \omega t) \cos^2 \theta - \\ - \sin(Kx_c - \omega t) \sin \theta \cos \theta] + \\ + P_o (\ddot{x}_c \sin \theta \cos \theta - \ddot{z}_c \cos^2 \theta) - P_1 \cos \theta\} + \\ + C_N \hat{i}_z \{\omega^2 \xi_o Q_o [\sin(Kx_c - \omega t) \sin^2 \theta - \cos(Kx_c - \omega t) \\ \sin \theta \cos \theta] + P_o (\ddot{x}_c \sin \theta \cos \theta - \ddot{z}_c \sin^2 \theta) + \\ + P_1 \sin \theta\}$$

$$4. C_T \int dB \bar{A}_{RT} = C_T \hat{i}_x \{\omega^2 \xi_o Q_o [\cos(Kx_c - \omega t) \sin^2 \theta + \\ + \sin(Kx_c - \omega t) \sin \theta \cos \theta] + \\ + P_o (-\ddot{x}_c \sin^2 \theta - \ddot{z}_c \sin \theta \cos \theta) + \\ + P_1 \sin \theta\} + C_T \hat{i}_z \{\omega^2 \xi_o Q_o [\cos(Kx_c - \omega t) \sin \theta \cos \theta + \\ + \sin(Kx_c - \omega t) \cos^2 \theta] + P_o (-\ddot{x}_c \sin \theta \cos \theta - \\ - \ddot{z}_c \cos^2 \theta) + P_1 \cos \theta\}$$

$$5. - \int_{-l}^{u_3} dB \bar{g} = g \int_{-l}^{u_2} dB \hat{i}_z + g \int_{-l}^{-z_o \sin(Kx_c - \omega t) / \cos \theta} dB \hat{i}_z$$

Also; $dB = \rho S_o dz'$, where S_o is the cross-sectional area of the disk of height dz' . Then;

$$-\int_l^{u_3} dB \bar{g} = \hat{i}_z [P_0 g - \rho s_{o2} g \xi_o \sin(Kx_c - \omega t) / \cos\theta]$$

where; $s_{o2} = \pi r_2^2$

$$6. \int dM \bar{g} = - Mg \hat{i}_z$$

Integrals of equation (2.2) can also be written
as:

$$1. \int dM (\bar{R}_{cp} \times \bar{A}_{Ep}) = \int dM z'^2 \ddot{\theta} \hat{i}_y = I_{yy} \ddot{\theta} \hat{i}_y$$

$$2. \int dB (\bar{R}_{cp} \times \bar{A}_{Ew}) = \hat{i}_y \{ \omega^2 \xi_o Q_1 [\cos(Kx_c - \omega t) \cos\theta - \\ - \sin(Kx_c - \omega t) \sin\theta] \}$$

$$3. C_N \int dB (\bar{R}_{cp} \times \bar{A}_{RN}) = C_N \hat{i}_y \{ \omega^2 \xi_o Q_1 [\cos(Kx_c - \omega t) \cos\theta - \\ - \sin(Kx_c - \omega t) \sin\theta] - P_1 \cos\theta \ddot{x}_c + \\ + P_1 \sin\theta \ddot{z}_c - P_2 \ddot{\theta} \}$$

$$4. C_T \int dB (\bar{R}_{cp} \times \bar{A}_{RT}) = 0$$

$$5. - \int_l^{u_3} dB (\bar{R}_{cp} \times \bar{g}) \approx - \int_l^{u_2} dB (\bar{R}_{cp} \times \bar{g}) \\ = \hat{i}_y (-P_1 g \sin\theta)$$

6. $\int dM(\bar{R}_{cp} \times \bar{g}) = 0$

Viscous Drag Forces and Moments: For a tuned spar buoy the viscous drag forces are assumed to be acting in normal and tangential directions proportional to their respective drag coefficients and areas.

$$\begin{aligned} \vec{v}_{Bw} &= \hat{i}_x [v_{ox} + \phi_x - \dot{x}_c - z_p' \dot{\theta} \cos \theta] + \\ &+ \hat{i}_z [v_{oz} + \phi_z - \dot{z}_c + z_p' \dot{\theta} \sin \theta] \\ &= \hat{i}_x [(v_{ox} + \phi_x - \dot{x}_c) \cos \theta \\ &- (v_{oz} + \phi_z - \dot{z}_c) \sin \theta - z_p' \dot{\theta}] \\ &+ \hat{i}_z [(v_{ox} + \phi_x - \dot{x}_c) \sin \theta \\ &+ (v_{oz} + \phi_z - \dot{z}_c) \cos \theta] \\ &= \hat{i}_x v_{Bwx} + \hat{i}_z v_{Bwz}, \end{aligned}$$

Drag force components can now be written:

$$DF_x = \rho C_{DN} \int r |v_{Bwx}| |v_{Bwx}| dz'$$

$$\begin{aligned} DF_z &= \rho C_{DT} \pi \int r |v_{Bwz}| |v_{Bwz}| dz' \\ &+ \frac{1}{2} \rho C_{Dp} \pi \{r_1^2 |v_b| v_b + (r_1^2 - r_2^2) |v_s| v_s\} \end{aligned}$$

Here; C_{DN} and C_{DT} are normal and tangential drag coefficients. C_{DP} is the pressure drag coefficient due to the bottom, and the step, of the tuned spar buoy.

$$V_s = V_{Bwz}, (z' = h_1 - z_c)$$

and $V_b = V_{Bwz}, (z' = -z_c)$

Also; $DM = \rho C_{DN} \int r |V_{Bwx}| |V_{Bwx}| z'_p dz'$

Using the transformation matrix:

$$\begin{Bmatrix} DF_x \\ DF_z \end{Bmatrix} = \begin{bmatrix} \cos\theta & \sin\theta \\ -\sin\theta & \cos\theta \end{bmatrix} \begin{Bmatrix} DF_{x'} \\ DF_{z'} \end{Bmatrix}$$

Added Mass Force Due to the Step and Bottom Base

of the Tuned Spar: In addition to the forces mentioned above, an added mass force proportional to the tangential body acceleration (\bar{A}_{Et}) and acting perpendicular to the step and the bottom end of the tuned spar is considered. Lamb (1945) in his analysis of a cylindrical spar moving in still water, gives an added mass coefficient equal to $4/3\pi r^3$. Following representation is used in this analysis for this force (\bar{AM}).

$$\overline{AM} = \frac{4}{3} \alpha \rho \left[r_1^3 \bar{A}_{Et} \Big|_{z'=-z_c} + (r_1 - r_2)^3 \bar{A}_{Et} \Big|_{z'=h_1 - z_c} \right] \quad (2.6)$$

where; $\bar{A}_{Et} = (\bar{A}_{Ep} \cdot \hat{i}_{z'}) \hat{i}_{z''}$, and α is a constant.

\overline{AM} is added to the left hand side of equation (2.1).

$\overline{R}_{cp} \times \overline{AM}$ would be equal to zero.

Combining all these forces and moments; the matrix coefficients of equation (2.3) can be written as:

$$M_{11} = M + P_o (C_N \cos^2 \theta + C_T \sin^2 \theta) +$$

$$\frac{4}{3} \alpha \rho [r_1^3 + (r_1 - r_2)^3] \sin^2 \theta$$

$$M_{12} = P_o \sin \theta \cos \theta (C_T - C_N) +$$

$$\frac{4}{3} \alpha \rho [r_1^3 + (r_1 - r_2)^3] \sin \theta \cos \theta$$

$$M_{13} = C_N P_1 \cos \theta$$

$$M_{21} = P_o \sin \theta \cos \theta (C_T - C_N) +$$

$$\frac{4}{3} \alpha \rho [r_1^3 + (r_1 - r_2)^3] \sin \theta \cos \theta$$

$$M_{22} = M + P_o (C_N \sin^2 \theta + C_T \cos^2 \theta) +$$

$$\frac{4}{3} \alpha \rho [r_1^3 + (r_1 - r_2)^3] \cos^2 \theta$$

$$M_{23} = - C_N P_1 \sin \theta$$

$$M_{31} = C_N P_1 \cos \theta$$

$$M_{32} = - C_N P_1 \sin \theta$$

$$M_{33} = I_{yy} + C_N P_2$$

$\{v\} = [\dot{x}_c, \dot{z}_c, \dot{\theta}]$; which is a column vector.

$$F_{D1} = \omega^2 \xi_o Q_o [\cos(Kx_c - \omega t) (1 + C_N \cos^2 \theta + C_T \sin^2 \theta) + \sin(Kx_c - \omega t) \sin \theta \cos \theta (C_T - C_N)]$$

$$F_{D2} = \omega^2 \xi_o Q_o [\sin(Kx_c - \omega t) (1 + C_N \sin^2 \theta + C_T \cos^2 \theta) + \cos(Kx_c - \omega t) \sin \theta \cos \theta (C_T - C_N)]$$

$$F_{D3} = \omega^2 \xi_o Q_1 [\cos(Kx_c - \omega t) \cos \theta - \sin(Kx_c - \omega t) \sin \theta] (1 + C_N)$$

$$r_{G1} = 0.$$

$$F_{G2} = P_o g - \rho S_{o2} g \xi_o \sin(Kx_c - \omega t) / \cos \theta - Mg$$

$$F_{G3} = - P_1 g \sin \theta$$

$$F_{A1} = C_T P_1 \sin \theta \dot{\theta}^2 + DF_x - \frac{4}{3} \alpha [r_1^3 + (r_1 - r_2)^3] z_c \sin \theta \dot{\theta}^2$$

$$F_{A2} = C_T P_1 \cos \theta \dot{\theta}^2 + DF_z + \frac{4}{3} \alpha [r_1^3 + (r_1 - r_2)^3]$$

$$(h_1 - z_c) \cos \theta \dot{\theta}^2$$

and $F_{A3} = DM$

Three-Dimensional Analysis: For small angles the appropriate transformation matrix reduces to:

$$\begin{pmatrix} \hat{i}_x' \\ \hat{i}_y' \\ \hat{i}_z' \end{pmatrix} = \begin{bmatrix} 1 & & -\theta \\ -\psi & 1 & \phi \\ \theta & -\phi & 1 \end{bmatrix} \begin{pmatrix} \hat{i}_x \\ \hat{i}_y \\ \hat{i}_z \end{pmatrix}$$

In this analysis we let $C_N = 1.0$, $C_T = 0.0$, and define:

$$[\ddot{R}_{oc}]_E = \hat{i}_x \ddot{x}_c + \hat{i}_y \ddot{y}_c + \hat{i}_z \ddot{z}_c$$

$$\ddot{w}_{EB} = \hat{i}_x \dot{\phi} + \hat{i}_y \dot{\theta} + \hat{i}_z \dot{\psi}$$

and $\bar{R}_{cp} = z_p \hat{i}_z'$

$$\therefore \bar{A}_{Ep} = \hat{i}_x (\ddot{x}_c + \ddot{z}_p) + \hat{i}_y (\ddot{y}_c + \ddot{z}_p) + \hat{i}_z \ddot{z}_c$$

and; $\bar{A}_{Ew} = \omega^2 i_o e^{j\bar{K}z_w} [\hat{i}_x \cos \theta \cos(\bar{K} \cdot \bar{s} - t) + \hat{i}_y \sin \theta \cos(\bar{K} \cdot \bar{s} - t) + \hat{i}_z \sin(\bar{K} \cdot \bar{s} - t)]$

Integrals of equation (2.1) can now be written
as:

$$1. \int dM \bar{A}_{Ep} = M (\hat{i}_x \ddot{x}_c + \hat{i}_y \ddot{y}_c + \hat{i}_z \ddot{z}_c)$$

$$2. \int dB \bar{A}_{Ew} = \omega^2 i_o Q_o [\hat{i}_x \cos \theta \cos(\bar{K} \cdot \bar{s} - t) + \hat{i}_y \sin \theta \cos(\bar{K} \cdot \bar{s} - t) + \hat{i}_z \sin(\bar{K} \cdot \bar{s} - t)]$$

also; $\bar{A}_{RN} = \hat{i}_x (\ddot{i}_x - \ddot{x}_c - \ddot{z}_p + \ddot{z}_c) + \hat{i}_y (\ddot{i}_y - \ddot{y}_c + \ddot{z}_p - \ddot{z}_c) + \hat{i}_z (\ddot{i}_z - \ddot{z}_c)$

$$3. \int dB \bar{A}_{RN} = \hat{i}_x (\omega^2 i_o \cos \theta Q_o \cos(\bar{K} \cdot \bar{s} - t) - P_o \ddot{x}_c - P_1 \ddot{z}_c + \hat{i}_y \ddot{z}_c + \hat{i}_z \ddot{y}_c) \sin \theta Q_o \cos(\bar{K} \cdot \bar{s} - t) -$$

$$P_o \ddot{y}_c + P_1 \ddot{z}_c - P_o \ddot{z}_c + \hat{i}_z P_o (\ddot{x}_c - \ddot{y}_c)$$

$$4. - \int_{\ell}^u dB \bar{g} = \int_{\ell}^u dB g \hat{i}_z + \int_{\ell}^u dB g \hat{i}_z \\ = \hat{i}_z (P_o q - \omega S_o 2 q S_o \sin(\bar{K} \cdot \bar{s} - \omega t))$$

$$5. \int dM \bar{g} = - Mg \hat{i}_z$$

Similarly integrals of equation (2.2) can be written as:

$$1. \int dM (\bar{R}_{cp} \times \bar{A}_{EP}) = \hat{i}_x I_{xx} \ddot{\phi} + \hat{i}_y I_{yy} \ddot{\theta}$$

where; $I_{xx} = I_{yy} = \int_0^H dM z'^2$

$$2. \int dB (\bar{R}_{cp} \times \bar{A}_{EW}) = \hat{i}_x \{-\omega^2 \xi_o Q_1 \sin \beta \cos(\bar{K} \cdot \bar{S} - \omega t)\} \\ + \hat{i}_y \{\omega^2 \xi_c Q_1 \cos \beta \cos(\bar{K} \cdot \bar{S} - \omega t)\}$$

$$3. \int dB (\bar{R}_{cp} \times \bar{A}_{RN}) = \hat{i}_x \{-\omega^2 \xi_o Q_1 \sin \beta \cos(\bar{K} \cdot \bar{S} - \omega t) + P_1 \ddot{y}_c - P_2 \ddot{\phi} \\ + P_1 \ddot{\phi} z_c\} + \hat{i}_y \{\omega^2 \xi_o Q_1 \cos \beta \cos(\bar{K} \cdot \bar{S} - \omega t) \\ - P_1 \ddot{x}_c - P_2 \ddot{\theta} + P_1 \ddot{\theta} z_c\} - \hat{i}_z P_1 \{\ddot{\theta} y_c + \ddot{\phi} x_c\}$$

$$4. - \int_l^{u_3} dB (\bar{R}_{cp} \times \bar{g}) = - \int_l^{u_2} dB (\bar{R}_{cp} \times \bar{g}) \\ = \hat{i}_x (-P_1 \phi g) + \hat{i}_y (-P_1 \theta g)$$

$$5. \int dM (\bar{R}_{cp} \times \bar{g}) = 0$$

Viscous drag Forces and Moments:

$$\begin{aligned}
 \bar{v}_{Bw} &= \hat{i}_x [v_{ox} + \dot{\phi}_x - \dot{z}_c - z_p' \dot{\theta}] + \\
 &\quad \hat{i}_y [v_{oy} + \dot{\phi}_y - \dot{y}_c + z_p' \dot{\phi}] + \\
 &\quad \hat{i}_z [v_{oz} + \dot{\phi}_z - \dot{z}_c] \\
 &= \hat{i}_x [v_{ox} + \dot{\phi}_x - \dot{x}_c - z_p' \dot{\theta} + v_{oy} \psi - \dot{y}_c \psi - v_{oz} \theta + \dot{z}_c \theta] \\
 &\quad + \hat{i}_y [-v_{ox} \psi + \dot{y}_c + v_{oy} + \dot{\phi}_y - \dot{y}_c + z_p' \dot{\phi} + v_{oz} \phi - \dot{z}_c \phi] \\
 &\quad + \hat{i}_z [v_{ox} \theta - \dot{x}_c \theta - v_{oy} \phi + \dot{y}_c \phi + v_{oz} + \dot{\phi}_z - \dot{z}_c] \\
 &= \hat{i}_x, v_{Bwx} + \hat{i}_y, v_{Bwy} + \hat{i}_z, v_{Bwz}
 \end{aligned}$$

Hence; $DF_x = \rho C_{DN} \int r \sqrt{v_{Bwx}^2 + v_{Bwy}^2} (v_{Bwx}) dz'$

$$DF_y = \rho C_{DN} \int r \sqrt{v_{Bwx}^2 + v_{Bwy}^2} (v_{Bwy}) dz'$$

and, $DF_z = \rho C_{DT} \pi \int r |v_{Bwz}| v_{Bwz} dz' +$

$$\frac{1}{2} \rho C_{DP} \pi (r_1^2 |v_b| v_b + (r_1^2 - r_2^2) |v_s| v_s)$$

Using the transformation matrix:

$$\begin{Bmatrix} DF_x \\ DF_y \\ DF_z \end{Bmatrix} = \begin{bmatrix} 1 & -\psi & \theta \\ \psi & 1 & -\phi \\ -\theta & \phi & 1 \end{bmatrix} \begin{Bmatrix} DF_{x'} \\ DF_{y'} \\ DF_{z'} \end{Bmatrix}$$

Also $\overline{DM} = \int (\bar{R}_{cp} \times d\overline{DF})$
 $= i_x' (DM_{x'}) + i_y' (DM_{y'})$

Therefore:

$$\begin{Bmatrix} DM_x \\ DM_y \\ DM_z \end{Bmatrix} = \begin{bmatrix} 1 & -\psi & \theta \\ \psi & 1 & -\phi \\ -\theta & \phi & 1 \end{bmatrix} \begin{Bmatrix} DM_{x'} \\ DM_{y'} \\ 0 \end{Bmatrix}$$

Combining all these forces and equation (2.6) of additional added mass, we can write the non-zero elements of matrices in equation (2.3) as:

$$M_{11} = M + P_o = M_{22}$$

$$M_{13} = 4/3 \alpha_0 [r_1^3 + (r_1 - r_2)^3] \theta - P_c \theta = M_{31}$$

$$M_{15} = P_1 = M_{51}$$

$$M_{23} = P_o \phi - 4/3 \alpha_0 [r_1^3 + (r_1 - r_2)^3] \phi = M_{32}$$

$$M_{24} = -P_1 = M_{42}$$

$$M_{33} = M + 4/3 \alpha \rho [r_1^3 + (r_1 - r_2)^3]$$

$$M_{43} = -P_1 \phi$$

$$M_{44} = I_{xx} + P_2$$

$$M_{53} = -P_1 \theta$$

$$M_{55} = I_{yy} + P_2$$

$$M_{61} = P_1 \phi \quad M_{62} = P_1 \theta$$

$\{v\} = [\dot{x}_c, \dot{y}_c, \dot{z}_c, \dot{\phi}, \dot{\theta}, \dot{\psi}]$ is a column vector.

$$F_{D1} = 2\omega^2 \xi_o Q_o \cos \beta \cos(\bar{K} \cdot \bar{S} - \omega t)$$

$$F_{D2} = 2\omega^2 \xi_o Q_o \sin \beta \cos(\bar{K} \cdot \bar{S} - \omega t)$$

$$F_{D3} = \omega^2 \xi_o Q_o \sin(\bar{K} \cdot \bar{S} - \omega t)$$

$$F_{D4} = -2\omega^2 \xi_o Q_1 \sin \beta \cos(\bar{K} \cdot \bar{S} - \omega t)$$

$$F_{D5} = 2\omega^2 \xi_o Q_1 \cos \beta \cos(\bar{K} \cdot \bar{S} - \omega t)$$

$$F_{G3} = P_0 g - \rho S_{02} g \xi_0 \sin(\bar{K} \cdot \bar{\xi} - \omega t) - Mg$$

$$F_{G4} = - P_1^4 g$$

$$F_{G5} = - P_1^5 g$$

and $\{F_A\} = [DF_x, DF_y, DF_z, DM_x, DM_y, DM_z]$ is a column vector.

As can be seen from these matrix elements, the sixth degree of freedom corresponding to ψ does not drop out; but M_{66} equals zero. M_{66} is introduced in the equations for computational purposes. M_{66} is given by:

$$M_{66} = \frac{\rho \pi}{2} [r_1^4 h_1 + r_2^4 (H-h_1)]$$

which represents the moment of inertia of a tuned spar about its longitudinal axis.

2.1.2 Other Shapes

To obtain the velocity potential function ϕ for any shapes other than for simple geometries and small body motions is hardly ever possible. Hence to obtain any reasonable solution to this problem one has to depend on empirical approaches. Solution to these problems has thus been left out of this report. In order to use the

analysis and computer programs of this report, the readers will have to substitute their own elements for $[M]$, $\{F_D\}$, $\{F_G\}$, and $\{F_A\}$ matrices of equation 2.3; pertinent to the particular surface buoy in question.

2.2 Mooring Line

A mooring line connects a surface or a subsurface buoy to the anchor. In this report, a line attached to a buoy but not to an anchor is also considered a mooring line. Such a line could be connecting a drogue with the surface buoy or be an instrument line hanging from a moored surface buoy. In general a mooring line is made of any type or number of materials (steel, nylon, dacron, etc.) and has any type or number of instruments (including subsurface floats) inserted along its length.

The mathematical model of mooring line dynamics will be formulated in two different approaches. The "first" approach is called the "continuous line formulation". In this approach the mooring line differential equations, with respect to the spatial coordinate s , are integrated incrementally down the mooring line, to obtain its dynamic equilibrium at any instant of time. Velocities and accelerations of the mooring line differential elements and the instruments (including subsurface floats) inserted in the mooring line are computed by differentiating

positions found by the dynamic equilibriums. This approach was used to model the low frequency motion of a subsurface mooring system, as presented later in the report. Exciting forces exerted on the mooring line by the wave system are neglected and so are the wave-damping forces. Viscous drag effects due to the velocity field generated by the surface waves is included. This approach was found to be computationally inefficient, and hard to solve numerically (due to the differentiation of positions to find velocities and accelerations) for the high frequency motion of a surface moored system.

For the high frequency motion of a surface moored system a "second" approach called the "lumped parameter formulation" is presented. Here exciting forces exerted on the mooring line by the wave system are taken equal to the "Froude-Krylov" forces, as it is assumed that the presence of the mooring line does not disturb the wave particle motion. Again, viscous drag effects due to the velocity field generated by the surface waves are included, and the wave-damping forces are neglected. In both approaches, a velocity profile (could-be time varying) can be present along with the surface wave. Both formulations are presented in three-dimensions and can be reduced to two-dimensions when needed.

2.2.1 Continuous Line Formulation

On a differential element of a continuous mooring line the forces acting are: (a) the constant force due to gravitational attraction, (b) the variable tensile forces transmitted from the adjoining elements, and (c) the variable pressure (normal) and shear (tangential) forces applied by the fluid. The fluid forces can be broken down into (1) the hydrostatic pressure force, (2) the pressure force due to the acceleration of the fluid by the element (the so-called added mass force), and (3) the viscous drag forces due to fluid relative velocity, which have both pressure (normal) and shear (tangential) components. Internal damping forces are neglected in this analysis as these are assumed small compared to tensile and viscous drag forces. Exciting and damping forces due to the wave system are also neglected. From Newton's second law of mechanics the above forces should equal the mass of the differential element multiplied by its acceleration. By computing these forces the differential equations for the mooring line dynamic equilibrium are derived as follows:

The mooring line is considered to be a cylindrical slender body. A free body diagram of a differential element of length ds of the mooring line is shown in Figure 2.5.

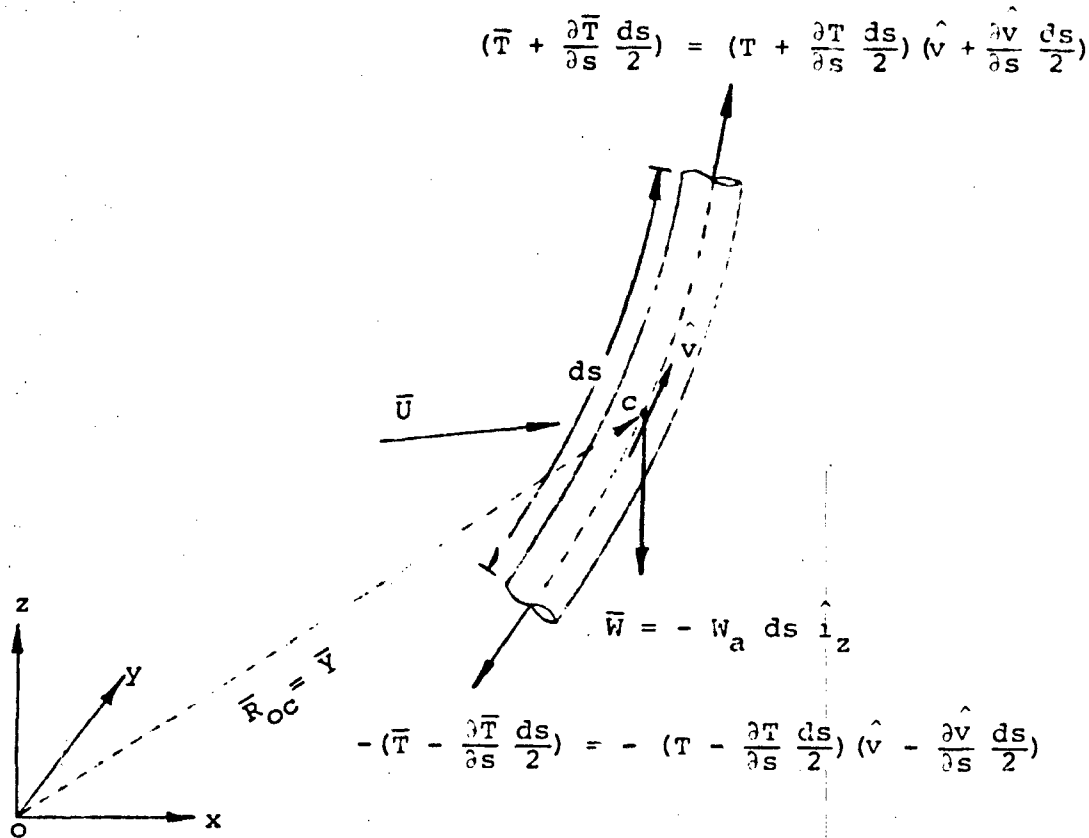


Figure 2.5 Mooring Line Differential Element

The internal tension and the inclination of the line segment change to keep all the above-mentioned forces in equilibrium. In Figure 2.5 \hat{v} is a unit vector along the mooring line given by:

$$\hat{v} = \hat{i}_x \cos \phi_1 + \hat{i}_y \cos \phi_2 + \hat{i}_z \cos \phi_3$$

\vec{T} is a tension vector, and \vec{U} is a fluid velocity vector (obtained from the current profile and the velocity field generated by the surface wave). The relative velocity vector \vec{UR} is given by:

$$\vec{UR} = \vec{U} - \dot{\vec{Y}}_c$$

where; $\vec{U} = \hat{i}_x U_x + \hat{i}_y U_y + \hat{i}_z U_z$

and, $\dot{\vec{Y}}_c = \hat{i}_x \dot{x}_c + \hat{i}_y \dot{y}_c + \hat{i}_z \dot{z}_c$ is the velocity of point c on the differential segment.

The viscous drag forces are computed according to the square drag law and are assumed to act in normal and tangential directions to the cylindrical line, proportional to their respective drag coefficients and areas.

Let: $\vec{UR} = \vec{UTR} + \vec{UNR}$

where; $\vec{UTR} = (\vec{UR} \cdot \hat{v}) \hat{v}$

and, $\vec{UNR} = \vec{UR} - \vec{UTR}$

From \vec{UNR} and \vec{UTR} , normal (\vec{DN}) and tangential (\vec{DT}) drag forces can be calculated using the pertinent drag coefficients (C_{DN} and C_{DT}). Representative areas of the differential element 'ds' can be calculated using the

reduced diameter and stretched length. These are given by dA_N and dA_T . The standard formulation is given by:

$$\overline{DN}ds = \rho/2 (C_{DN}) (dA_N) |\overline{UNR}| \overline{UNR}$$

and $\overline{DT}ds = \rho/2 (C_{DT}) (dA_T) |\overline{UTR}| \overline{UTR}$

The constant force due to gravitational attraction is $\bar{W} = - W_a ds \hat{i}_z$. Here, W_a is the weight in air per unit stretched length of the mooring line. \bar{W} is resolved into normal (\overline{WN}) and tangential (\overline{WT}) components as:

$$\overline{WT} = (\bar{W} \cdot \hat{v}) \hat{v} = - W_a ds \cos \phi_3 \hat{v}$$

and $\overline{WN} = \bar{W} - \overline{WT}$
 $= - W_a ds (\hat{i}_z - \hat{v} \cos \phi_3)$

The hydrostatic pressure force on the differential element by the surrounding fluid is given by the weight of the fluid displaced minus the hydrostatic pressure forces on the end cross-sections of the element. Or,

$$\overline{FH}ds = (W_a - W_w) ds \hat{i}_z - \pi r^2 [\hat{v}(P_b - P_t) - \frac{1}{2} \frac{\partial \hat{v}}{\partial s} ds (P_b + P_t)]$$

where, w_w is the weight in water per unit stretched length, and r is the reduced radius due to stretch of the mooring line. P_b and P_t are the hydrostatic pressures at the bottom and top ends of the differential element. Assume;

$$(P_b - P_t) = \rho g ds \cos\phi_3$$

$$\frac{P_b + P_t}{2} = P_c$$

and $w_a - w_w = \rho g \pi r^2$

$$\therefore \overline{FH} ds = (w_a - w_w) ds \left\{ (\hat{i}_z - \hat{v} \cos\phi_3) + \frac{P_c}{\rho g} \frac{\partial v}{\partial s} \right\}$$

Here, P_c is the hydrostatic pressure at the midpoint c of the differential element.

For a continuous cylindrical body it is also assumed that the body motion accelerates water only in the direction normal to its longitudinal axis. The inertia forces due to body's (differential element) own acceleration and the so called "added mass" term can now be written as:

$$\overline{IF} \, ds = - \frac{W_a}{g} \, ds \, \ddot{\overline{Y}} - \frac{(W_a - W_w)}{g} \, ds \, \ddot{\overline{YN}}$$

where; $\ddot{\overline{YN}} = \ddot{\overline{Y}} - \ddot{\overline{YT}}$

$\ddot{\overline{YT}} = (\ddot{\overline{Y}} \cdot \hat{v}) \hat{v}$; and the added mass of the differential element is assumed to be the mass of water displaced by this element.

Combining all these forces, the force equilibrium is written as:

$$\left(T + \frac{\partial T}{\partial s} \frac{ds}{2} \right) \left(\hat{v} + \frac{\partial \hat{v}}{\partial s} \frac{ds}{2} \right) - \left(T - \frac{\partial T}{\partial s} \frac{ds}{2} \right) \left(\hat{v} - \frac{\partial \hat{v}}{\partial s} \frac{ds}{2} \right) +$$

$$\overline{DN} \, ds + \overline{DT} \, ds - W_a \, ds \cos\phi_3 \hat{v} -$$

$$W_a \, ds (\hat{i}_z - \hat{v} \cos\phi_3) +$$

(2.7)

$$(W_a - W_w) ds (\hat{i}_z - \hat{v} \cos\phi_3) +$$

$$\frac{P_C}{\rho g} \frac{\partial \hat{v}}{\partial s} - \frac{W_a}{g} \, ds \, (\ddot{\overline{YN}} + \ddot{\overline{YT}}) - \frac{(W_a - W_w)}{g} \, ds \, \ddot{\overline{YN}} = 0$$

Or, $\left(\frac{\partial T}{\partial s} \right) \hat{v} = (-DT + W_a \cos\phi_3 + \frac{W_a}{g} \dot{YT}) \hat{v}$ (2.8)

and

$$\left\{ T + \frac{P_c (W_a - W_w)}{g} \right\} \frac{\partial \hat{v}}{\partial s} = - \bar{DN} + W_w (\hat{i}_z - \hat{v} \cos \phi_3) + \left(\frac{2W_a - W_w}{g} \right) \frac{\partial \bar{y}}{\partial s} \quad (2.9)$$

Also we can write:

$$\frac{\partial \bar{y}}{\partial s} = v \quad (2.10)$$

Here T , the tension, \hat{v} , the unit vector along the mooring line, and \bar{y} , the geometric displacement vector are the dependent variables of interest. Equations (2.8) and (2.9) can be simplified if we define a new variable called the effective tension (T_e) similar to the one described in GOODMAN and BRESLIN (1976).

$$T_e = T + \frac{P_c (W_a - W_w)}{\rho g} \quad (2.11)$$

Differentiating T_e with respect to s

$$\begin{aligned} \frac{\partial T_e}{\partial s} &= \frac{\partial T}{\partial s} + \frac{W_a - W_w}{\rho g} \frac{\partial P_c}{\partial s} \\ &= \frac{\partial T}{\partial s} - (W_a - W_w) \cos \phi_3 \end{aligned} \quad (2.12)$$

Substituting (2.11) and (2.12) in (2.8) and (2.9) we obtain:

$$\frac{\partial T_e}{\partial s} = -DT + W_w \cos\phi_3 + \frac{W_a}{g} \ddot{Y_T} \quad (2.13)$$

and $T_e \frac{\partial v}{\partial s} = -\overline{DN} + W_w (\dot{i}_z - \hat{v} \cos\phi_3) +$

$$\left(\frac{2W_a - W_w}{g} \right) \ddot{\overline{YN}} \quad (2.14)$$

Equations (2.13) and (2.14) are derived for a line of an arbitrary stretched length and of consequent reduced diameter. Also we assume, as reasoned in GOODMAN and BRESLIN (1976) for materials obeying Hooke's law, that the effective tension and not the actual tension controls the extensibility of the mooring line. The extension of the mooring line is caused by (1) pulling on the line due to tension and (2) squeezing of the line due to hydrostatic pressure. Volume I (CHHABRA, 1973) plotted non-linear curves between tension and elongation of various mooring cables and ropes. Using the effective tension instead of the actual tension, mooring line stretch and the consequent reduced diameter from some initial reference state are found as discussed in Volume I.

The analysis also allows for an arbitrary number of intermediate bodies such as sensor packages and subsurface floats inserted in the mooring line. For this case equations (2.13) and (2.14) are replaced by:

$$\bar{T}_e|_{n+1} = \bar{T}_e|_n + \bar{F} \quad (2.15)$$

Here, \bar{F} is the summation of gravitational attraction, fluid, and inertia forces of the body inserted between n , the differential element above the body, and $n+1$, below it.

For cylindrical packages, the viscous drag representation remains similar to the one for cylindrical mooring line. For a spherical or any other shaped package this viscous drag force is computed as:

$$\bar{D}\bar{A} = \rho/2 C_{Db} A_{Db} |\bar{U}\bar{R}| \bar{U}\bar{R}$$

where; C_{Db} and A_{Db} are the appropriate drag coefficient and area.

The gravitational force and the hydrostatic pressure force are combined to give:

$$\bar{N}\bar{B} = - W_{wb} \hat{i}_z$$

where; w_{wb} is the weight in water of the inserted body.

Inertia forces for cylindrical packages are changed slightly from that of a continuous cylindrical mooring line. Here the assumption of the body motion accelerating water only in the direction normal to its longitudinal axis is dropped. Instead two added mass terms; one normal and the other tangential to the longitudinal axis are used. For cylindrical packages inertia force is given by:

$$\overline{IF}_b = - (m_b \ddot{\bar{Y}} + m_{nb} \ddot{\bar{Y}}_N + m_{tb} \ddot{\bar{Y}}_T)$$

and for any other shape this force is:

$$\overline{IF}_b = - (m_b + m_{ab}) \ddot{\bar{Y}}$$

Here; m_b is the mass, m_{nb} and m_{tb} are the normal and tangential components of added mass for cylindrical bodies, and m_{ab} is the added mass for any other shaped body.

Summation of gravitational attraction, inertia, and fluid forces gives \bar{F} . Integration of equations (2.10), (2.13), (2.14) and (2.15) along the spatial coordinate, s , of the mooring line gives the dynamic equilibrium of the

mooring system at discrete times. At any time these four equations can be solved for positions, $\bar{Y}(t)$, of the mooring system. Positions \bar{Y} are calculated at short enough time intervals, Δt_s , so that velocities $\dot{\bar{Y}}$ and accelerations $\ddot{\bar{Y}}$ during these time intervals can be computed as piecewise constant. Accelerations are neglected at t_0 and t_1 , velocities are neglected at t_0 .

2.2.2 Lumped Parameter Formulation

In this formulation, the mooring line is reduced to a discretized dynamic system which is solved by a lumped parameter approach. All forces acting on the mooring line and the inserted packages are transferred to a fixed number of nodes (say N). If each node has q degrees of freedom then $N \times q$ simultaneous differential equations, q for each node, describing these nodes can be solved simultaneously by using any of the numerical integration techniques. Once again the forces transferred at each node (lumped mass) are the same as listed in 2.2.1, with the exception of Froude-Krylov forces which are not neglected here. The forces for the n^{th} mass for a N node system are derived next.

Consider the discretized dynamic system as shown in Figure 2.6, where an N-mass system is shown. In this figure \hat{v}_n is a unit vector along the n^{th} segment

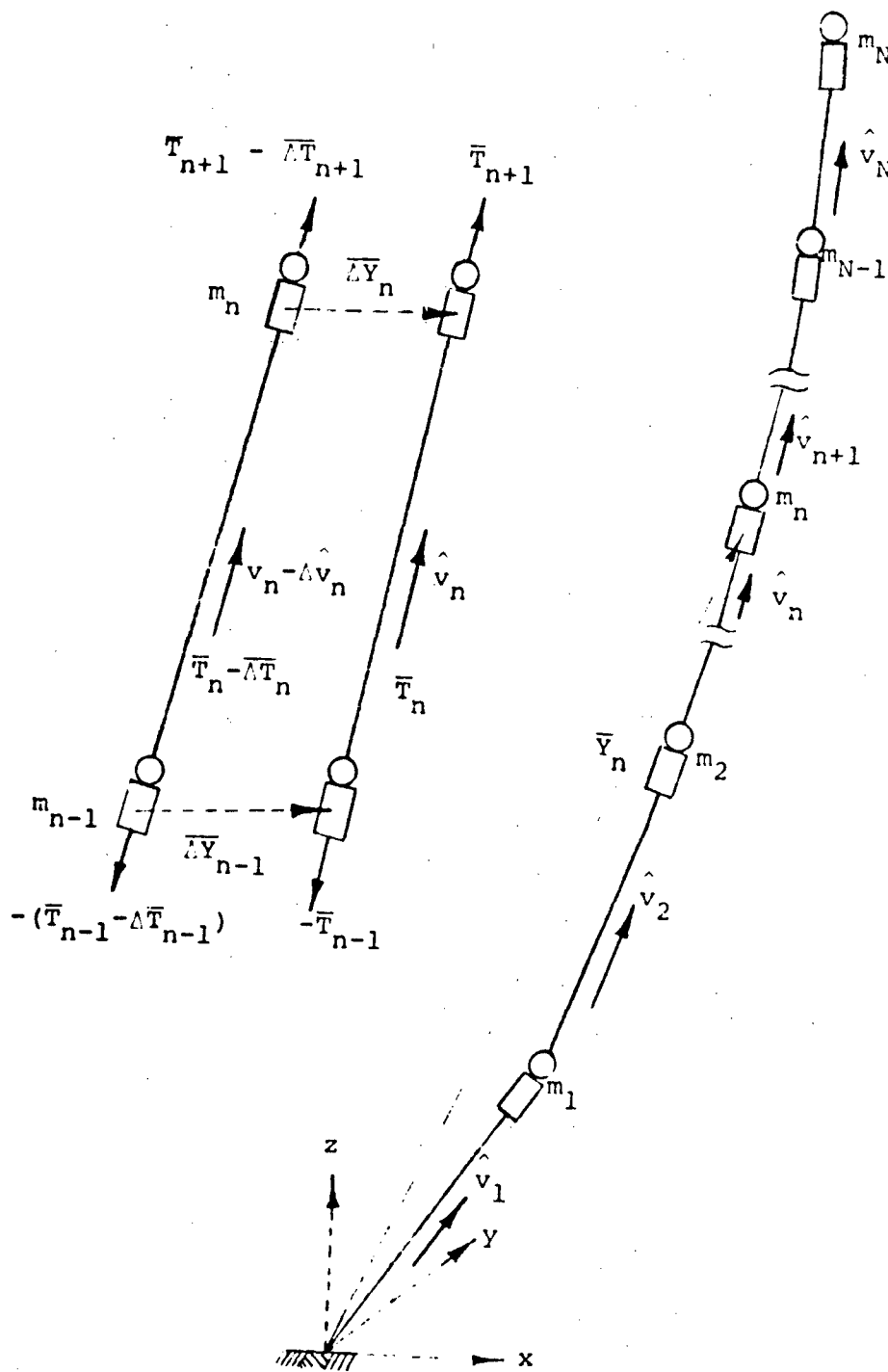


Figure 2.6 N-Mass System

(below the n^{th} mass). This can be written as:

$$\hat{v}_n = \hat{i}_x \cos\phi_{1n} + \hat{i}_y \cos\phi_{2n} + \hat{i}_z \cos\phi_{3n}$$

\bar{T}_n , \bar{T}_{n+1} are the tension vectors, and \bar{U}_n is the fluid velocity vector at the location of the n^{th} mass. A typical mass could consist of cylindrical components, spherical components, and any other shaped components. The transfer of all adjacent forces to a typical n^{th} mass is done as explained below.

Viscous drag forces acting on the mooring system have to be transferred at 'N' nodes. Any scheme devised for this transfer should take into account the different behavior of cylindrical and spherical components of the mooring system. Let $\bar{D}\bar{N}_n$ be the drag force transferred to n^{th} node which is equivalent to contribution of normal drag forces on cylindrical components lumped at the n^{th} node. Similarly, $\bar{D}\bar{T}_n$ is the drag force on n^{th} node equivalent to tangential drag forces on cylindrical components lumped at the n^{th} node. $\bar{D}\bar{A}_n$ is the drag force acting on the n^{th} node in the direction of the relative velocity $\bar{U}\bar{R}_n$, and is a contribution from spherical or any other shaped components lumped at the n^{th} node. These forces are given by :

$$\overline{DN}_n = (CDIN)_n |\overline{UNR}_n| \overline{UNR}_n$$

$$\overline{DT}_n = (CDIT)_n |\overline{UTR}_n| \overline{UTR}_n$$

$$\overline{DA}_n = (CDIA)_n |\overline{UR}_n| \overline{UR}_n$$

and $\overline{DF}_n = \overline{DN}_n + \overline{DT}_n + \overline{DA}_n$ (2.16)

Here; \overline{U}_n is computed from the current profile and the velocity of water due to surface waves at the location of the n^{th} mass which is exponentially attenuated with depth. CDIN, CDIT, and CDIA are the appropriate drag coefficients multiplied by respective areas.

The gravitational forces and the hydrostatic pressure forces are combined for all the transferred components to give:

$$\overline{NB}_n = - w_{wn} \hat{i}_z \quad (2.17)$$

Inertia forces for the components, in general, are given by:

$$\begin{aligned} \overline{IF}_n = & - (m_n + m_{an}) \ddot{\overline{Y}}_n - m_{nn} \ddot{\overline{YN}}_n \\ & - m_{tn} \ddot{\overline{YT}}_n \end{aligned} \quad (2.18)$$

This representation is similar to the one used for inserted bodies in the continuous line formulation.

The tensile forces acting on the n^{th} mass change in direction as well as magnitude with the motion of the nodes. The direction can be obtained by \bar{Y}_n and \bar{Y}_{n-1} (refer Figure 2.6); but as the present problem is one of large displacements the magnitude is determined at each integration step by updating its value at the beginning of the time step by the stiffness force due to the incremental deformation during this time step. Let the incremental change in length of the n^{th} segment ΔL_n be:

$$\Delta L_n = \bar{Y}_n - \bar{Y}_{n-1}$$

For small \bar{Y}_n and \bar{Y}_{n-1} :

$$\Delta L_n \approx \Delta L_n \cdot \hat{v}_n = \\ \left[-\cos\phi_{1n} - \cos\phi_{2n} - \cos\phi_{3n} \cos\phi_{1n} \cos\phi_{2n} \cos\phi_{3n} \right] \begin{Bmatrix} \bar{Y}_{n-1} \\ \bar{Y}_n \end{Bmatrix}$$

If k_n (stiffness coefficient) is defined as the force required at node n for a unit displacement along \hat{v}_n ; then the change in tension magnitude ΔT_n is:

$$\Delta T_n = k_n \Delta L_n$$

or; $\bar{T}_n = (T_n - \Delta T_n) \hat{v}_n + \Delta T_n \hat{v}_n$

Also, as tension vectors \bar{T}_n and \bar{T}_{n+1} are acting at the n^{th} mass, we have:

$$\bar{TF}_n = \bar{T}_{n+1} - \bar{T}_n \quad (2.19)$$

Froude-Krylov force on the submerged 'mass n' is assumed to be given by the product of mass of water displaced by the ' n^{th} mass' and the acceleration of water at that location which is exponentially attenuated with depth. Or,

$$\bar{FF}_n = m_{dn} g \xi_0 e^{|K| z_n} \left[\hat{i}_x K_x \cos(\bar{K} \cdot \bar{S} - \omega t) + \hat{i}_y K_y \cos(\bar{K} \cdot \bar{Z} - \omega t) + \hat{i}_z |K| \sin(\bar{K} \cdot \bar{S} - \omega t) \right] \quad (2.20)$$

where, m_{dn} is the mass of water displaced by the n^{th} mass.

Combining equations (2.16) through (2.20) for all nodes and taking into account all the boundary conditions, the force balance reduces in matrix notation to:

$$[\bar{M}] \ddot{\{Y\}} = \{\bar{DF}\} + \{\bar{CF}\} + \{\bar{TF}\} + [\bar{K}] \{\Delta Y\} + \{\bar{FF}\} \quad (2.21)$$

where; $[M]$ is a matrix of appropriate inertia terms.
 $[K]$ is a matrix of stiffness terms.
 $\{TF\}$ is an array of tension components at the nodes.
 $\{DF\}$ is an array of appropriate viscous drag terms.
 $\{CF\}$ is an array of constant nodal forces
 (gravitational and hydrostatic).
 $\{FF\}$ is an array of Froude-Krylov forces.
 $\{Y\}$ is an array of accelerations at the nodes.
and $\{\Delta Y\}$ is an array of incremental deformations of
 the nodes.

Derivation of Matrices: In equation (2.21), the order of each matrix and array is equal to the number of nodes (N) multiplied by degrees of freedom ($q = 3$) per node. For simplicity the masses were assumed to be lumped at ' N ' nodes, in which case the off-diagonal terms in the mass matrix are zero, i.e., force at node ' i ' due to an acceleration at node ' j ' equals zero. A consistent mass matrix analysis can be done to allow for distributed mass.

Mass Matrix - $[M]$:

$$[M] = \begin{bmatrix} M_1 & & & & & \\ & M_2 & & & & \\ & & M_3 & & & \\ & & & \ddots & & \\ & & & & M_n & \\ & & & & & \ddots \\ & & & & & & M_{N-1} \\ & & & & & & & M_N \end{bmatrix}$$

where; M_1, M_2, \dots, M_N are 3×3 matrices given by:

$$M_n = \begin{bmatrix} m_n + m_{an} + m_{nn} \sin^2 \phi_{1n} & (m_{tn} - m_{nn}) \cos \phi_{1n} \cos \phi_{2n} & (m_{tn} - m_{nn}) \cos \phi_{1n} \cos \phi_{3n} \\ (m_{tn} - m_{nn}) \cos \phi_{2n} \cos \phi_{1n} & m_n + m_{an} + m_{nn} \sin^2 \phi_{2n} & (m_{tn} - m_{nn}) \cos \phi_{2n} \cos \phi_{3n} \\ (m_{tn} - m_{nn}) \cos \phi_{3n} \cos \phi_{1n} & (m_{tn} - m_{nn}) \cos \phi_{3n} \cos \phi_{2n} & m_n + m_{an} + m_{nn} \sin^2 \phi_{3n} \end{bmatrix}$$

m_n = mass lumped at the n^{th} node.

m_{an} = added mass at n^{th} node due to non-cylindrical components

and m_{nn}, m_{tn} = Normal and tangential components of added mass at n^{th} node due to cylindrical components

Stiffness Matrix [K] - 4 Mass System

$$[K] = \begin{bmatrix} K^1 + K^2 & -K^2 & 0 & 0 \\ -K^2 & K^2 + K^3 & -K^3 & 0 \\ 0 & -K^3 & K^3 + K^4 & -K^4 \\ 0 & 0 & -K^4 & K^4 \end{bmatrix}$$

where; K^S are 3×3 matrices whose elements are given by

$$K_{ij}^S = k_s \cos_{i,s} \cos_{j,s}$$

k_s = Stiffness coefficient for segment s.

and $\cos_{i,s}$ = $\cos\phi_i$ of segment s.

{TF}, {DF}, {CF}, {FF}, {Y} and $\{\Delta Y\}$ are column matrices. These matrices can be written as

$$\{TF\} = \begin{Bmatrix} -(T_1 - \Delta T_1) \cos_{1,1} + (T_2 - \Delta T_2) \cos_{1,2} \\ -(T_1 - \Delta T_1) \cos_{2,1} + (T_2 - \Delta T_2) \cos_{2,2} \\ -(T_1 - \Delta T_1) \cos_{3,1} + (T_2 - \Delta T_2) \cos_{3,2} \\ \cdot \\ \cdot \\ -(T_{N-1} - \Delta T_{N-1}) \cos_{3,N-1} + (T_N - \Delta T_N) \cos_{3,N} \\ -(T_N - \Delta T_N) \cos_{1,N} \\ -(T_N - \Delta T_N) \cos_{2,N} \\ -(T_N - \Delta T_N) \cos_{3,N} \end{Bmatrix} \quad \{FF\} = \begin{Bmatrix} FF_{1,1} \\ FF_{2,1} \\ FF_{3,1} \\ \cdot \\ \cdot \\ \cdot \\ FF_{1,N} \\ FF_{2,N} \\ FF_{3,N} \end{Bmatrix}$$

$$\{DF\} = \begin{Bmatrix} DF_{1,1} \\ DF_{2,1} \\ DF_{3,1} \\ \cdot \\ \cdot \\ DF_{1,N} \\ DF_{2,N} \\ DF_{3,N} \end{Bmatrix}; \quad \{CF\} = \begin{Bmatrix} CF_{1,1} \\ CF_{2,1} \\ CF_{3,1} \\ \cdot \\ \cdot \\ CF_{1,N} \\ CF_{2,N} \\ CF_{3,N} \end{Bmatrix}; \quad \{\ddot{Y}\} = \begin{Bmatrix} \ddot{Y}_{1,1} \\ \ddot{Y}_{2,1} \\ \ddot{Y}_{3,1} \\ \cdot \\ \cdot \\ \ddot{Y}_{1,N} \\ \ddot{Y}_{2,N} \\ \ddot{Y}_{3,N} \end{Bmatrix}; \quad \{\Delta Y\} = \begin{Bmatrix} \Delta Y_{1,1} \\ \Delta Y_{2,1} \\ \Delta Y_{3,1} \\ \cdot \\ \cdot \\ \Delta Y_{1,N} \\ \Delta Y_{2,N} \\ \Delta Y_{3,N} \end{Bmatrix}$$

Equation (2.21) can be re-written as

$$\begin{aligned} \ddot{\{Y\}} &= [M]^{-1} \{TF\} + [M]^{-1} [K] \{\Delta Y\} + \\ &[M]^{-1} \{DF\} + [M]^{-1} \{FF\} + [M]^{-1} \{CF\} \end{aligned}$$

These $3N$ second-order differential equations can be reduced to a set of $6N$ first-order differential equations which can be solved by any of the numerical methods.

2.3

Attachment Between Surface Buoy and a Mooring Line

Figure 2.7 shows the attachment between a surface buoy and a mooring line. Let the attachment point be 'a', which is fixed rigidly to the buoy.

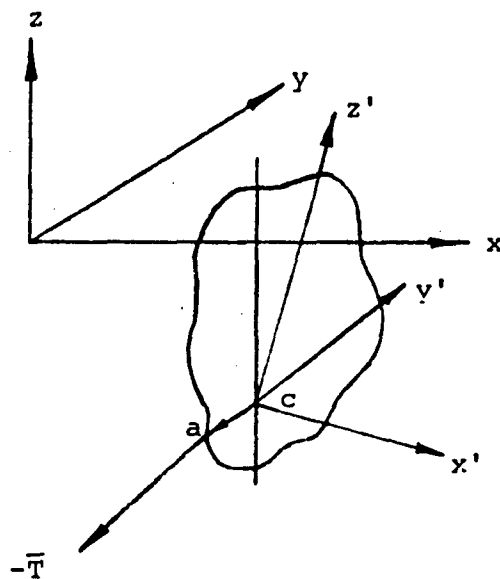


Figure 2.7 Attachment Between Surface Buoy and a Mooring Line

In addition to all the other forces acting on the surface buoy as outlined in Section 2.1; a tension vector \bar{T} is acting at point a, which should be included in the force balance.

$$\bar{T} = \hat{T}_v = \hat{T}_x i_x + \hat{T}_y i_y + \hat{T}_z i_z \quad (2.22)$$

also let vector \bar{R}_{ca} be given by:

$$\bar{R}_{ca} = \hat{i}_x' x_a' + \hat{i}_y' y_a' + \hat{i}_z' z_a'$$

Taking moment of \bar{T} about point c we obtain:

$$\bar{TM} = - \bar{R}_{ca} \times \bar{T} \quad (2.23)$$

for inclusion in the moment balance.

Two Dimensional Analysis:

$$\begin{aligned}\bar{R}_{ca} &= \hat{i}_x' x_a' + \hat{i}_z' z_a' \\ &= \hat{i}_x (x_a' \cos\theta + z_a' \sin\theta) + \hat{i}_z (z_a' \cos\theta - x_a' \sin\theta)\end{aligned}$$

and; $\bar{TM} = \hat{i}_y [T_z (x_a' \cos\theta + z_a' \sin\theta) - T_x (z_a' \cos\theta - x_a' \sin\theta)]$

Three Dimensional Analysis:

$$\begin{aligned}\bar{R}_{ca} &= \hat{i}_x (x_a' - \psi y_a' + \theta z_a') + \hat{i}_y (\psi x_a' + y_a' - \phi z_a') + \\ &\quad \hat{i}_z (-\theta x_a' + \phi y_a' + z_a')\end{aligned}$$

And; $\overline{T_M} = \hat{i}_x [T_y (-\theta x'_a + \phi y'_a + z'_a) - T_z (\psi x'_a + y'_a - \phi z'_a)] +$
 $\hat{i}_y [T_z (x'_a - \psi y'_a + \theta z'_a) - T_x (-\theta x'_a + \phi y'_a + z'_a)] +$
 $\hat{i}_z [T_x (\psi x'_a + y'_a - \phi z'_a) - T_y (x'_a - \psi y'_a + \theta z'_a)]$

Change in mooring line tension magnitude due to buoy rotation
(coefficients in the stiffness matrix).

Two Dimensional Analysis:

Rotate \bar{R}_{ca} through $\Delta\theta$ to obtain \bar{R}_{ca_1}

$$\bar{R}_{ca_1} = \begin{bmatrix} 1 & \Delta\theta \\ -\Delta\theta & 1 \end{bmatrix} \begin{bmatrix} \cos\theta & \sin\theta \\ -\sin\theta & \cos\theta \end{bmatrix} \begin{Bmatrix} x'_a \\ z'_a \end{Bmatrix}$$

For small rotations change in tension magnitude ΔT is given by

$$\Delta T = k(\bar{R}_{ca_1} - \bar{R}_{ca}) \cdot \hat{v}$$

where k is the stiffness coefficient for the line segment attached to the surface buoy.

If $\hat{v} = \hat{i}_x \cos\phi + \hat{i}_z \sin\phi$

$$\Delta T = k[\cos\phi(z'_a \cos\theta - x'_a \sin\theta) + \sin\phi(-z'_a \sin\theta - x'_a \cos\theta)]\Delta\theta$$

Three Dimensional Analysis:

$$\bar{R}_{ca_1} = \begin{bmatrix} 1 & -\Delta\psi & \Delta\theta \\ \Delta\psi & 1 & -\Delta\phi \\ -\Delta\theta & \Delta\phi & 1 \end{bmatrix} \begin{bmatrix} 1 & -\psi & \theta \\ \psi & 1 & -\alpha \\ -\theta & \alpha & 1 \end{bmatrix} \begin{Bmatrix} x'_a \\ y'_a \\ z'_a \end{Bmatrix}$$

and;

$$\Delta T = k \begin{bmatrix} \cos \phi_2 (\theta x'_a - y'_a - z'_a) & \cos \phi_1 (-\alpha x'_a + \psi y'_a + z'_a) & \cos \phi_1 (-\psi x'_a - y'_a + \alpha z'_a) \\ + \cos \phi_3 (\psi x'_a + y'_a - \phi z'_a) & + \cos \phi_3 (-x'_a + \psi y'_a - \theta z'_a) & + \cos \phi_2 (x'_a - \psi y'_a + \theta z'_a) \end{bmatrix} \cdot \begin{Bmatrix} \Delta\alpha \\ \Delta\psi \\ \Delta\theta \end{Bmatrix}$$

If more than one mooring lines are attached to the surface buoy, as is the case of simulation study in Section 5.3, force and moment of both these lines are to be included in the appropriate equations. It is important to note that within the definition of the coordinate frame (fixed at the anchor) if a mooring line hangs from the buoy (as is the case in 5.3), $-\bar{T}$ of this section would be replaced by $+\bar{T}$. Also in this case ΔT would be given by

$$\Delta T = -k(\bar{R}_{ca_1} - \hat{\bar{R}}_{ca}) \cdot \hat{v}$$

2.4 Window Shade Drogue

Sometimes an alternative approach to mooring surface buoys is the use of surface trackable drogued drifting buoys. Such a buoy system employs a high drag device (or drogue) tethered to a trackable buoy at the surface. A drogue is subjected to the same forces (including the wave effects) as a differential element of the mooring line. A special case of drogues, the window shade drogue, as shown in Figure 2.3 is considered in this analysis. The drogue, modeled dynamically as a lumped parameter system (Figure 2.8), is reduced to strips. The mass, the acting forces, and the dynamic behavior of each strip is lumped at an assigned nodal point. Nodal masses are linked by suitably elastic lines.

The window shade drogue is a compliant sheet. Close observation of scale model drogues (Vachon, 1973) has revealed that it seems nearly locked to the local water mass insofar as motion normal to the sheet is concerned. However, in the tangential direction, it seems to slip through the local water mass rather easily. The forces were therefore described as follows: the wave forces (Froude-Krylov force; as it is assumed that there is no diffracted wave) acting on a material strip are estimated by calculating the force normal to the axis

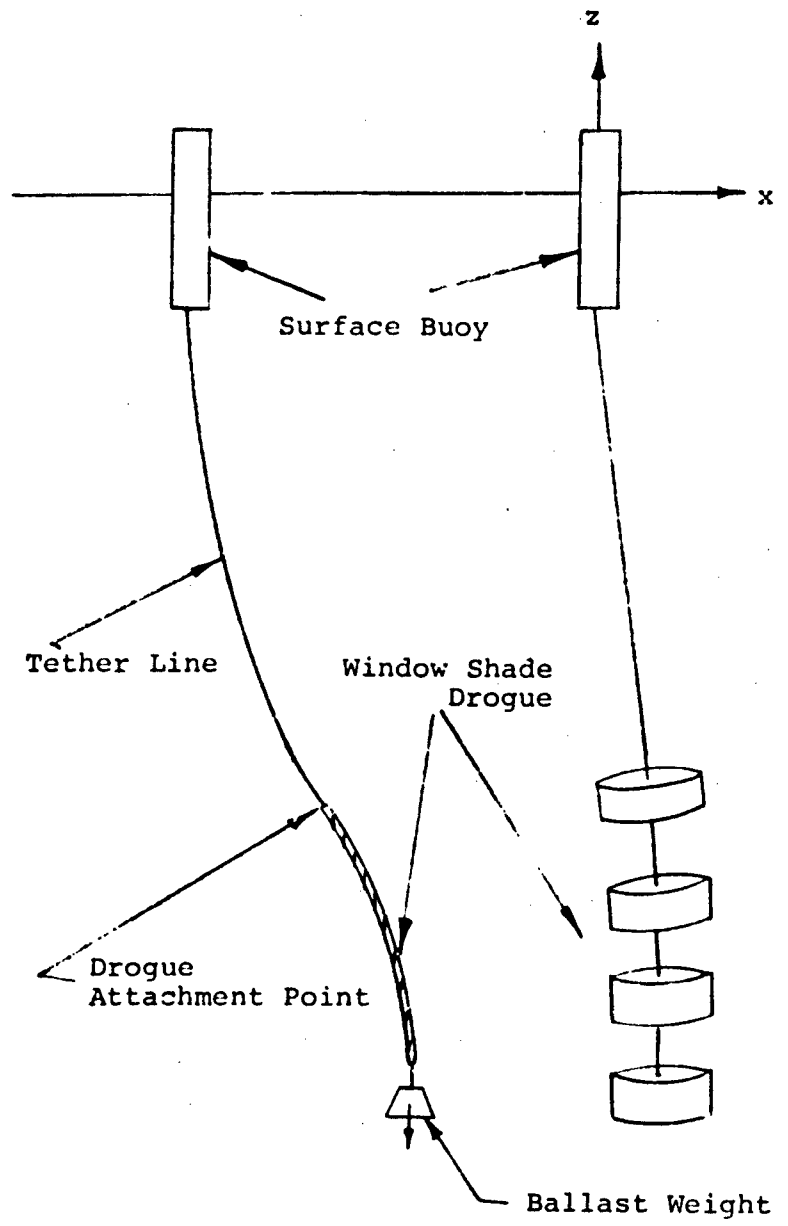


Figure 2.8 Drifting Drogued Buoy System

of revolution of a hypothetical cylindrical element, the diameter and length of which is equal to the breadth and length of the strip respectively. This force is given by the mass of the hypothetical water cylinder multiplied by the component of water acceleration normal to the cylinder's longitudinal axis. Or;

$$\overline{FF}_n = m_{dn} \cdot [\bar{A}_{Ew} - (\bar{A}_{Ew} \cdot \hat{v}_n) \hat{v}_n] \quad (2.24)$$

where w is the particle of water next to the n^{th} node, and m_{dn} is the mass of the hypothetical water cylinder. For inertia forces m_{an} and m_{tn} equal zero; whereas m_{nn} equals m_{dn} . The viscous drag of this strip in the normal direction is calculated using the frontal area of the strip and the drag coefficient measured in water-filled quarry tests (Vachon, 1975). The elemental strips of the drogue are assumed subject to tangential viscous drag calculated using the area of the strip and a tangential drag coefficient measured during drop tests in the ocean (Vachon, 1975).

Gravitational, hydrostatic pressure, and tensile forces on a drogue strip are similar to the ones outlined in Section 2.2 for a discretized dynamic system.

3.0 METHOD OF SOLUTION

Section 2 outlined all the necessary ingredients of the mathematical models used in this report. In this section some details of how to use these ingredients, to obtain a solution for a specific problem on hand, are given. For illustrative purposes a specific case study, of a spar buoy at the surface and a mooring line connecting this buoy with the anchor, will be discussed. Method of solution for both the two-dimensional and the three-dimensional analysis of the moored system will be outlined in

3.1. Section 3.2 outlines the approximate initial conditions for the steady state analysis of a spar buoy freely floating in a surface wave.

Another case study of a spar buoy at the surface and connected to a window shade drogue at a given depth is discussed in section 3.3.

3.1 Moored System Analysis

Two-Dimensional:

In this case, the current profile is in the same plane as the train of surface gravity waves having a single frequency and amplitude; and its direction parallel or anti-parallel to the direction of surface wave propagation.

Static Solution:

For the static solution, the analysis is started at the spar buoy. The pertinent static equations for the spar buoy (Section 2.1) with an attached mooring line (Section 2.3) are:

$$DF_x - T_x = 0 \quad (3.1)$$

$$P_o g - Mg + DF_z - T_z = 0 \quad (3.2)$$

and
$$-P_1 g \sin\theta + DM + T_z (x'_a \cos\theta + z'_a \sin\theta) - T_x (z'_a \cos\theta - x'_a \sin\theta) = 0 \quad (3.3)$$

Here; we have three equations and four (T_x , T_z , θ , h_s) unknowns, where h_s is the static draft of the spar buoy. Now if we assume a value for h_s , the other three unknowns can be solved by equations (3.1) through (3.3). The solution for the three unknowns T_x , T_z , and θ is found by iterating on the pitch angle θ . If θ is known; DF_x , DF_z , and DM can be computed explicitly. P_o and P_1 can be calculated if h_s is known and thus T_x and T_z are given by equations (3.1) and (3.2) respectively. Moment balance can now be performed by using equation (3.3)

to obtain the error. This error is minimized by iterating on the pitch angle θ .

Having solved the buoy force and moment balances for a assumed h_s the mooring line can be analyzed next.

For the continuous line formulation, a numerical integration is carried down the mooring line by dividing it into a finite number of segments. In this representation equations (2.13), (2.14), and (2.10) for two-dimensions can be written as:

$$\Delta T_e = (-DT + W_w \sin\phi) \Delta S \quad (3.4)$$

$$T_e \Delta \phi = [DN + W_w \cos\phi] \Delta S \quad (3.5)$$

and $\Delta Y = \hat{i}_x \Delta S \cos\phi + \hat{i}_z \Delta S \sin\phi \quad (3.6)$

Having found T_x and T_z (or T and ϕ) at the top of the mooring line equations (3.4) through (3.6) are used to find the configuration and the tension distribution along the mooring line. At the end of the mooring line the boundary condition of the ocean floor depth should be met. If not, the whole process is repeated with a new h_s ; thus computing the correct value of h_s for the given boundary condition. Whenever the mooring line is

discontinued to insert an intermediate body, the discontinuity is taken as a lumped mass and resolved as done below for the lumped parameter approach.

For the lumped parameter formulation, the configuration and the tension distribution along the mooring line can be found by (Section 2.2):

$$\bar{T}_n = \bar{T}_{n+1} - W_{wn} \hat{i}_z + \bar{DF}_n \quad (3.7)$$

where; \bar{T}_n is the tension vector below the n^{th} mass and \bar{T}_{n+1} above it.

Dynamic Solution:

Equations of Section 2.2 which are written for three-dimensional analysis can be easily reduced for the two dimensional problem. Using the lumped parameter approach for the mooring line; equations (2.21) are combined with equations (2.3), (2.22), and (2.23) to obtain a global matrix equation for the mooring/buoy system. Stiffness coefficients for the change in mooring line tension magnitude due to buoy rotation are obtained from Section 2.3. This matrix equation can be solved in the time domain using various numerical integration techniques. Integrals of P_i and Q_i , given in Section 2.1,

are computed exactly; whereas the integrals for viscous drag forces and moments DF_x , DF_z , and DM are computed numerically by dividing the spar buoy in disks of height dz' . The composit matrices are of order $2N + 3$. Matrices $[M]$, $\{TF\}$, $\{K\}$, $\{DF\}$, $\{FF\}$, $\{FD\}$, $\{FG\}$, and $\{FA\}$ are computed at each time step of the integration.

For the continuous line formulation; the matrices of equation (2.3) combined with equations (2.22) and (2.23) can be solved for \bar{T} in equation (2.22) if the buoy draft h_o is known. Then integration of equations (2.13), (2.14), (2.10), and (2.15) along the spatial coordinate, s , of the mooring line gives the dynamic equilibrium of the mooring system at discrete times. Iteration on the unknown h_o may be necessary to meet the boundary condition of the ocean floor depth.

Three Dimensional:

Here; the train of surface gravity waves having a single frequency and amplitude, can propagate in a general direction. The current profile is also three-dimensional and can vary, in magnitude and direction, with depth.

Static Solution:

The pertinent static equations for the spar buoy (Section 2.1) with an attached mooring line (Section 2.3) are:

$$-\int dB\bar{g} + \int dM\bar{g} + \bar{DF} - \bar{T} = 0 \quad (3.8)$$

and; $-\int dB(\bar{R}_{cp} \times \bar{g}) + \bar{DM} + \bar{TM} = 0 \quad (3.9)$

Integrations for dB are over the static draft of the buoy, and integration for DM is over the length of the buoy.

Equations (3.8) and (3.9) can be written as:

$$P_0 g \hat{i}_z - Mg \hat{i}_z + \bar{DF} - \bar{T} = 0 \quad (3.10)$$

and $\begin{Bmatrix} \phi \\ \theta \\ \psi \end{Bmatrix} = [S]^{-1} \{F\} \quad (3.11)$

where; $[S]$ is a 3×3 matrix with components given by:

$$S_{11} = P_0 g \ell_1 + DF_z \ell_2 - T_y y'_a - T_z z'_a$$

$$S_{12} = T_y x'_a ; \quad S_{13} = T_z x'_a$$

$$S_{21} = T_x y'_a ; \quad S_{23} = T_z y'_a$$

$$S_{22} = P_o g \ell_1 + DF_z \ell_2 - T_x x'_a - T_z z'_a$$

$$S_{31} = - DF_x \ell_2 + T_x z'_a$$

$$S_{32} = - DF_y \ell_2 + T_y z'_a$$

$$S_{33} = - T_x x'_a - T_y y'_a$$

and $\{F\}$ is a 3×1 array

$$F_1 = - DF_y \ell_2 + T_y z'_a - T_z y'_a$$

$$F_2 = DF_x \ell_2 - T_x z'_a + T_z x'_a$$

$$F_3 = T_x y'_a - T_y x'_a$$

also $P_o = \begin{cases} dB; & \text{and } \ell_1, \ell_2 \text{ are the distances between} \\ & \text{center of gravity and center of buoyancy and center of} \end{cases}$

drag respectively. For the static case we also assume (small angles):

$$DF_x \propto |V_{Bwx}| V_{Bwx}$$

$$DF_y \propto |V_{Bwy}| V_{Bwy}$$

and $DF_z \propto |V_{Bwz}| V_{Bwz}$

$\therefore \bar{T}$ and ϕ , θ , and ψ can be solved explicitly from equations (3.10) and (3.11) if h_s is known. h_s is determined by iteration on the boundary condition of the ocean floor depth.

Mooring line solution is similar to the one presented for the two-dimensional analysis.

Dynamic Solution:

This dynamic solution is similar to the one for two-dimensional analysis except that the order of matrices in this case is $3N + 6$.

3.2 Initial Conditions for the Steady-State Analysis of a Spar Buoy

Two-Dimensional Analysis:

Let $C_N = 1.0$, $C_T = 0.0$, and $x_C = 0.0$. Also assuming small pitch of the buoy and neglecting viscous

drag forces, the equations of motion for a spar buoy become:

$$2M\ddot{x}_c + P_1\ddot{\theta} = 2\omega^2\xi_o Q_o \cos\omega t \quad (3.12)$$

$$\begin{aligned} M^*\ddot{z}_c + \rho S_{o2} g z &= -\omega^2 \xi_o Q_o \sin\omega t \\ &+ \rho S_{o2} g \xi_o \sin\omega t \end{aligned} \quad (3.13)$$

and $P_1\ddot{x}_c + (I_{yy} + P_2)\ddot{\theta} + P_1 g \theta = 2\omega^2 \xi_o Q_1 \cos\omega t \quad (3.14)$

where, $M^* = M + 4/3 \rho [r_1^3 + (r_1 - r_2)^3]$

Surge Equation 3.12:

Let $P_1\ddot{\theta} \ll 2M\ddot{x}_c$ and $x = C_1 \sin\omega t + C_2 \cos\omega t + C_3$.

Now differentiating x twice and substituting in (3.12) we obtain

$$x = -\xi_o Q_o \cos\omega t / M + C_3$$

and $\dot{x} = \omega \xi_o Q_o \sin\omega t / M + C_3 t$

Hence $\dot{x}(0) = 0$

and $x(0) = -\xi_o Q_o / M$

Heave equation (3.13)

Let $z = C_1 \sin \omega t + C_2 \cos \omega t + C_3$

Differentiating twice and substituting in equation (3.13) we obtain:

$$C_2 = C_3 = 0$$

and $C_1 = \xi_o (\rho s_{o2} g - \omega^2 Q_o) / (\rho s_{o2} g - M^* \omega^2)$

Hence, $z(0) = 0$

$$\dot{z}(0) = \omega C_1$$

Pitch Equation 3.14:

Substituting \ddot{x}_c from equation (3.12) into equation (3.14) we obtain:

$$\ddot{A}\theta + B\theta = C \cos \omega t \quad (3.15)$$

where, $A = (I_{yy} + P_2 - P_1^2/2M)$

$$B = P_1 g$$

and $C = (2\omega^2 \xi_0 Q_1 - P_1 \omega^2 \xi_0 Q_0 / M)$

Now let $\theta = C_1 \sin \omega t + C_2 \cos \omega t + C_3$

Differentiating θ twice and substituting in equation
(3.15) gives:

$C_1 = C_3 = 0$

and $C_2 = C / (B - A\omega^2)$

Or, $\theta = \frac{C}{B - A\omega^2} \cos \omega t$

Hence,

$$\theta(0) = \frac{\omega^2 \xi_0 (2Q_1 - P_1 Q_0 / M)}{P_1 g - \omega^2 (I_{yy} + P_2^2 - P_1^2 / 2M)}$$

and $\dot{\theta}(0) = 0$

Three Dimensional Analysis:

Similarly; for the three dimensional case with
wave direction at an angle β with the x-axis we have:

$$x(o) = - \xi_o \cos\beta Q_o/M$$

$$y(o) = - \xi_o \sin\beta Q_o/M$$

$$z(o) = 0.$$

$$\dot{x}(o) = \dot{y}(o) = 0$$

$$\dot{z}(o) = \frac{\omega \xi_o (\rho S_o 2g - \omega^2 Q_o)}{\rho S_o 2g - M * \omega^2}$$

$$\phi(o) = - \frac{\omega^2 \xi_o \sin\beta (2Q_1 - P_1 Q_o/M)}{P_1 g - \omega^2 (I_{yy} + P_2 - P_1^2 / 2M)}$$

$$\theta(o) = \frac{\omega^2 \xi_o \cos\beta (2Q_1 - P_1 Q_o/M)}{P_1 g - \omega^2 (I_{yy} + P_2 - P_1^2 / 2M)}$$

$$\psi(o) = 0$$

$$\dot{\phi}(o) = \dot{\theta}(o) = \dot{\psi}(o) = 0.$$

3.3 Drifting Drogued Spar Buoy

In this analysis the drogue and the mooring line connecting it to the spar buoy are modeled dynamically as a lumped parameter system.

Two-Dimensional Analysis

Static Solution:

The pertinent static equations for the spar buoy
(Section 2.1) with an attached mooring line (Section 2.3)
are:

$$DF_x + T_x = 0 \quad (3.16)$$

$$P_0 g - Mg + DF_z + T_z = 0 \quad (3.17)$$

and $-P_1 g \sin\theta + DM - T_z (x'_a \cos\theta + z'_a \sin\theta)$

$$+ T_x (z'_a \cos\theta - x'_a \sin\theta) = 0 \quad (3.18)$$

Here; we have three equations and five (v_s , h_s , T_x , T_z , θ) unknowns where v_s is the static velocity of the drogued drifting system. These equations are solved by iterating on v_s and θ . Assuming a value for v_s , T_x and T_z can be calculated by known weights, buoyancies, viscous drag forces, and elastic characteristics of the system beneath the spar. Now if a value for θ is assumed equation (3.17) is solved for h_s and the error in equation (3.18) is found. This error is minimized by iterations on θ . Next v_s is iterated upon to satisfy equation (3.16).

Dynamic Solution

This solution is similar to the lumped parameter solution discussed in Section 3.1.

Three Dimensional Analysis

Static Solution:

Here the pertinent equations (static) remain the same as Section 3.1 except for replacing $-\bar{T}$ by $+\bar{T}$ and $+ \bar{TM}$ by $-\bar{TM}$.

Also; following similar reasoning of small angles \bar{T} , ϕ , θ , and ψ can be solved explicitly from equations (3.10) and (3.11) with new \bar{T} and \bar{TM} if V_s is known. V_s is determined by iteration on the equation similar to (3.10).

Dynamic Solution

This solution is similar to the one in Section 3.1 .

4.0 COMPUTER PROGRAM DETAILS

This section will describe the various computer programs written for the theoretical analysis presented in Section 2 and using solution methods of Section 3.

Description of the programs is general and specific details can be found in the program listings presented in Appendix A. All computer programs are written in FORTRAN IV and have been run for many case studies on the CSDL AMDAHL 470 V6 computer. Input data required for these programs is also explained in this section. Some of the simulations, along with the accompanying input data, are presented in Section 5.

Computer programs written for the surface moored and drifting systems are tabulated in Table 4.1. Programs for subsurface moored systems are tabulated in Table 4.2. Program listings for some of these computer programs are presented in Appendix A. Listings not presented are duplications of what is presented and can be obtained after minor modifications.

4.1 Surface Moored/Drifting Systems

Computer program SD3.FORT is coded for the three-dimensional analysis of surface moored and drifting systems presented in Section 2. Four case studies can be simulated by this program:

1. A freely floating spar buoy.

FILE NAME	MOORING SYSTEM	DEGREES OF FREEDOM	PHYSICAL FORCES	INPUT ENVIRONMENT (Forcing Function)
SD3.FORT	Cylindrical spar buoy analysis. Tuned spar buoy analysis. Cylindrical or tuned spar buoy anchored by a mooring line. Cylindrical or tuned spar buoy anchored by a mooring line and an instrument line hanging from the buoy. Drifting drogue? buoy (cylindrical or tuned spar) analysis.	Surface buoy-six Mooring line-three	All applicable forces of Section 2.	Surface wave and constant absolute current profile.
SD2.FORT	Same as above	Surface buoy-three Mooring line-two	All applicable forces of Section 2.	Surface wave and constant absolute current profile.
BUOY.FORT	Cylindrical spar buoy analysis. Tuned spar buoy analysis.	Buoy-six	All applicable forces of Section 2.	Surface wave and constant absolute current profile.
MDE.FORT	Cylindrical or tuned spar buoy anchored by a mooring line and an instrument line hanging from the buoy.	Surface buoy-six Mooring line-three	All applicable forces of Section 2.	Surface wave and constant absolute current profile.
DDB.FORT	Drifting drogued buoy analysis (cylindrical or tuned spar)	Surface buoy-six Mooring line-three	All applicable forces of Section 2.	Surface wave and constant absolute current profile.

TABLE 4.1 Programs for Surface Moored/Drifting Systems

FILE NAME	MOORING SYSTEM	DEGREES OF FREEDOM	PHYSICAL FORCES	INPUT ENVIRONMENT (forcing function)
SSD3.FORT	Subsurface moored system.	Three	All applicable forces from Section 2.	Time varying relative current profile.
SSD31.FORT	Subsurface moored system.	Three	All applicable forces from Section 2.	Time varying absolute current profile.
SSS3.FORT	Subsurface moored system.	Three	All applicable forces from Section 2 except inertia forces.	Time varying relative current profile.

TABLE 4.2 Programs for Subsurface Moored Systems

2. A spar buoy anchored with a lumped parameter mooring line.
3. A spar buoy anchored with a lumped parameter mooring line and a lumped parameter mooring line hanging from the buoy.
4. A spar buoy attached to a window shade drogue.

SD2.FORT does the same simulations as SD3.FORT, but is coded for the two dimensional analysis of Section 2. Computer programs BUOY.FORT, MDE.FORT, and DDB.FORT are subsets of the computer program SD3.FORT. BUOY.FORT simulates case study 1, MDE.FORT simulates case study 3, and DDB.FORT simulates case study 4. All these programs use the lumped parameter formulation for the mooring line. Input data necessary for these programs is outlined below.

Input Data Required for Computer Program
SD3.FORT (All units in F.P.S.)

General data:

NM: Number of nodes (masses). Equals one for case study 1.

NB: Number of the surface buoy. Starting from the anchor, the number of the node (anchor is not counted as a node) where

the buoy is located. NM = NB for case study 3. NB equals one for case studies 1 and 4.

ND: Number of the first node on the drogue.

NST: Number of steps. This is used for dividing the spar buoy in NST strips for integration of viscous drag forces and moments over the entire submerged buoy.

NC: Number of cycles, i.e. number of surface waves for which the simulations are to be done.

MOOR: Index for case study control. Equals zero for case study 1; one for case studies 2 and 3, and two for case study 4.

DEPTH: Ocean depth.

DT: Integration time step ΔT .

TMAX: Maximum time of simulation.

T2: Time interval for simulation printout.

Buoy Data:

RD1, RD2: Two radii (r_1 and r_2) of the tuned spar buoy. RD1 is for the drum and equals RD2 for a cylindrical spar.

ZCG: Distance ($Z_C > 0$) between centroid of the spar base and its C.G.

RGYR: Radius of gyration of the buoy about any axis in the horizontal plane.

HMAX: Length of the spar buoy (H).

CDL: Normal viscous drag coefficient (C_{DN}) used for the spar. πC_{DT} is found by multiplying CDLx0.02

HST: Length of the drum for the tuned spar buoy (h_1). For cylindrical spar HST is some arbitrary number between zero and the submerged depth of the spar.

CON: Added mass coefficient (C_N) for the buoy. (Used & read in SD2.FORT only).

COT: Added mass coefficient (C_T) for the buoy. (Used & read in SD2.FORT only).

CDP: Viscous drag coefficient for the base and step of the tuned spar (C_{DP}).

ALPHA: Added mass coefficient for the base and step of the tuned spar (α).

Mooring Line Data:

W(I): Weight in water (ω_{wi}) of components lumped at the Ith node. Equals weight in air for the buoy (NBth node)

- CM(I): Mass of components lumped at the I^{th} node (m_i).
- CMS(I): Added mass of spherical components lumped at the I^{th} node (m_{ai}).
- CMD(I): Mass of water displaced by components lumped at the I^{th} node (m_{di}).
- CMN(I),
CMT(I): Normal and tangential components of added mass of cylindrical components lumped at the I^{th} node (m_{ni} and m_{ti}).
- SL(I): Slack length of the mooring line proceeding the I^{th} node (L_i).
- EK(I): Elastic coefficient for SL(I) (k_i).
- CDIN(I),
CDIT(I): Normal and tangential viscous drag constants ($1/2 \rho C_D A_D$) of cylindrical components lumped at the I^{th} node.
- CDIA(I): Viscous drag constant of non-cylindrical components lumped at the I^{th} node.
- DEP(I): Depth (less than zero) of the I^{th} node (approximate) (z_i).

Attachment Data:

XC1,YC1, Coordinates of the attachment point
SC1: between spar and the anchoring line
in spar buoy coordinate frame (x' ,
 y' , z').

XC2,YC2, Coordinates of the attachment point
ZC2: between the spar and the instrument
line in x' , y' , z' frame.

Current Profile Data:

V(IJ,I): Absolute velocity of water in J^{th}
(x , y , and z) direction at the depth
of I^{th} node.

Surface Wave Data:

WE: Frequency (ω) of the surface wave.
AMP: Amplitude (ξ_0) of the surface wave.
BETA: Wave direction (β).

All of the input data are read in the main program. The main program calls subroutines: (a) STATIC; which calculates the mean configuration or steady state (static) solution without any surface wave forcing. (b) BUOYS; which calculates the mass matrix [M] for the spar buoy. (c) DBDRG, which calculates the viscous drag

forces/moment on the spar buoy. (d) MINVER, which inverts a matrix. (e) MATRIX, which calculates the wave exciting plus hydrostatic forces on the spar buoy, the stiffness matrix [K], the remaining mass matrix for the mooring lines, viscous drag forces on the mooring lines, Froude Krylov forces on the mooring lines, and the tension force components at each node. It also integrates the differential equations of motion. (f) NEXT, which updates the geometry of the system.

Before finding the steady state dynamic response of a system to a sinusoidal surface wave, an equivalent current profile has to be determined to compute the mean configuration of the system. This current profile depends on the original current profile plus the contribution due to the surface wave. In effect it is a rectification of the time constant current profile by the oscillatory velocity field generated by the surface wave. From Section 2.1 we have:

$$\bar{v}_{EW} = \hat{i}_x (v_{ox} + \phi_x) + \hat{i}_y (v_{oy} + \phi_y) \\ + \hat{i}_z (v_{oz} + \phi_z)$$

also; $|\bar{v}_{EW}|^2 = (v_{ox} + \phi_x)^2 + (v_{oy} + \phi_y)^2 + (v_{oz} + \phi_z)^2$

And as viscous drag forces determine the moored or drifting system configurations for the static solution, and these are proportional to $|\bar{V}_{EW}| \bar{V}_{EW}$, the square root of mean ($|\bar{V}_{EW}| \bar{V}_{EW}$) over a wave period (T) would give the equivalent rectified current vector at this location.

Let; $\bar{E} = \frac{1}{\omega T} \int_0^{\omega T} |\bar{V}_{EW}| (\bar{V}_{EW}) d(\omega t)$
 $= \hat{i}_x E_x + \hat{i}_y E_y + \hat{i}_z E_z$

Now the equivalent current vector can be written as:

$$\bar{V}_{eq} = \bar{E}/EE$$

where: $EE = \sqrt{|\bar{E}|}$

This calculation to find \bar{V}_{eq} , before a static solution is performed, is done in the main program. The numerical integration of differential equations in the subroutine MATRIX was performed by the rectangular rule, which was found adequate for all case studies simulated.

4.2 Subsurface Moored Systems

Computer program SSD3.FORT is coded for the three dimensional analysis of subsurface moored systems

(continuous line formulation) given in Section 2. The program simulates the response of a subsurface moored system to the time varying current fields. SSD3.FORT reads in the relative (relative to the mooring system) velocity profile in the three orthogonal x, y, and z directions. From these three components the viscous drag forces can be computed directly. These components of the relative velocity could be the ones measured by current sensors on the mooring line. Alternatively, SSD31.FORT reads in the absolute (relative to the mean floor) velocity profile in the three orthogonal (x, y, and z) directions. Profile is read in as amplitudes of the sinusoidally varying currents. All components (varying with depth) are driven by a single frequency. In addition a surface wave of given amplitude, frequency, and direction generates velocity field exponentially attenuated in depth. The program computes the total absolute velocity and then subtracts the mooring line velocity from this absolute velocity to compute the viscous drag forces. SSS3.FORT is the same as SSD3.FORT but it neglects all inertia forces of the mooring system. All three programs use the continuous line formulation of the mooring line, given in Section 2, as the mathematical model. Input data, except

for the input forcing function (velocity profiles and surface wave) are the same for all three programs and are detailed below:

General Data:

- NI: Number of intermediate bodies
(instrument clusters or inserted floats) to be included in the analysis.
- NP: Number of mooring parts (each mooring part can have different properties).
- NS: Number of segments the continuous line is to be divided in.
- NPT: Number of dynamic equilibriumsto be performed.
- IKK: Number of locations the velocity profile changes along the ocean depth.
- DEPTH: Depth of the ocean. (Meters)
- DDT: Approximate depth of the mooring line top. (Meters)
- ER: Used for iteration on the boundary condition of ocean depth. If DDT is known with reasonable accuracy, ER is not required. (Meters)
- ER1: Used for error control in SSD31.FORT.

Instrument Data:

PI(J) Position of the Jth instrument in slack length distance from the top. (Meters)

SI(J): Length of the Jth instrument. Equals zero for non-cylindrical instruments. (Meters)

ZM(J): Mass of the Jth instrument (m_j). (Slugs)

ZMC(J): Normal added mass component (m_{nj}) for cylindrical instruments. (Slugs)

ZMV(J): Added mass (m_{aj}) of the Jth instrument for a non-cylindrical instrument. Tangential added mass component (m_{tj}) for cylindrical instruments. (Slugs)

F(3,J): Weight in water (w_{wj}) of the Jth instrument. (Pounds)

CDIN(J), CDIT(J): Normal and tangential viscous drag constants ($1/2 \rho C_D A_D$) of the instruments. CDIT is not used for spherical instruments. (F.P.S. units)

Mooring Line Data:

DIAL(I): Nominal diameter of the Ith mooring part. (Inches)

SLL(I): Slack length of the Ith mooring part. (Meters)

AWL(I): Weight in air per unit slack length of the Ith mooring part (w_a). (lbs/M)

WWL(I): Weight in water per unit slack length of the Ith mooring part (w_w). (lbs/M)

TPL(I): Transient peak load on the Ith mooring part. For materials which obey Hook's law this is substituted with the Young's modulus of elasticity. (Refer volume 1 CHHABRA, 1973). (lbs. or lbs/in²)

CO1(I), CO2(I),
PO1(I), PO2(I),
AO(I): Constants for stress-strain relationships of mooring line materials. (CHHABRA, 1973). CO1 is used for jacket diameter (in.) in jacketed wire rope.

CDN(I), CDT(I): Normal and tangential drag coefficients of the Ith mooring part. (C_{DN} and C_{DT})

Current Profile Data:

D(I): Depths, greater than zero, where the current changes direction. I goes from 1 to IKK. (Meters)

V(I,J): For SSD3.FORT: Relative velocity in the Ith (x, y, and z) direction for the Jth zone. J goes from 1 to IKK + 1.
(mm/sec)

For SSD31.FORT: Absolute velocity amplitude in the I^{th} direction for the J^{th} zone. Following data are used only in SSD31.FORT.

WE: Frequency of current profile amplitudes $V(I,J)$. (Rad/sec)
DT: Time step for calculation of the mooring system dynamic equilibrium.
T2: Time step for simulation output.
TMAX: Maximum time for simulation.
WS: Surface wave frequency (.). (Rad/sec)
AMP: Surface wave amplitude (ζ_0). (mm)
BETA: Surface wave direction (°). (Radians)

All of input data are read in the main program.

The main program calls subroutine MOTION which calculates the dynamic equilibrium of the subsurface mooring system at discrete times. Subroutine MOTION calls subroutine FORCES, whenever an instrument package or a subsurface float is encountered in the mooring line incremental integration scheme. Both MOTION and FORCES call subroutine SPEED to find the current for viscous drag calculations.

5.0 CASE STUDIES/SIMULATIONS

This section presents computer simulations of specific case studies; using the computer programs outlined in Section 4. All simulations are done in the time-domain. Simulations of the freely floating spar buoy, as presented in Section 5.1, were combined to obtain the response amplitude operator (RAO) vs K_h (wave number multiplied by the appropriate buoy draft). Section 5.2 presents the subsurface moored system simulations. Section 5.3 gives simulations of a surface moored system, and Section 5.4 presents simulations of a drifting drogued buoy.

5.1 Spar Buoy

Both the two-dimensional computer program (SD2.FORT) and the three-dimensional computer program (SD3.FORT) are used to simulate each of the two spar buoys; one cylindrical, and the other tuned presented in Sections 5.1.1 and 5.1.2 respectively. RAO vs K_h plots are presented for the two-dimensional simulations of cylindrical and tuned spar buoys.

5.1.1 Cylindrical Spar

The spar buoy (Figure 5.1) used in these simulations was tested in a series of wave tank tests to

derive empirical response data for comparison with the computer simulations. This comparison has not been presented in this report. The dimensions

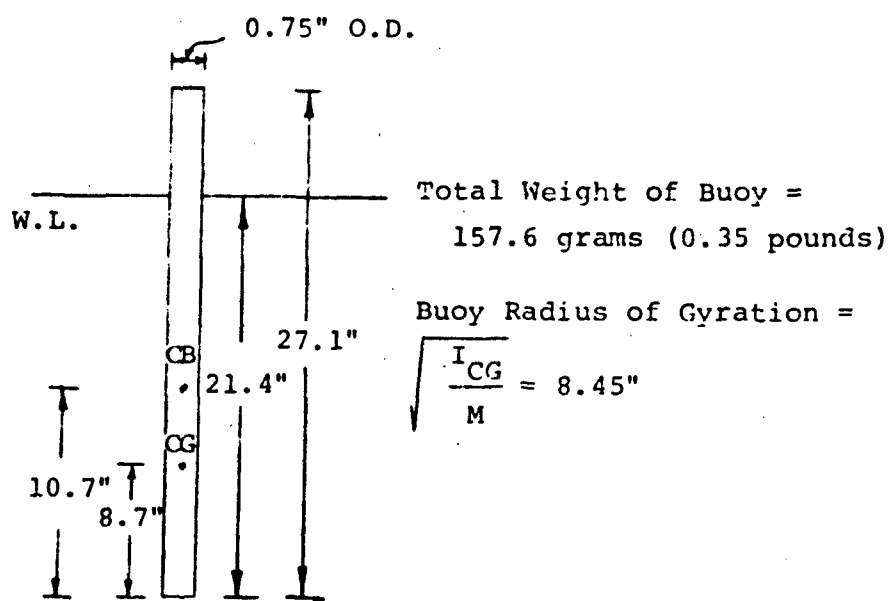


Figure 5.1 Scale Model Spar Buoy Description

and characteristics of this scale model spar buoy are shown in Figure 5.1.

Two Dimensional Simulations

Figures 5.2, 5.3, and 5.4 present the typical surge, heave, and pitch response of the buoy to surface waves of

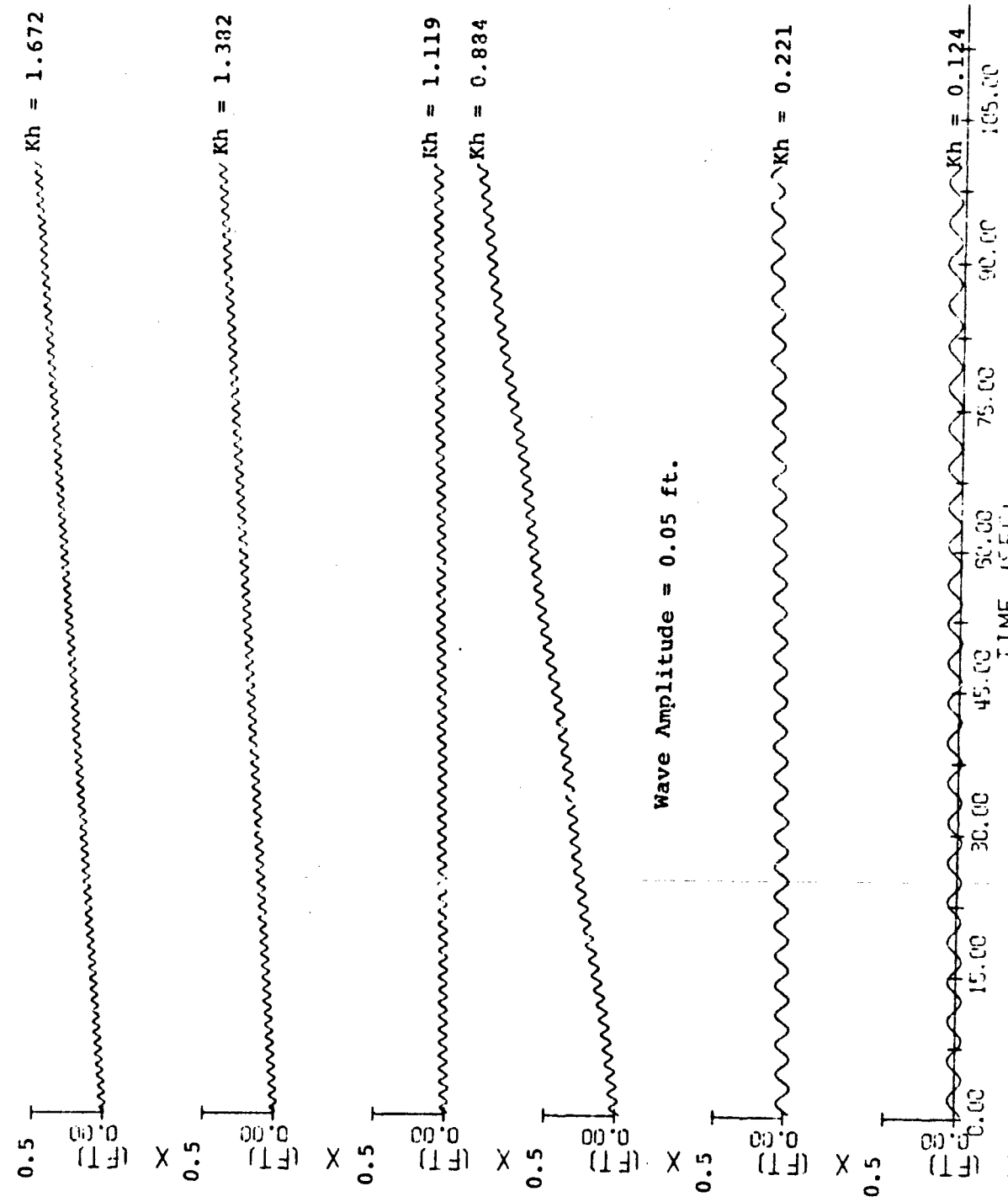


Figure 5.2 Surge Motions of the Freely Floating Cylindrical Spar Buoy

-100-

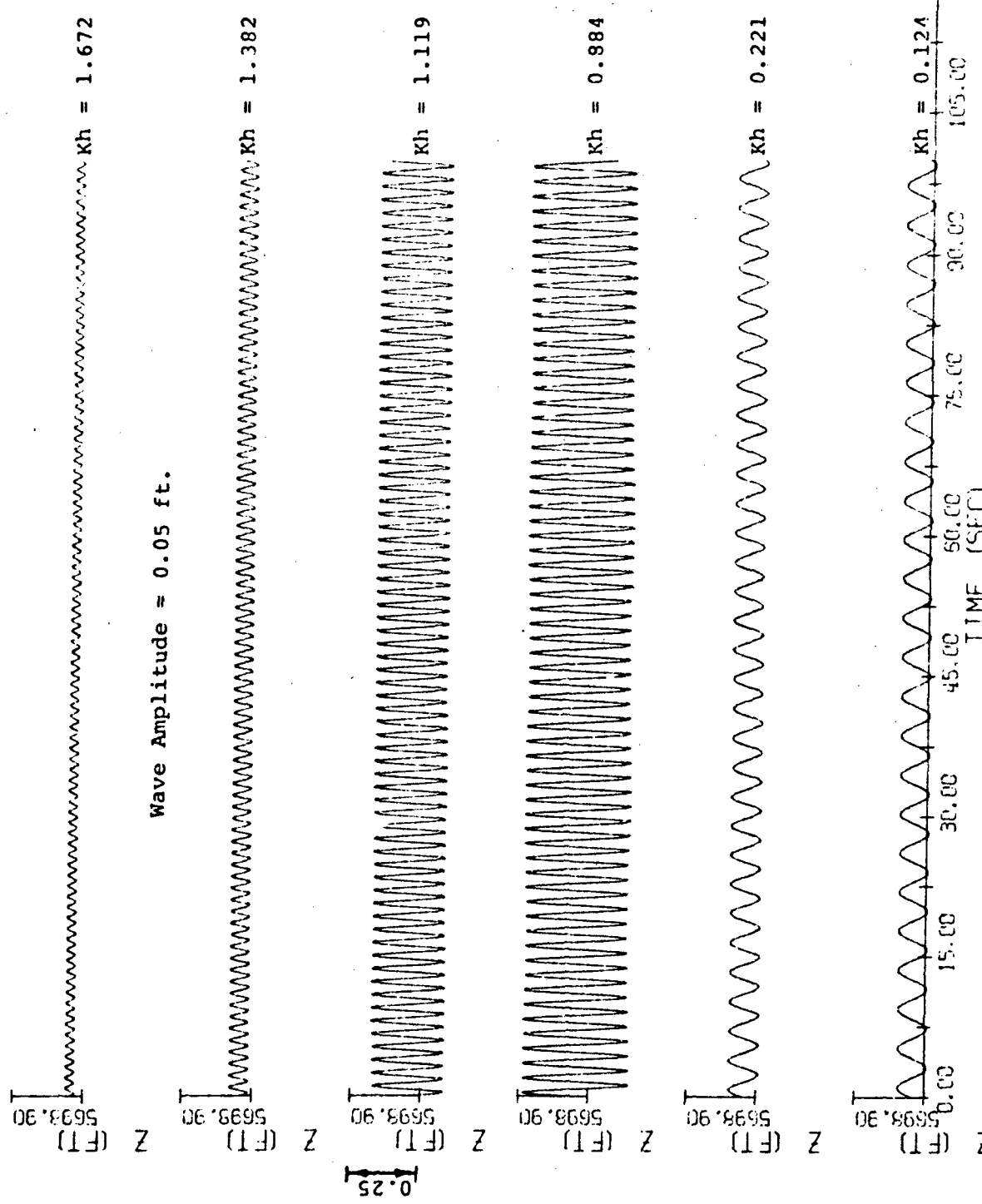


Figure 5.3 Heave Motions of the Freely Floating Cylindrical Spar Buoy

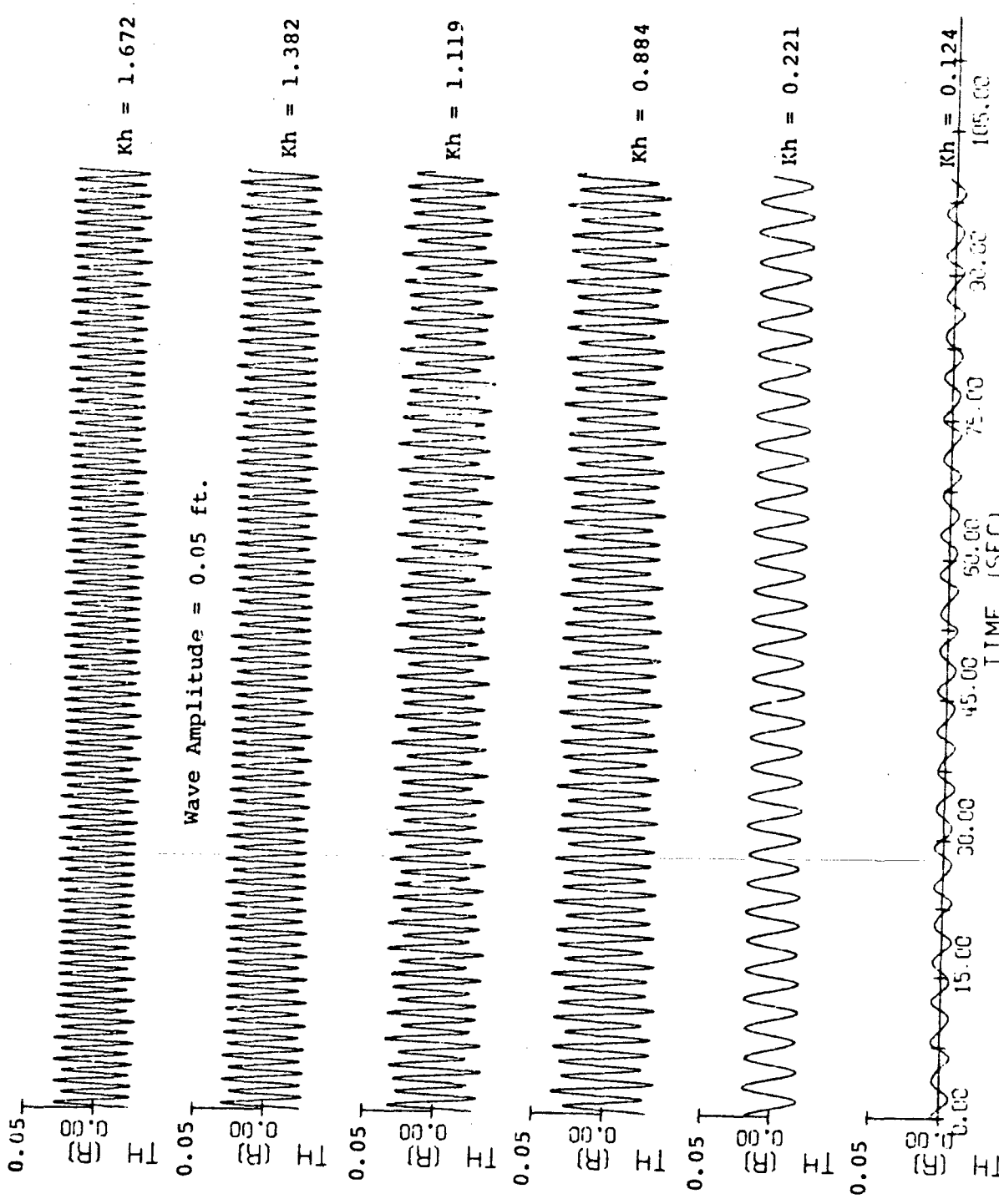


Figure 5.4 Pitch Motions of the Freely Floating Cylindrical Spar Buoy

amplitude 0.05 ft. and different frequencies. Table 5.1 is the input data used in conjunction with the computer program SD2.FORT to obtain these simulations. Noteworthy is the fact that the viscous (CDL) and pressure (CDP) drag coefficients in this study equal zero. Surge drift evident in Fig. 5.2 is due to the bias or rectification of wave exciting forces, which would be present for example if an oscillatory hydrodynamic force were to act on a heaving body whose motions were at varying with this force. Simulations for the same data as Table 5.1 and viscous and pressure drag coefficients equal to 1.0 are shown in Figures 5.5, 5.6, and 5.7.

Comparison between the surge motions of Figures 5.2 and 5.5 shows the effect of viscous drag on surge drift. Surge drift due to viscous drag occurs as the submerged area of the spar and its inclination vary over a wave period, and is a function of their phase relationships. This drift is most predominant near resonance. In this case heave resonance occurs at $K_h = 1.0$, and pitch resonance occurs at $K_h = 0.4$. Heave motions (Figures 5.3 and 5.6) are not effected much by viscous drag because the tangential drag due to CDL and CDP is comparatively small. Comparison of Figures 5.4 and 5.7 shows that the system frequency present in the top four curves of Figure 5.4, due to approximate initial conditions, is damped out in Figure 5.7 due to viscous drag damping. Otherwise, the amplitudes do not show much change.

SD2C.DATA						
00010	1	0	25	6	0 5700.	0.020
00020	0.03125	0.03125	0.725	6	0.704	2.258
00021	1.0	0.0	0.0	6	1.0	0.0
00055	0.35	0.	0.	6	0.	0.
00090	0.	0.	0.	6	0.	0.
00105	0.	0.	0.	6	0.	-18.
00110	0.0					
00120	1.50	0.05				
00130	2.00	0.05				
00140	4.00	0.05				
00150	4.50	0.05				
00160	5.00	0.05				
00170	5.50	0.05				
READY						

Table 5.1 Input Data for the 2-D Analysis of the Cylindrical Spar Buoy

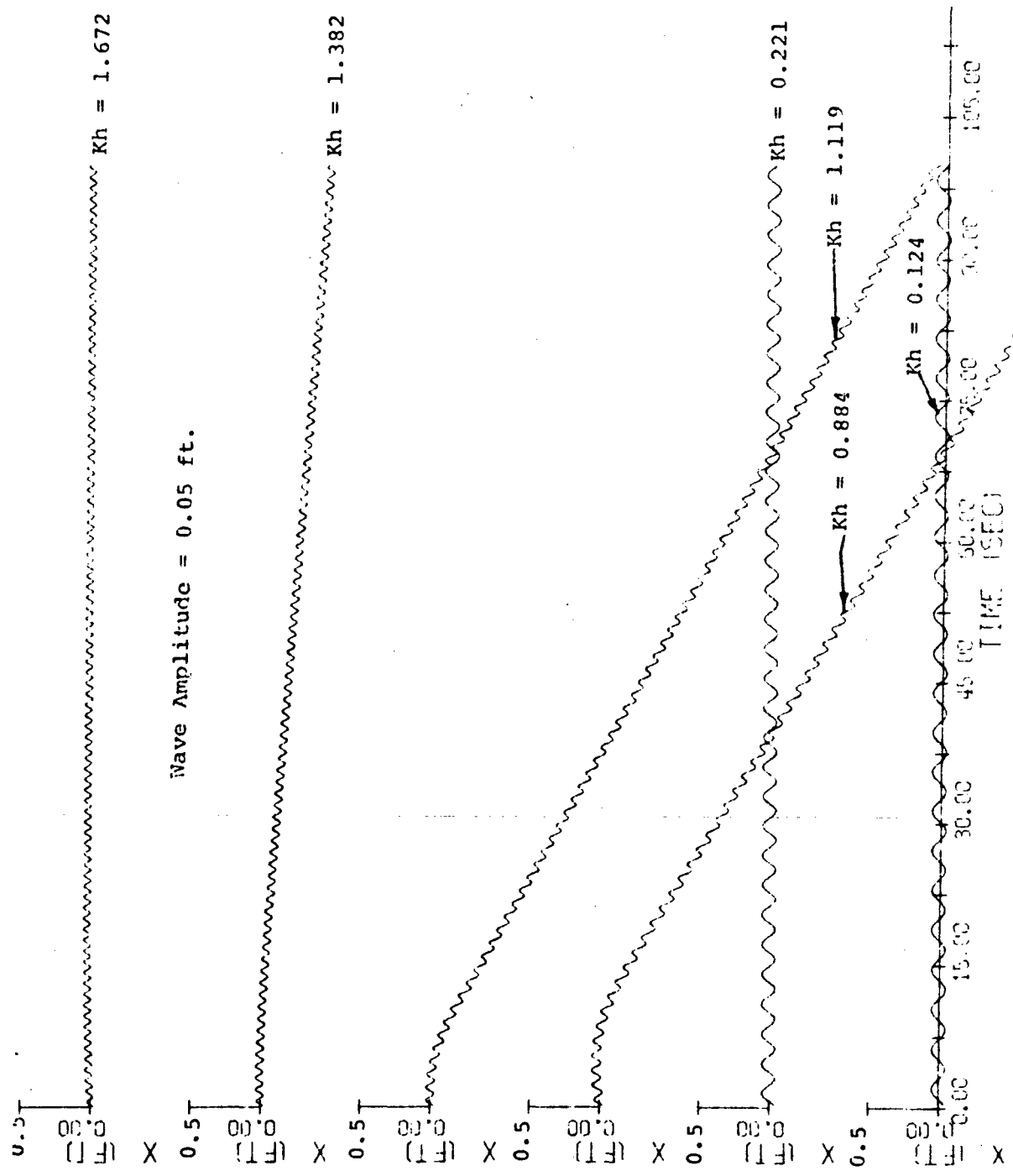


Figure 5.5 Surge Motions of the Freely Floating Cylindrical Spar Buoy

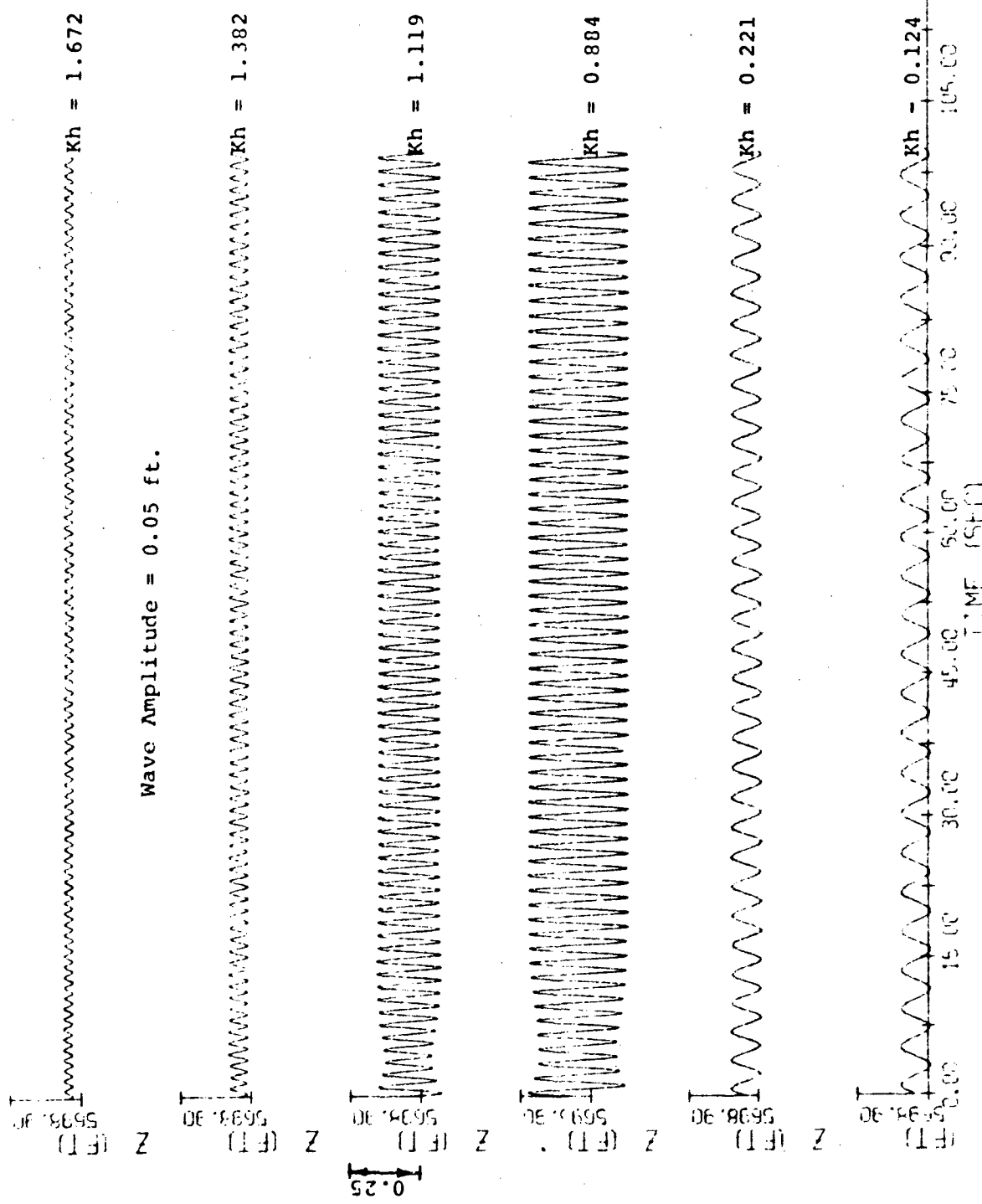


Figure 5.6. Free Motions of the Freely Floating Cylindrical Spar Buoy

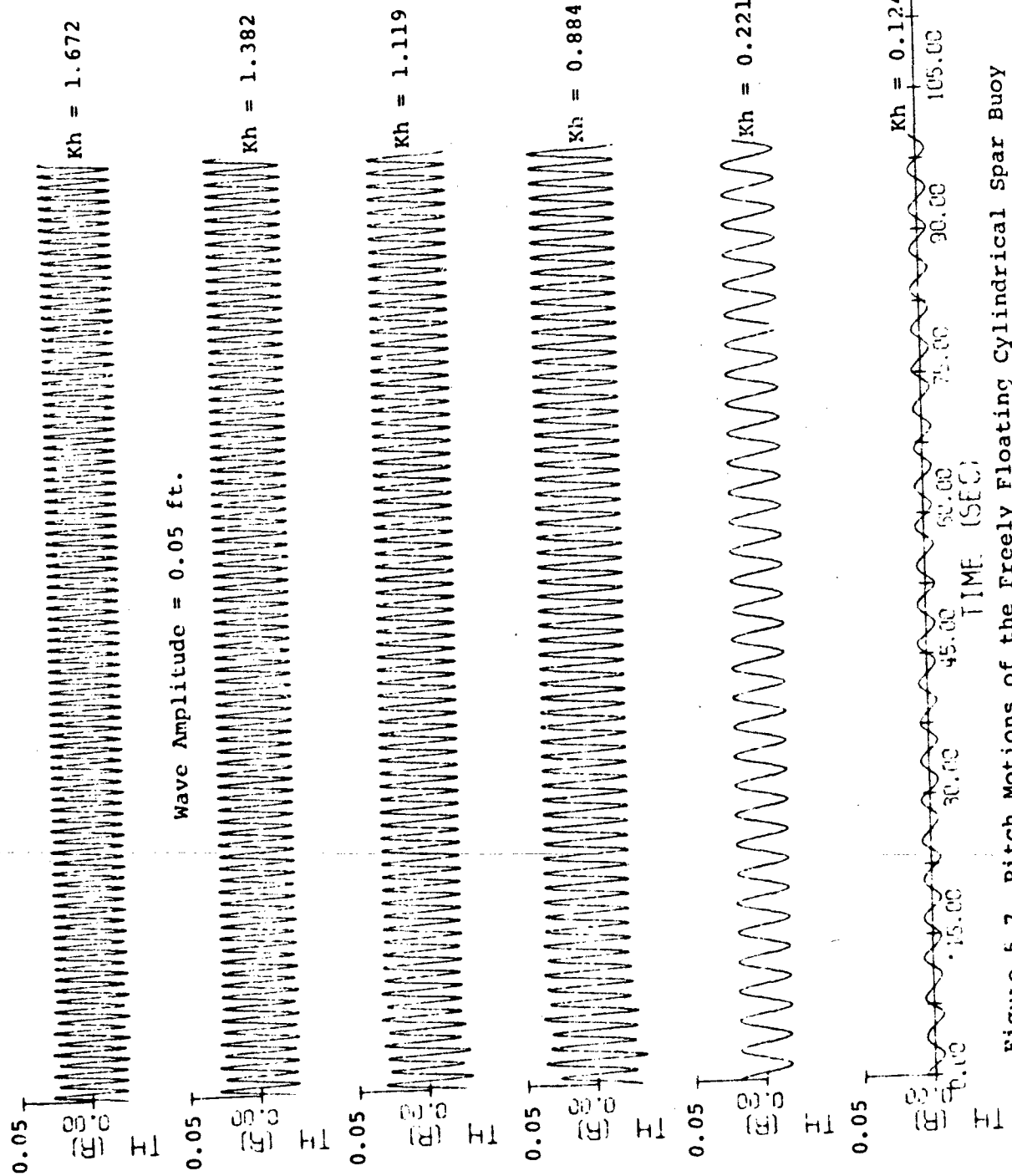


Figure 5.7 Pitch Motions of the Freely Floating Cylindrical Spar Buoy

Response amplitudes of surge, heave, and pitch; and surge drift as calculated from the steady state portions of the times histories presented in Figures 5.2 through 5.7, and other similar simulations are tabulated in Table 5.2. In this table column 1 tabulates the frequencies (ω) of waves studied. From these frequencies K_h is calculated and tabulated in column 2. Columns 3 through 6 are four columns of surge amplitude divided by ξ_0 . The first of these four columns presents the results of the undamped linear analytical solution as derived in Section 3.2. The second presents the computer simulation results with ξ_0 equal to 0.05 ft. and no viscous drag. Third and fourth present the computer simulation results with viscous drag and ξ_0 equal to 0.05 ft. and 0.25 ft. respectively. The simulated plots are shown for two wave amplitudes to emphasize the nonlinear response obtained by the nonlinear theory. Similarly columns 7 through 10 tabulate four columns of heave amplitude divided by ξ_0 , and columns 11 through 14 tabulate four columns of pitch amplitude divided by $K\xi_0$. $K\xi_0$ is the maximum wave slope. Analytical solution for surge drift was not found hence only three columns 15 through 17 are given for surge drift divided by $K\omega\xi_0^2$. $K\omega\xi_0^2$ is the mean "stokes drift" velocity at the mean free surface. Data points of Table 5.2 are plotted in Figures 5.8 through 5.11

ω	Kh	Surge Amplitude/ ξ_o				Heave Amplitude/ ξ_o				Pitch Amplitude/ ξ_o				Surge Drift/ $Kw^2 \xi_o^2$			
		1	2	3	4	1	2	3	4	1	2	3	4	1	2	3	4
1.50	0.12	-0.94	0.95	0.95	0.95	1.01	1.01	1.01	1.01	1.71	1.79	1.72	2.91	0.91	0.91	0.91	0.94
2.52	0.35	-0.84	0.86	0.75	1.09	1.13	1.23	1.19	1.19	7.94	5.42	6.37	-1.10				
2.69	0.40	-0.82	0.72			1.12		1.16		-26.52		8.22		-6.31			
2.85	0.45	-0.81	0.68	0.70	1.17	1.17	1.22	1.17	1.17	-7.97	6.76	4.01	-4.11	-0.48			
3.30	0.60	-0.75	0.67	0.67	1.39	1.39				-2.67	2.65			-0.61			
3.56	0.70	-0.72	0.66	0.65	1.69	1.68	1.62	1.62	1.62	-1.91	1.89	1.85	-0.43	0.13			
4.00	0.88	-0.66	0.61	0.64	0.85	3.79	3.75	3.53	3.97	-1.28	1.26	1.22	2.36	-7.91	0.19		
4.10	0.93	-0.65	0.53		6.18	4.23				-1.19	1.01			-11.88			
4.20	0.98	-0.64	0.53		21.35	4.30				-1.11	0.35			-12.45			
	1.00																
4.30	1.02	-0.63	0.51	-12.13	3.76					-1.04	0.86						
4.40	1.07	-0.61	0.53	-4.39	2.96					-0.98	0.90			-10.53			
4.50	1.12	-0.60	0.54	0.57	0.62	-2.56	2.57	2.15	1.34	-0.92	0.86	0.45	C.20	-5.63	-0.38	-7.58	
4.67	1.21	-0.58	0.52		-1.40		1.35		-0.83		0.82		-2.47				
5.00	1.38	-0.54	0.50	0.43	0.50	-0.64	0.64	0.64	0.64	-0.70	0.70	0.66	0.47	-0.47	-0.07		
5.50	1.67	-0.49	0.44	0.44	0.45	-0.27	0.27	0.28	0.28	-0.55	0.56	0.55	0.49	0.02	0.10		
6.72	2.50	-0.37	0.32	0.33	-0.05	0.05	0.06	0.06	-0.34	0.34	0.35	0.15	0.16				

TABLE 5.2 Dynamic Response (Surge, Heave and Pitch Amplitude; and Surge Drift) of a Cylindrical Spar Buoy to Waves

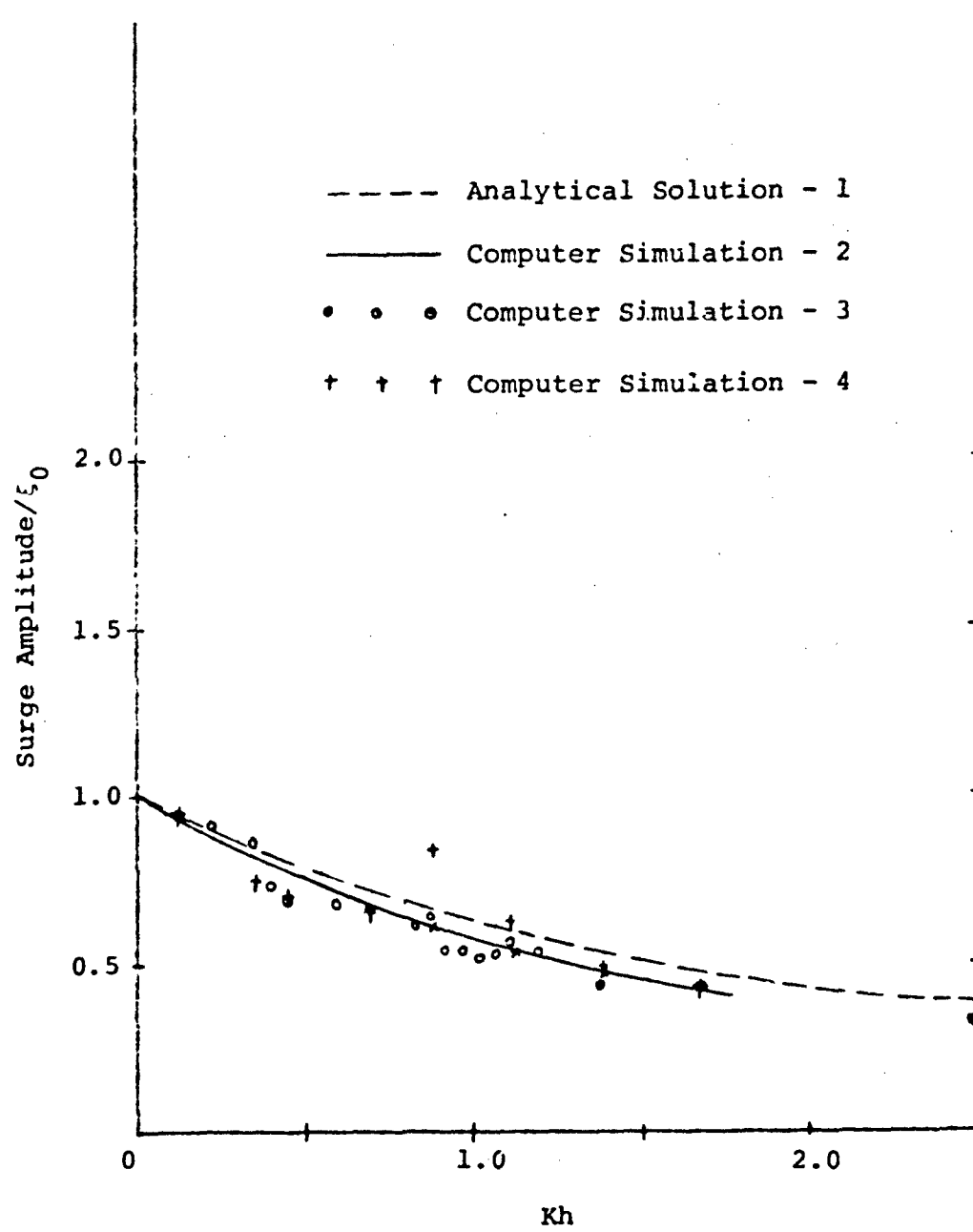


Figure 5.8 Surge Magnification Vs Kh

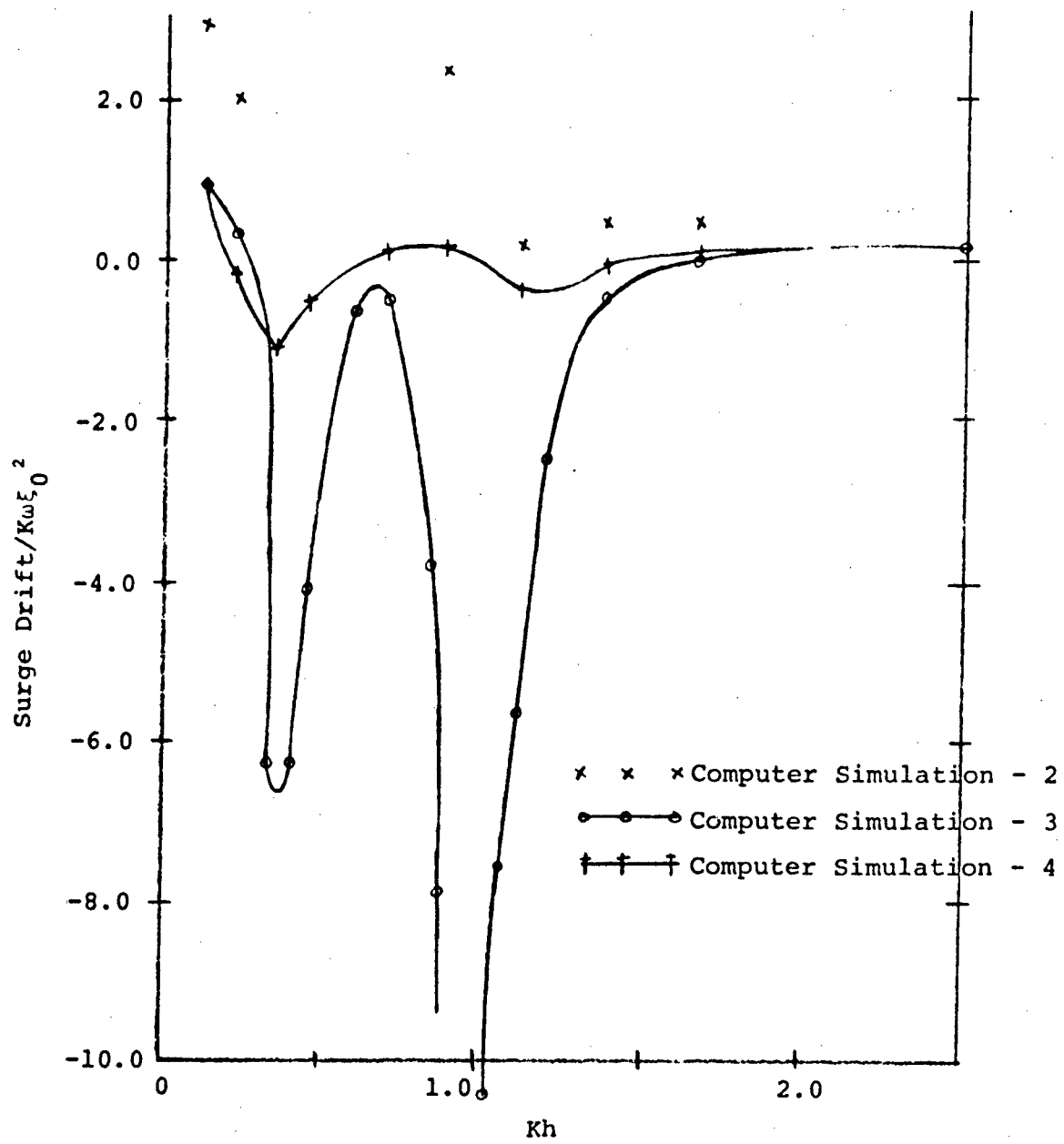


Figure 5.9 Surge Drift Vs Kh

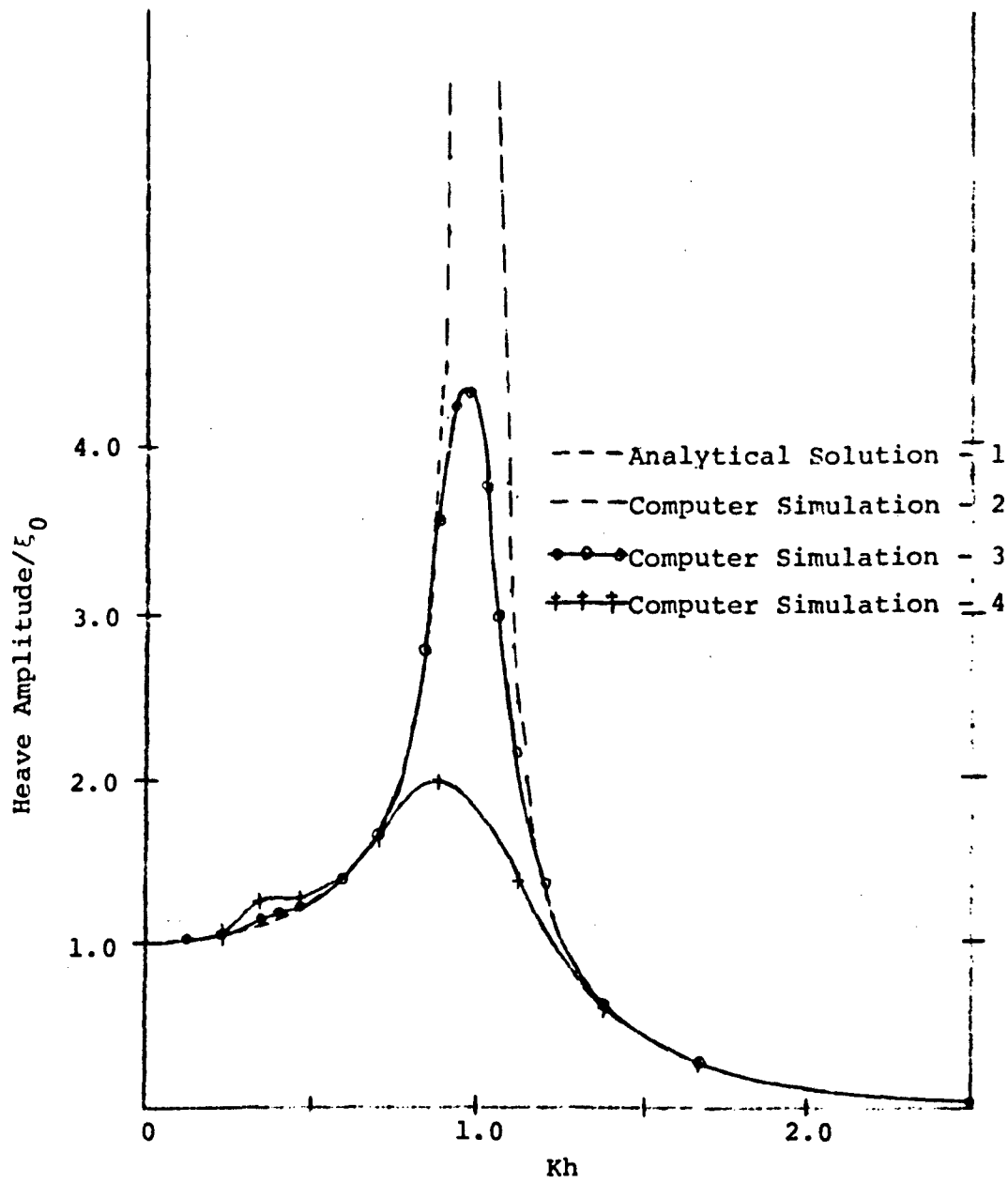


Figure 5.10 Heave Magnification Vs Kh

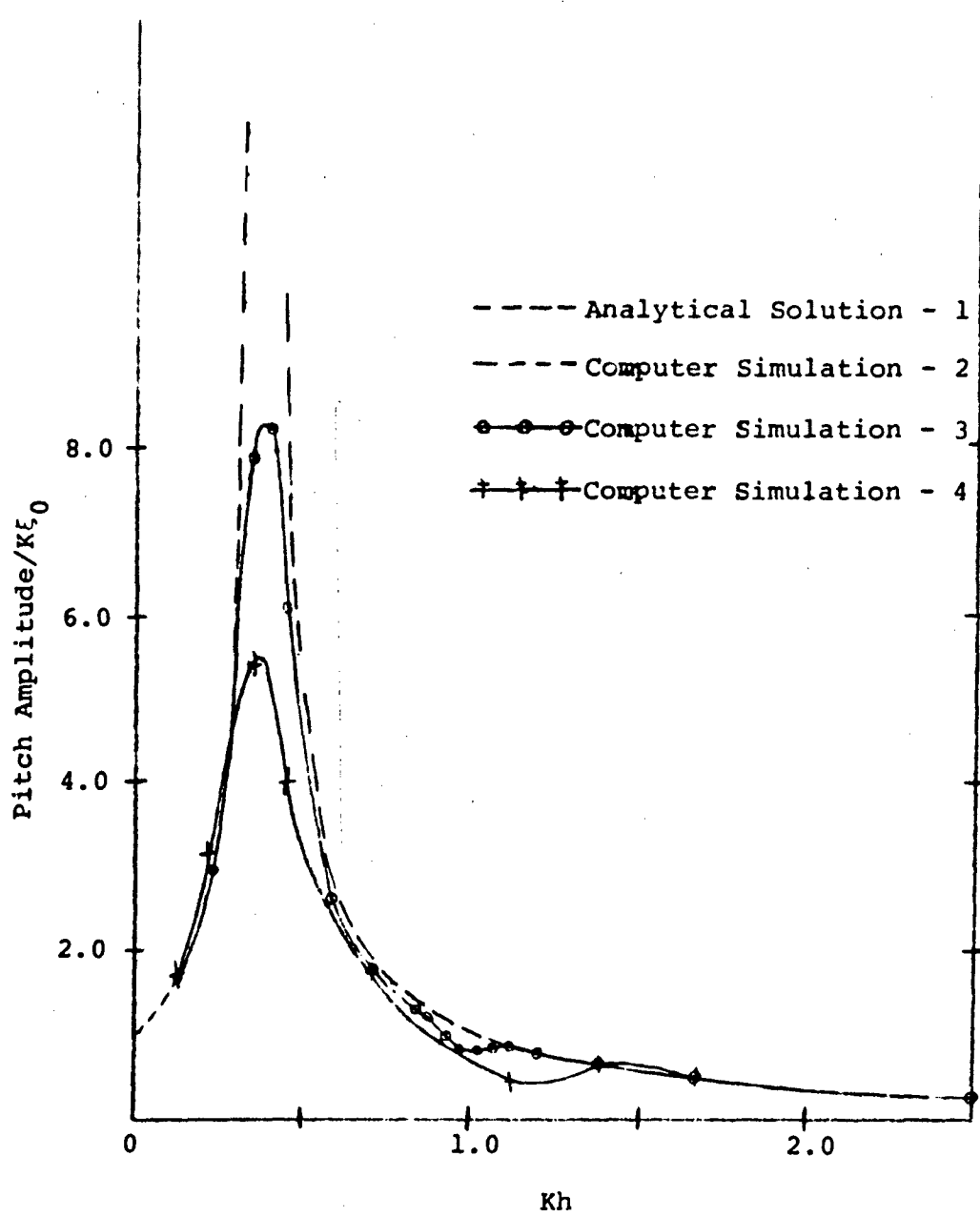
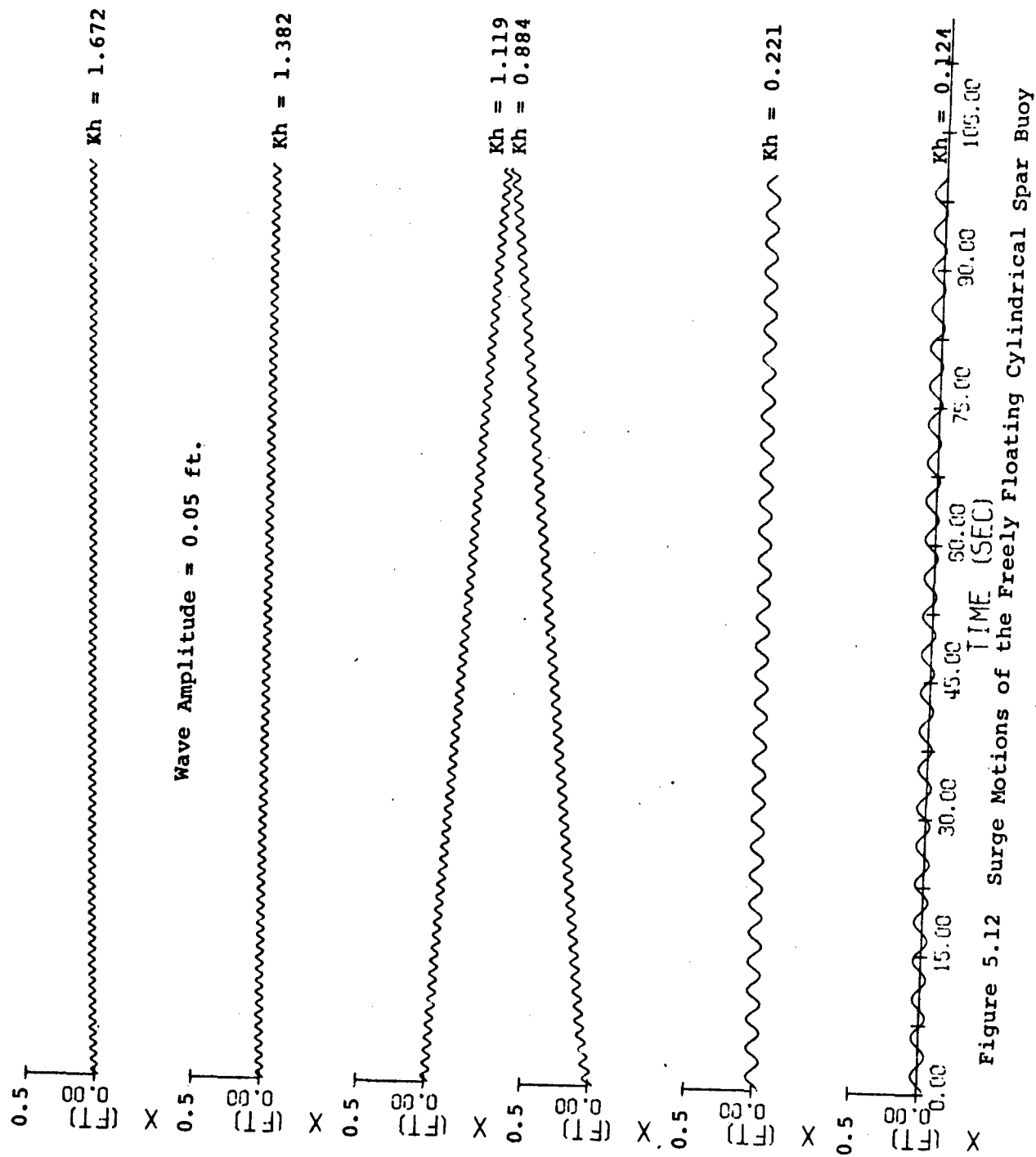


Figure 5.11 Pitch Magnification Vs Kh

to present plots of RAO vs Kh. Figure 5.8 shows the buoy surge per foot of wave amplitude as a function of Kh. For zero frequency this ratio is one and for increasing frequencies it decreases to zero. Figure 5.9 shows the buoy drift (in surge direction) per $K\omega\xi_0^2$ as a function of Kh. Figure 5.10 shows the buoy heave per foot of wave amplitude as a function of Kh. This ratio is one for zero frequency and exhibits resonance at Kh of approximately 1.0. The ratio decreases to zero with increasing frequencies. Figure 5.11 shows the buoy pitch per $K\xi_0$ as a function of Kh. This ratio is one at zero frequency and, after exhibiting resonance phenomenon at around 0.4 Kh, the ratio goes to zero with increasing frequencies. Figures 5.8 through 5.11 are further discussed in Section 6.

Three Dimensional Simulations

Figures 5.12 through 5.17 present the surge, sway, heave, roll, pitch and yaw responses of the buoy to surface waves of the same amplitude and frequencies as in Figures 5.5 and 5.7. Table 5.3 is the input data used in conjunction with the computer program SD3.FORT to obtain these simulations. Here the angle β , giving the wave propagation direction is zero. These simulations should give the same response as Figures 5.5 through 5.7. Comparing Figures 5.5 and 5.12, we see a lot of difference in the surge drifts. Figure 5.12 looks more like Figure 5.2 which



X Figure 5.12 Surge Motions of the Freely Floating Cylindrical Spar Buoy

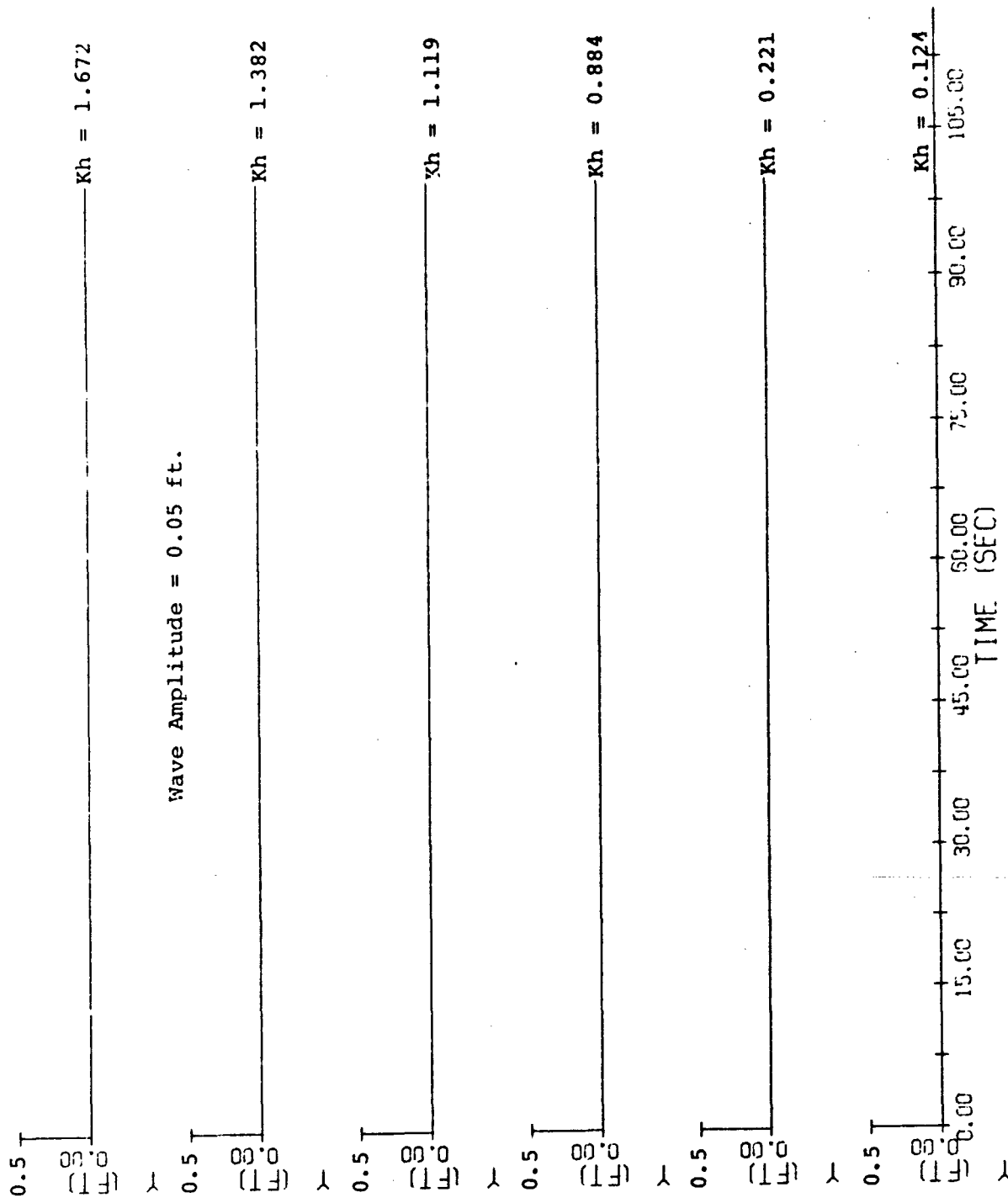


Figure 5.13 Sway Motions of the Freely Floating Cylindrical Spar Buoy

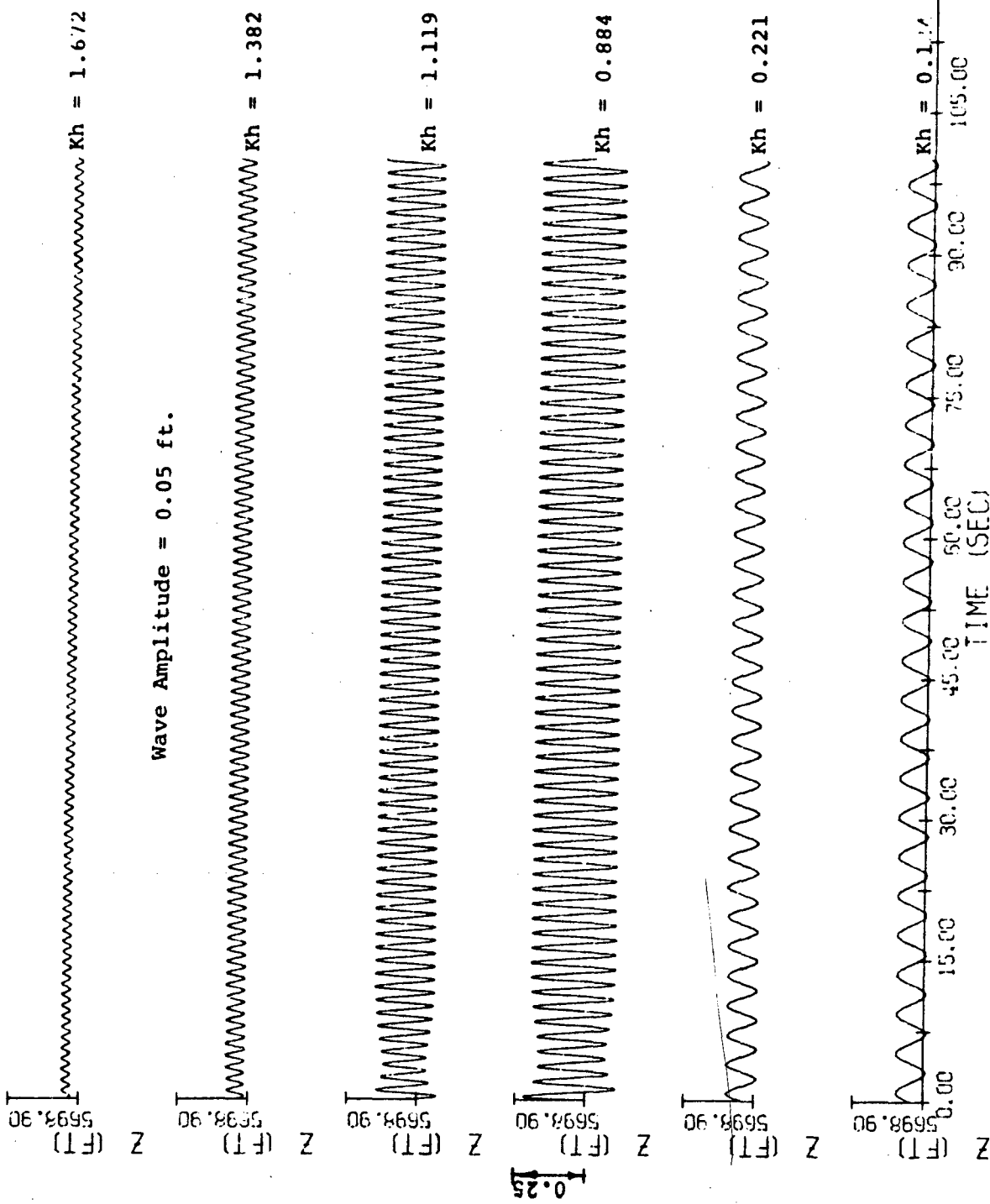


Figure 5.14 Heave Motions of the Freely Floating Cylindrical Spar Buoy

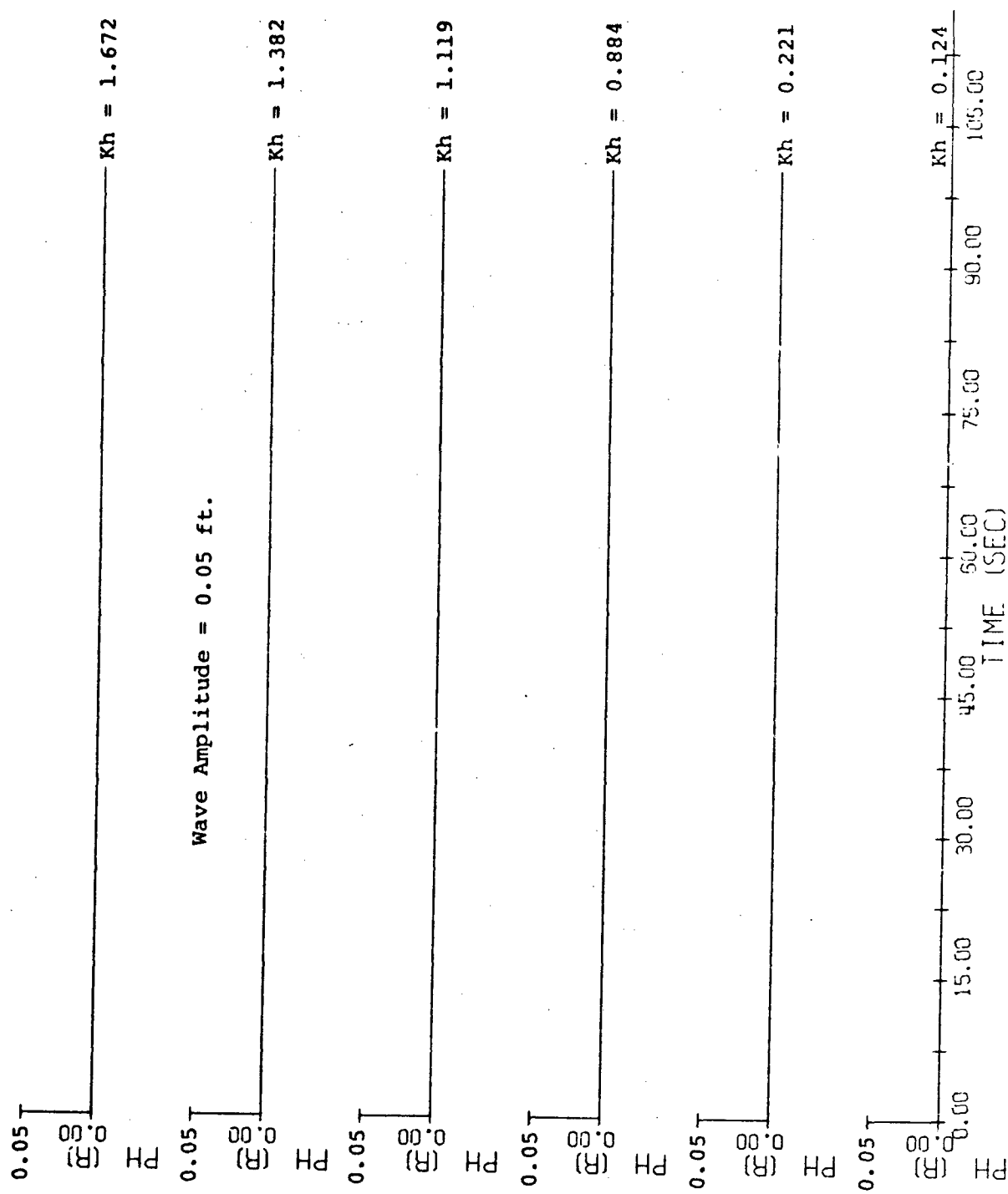


Figure 5.15 Roll Motions of the Freely Floating Cylindrical Spar Buoy

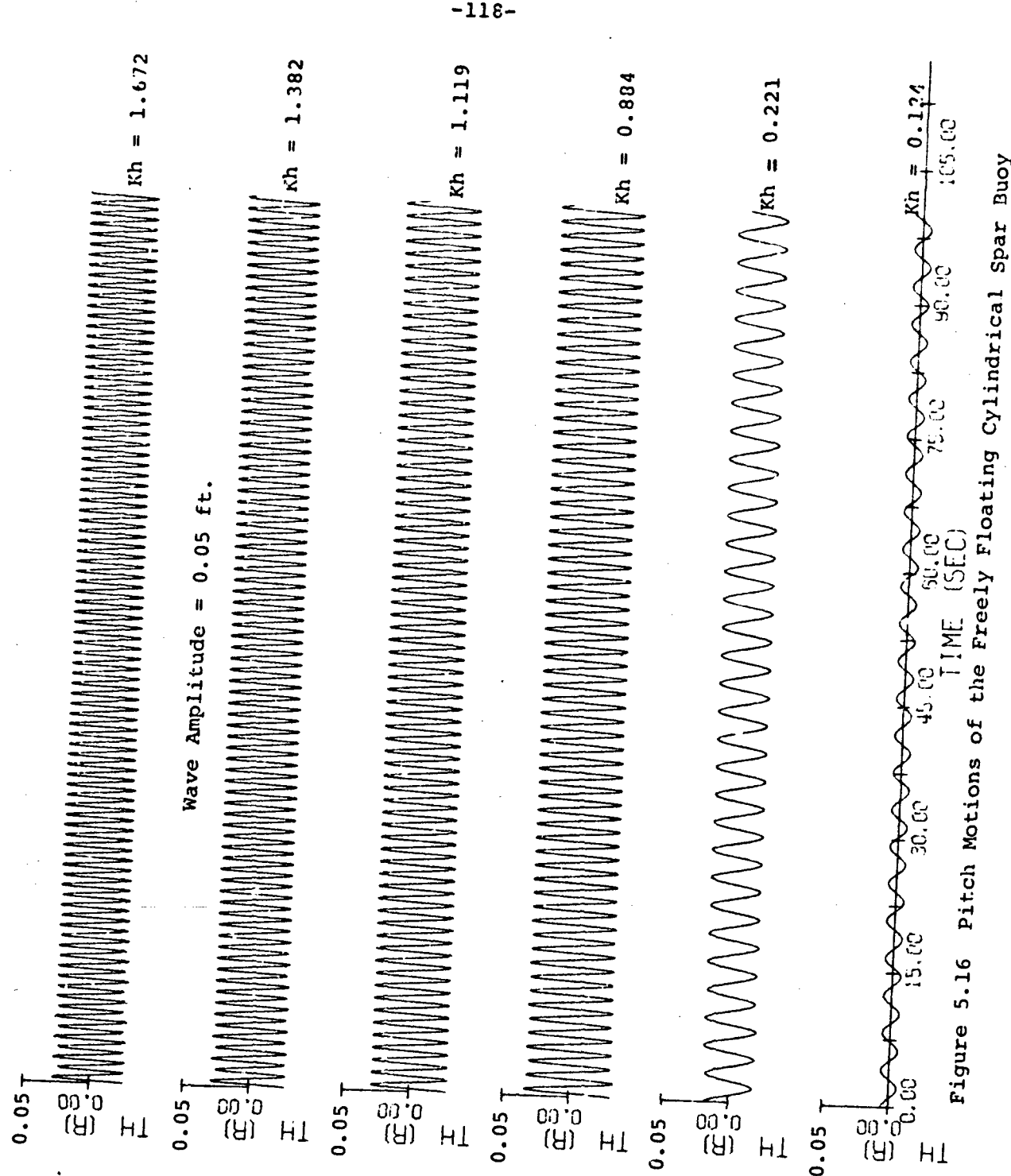


Figure 5.16 Pitch Motions of the Freely Floating Cylindrical Spar Buoy

-119-

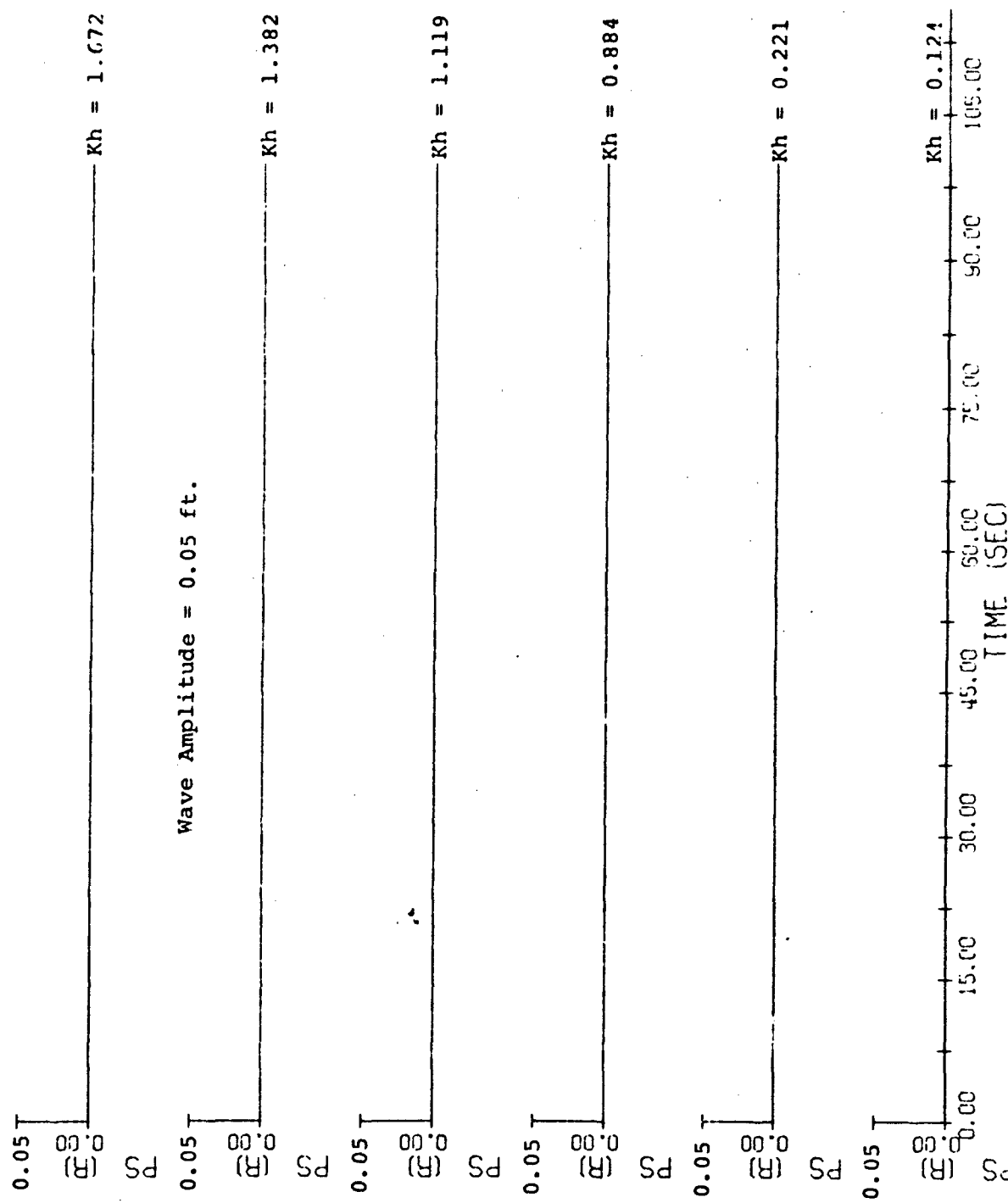


Figure 5.17 Yaw Motions of the Freely Floating Cylindrical Spar Buoy

SCBUOY.DATA							
00010	1	0	25	6	0 5700.	0.0020	100.0
00020	0.03125	0.03125	0.725	0.704	2.258	1.0	1.1
00021	1.	1.0					
00055	0.35	0.					
00090	0.	0.	0.	0.	0.	0.	
00105	0.	0.	0.	0.	0.	0.	-18.
00110	0.	0.	0.	0.	0.	0.	
00120	1.50	0.	0.	0.	0.	0.	
00130	2.00	0.	0.	0.	0.	0.	
00140	4.00	0.	0.	0.	0.	0.	
00150	4.50	0.	0.	0.	0.	0.	
00160	5.00	0.	0.	0.	0.	0.	
00170	5.50	0.	0.	0.	0.	0.	
READY							

Table 5.3 Input Data for the 3-D Analysis of the Cylindrical Spar Buoy

was obtained by neglecting viscous drag. Hence we see that the viscous drag effects on surge drift which show up in the two-dimensional non-linear simulations (Figure 5.5), do not show up in the three-dimensional simulation (Figure 5.12) where assumptions of small motions are made. This assumption may be in error the most near the resonance frequency (Heave resonance; $K_h = 1.0$. Pitch resonance; $K_h = 0.4$), where the two Figures 5.5 and 5.12 differ the most. Comparison of Figures 5.14 and 5.16 to Figures 5.6 and 5.7 shows only slight differences. Figures 5.13, 5.15, and 5.17 show no response as expected. Simulations for the same data as Table 5.3 but $\beta = \pi/4$ are presented in Figures 5.18 through 5.23. These figures show the resolution of surge in Figure 5.12 to surge and sway in Figures 5.18 and 5.19; and the resolution of pitch in Figure 5.16 to roll and pitch in Figures 5.21 and 5.22. Yaw response remains the same as expected.

5.1.2 Tuned Spar

The spar buoy used in these simulations along with its dimensions and characteristics is shown in Figure 5.24.

Two-Dimensional Simulations

Figures 5.25, 5.26, and 5.27 show the typical surge, heave, and pitch response of the buoy to surface waves of amplitude 0.5 ft. and different frequencies. Table 5.4 is the input data used in conjunction with the computer program SD2.FORT to obtain these simulations. Here again

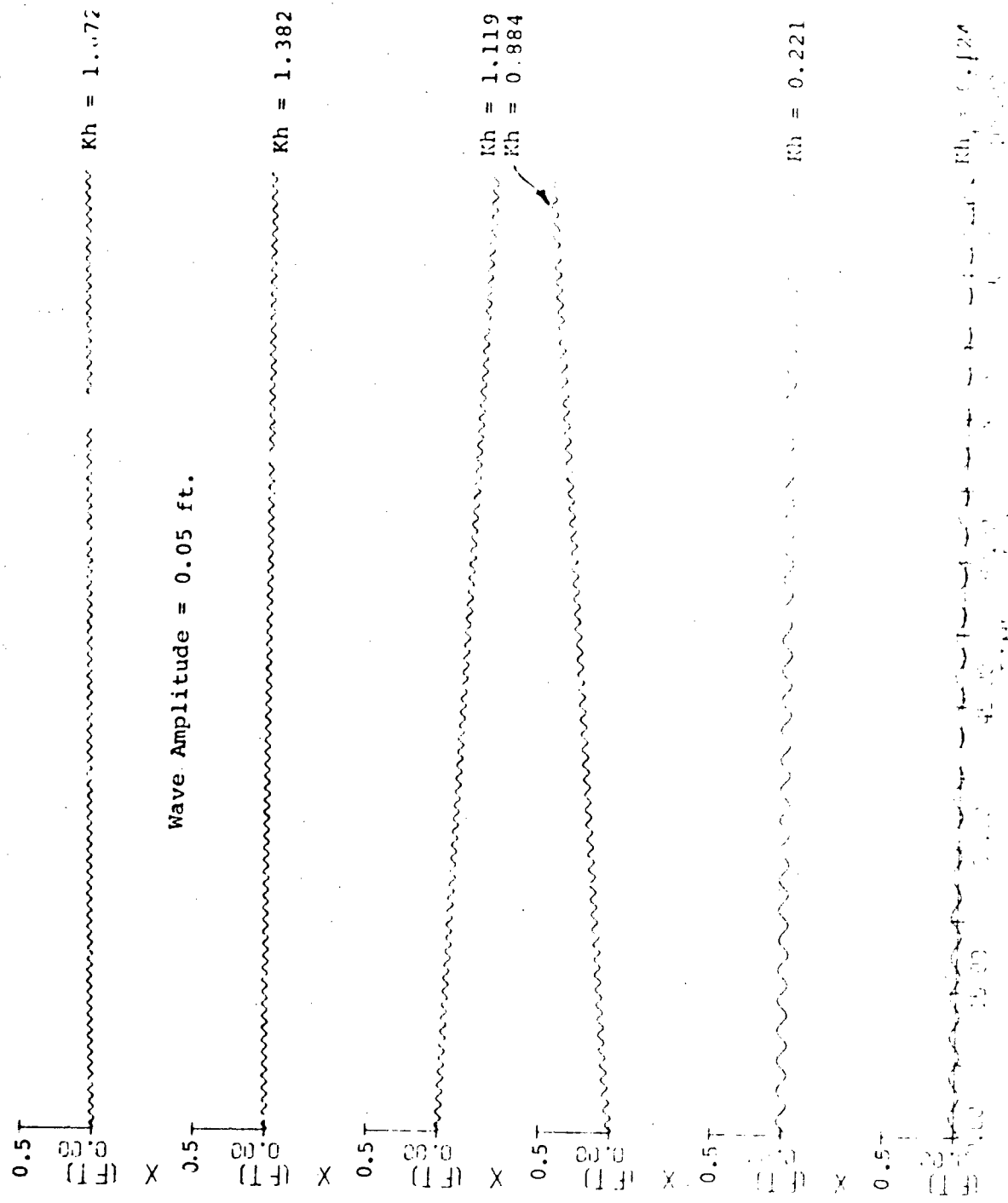


Figure 5.13 Surge Motions of the Freely Floating Cylindrical Ship with

-123-

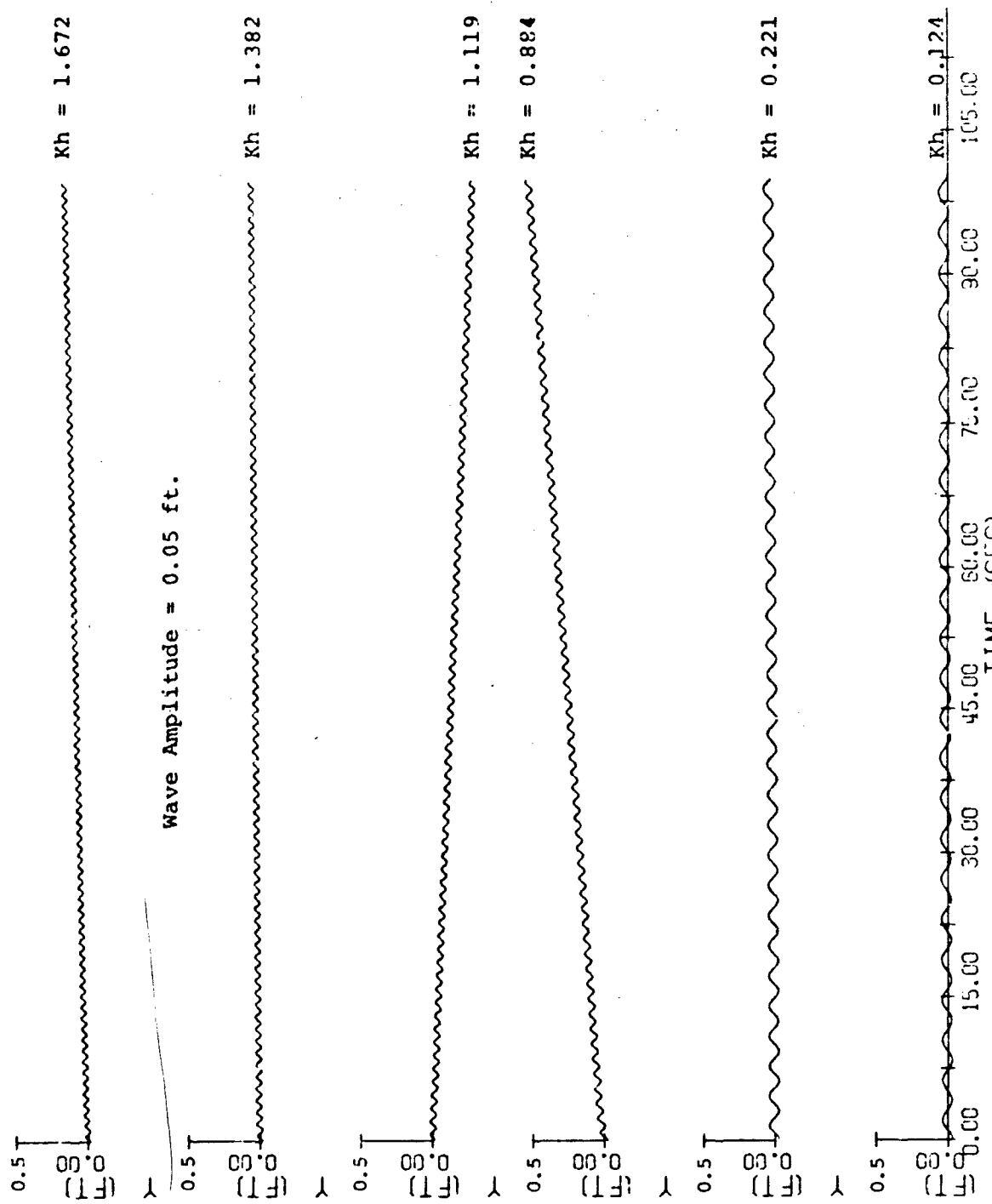


Figure 5.16 Sway Motions of the Freely Floating Cylindrical Spar Buoy

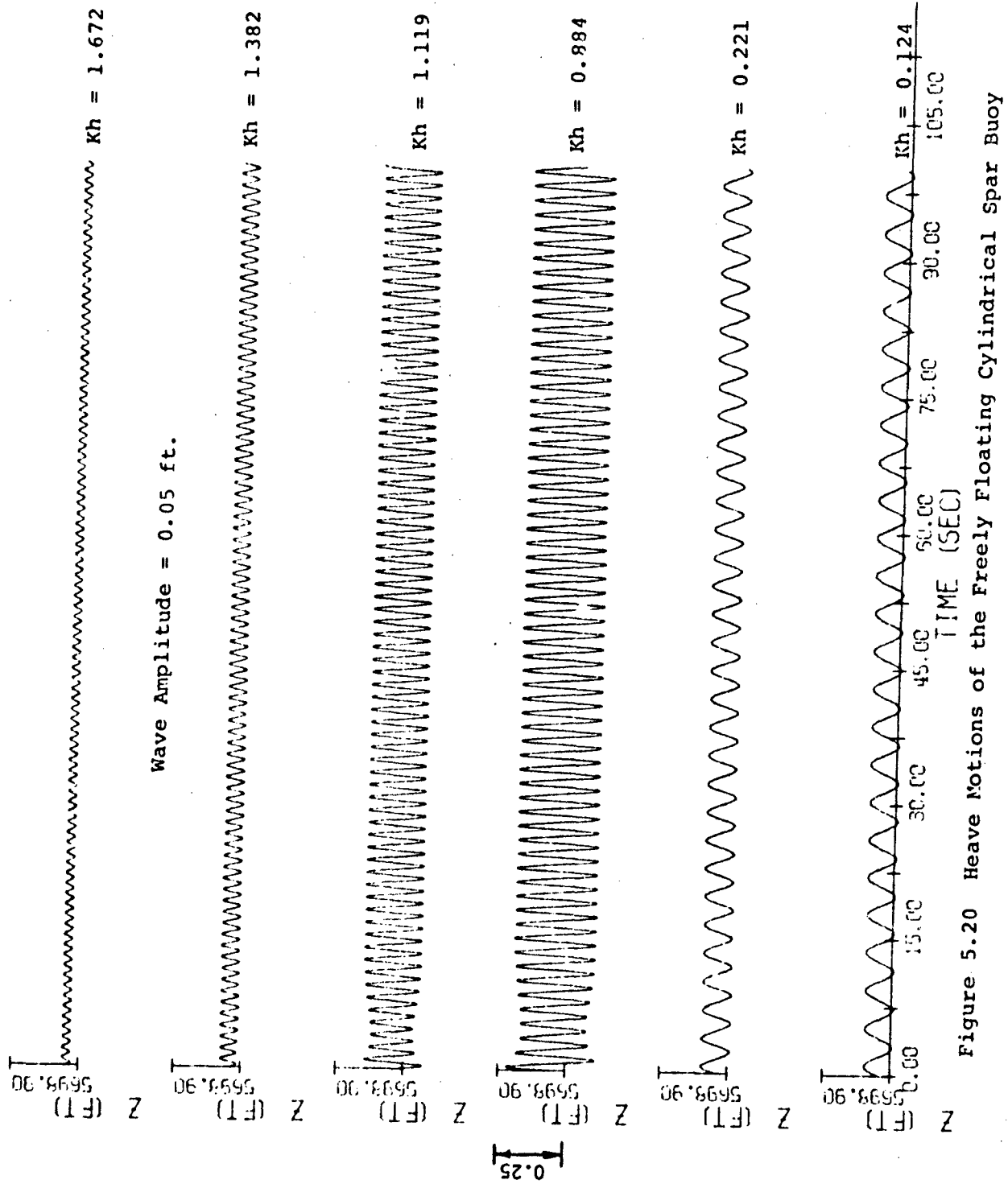


Figure 5.20 Heave Motions of the Freely Floating Cylindrical Spar Buoy

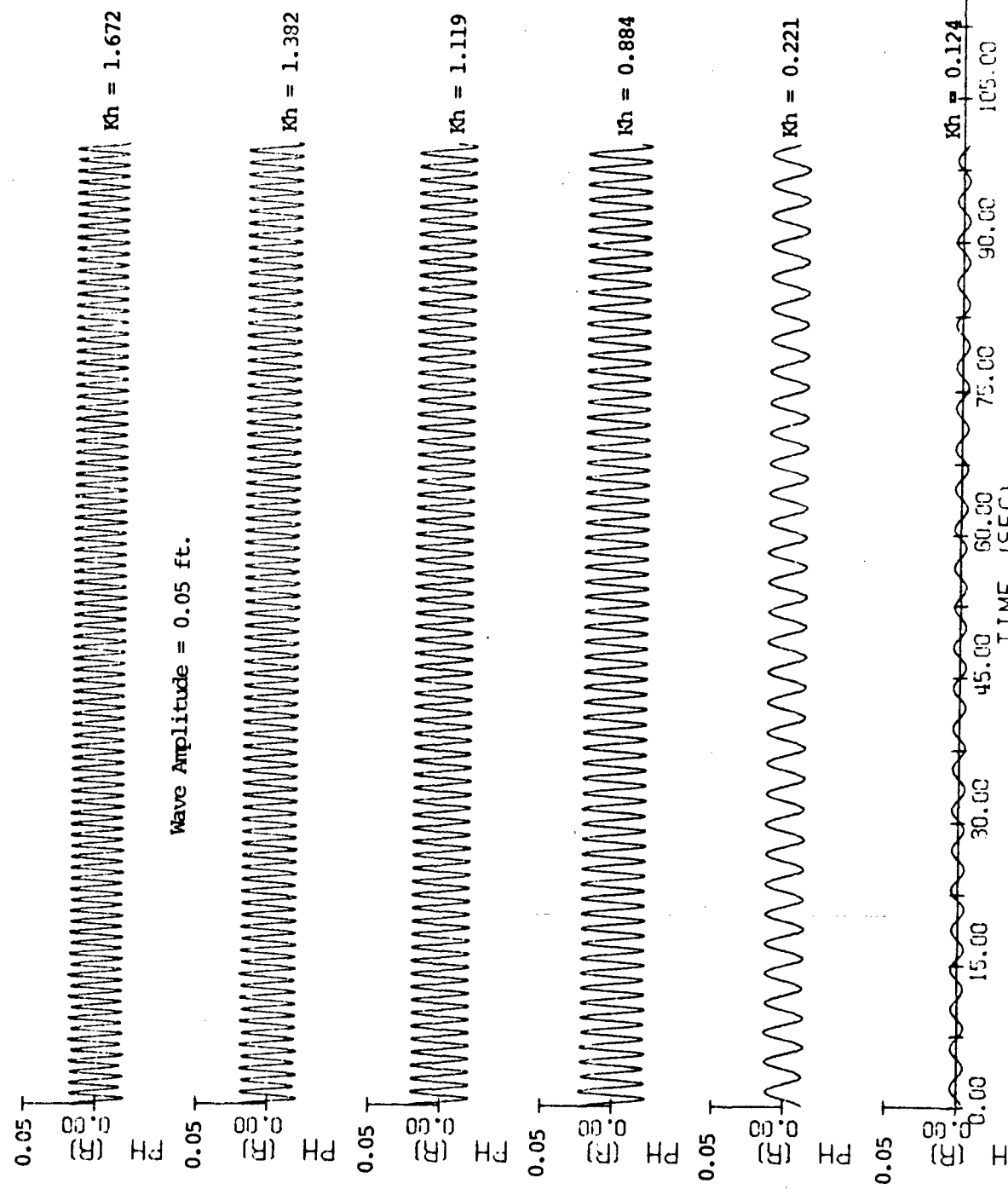


Figure 5.21 Roll Motions of the Freely Floating Cylindrical Spar Buoy

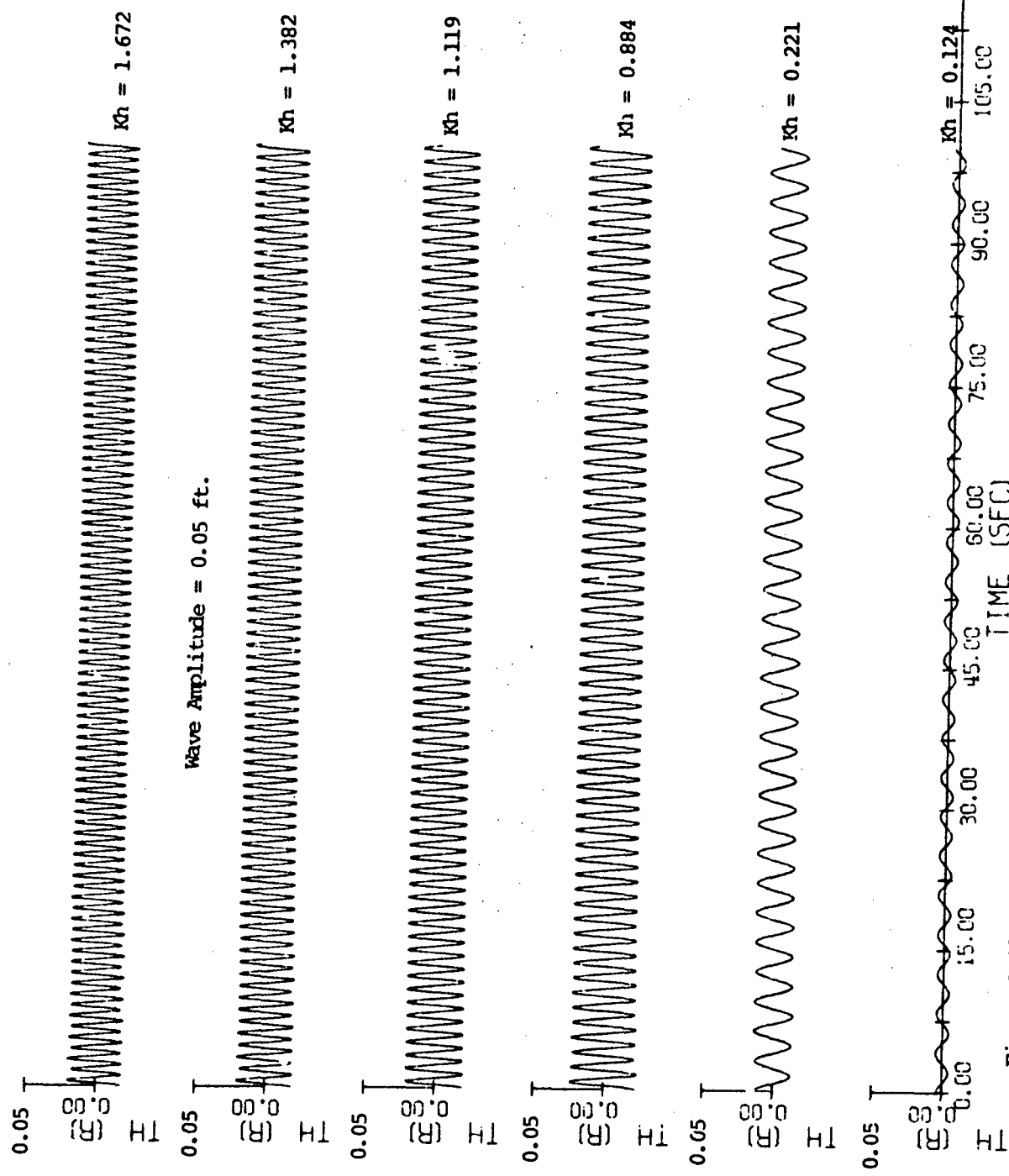


Figure 5.22 Pitch Motions of the Freely Floating Cylindrical Spar Buoy

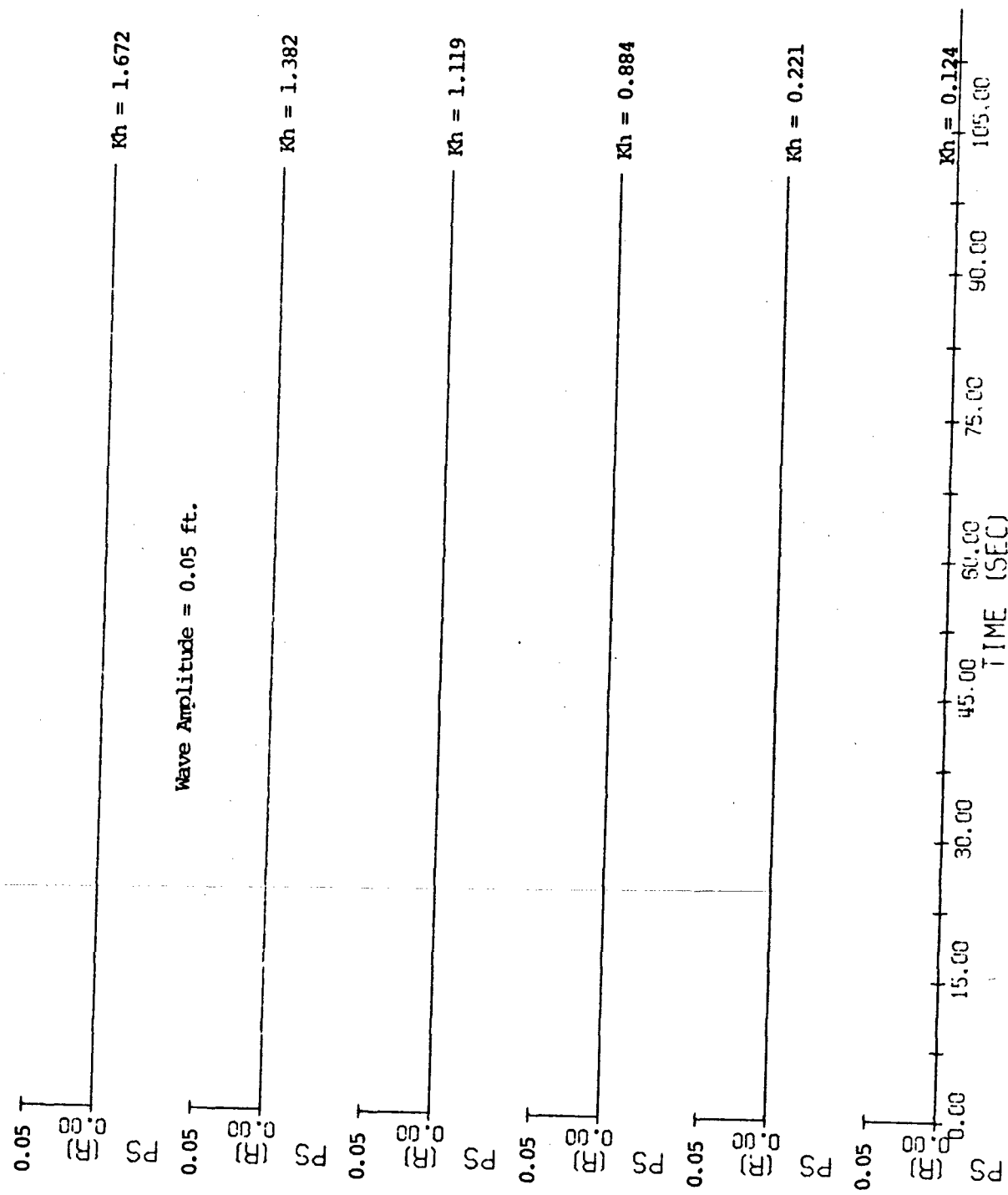
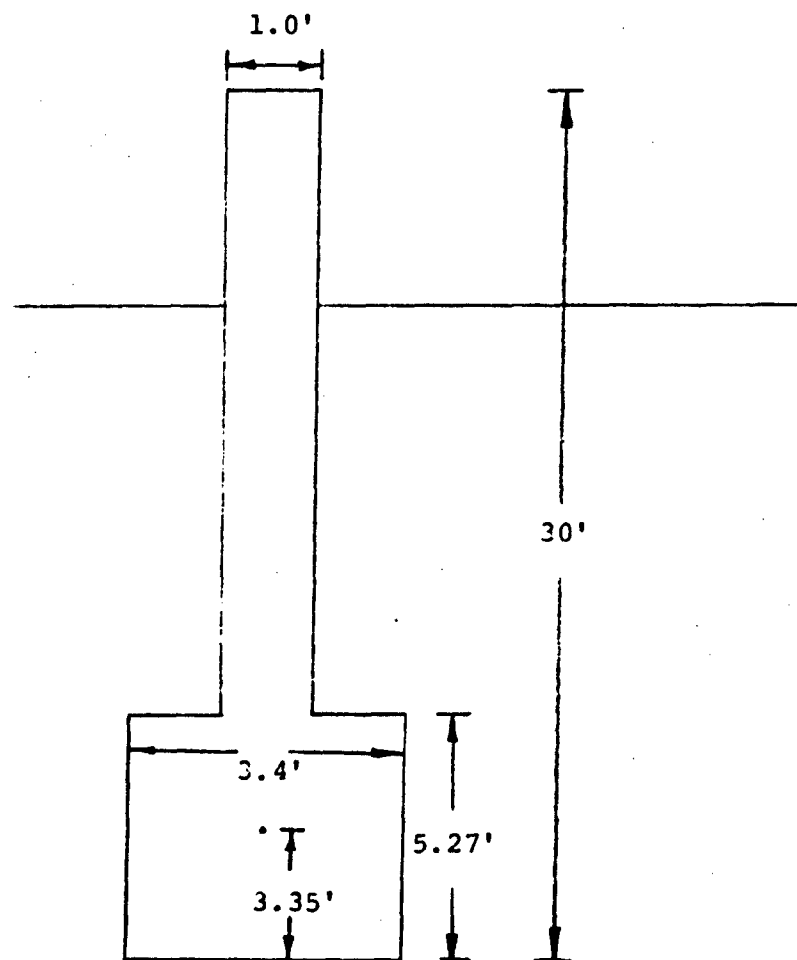


Figure 5.23 Yaw Motions of the Freely Floating Cylindrical Spar Buoy



Buoy Radius of Gyration = 5.11'

Total Weight of the Buoy = 3745.62 pounds

Figure 5.24 Tuned Spar Buoy Description

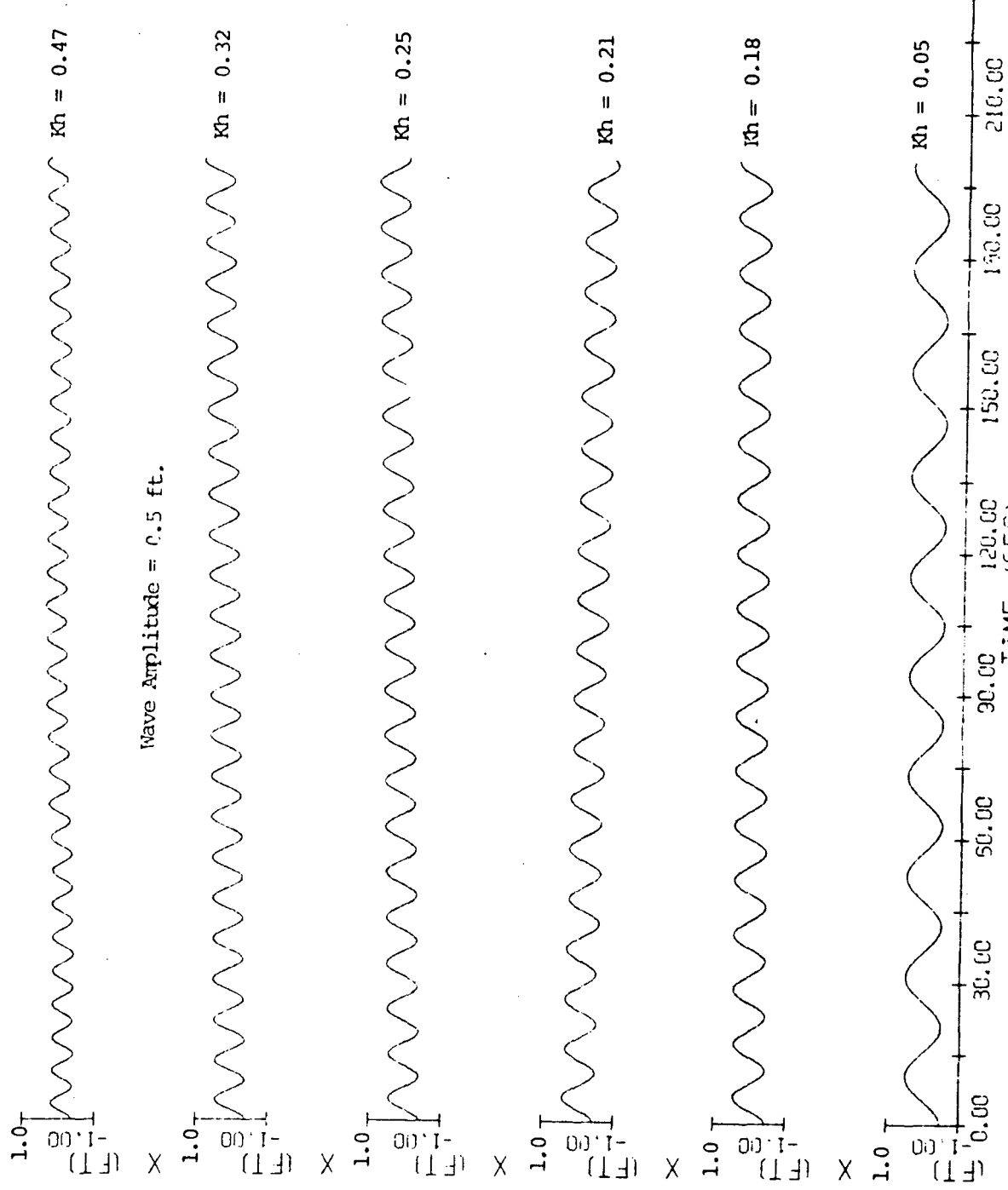


Figure 5.25 Surge motions of the freely floating 'tuned' spar buoy

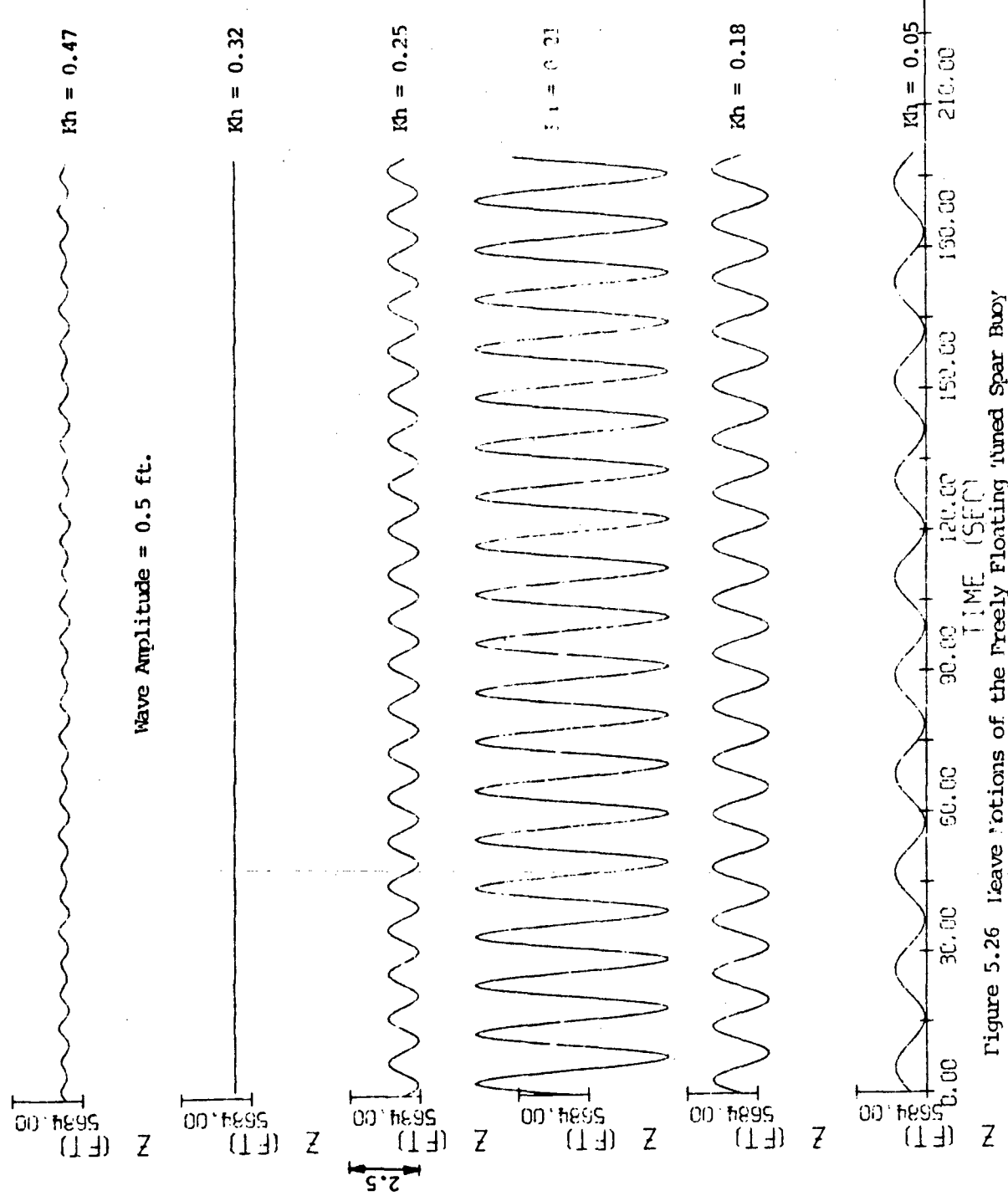


Figure 5.26 Leave motions of the freely floating 'tuned Spar Buoy'

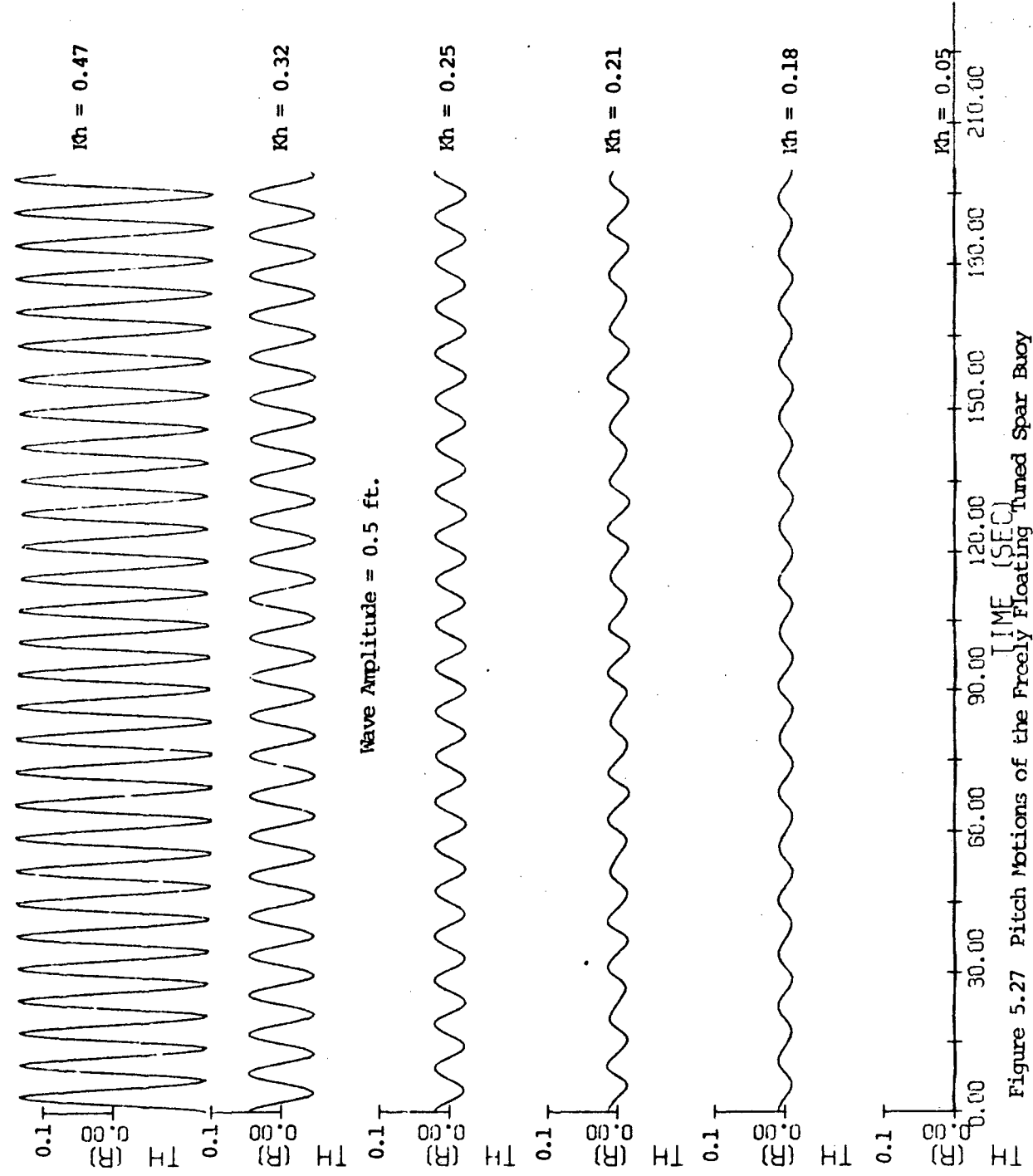


Figure 5.27 Pitch Motions of the Freely Floating Tuned Spar Buoy

SD2T.DATA	1	1	0	25	6	0	5700.	0.020	200.0	0.5
00010	1	1.7	0.5	3.35	5.11	30.				
00020				0.0	1.0					
00021	1.0		0.0	0.0	0.0					
00055	3745.62		0.0	0.0	0.0					
00090	0.0		0.0	0.0	0.0					
00105	0.0		0.0	0.0	0.0					
00110	0.0		0.0	0.0	0.0					
00120		0.30		0.5						
00130		0.55		0.5						
00140		0.60		0.5						
00150		0.66		0.5						
00160		0.74		0.5						
00170		0.90		0.5						
READY										

Table 5.4 Input Data for the 2-D Analysis of the Tuned Spar Buoy

viscous and pressure drag coefficients equal zero.

Figure 5.28 through 5.30 use the same data as Table 5.4 except that viscous and pressure drag coefficients are equal to 1.0. Once again comparisons between the two sets of figures (5.25 through 5.30) show similar differences as explained for the cylindrical spar buoy. In this case the heave resonance occurs at $Kh = 0.22$ and the pitch resonance at $Kh = 0.4$. Also in this case the viscous damping in heave and pitch responses is more pronounced.

Response amplitudes of surge, heave, and pitch; and surge drift as calculated from the steady-state portions of the time histories presented in Figures 5.25 through 5.30, and other similar simulations are tabulated in Table 5.5 which is similar to Table 5.2. In this case the wave amplitudes ξ_0 studied are 0.5 ft. and 2.5 ft. respectively. Data points of Table 5.5 are plotted in Figures 5.31 through 5.34 to presents plots of RAO vs Kh . These plots are similar to Figures 5.8 through 5.11. Figure 5.33b is an expanded view of Figure 5.33a, near the heave resonance frequency. The ratio between buoy heave and the wave amplitude is one at zero frequency and exhibits resonance at Kh of approximately 0.2. The ratio decreases to zero at Kh equal to 0.32, after which it increases a little before decreasing to zero with increasing frequencies. Such behavior, where the heave response is minimized at a given frequency is the main function of a tuned (as opposed to cylindrical) spar buoy.

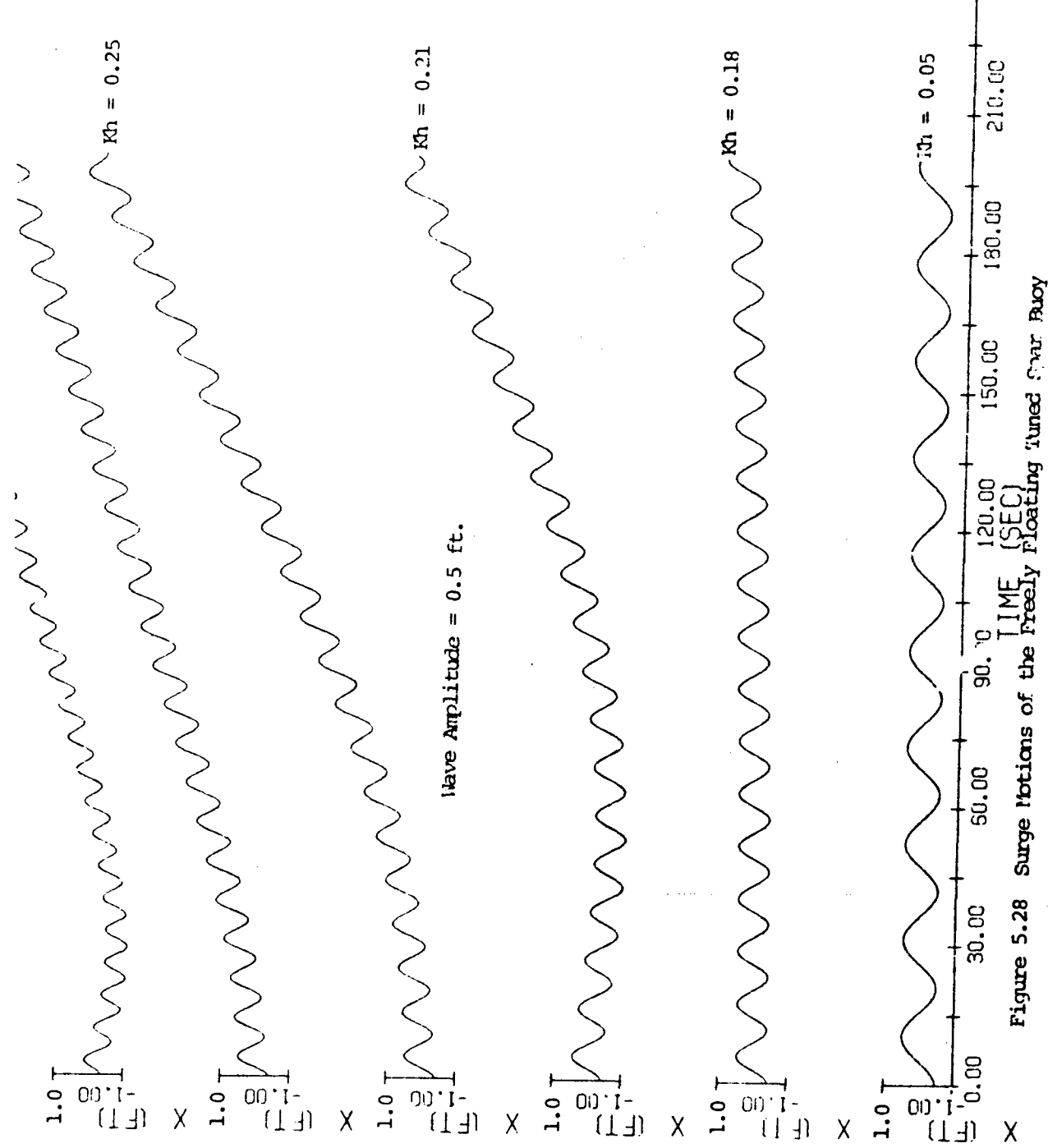


Figure 5.28 Surge Motions of the Freely Floating Tuned Smart Buoy

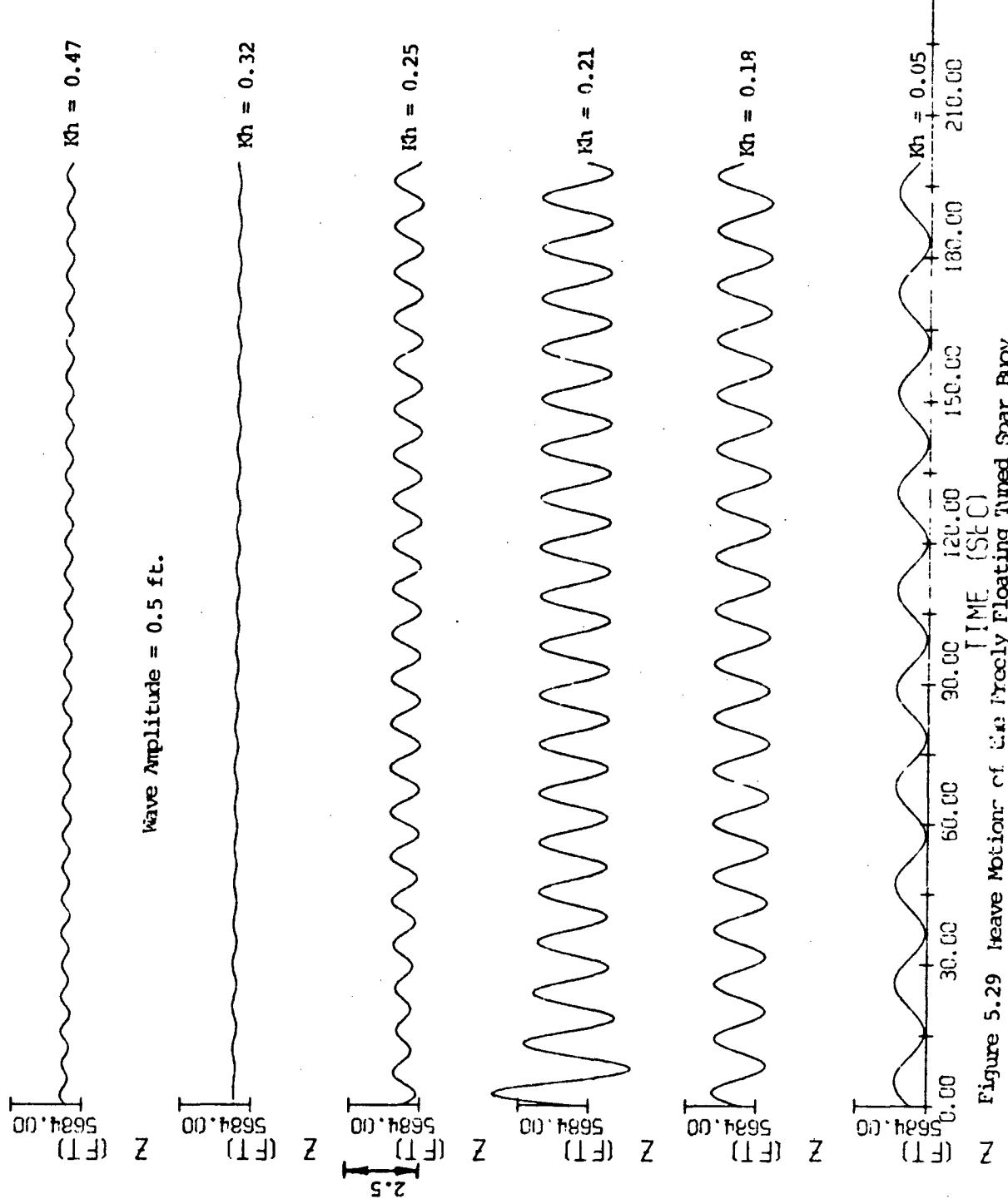


Figure 5.29 Heave Motion of the Freely Floating Tuned Spar Buoy

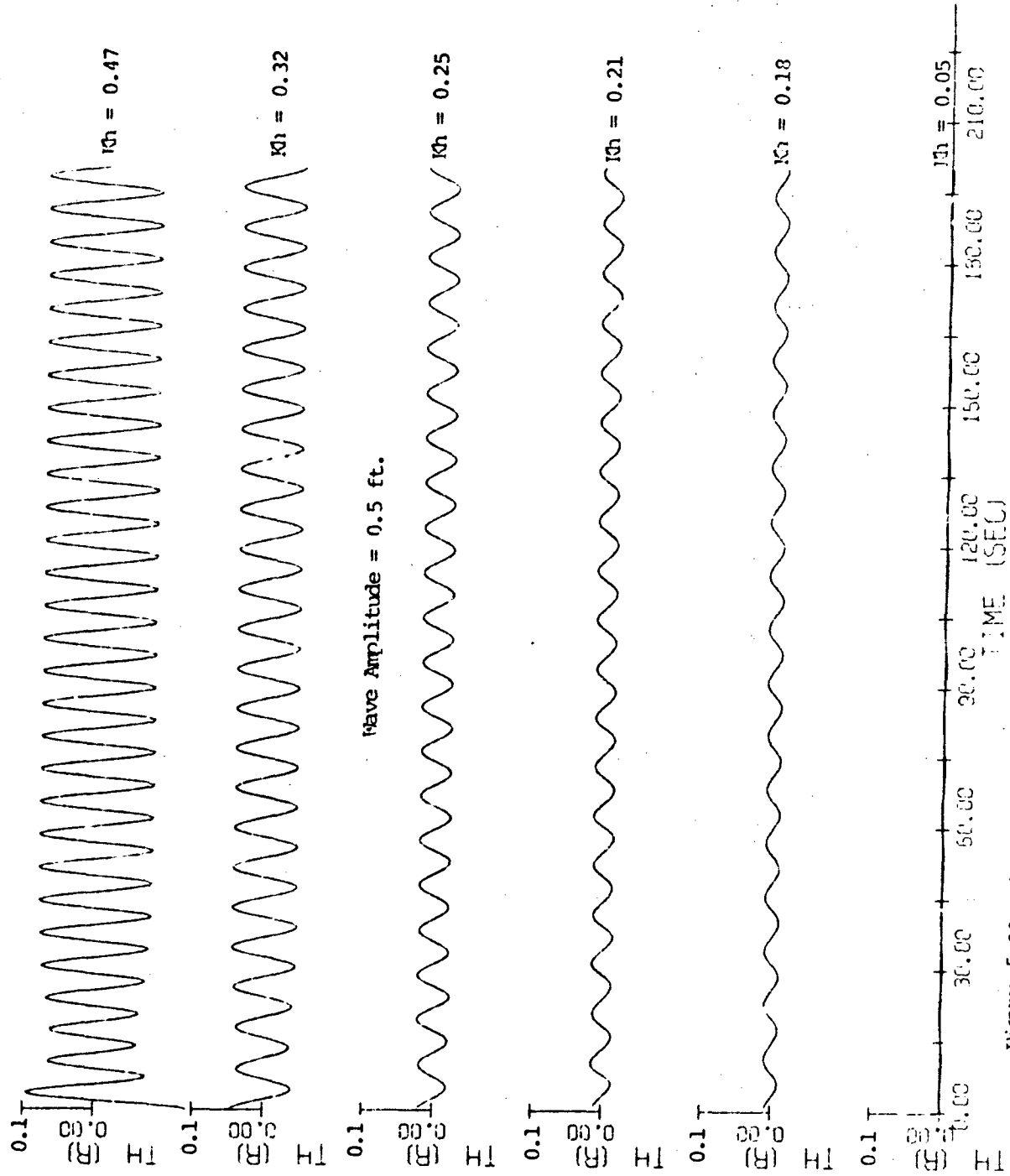


Figure 5.30 Pitch motions of the freely floating tuned Spar Buoy

ω	K_h	Surge Amplitude/%				Heave Amplitude/%				Pitch Amplitude/ k_b^2				Surge Drift/ kw_f^2			
		1	2	3	4	1	2	3	4	1	2	3	4	1	2	3	4
0.30	0.05	-0.96	0.96	0.96	0.96	1.05	1.05	1.05	1.05	1.21	1.23	1.23	1.23	1.38	1.38	1.41	0.48
0.55	0.18	-0.87	0.88	0.88	0.88	1.99	1.99	1.99	1.99	1.54	1.54	1.54	1.54	2.04	2.04	2.02	0.51
0.57	0.19	-0.87	0.87	0.88	0.88	2.58	2.58	2.58	2.58	2.27	2.51	2.51	2.51	2.17	2.17	2.17	4.13
0.59	0.20	-0.86	0.85	0.85	0.85	4.20	4.20	4.20	4.20	2.53	2.53	2.53	2.53	2.34	2.34	2.33	33.40
0.60	0.21	-0.85	0.86	0.82	0.85	6.87	6.87	6.87	6.87	2.50	1.46	1.46	1.46	2.43	2.77	2.53	2.44
0.63	0.23	-0.84	0.78	0.78	0.78	-4.15	-4.15	-4.15	-4.15	1.87	1.87	1.87	1.87	2.75	2.75	2.77	48.93
0.66	0.25	-0.82	0.84	0.81	0.81	0.81	0.81	0.81	0.81	-1.07	-1.07	-1.07	-1.07	0.86	3.10	3.26	2.94
0.70	0.29	-0.81	0.82	0.82	0.82	-0.29	-0.29	-0.29	-0.29	0.34	0.34	0.34	0.34	4.03	4.03	3.96	17.24
0.74	0.32	-0.79	0.82	0.81	0.81	0.77	0.77	0.77	0.77	-0.02	0.02	0.02	0.02	0.40	5.51	5.51	1.49
0.83	0.40	-0.74	0.67	0.67	0.67	0.21	0.21	0.21	0.21	0.24	0.24	0.24	0.24	35.79	35.79	7.81	15.61
0.90	0.47	-0.70	0.55	0.60	0.60	0.67	0.67	0.67	0.67	0.27	0.36	0.36	0.36	0.31	-10.62	11.34	6.44
1.01	0.59	-0.64	0.58	0.58	0.58	0.30	0.30	0.30	0.30	0.30	0.30	0.30	0.30	-3.43	-3.43	3.26	1.82
1.17	0.80	-0.55	0.51	0.51	0.51	0.28	0.28	0.28	0.28	0.26	0.26	0.26	0.26	-1.69	-1.69	1.67	1.55
1.61	1.50	-0.34	0.30	0.30	0.30	0.17	0.17	0.17	0.17	0.17	0.17	0.17	0.17	-0.62	-0.62	0.62	0.42

Table 5.5 Dynamic Response (Surge, Heave and Pitch Amplitude; and Surge Drift) of a Tuned Spar Buoy to Waves

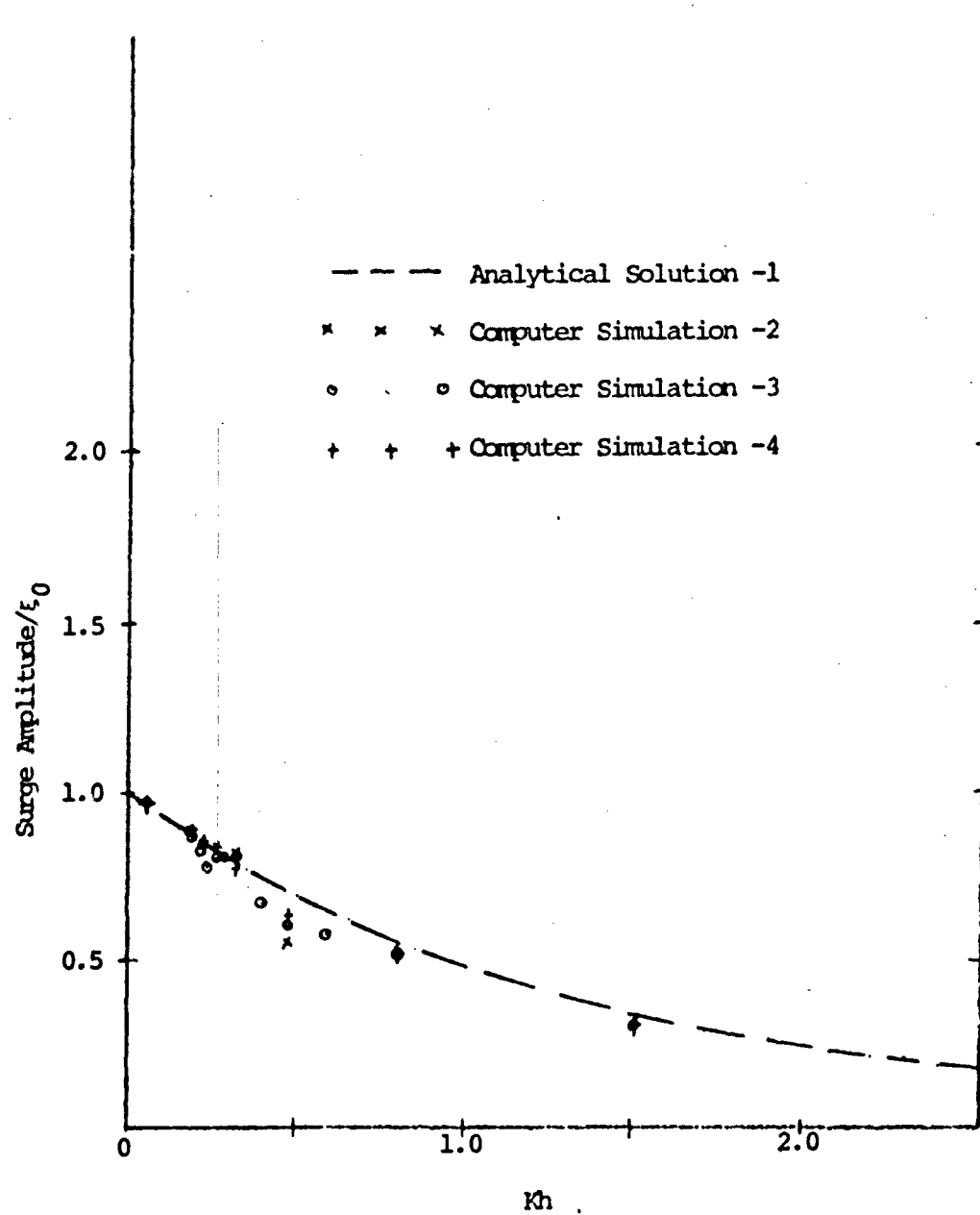


Figure 5.31 Surge Magnification Vs Kh

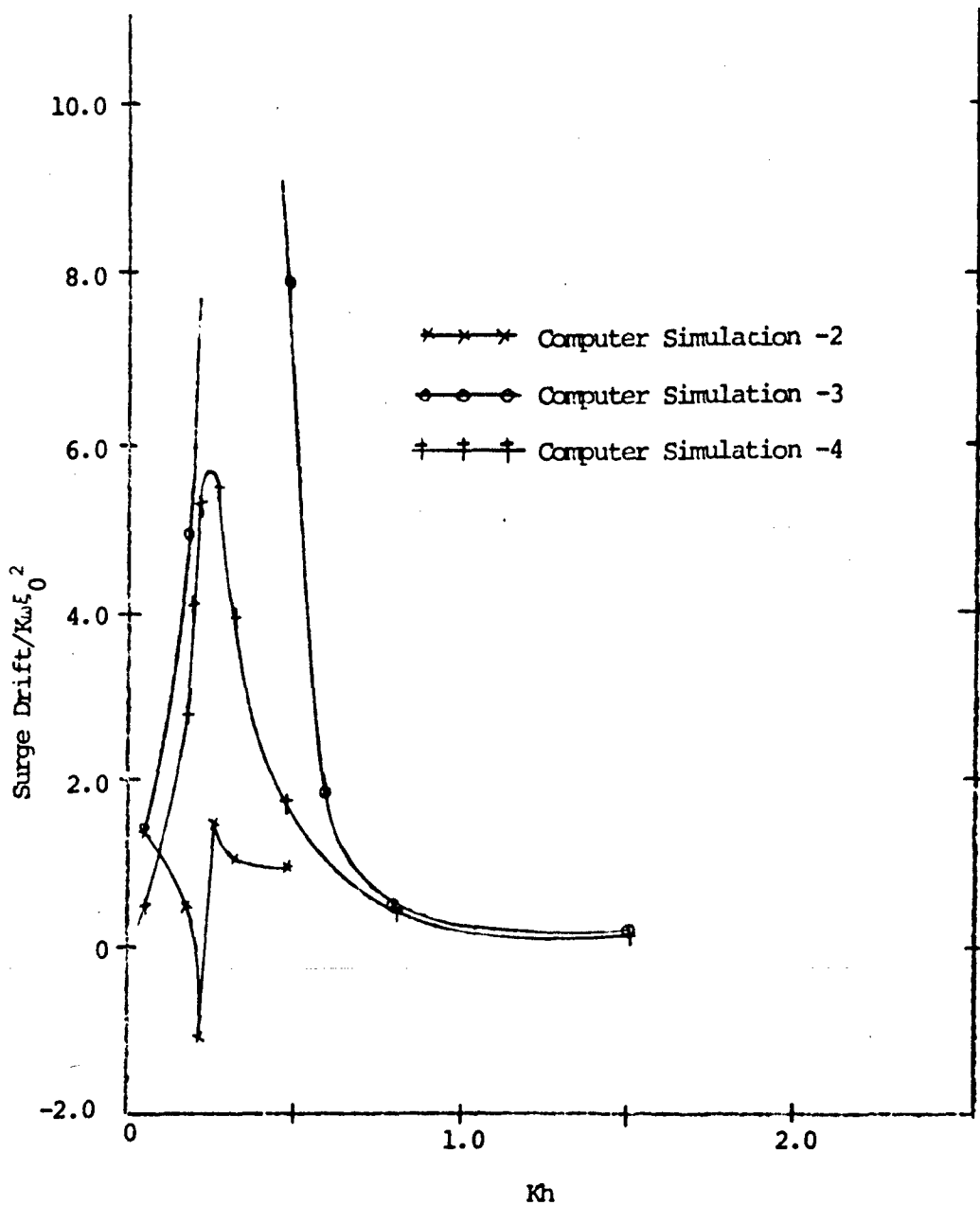


Figure 5.32 Surge Drift Vs Kh

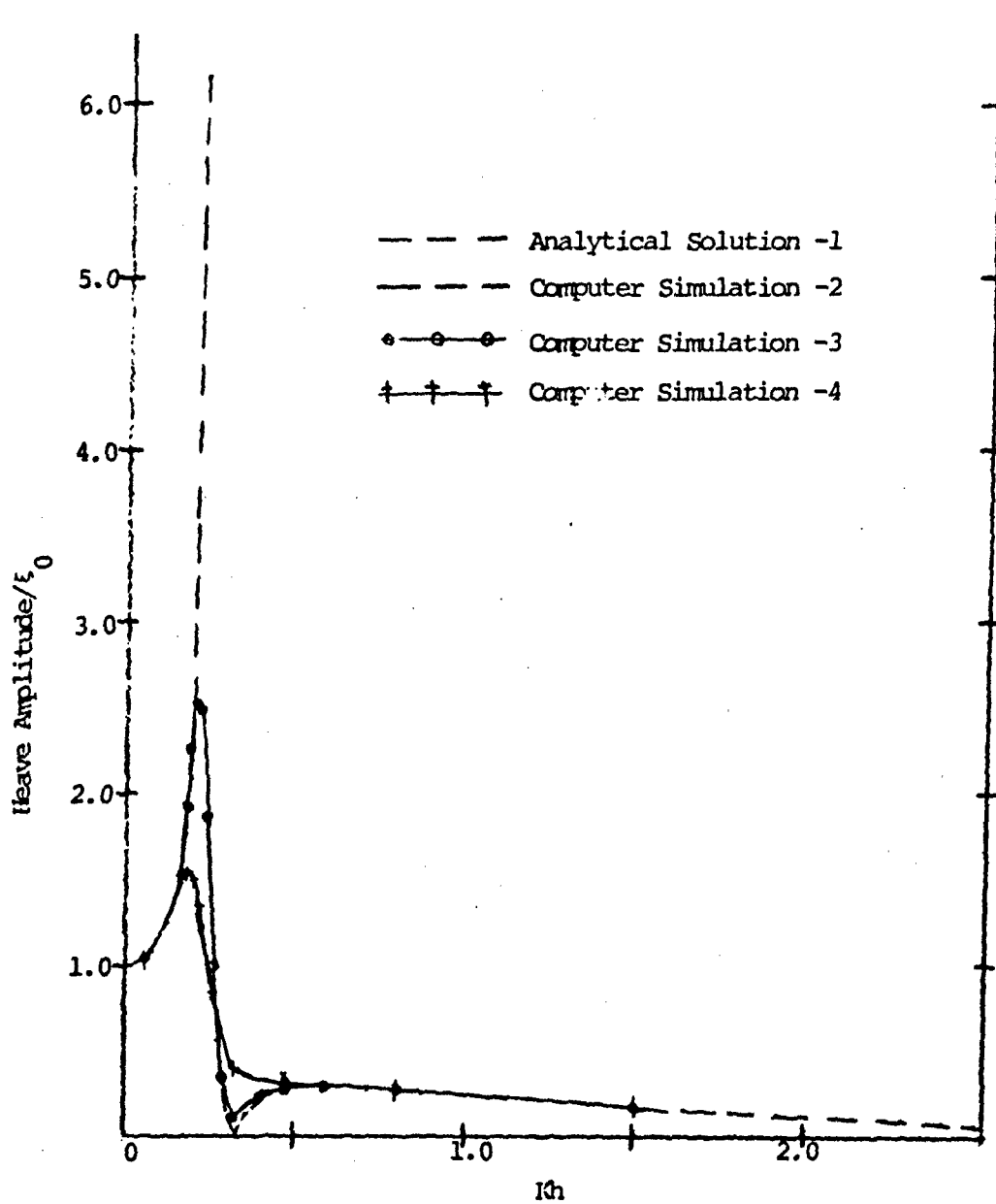


Figure 5.33a Heave Magnification Vs Kh

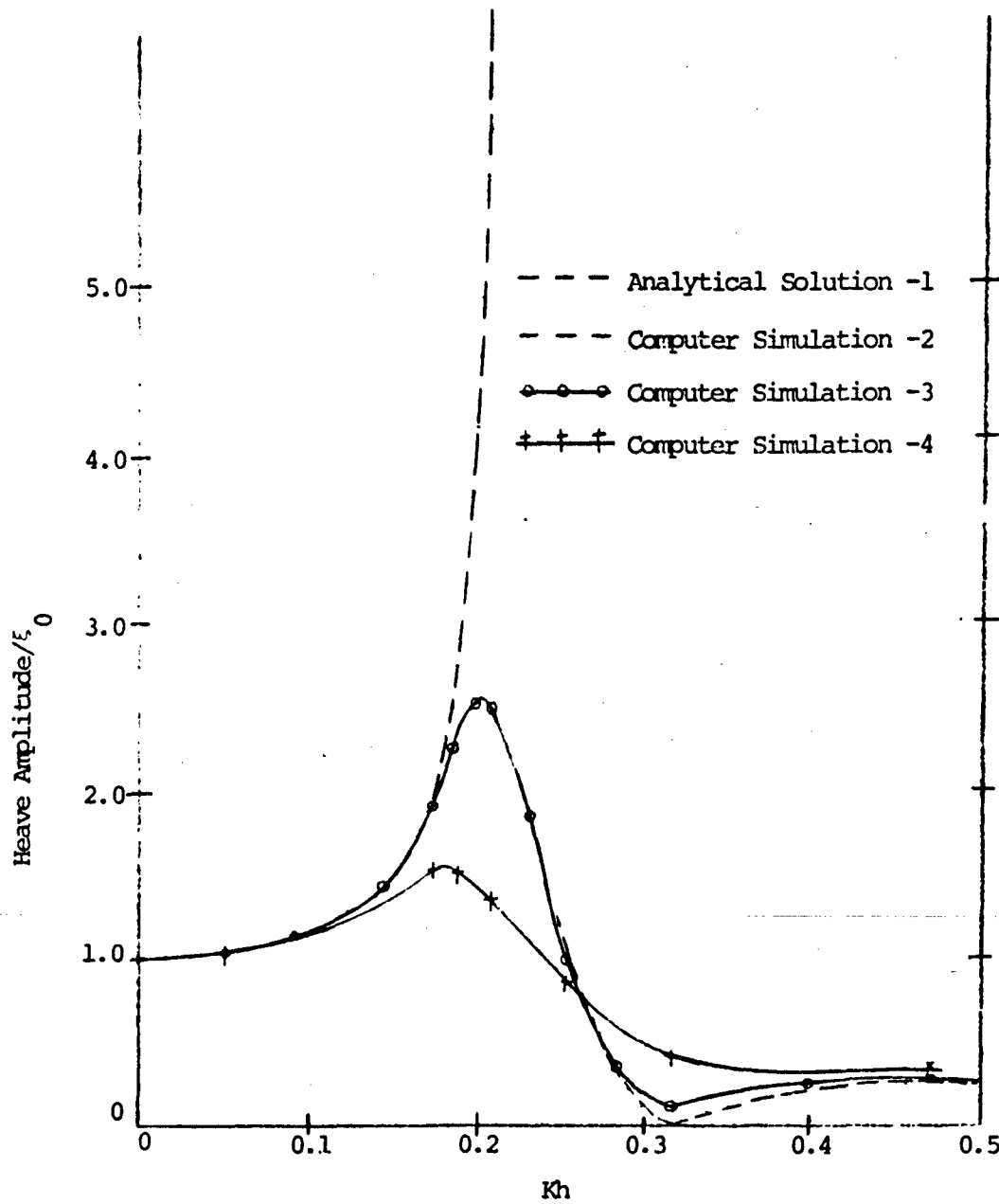


Figure 5.33b Expanded View of Figure 5.33a

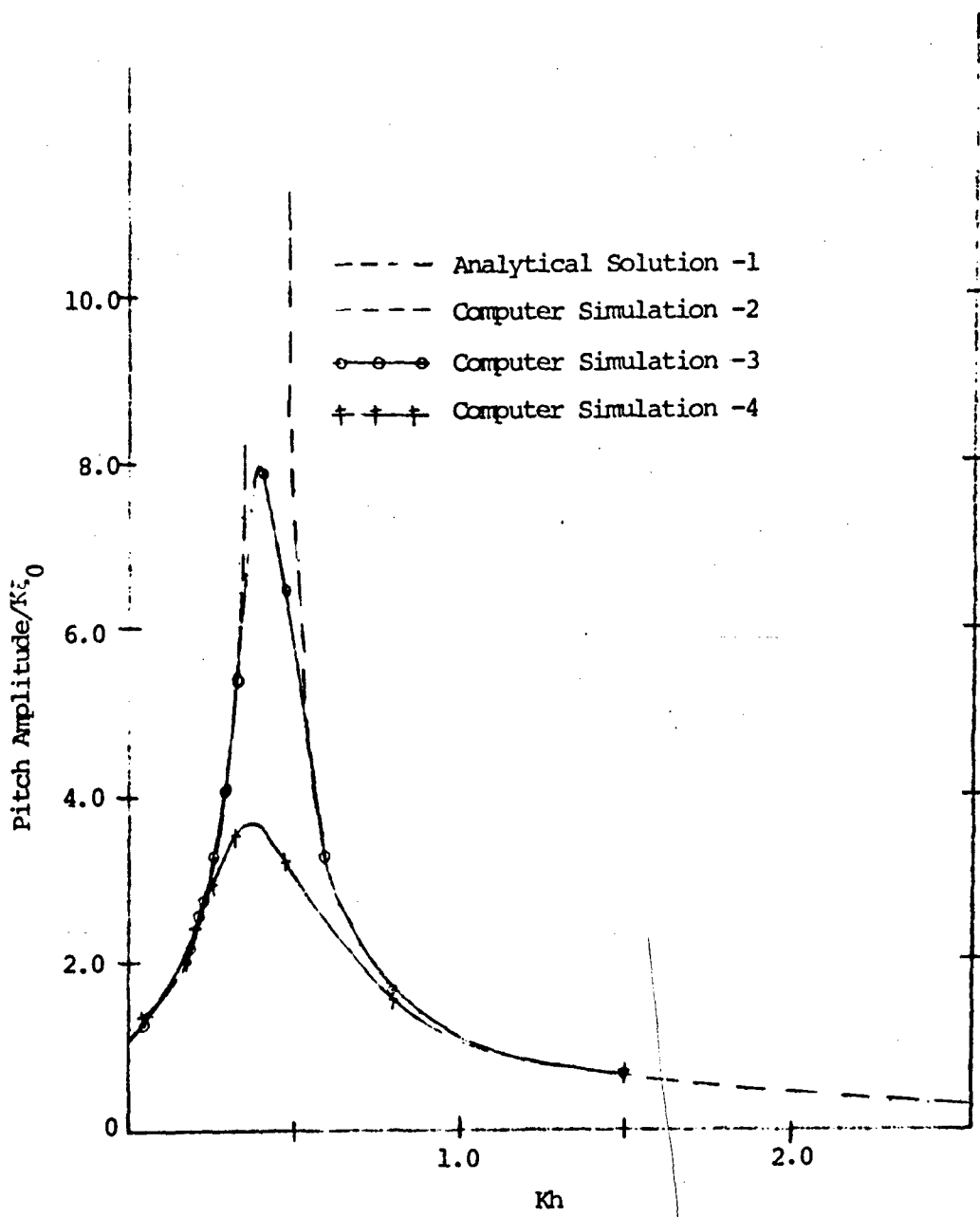


Figure 5.34 Pitch Magnification Vs Kh

Three-Dimensional Simulations

Figures 5.35 through 5.40 present the surge, sway, heave, roll, pitch, and yaw responses of the buoy to surface waves of the same amplitude and frequencies as in Figures 5.28 to 5.30.

Table 5.6 is the input data used in conjunction with the computer program SD3.FORT to obtain these simulations. Here β equals zero.

Differences between Figure 5.28 and 5.35 can be attributed directly to the assumptions of three-dimensional analysis. Simulations for the same data as Table 5.6 and $\beta = \pi/4$ are presented in Figures 5.41 through 5.46.

5.2 Subsurface Moored System

Three dimensional computer programs (S3S3.FORT, SSD3.FORT and SSD31.FORT) described in Section 4.2 are used for these simulations. Mooring system used as a case study for these simulations is shown in Figure 5.47. This mooring system was actually deployed during the MODE experiment and was called mooring No. 1 (station 481).

Figures 5.48 and 5.49 display the three coordinates (x , y , z) of the top of this mooring line in response to the relative velocity data displayed in Figures 5.50 and 5.51. This simulation is a part of the study (CHHABRA, 1976), where the current record from the topmost vector-averaging

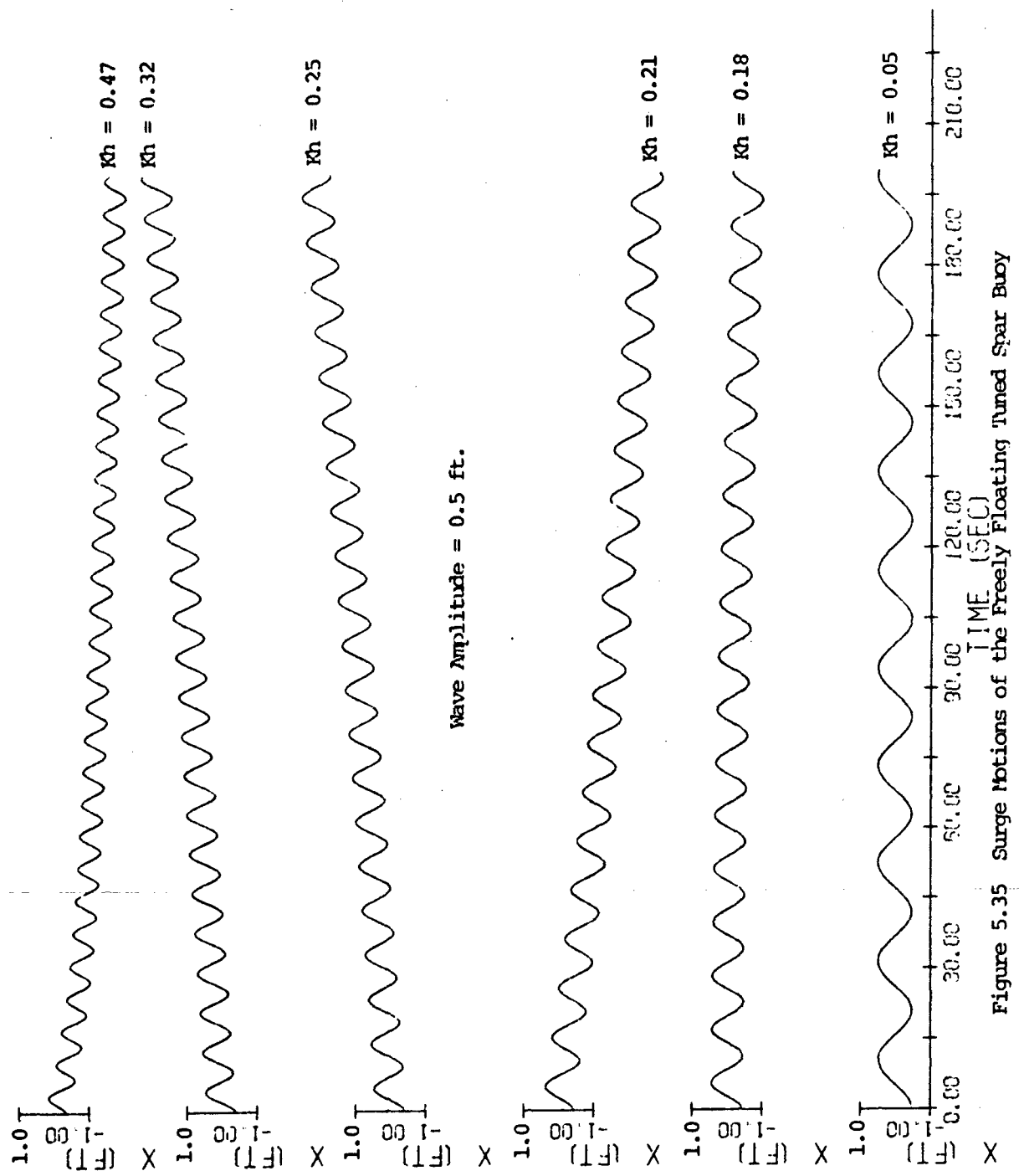


Figure 5.35 Surge Motions of the Freely Floating Tuned Spar Buoy

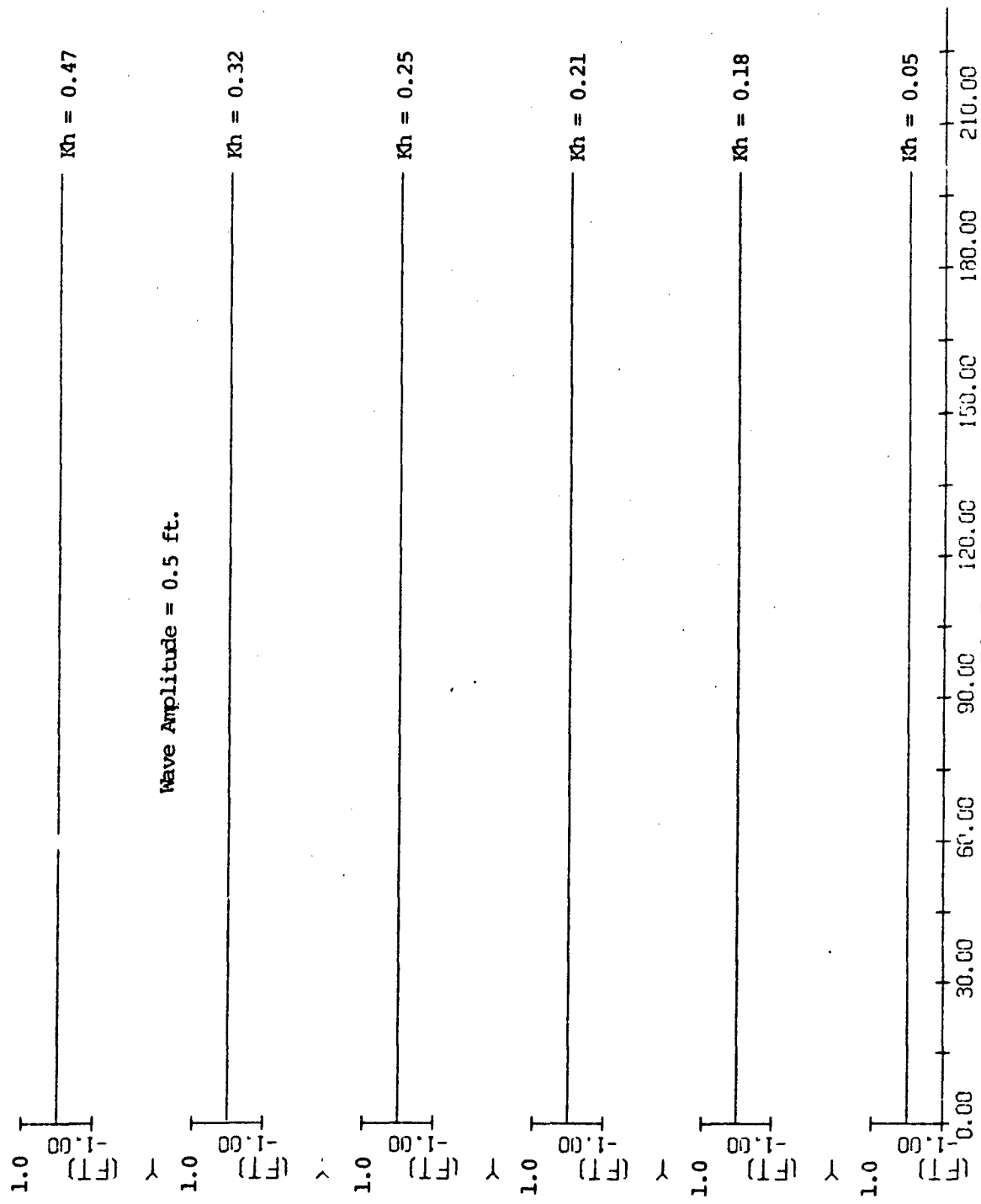


Figure 5.36 Sway Motions of the Freely Floating Tuned Spar Buoy

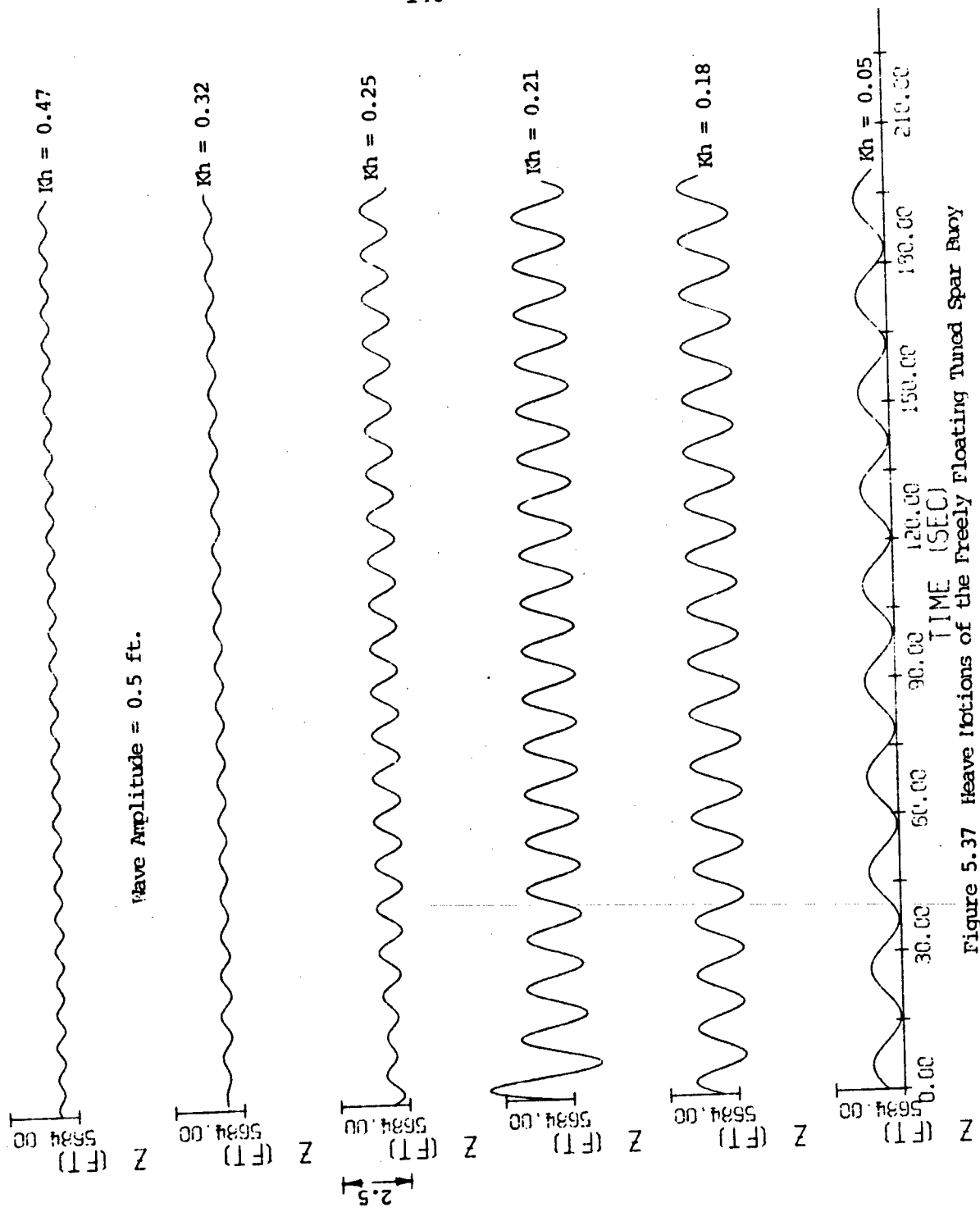


Figure 5.37 Heave motions of the freely floating tuned spar buoy

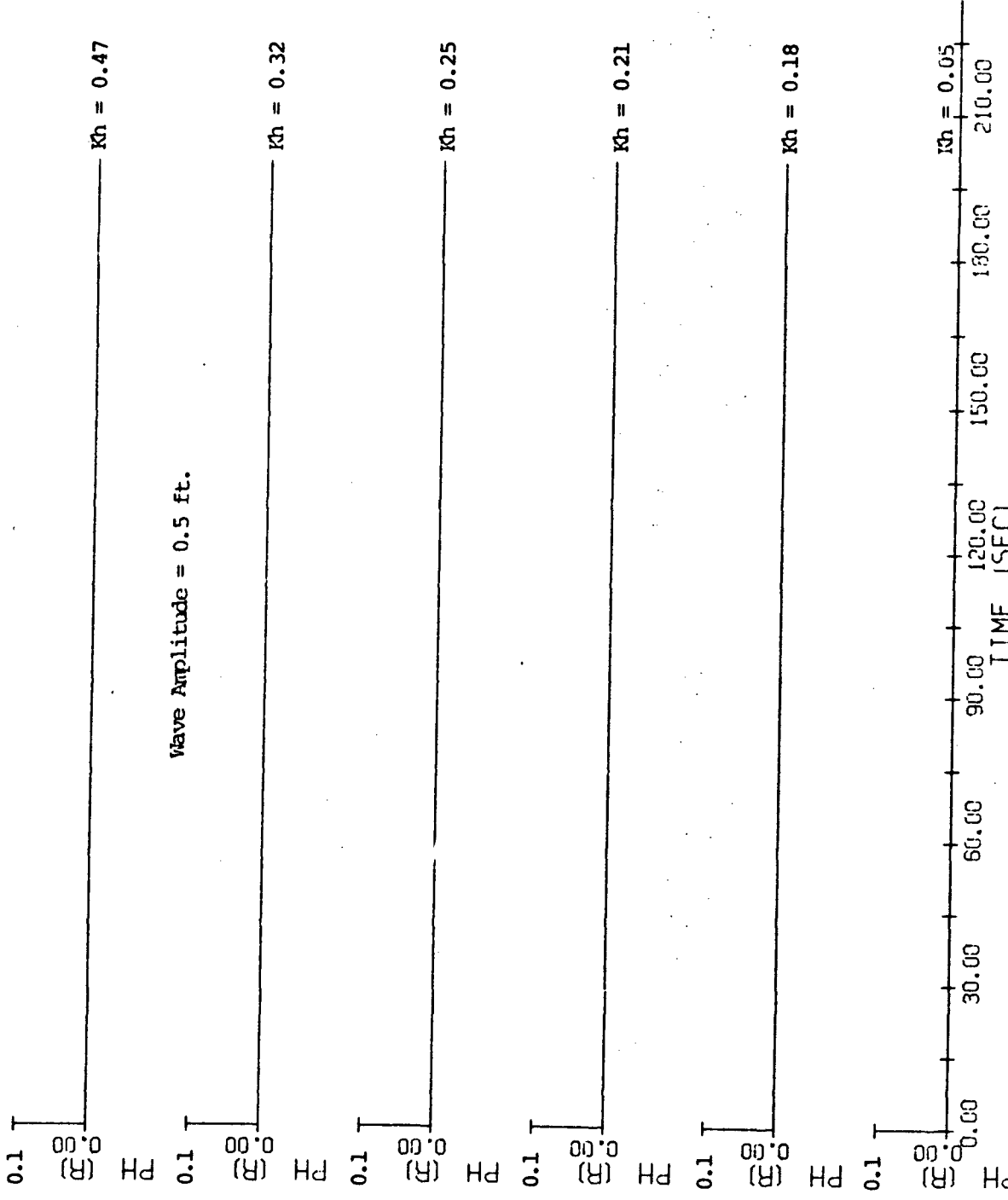


Figure 5.38 Roll Motions of the Freely Floating Tuned Spar Buoy

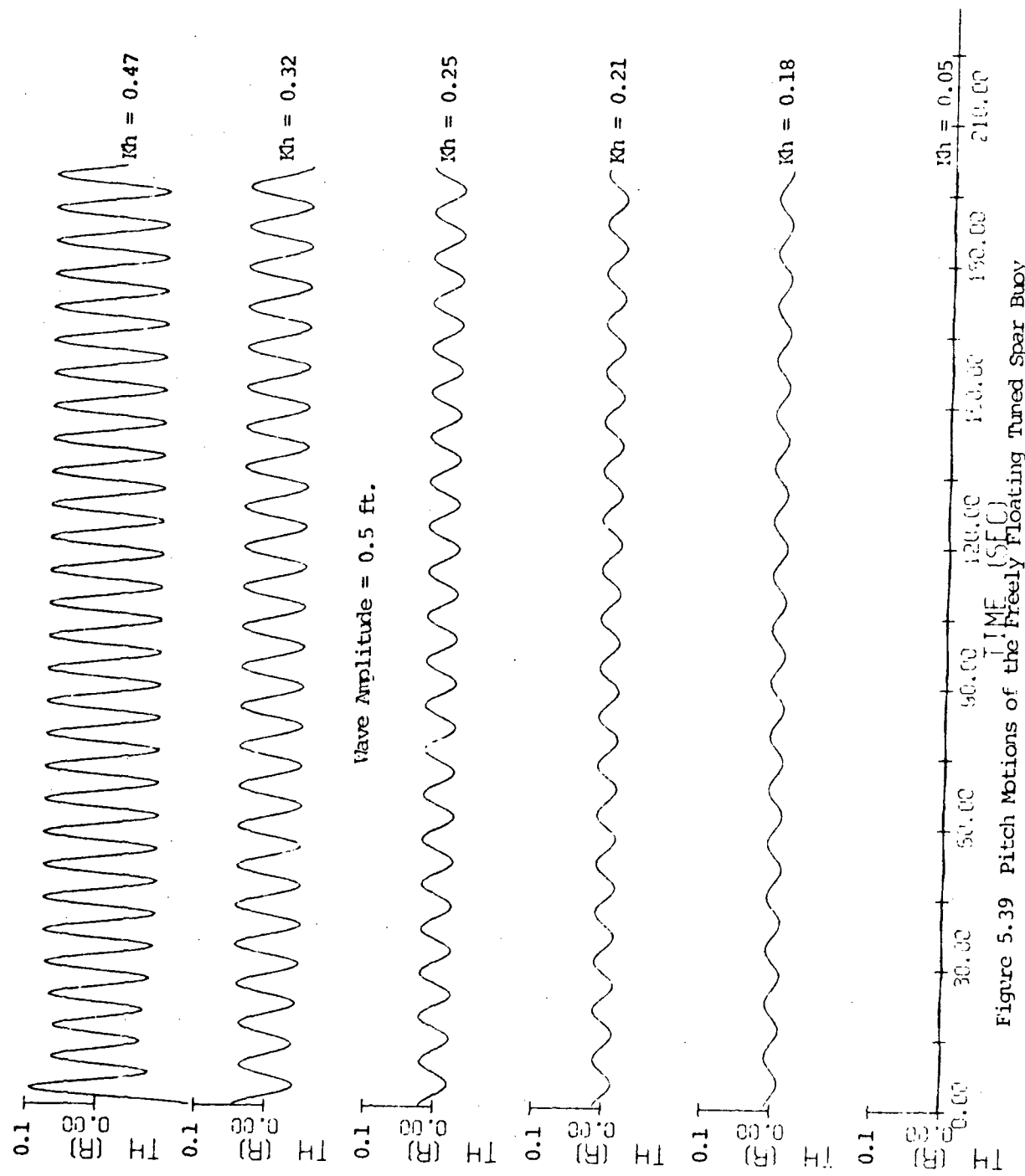


Figure 5.39 Pitch Motions of the Freely Floating Tuned Spar Buoy

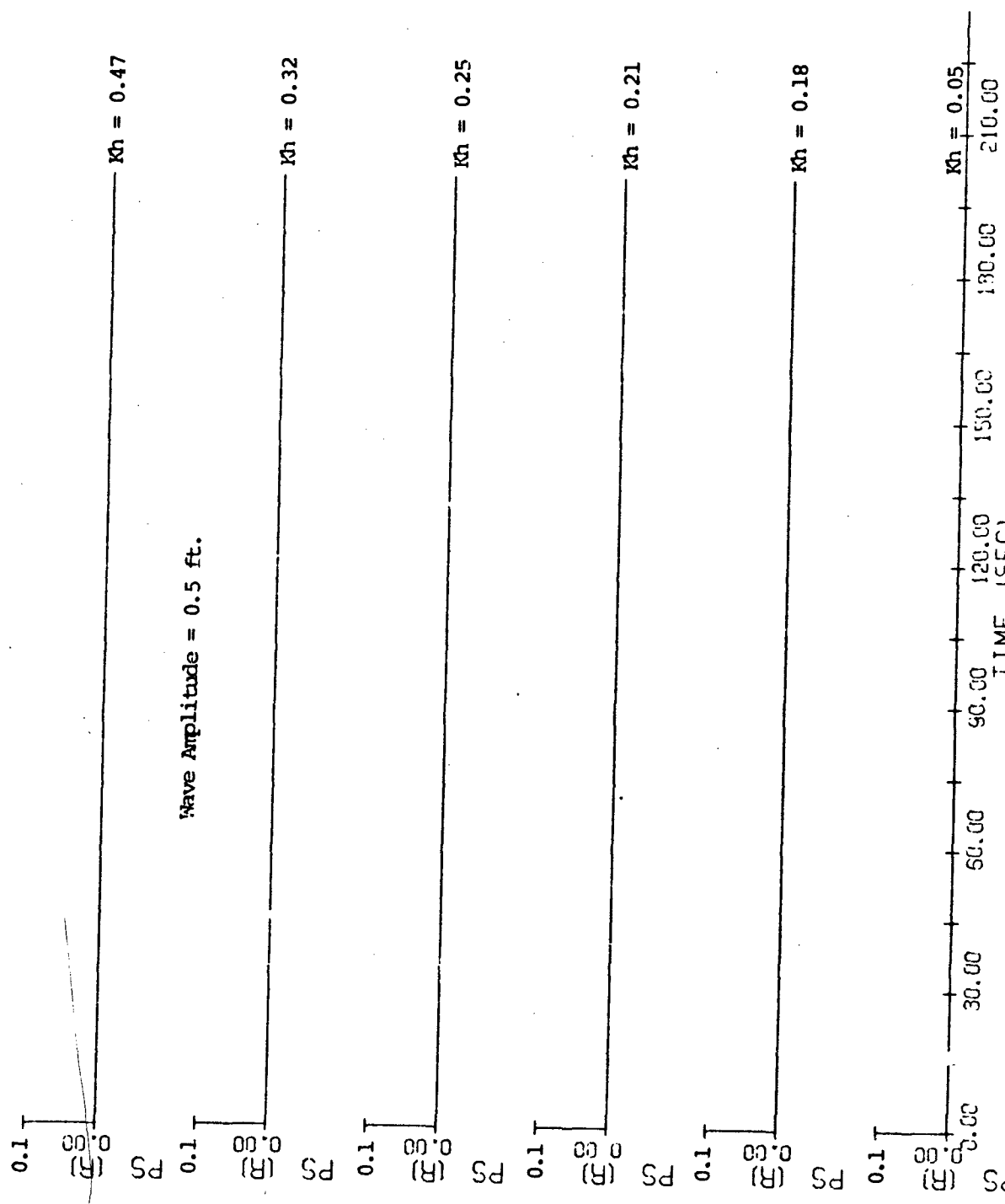


Figure 5.40 Yaw Motions of the Freely Floating Tuned Spar Buoy

STBUOY.DATA							
00010	1	1	0	25	6	0	5700.
00020	1.7	0.5	1.0	3.35	5.11	0.020	200.0
00021	1.0	1.0				30.	1.0
00055	3745.62	0.		0.	0.		5.27
00090	0.	0.		0.	0.		0.
00105	0.	0.		0.	0.		0.
00110	0.	0.		0.	0.		0.
00120	0.30	0.5		0.0	0.0		
00130	0.55	0.5		0.0	0.0		
00140	0.60	0.5		0.0	0.0		
00150	0.66	0.5		0.0	0.0		
00160	0.74	0.5		0.0	0.0		
00170	0.90	0.5		0.0	0.0		
READY							

Table 5.6 Input Data for the 3-D Analysis of the Tuned Star Buoy

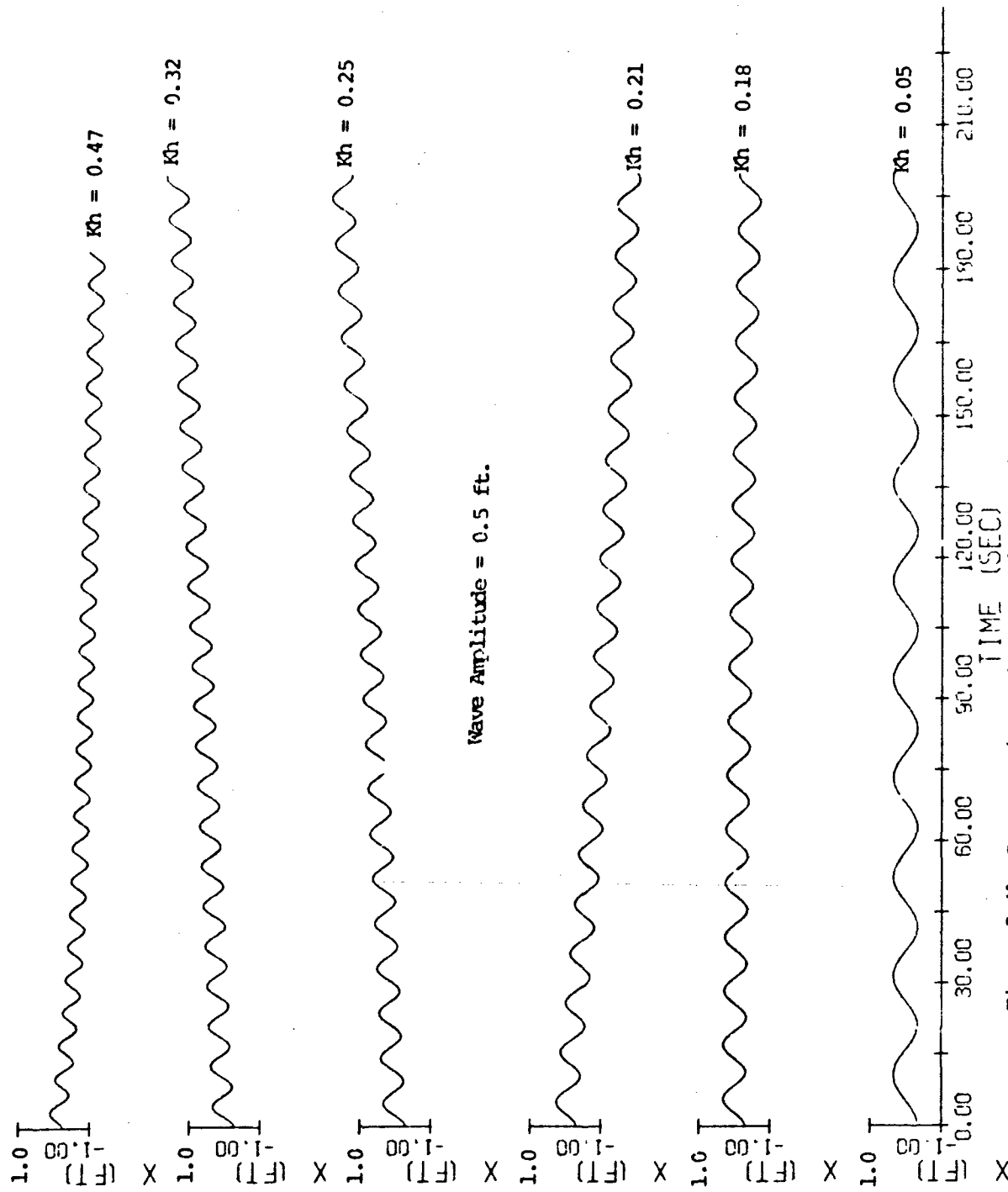


Figure 5.41 Surge Motions of the Freely Floating Tuned Spar Buoy

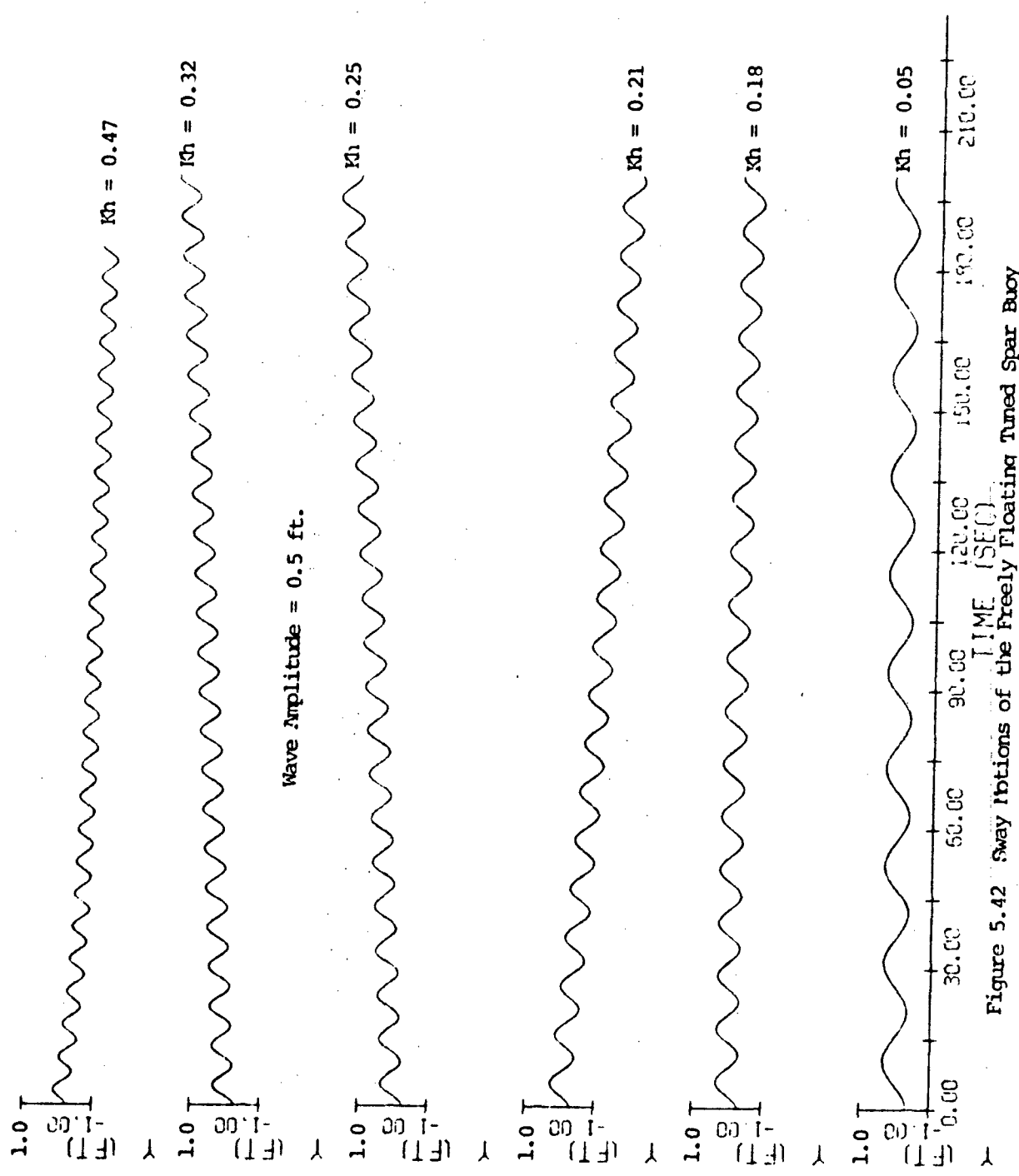


Figure 5.42 Sway Motions of the Freely Floating Tuned Spar Buoy

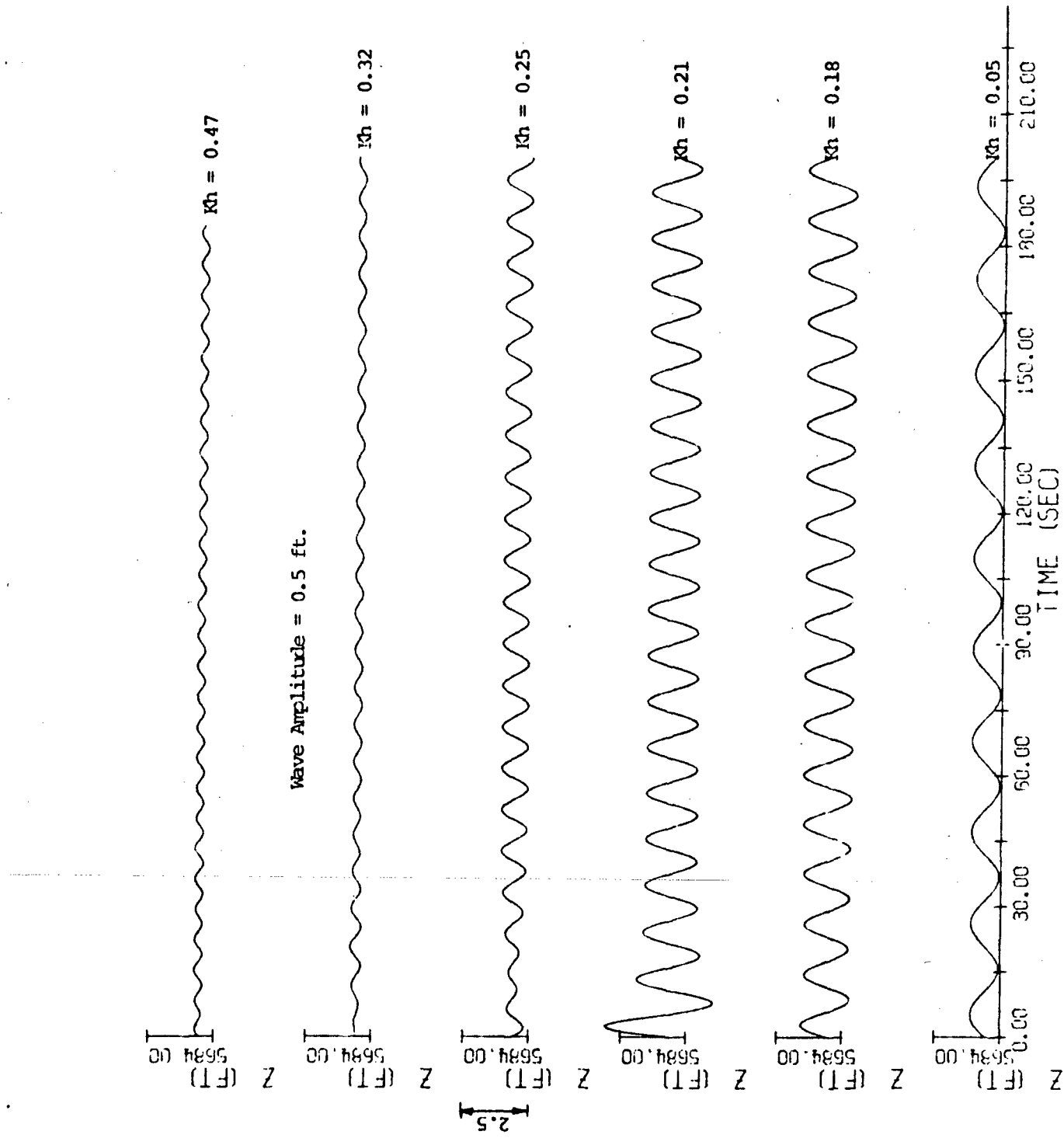


Figure 5.43 Heave motions of the freely floating Tuned Spar Buoy

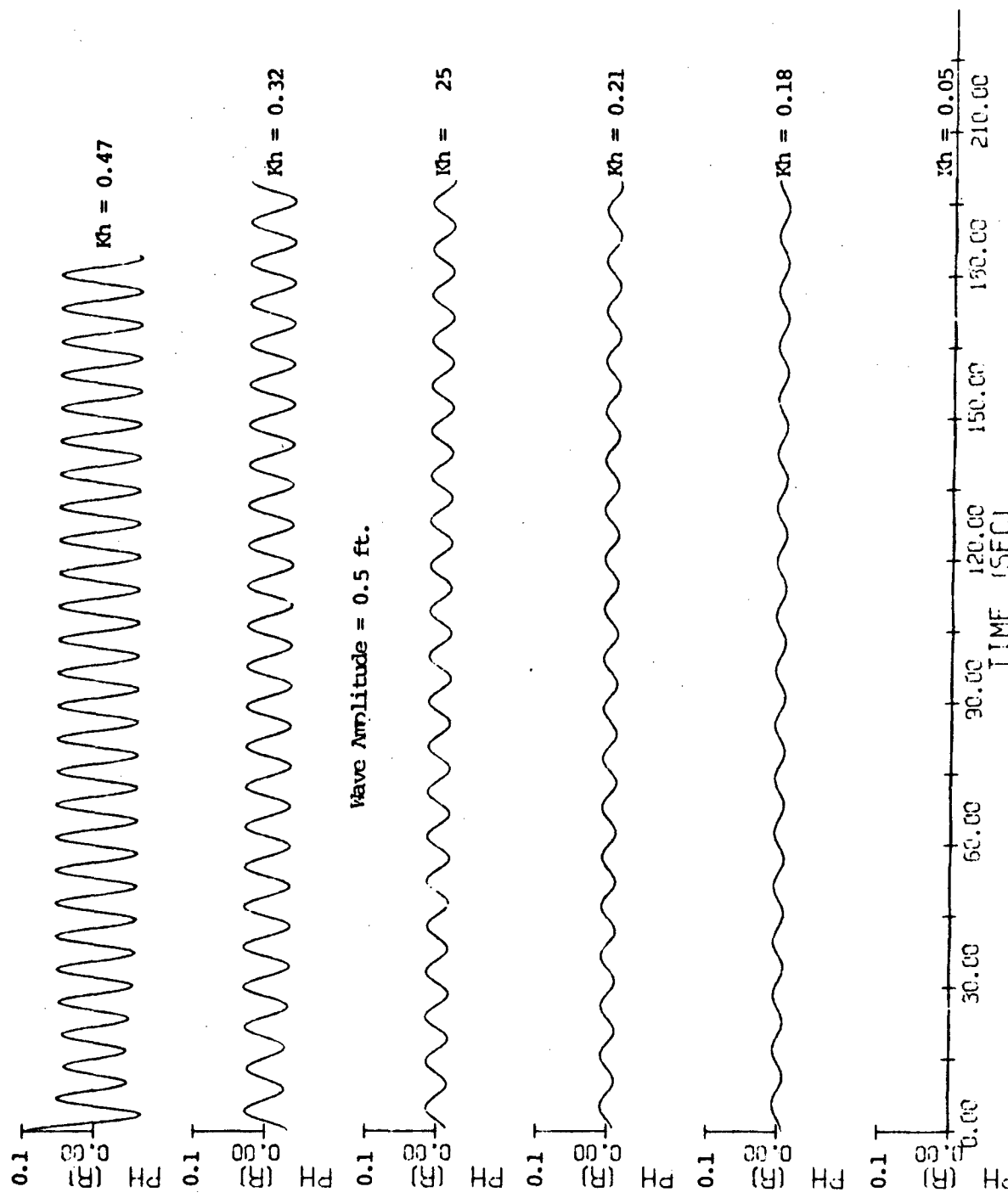


Figure 5.44 Roll motions of the freely floating tuned Spar Body

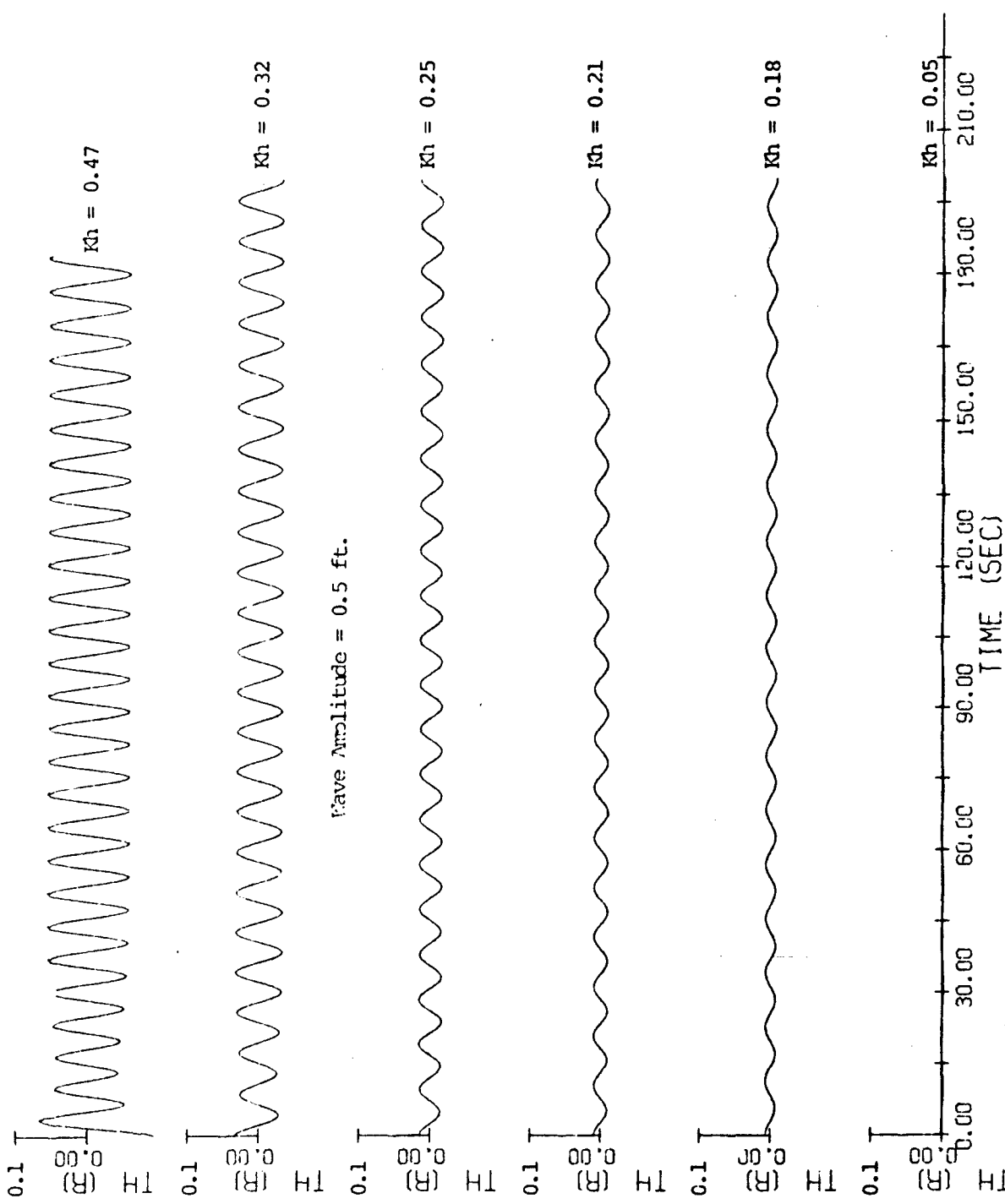


Figure 5.45 Pitch Rotations of the Freely Floating Tuned Spar Buoy

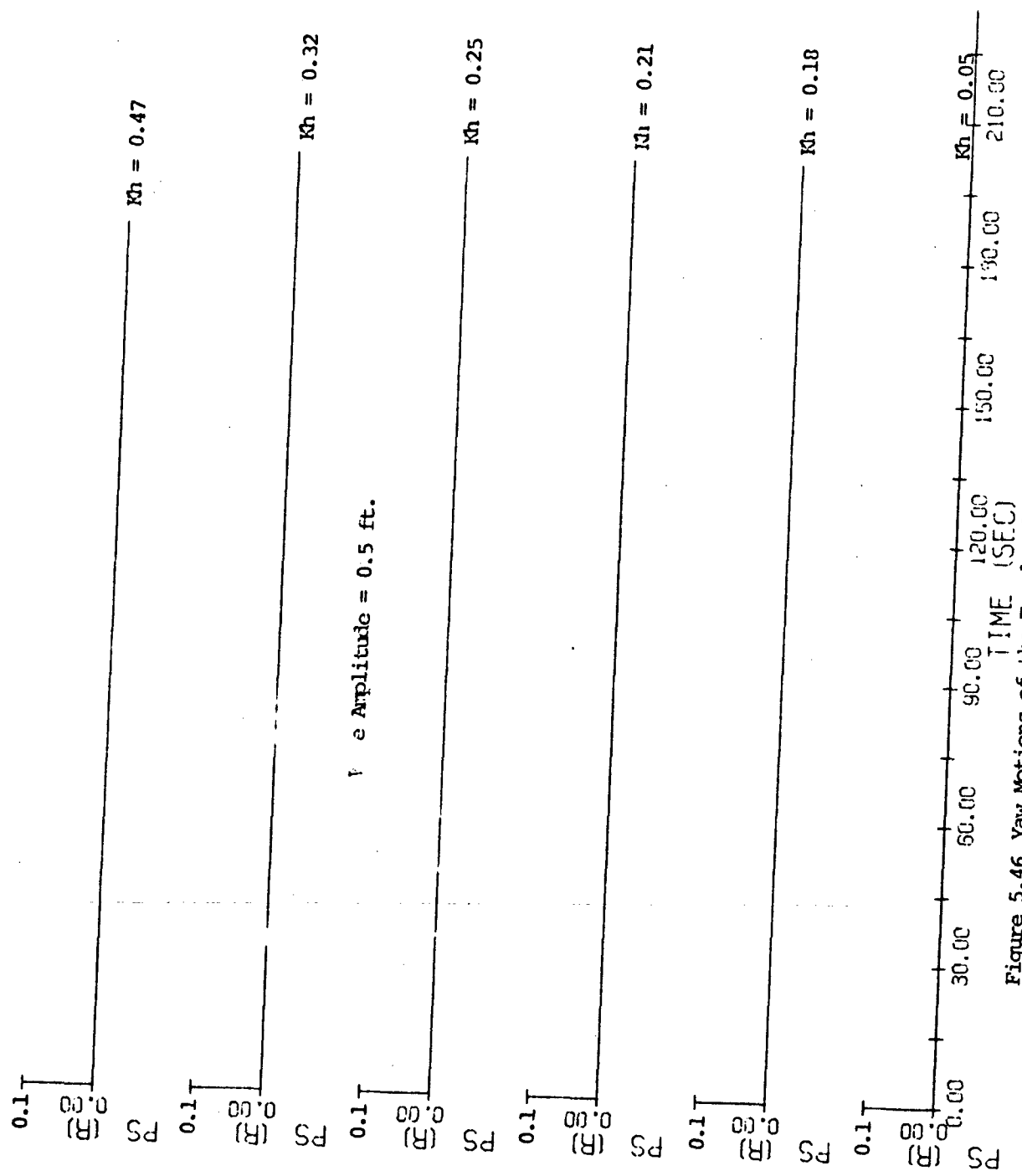


Figure 5.46 Yaw Motions of the Freely Floating Tuned Spar Buoy

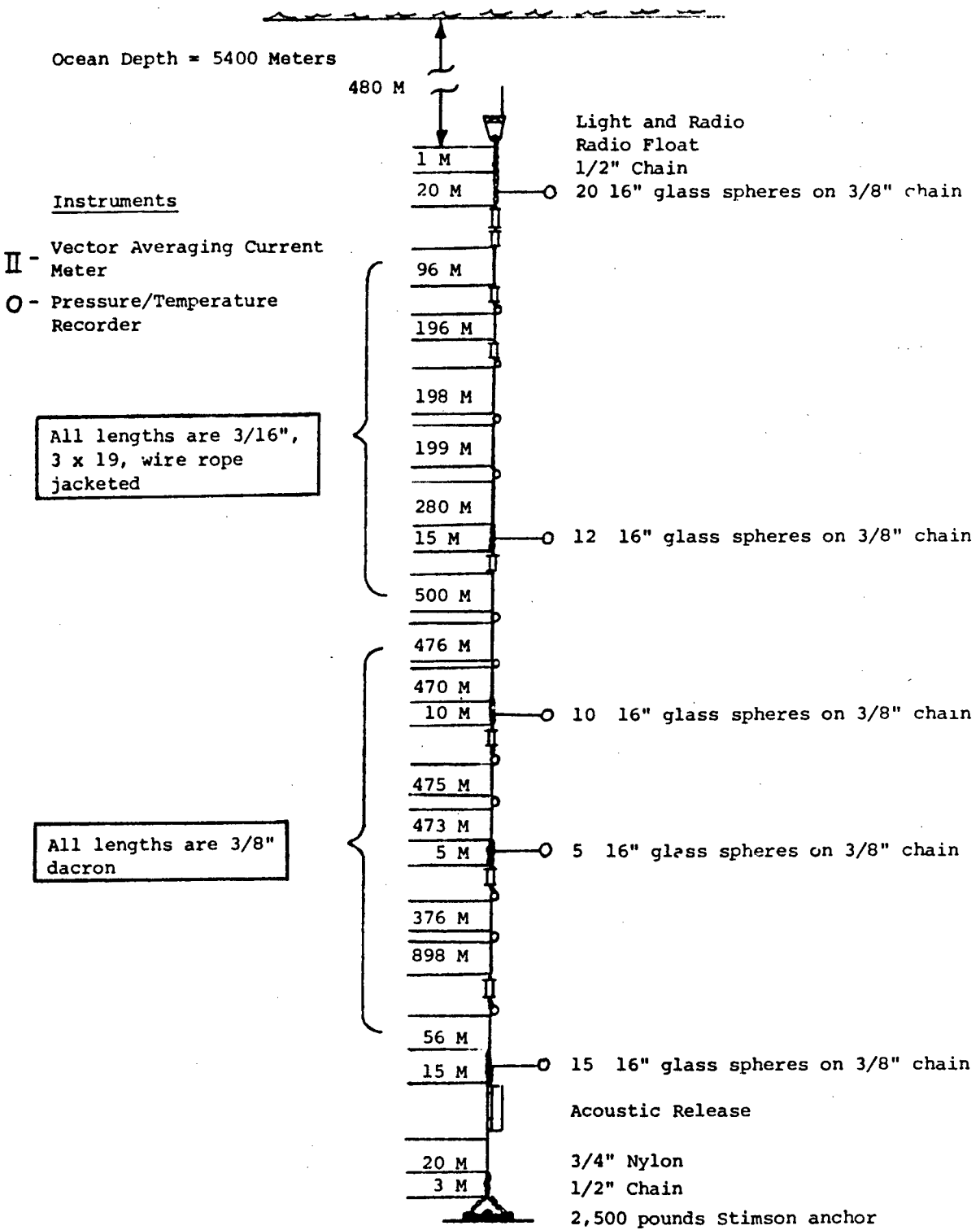


Figure 5.47 Subsurface Moored System

-158-

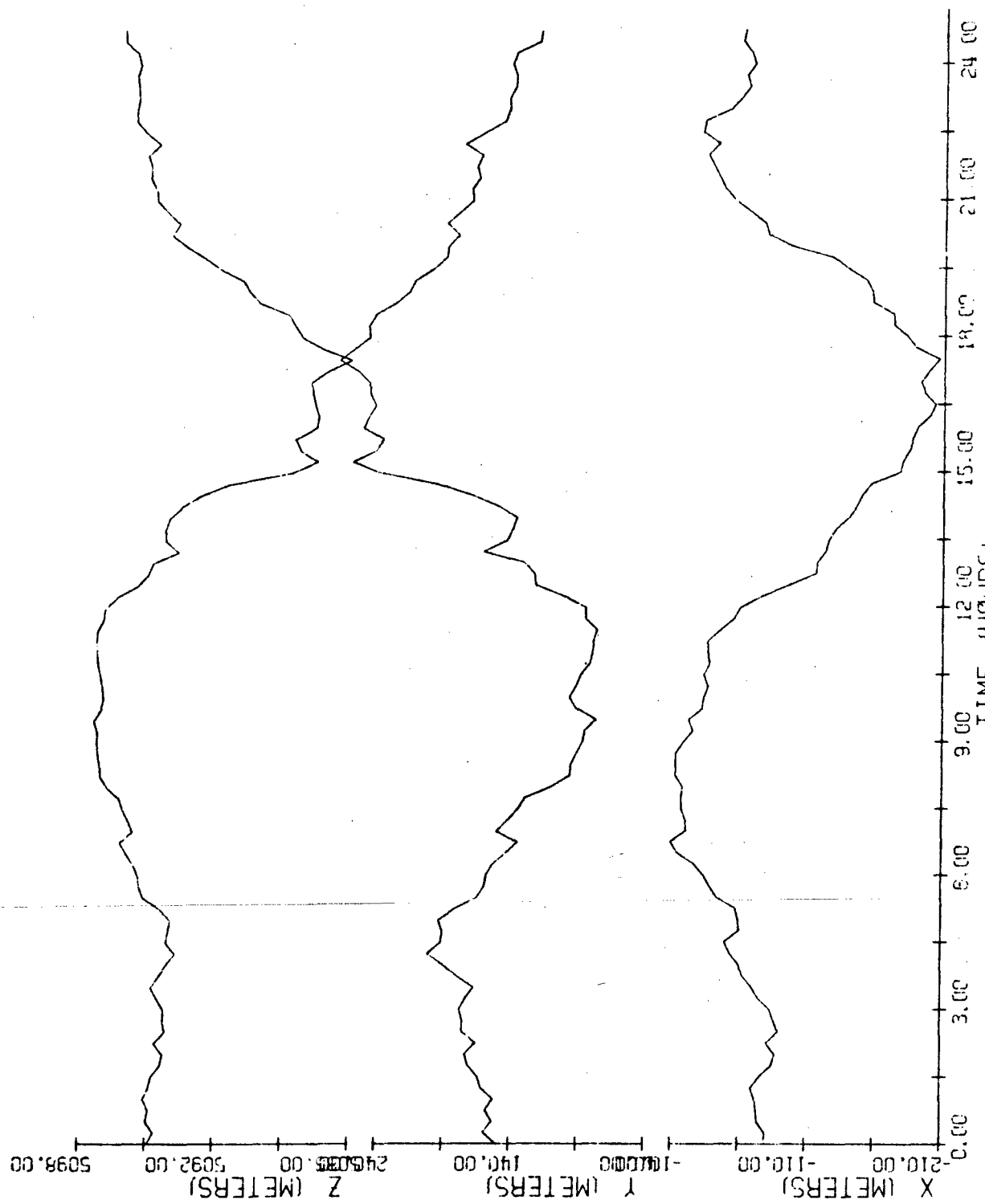


Figure 5.48 Motion of the Subsurface Moored System 10a

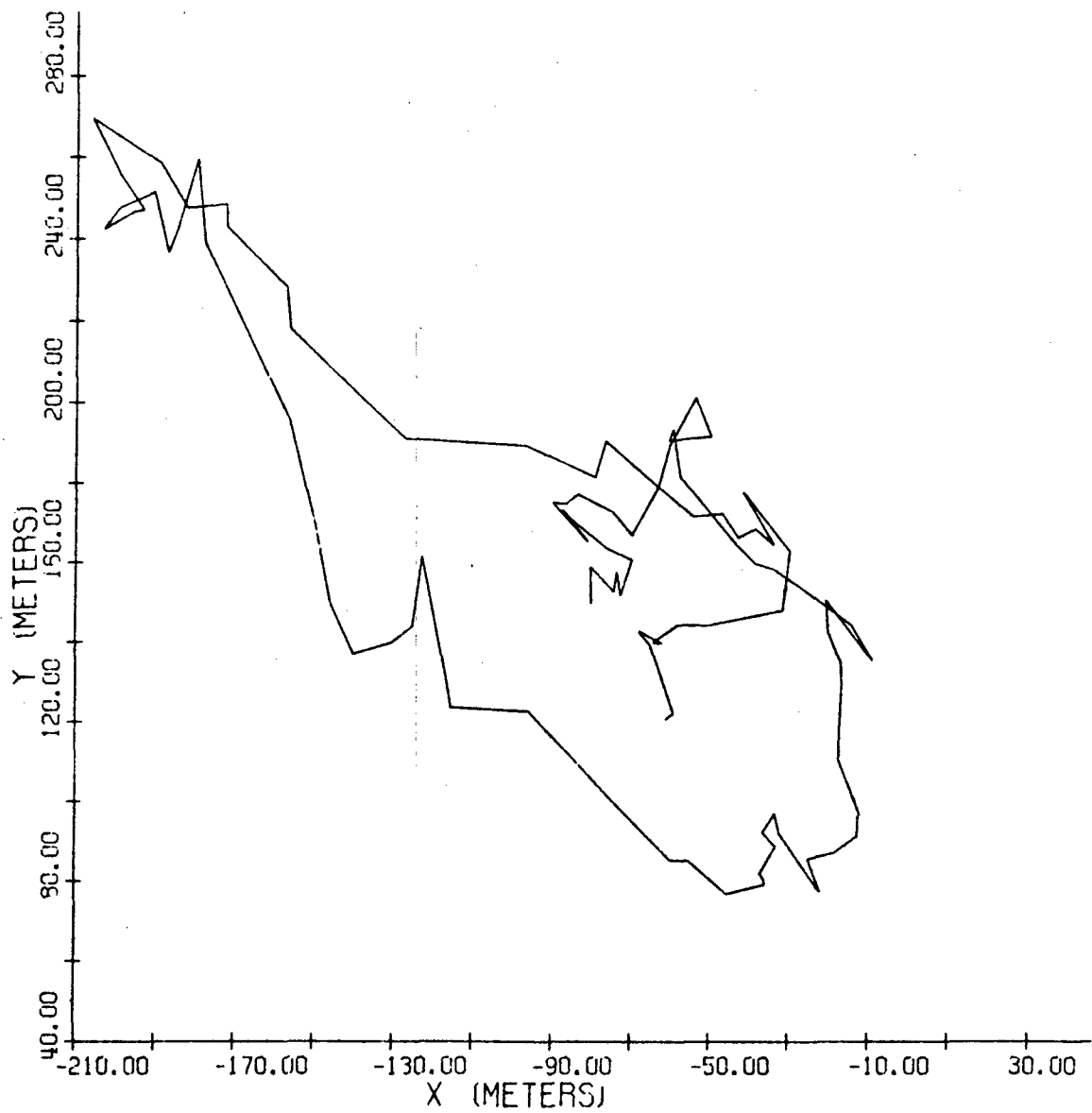


Figure 5.49 Trajectory of the Subsurface Moored System Top

VACM-EAST COMPONENTS

-160-

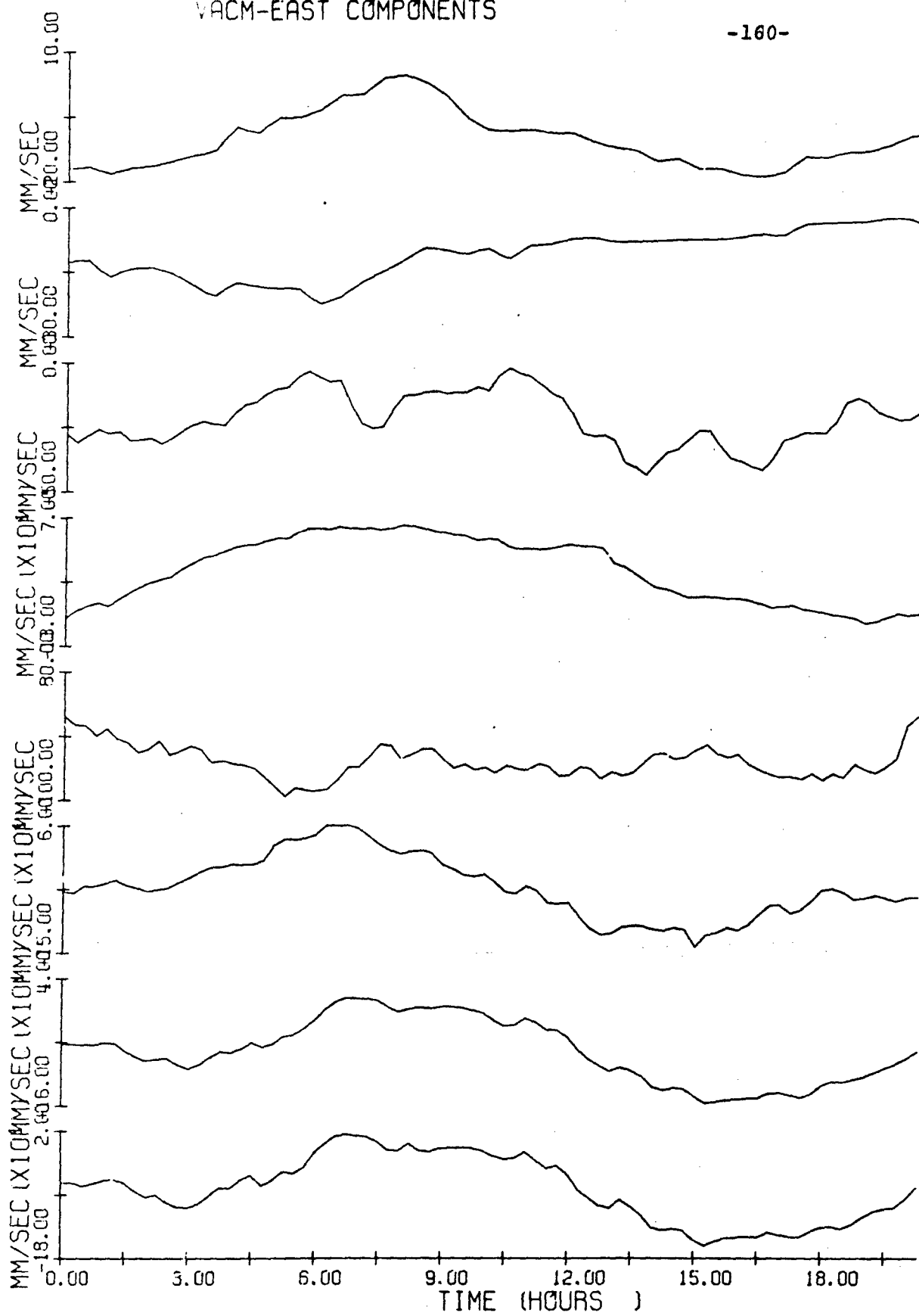


Figure 5.50 Relative Velocity Data for Subsurface Moored System

VACM-NORTH COMPONENTS

-161-

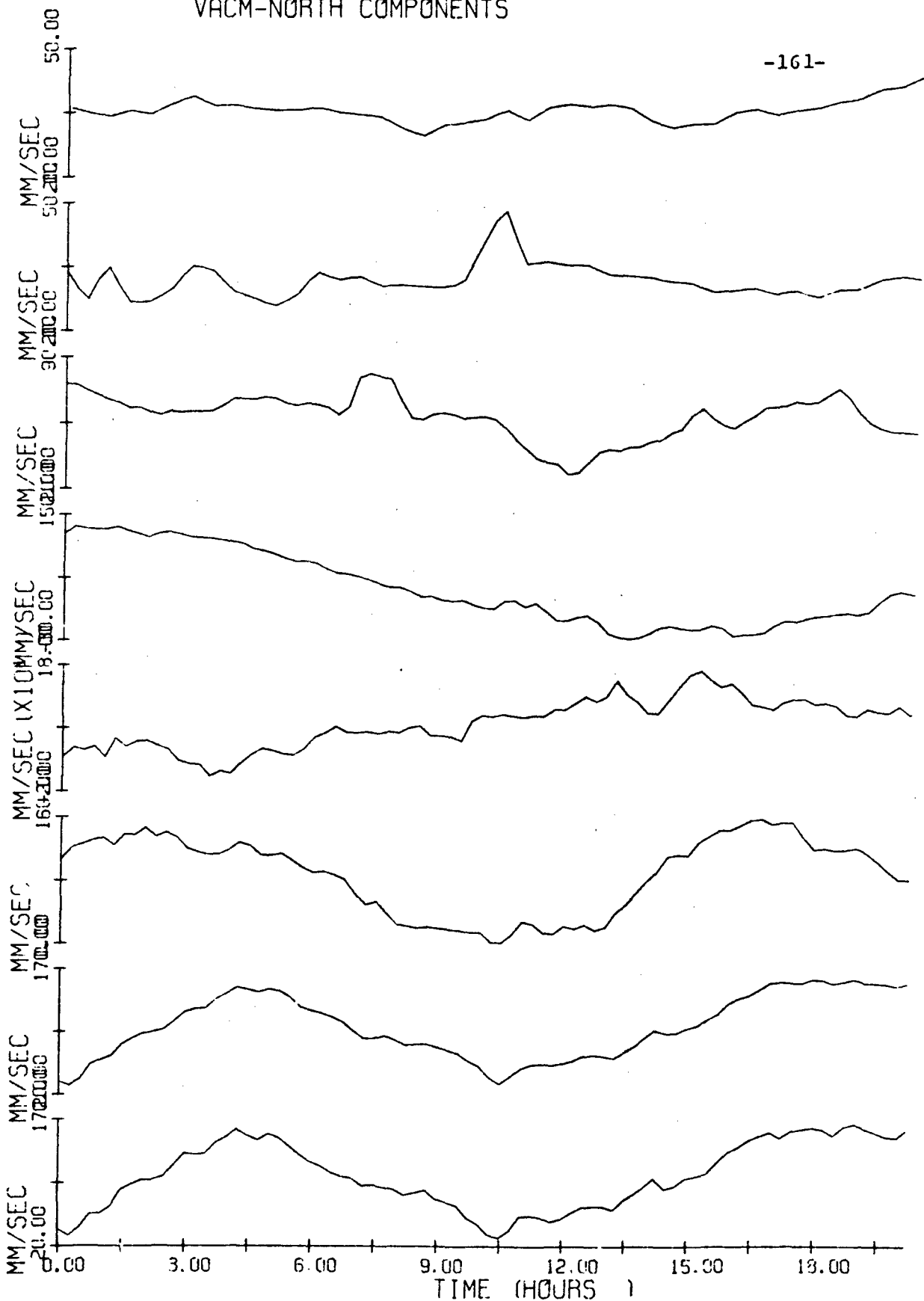


Figure 5.51 Relative Velocity Data for the Subsurface Moored System

current meter of this mooring was corrected for the effects of mooring motion, and power spectra of the uncorrected and corrected signals were compared. The relative velocity data as shown in Figures 5.50 and 5.51 was sampled every fifteen minutes at eight locations on this mooring line. Computer program SSS3.FORT was used for this simulation and no surface wave was assumed present. Figures 5.52 and 5.53 show this same response with the computer program SSD3.FORT, which calculates and includes inertia forces. Overlay of the two responses shows no noticeable difference. Input data used with these two computer programs, describing the system are shown in Tables 5.7 and 5.8.

Response of the top of this mooring line to hypothetical absolute velocity data (Figures 5.54 and 5.55), is shown in Figures 5.56 and 5.57. This simulation was done with computer program SSD31.FORT and the input data shown in Table 5.9. Surface wave was again assumed to be absent in this simulation.

5.3 Surface Moored System

The three-dimensional computer program SD3.FORT is used for this simulation. The surface moored system simulated is shown in Figure 5.58. This system of spar

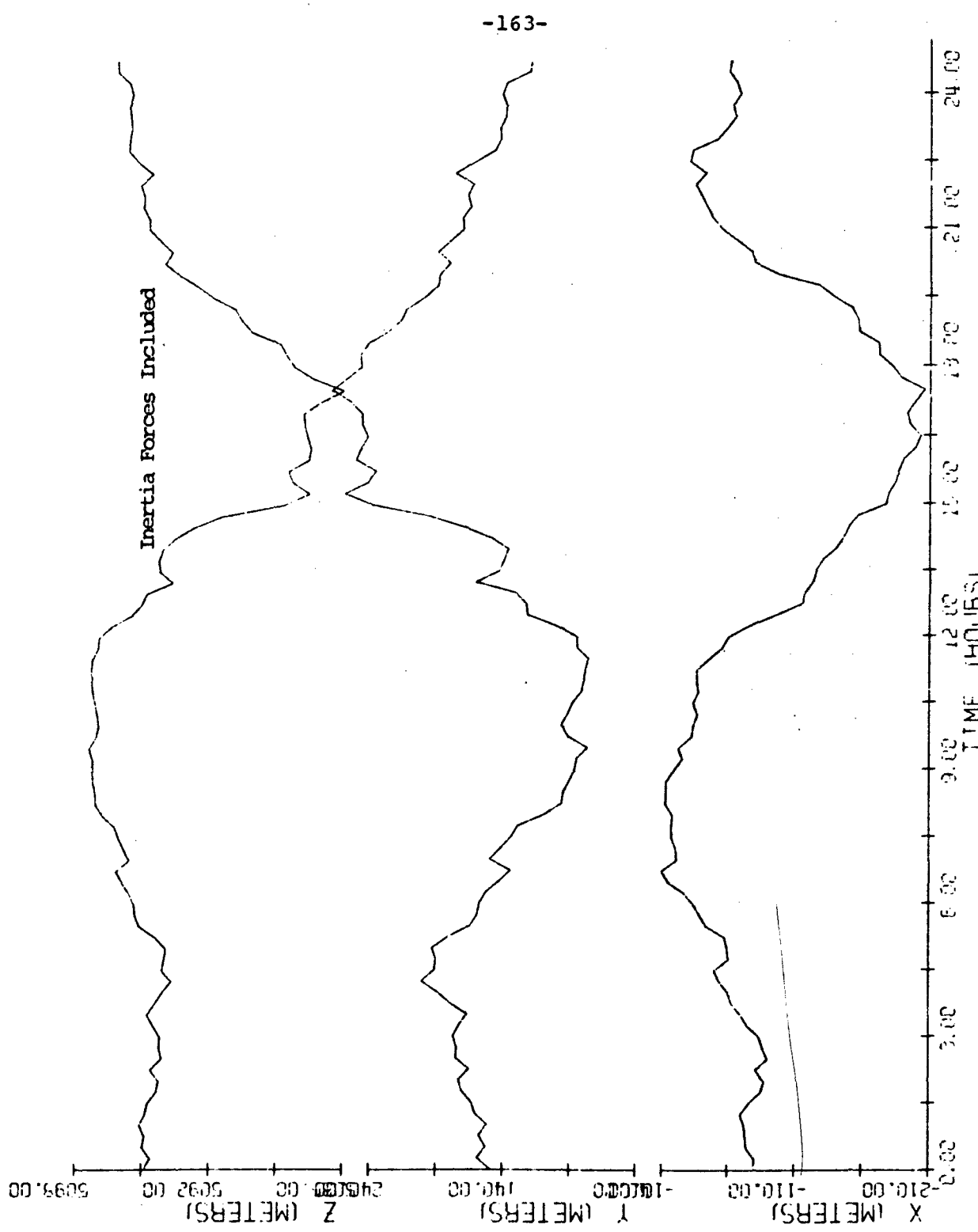


Figure 5.52 Motion of the Subsurface Moored System Top

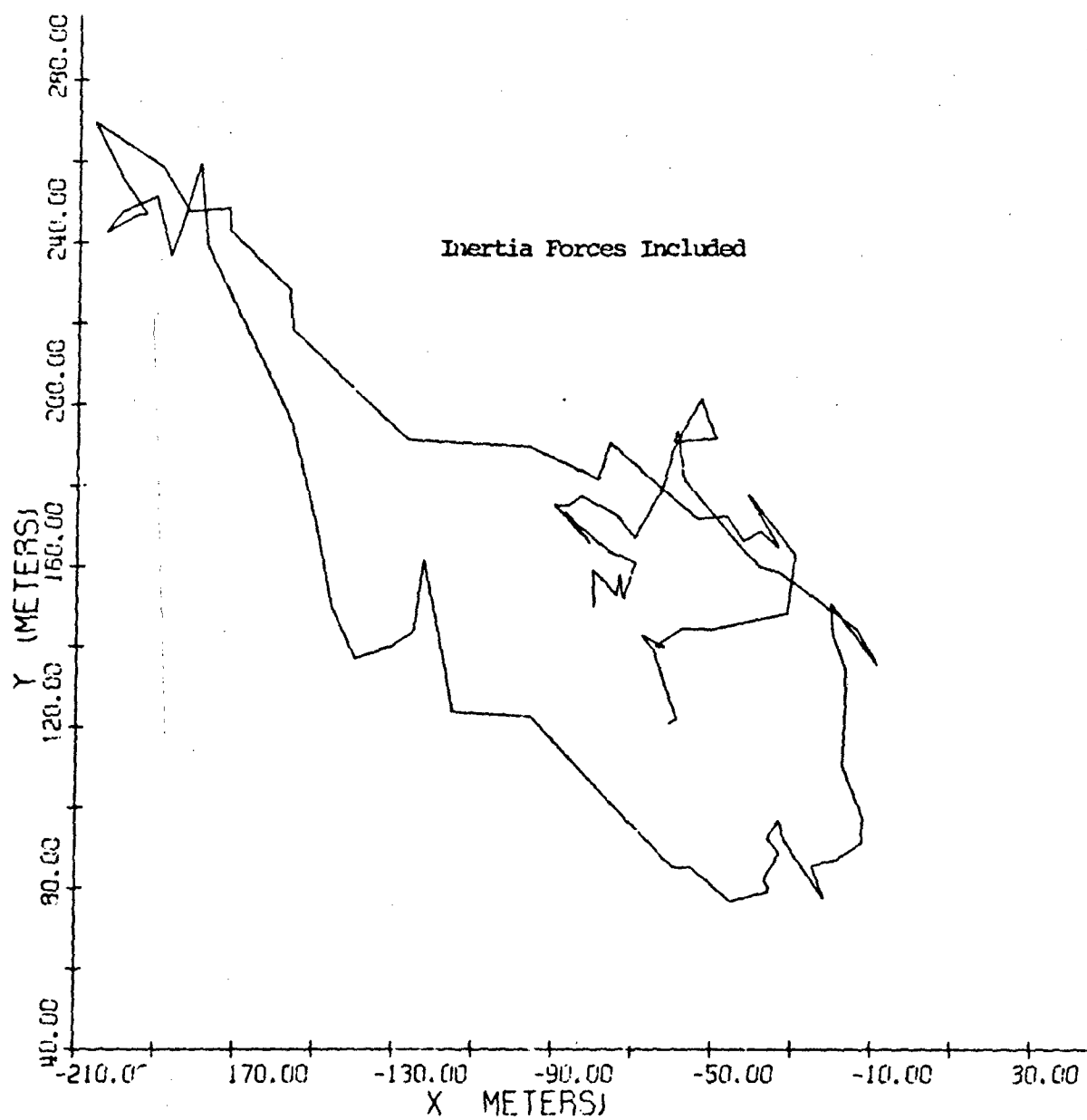


Figure 5.53 Trajectory of the Subsurface Moored System Top

SSS3.DATA		17	50	100	7	5462.	365.	3.	0.
00010	27	0.	0.	0.	0.	45.	1.75	0.	
00020	0.	0.	0.	0.	0.	976.	14.0	0.	
00030	0.0	0.	0.	0.	0.	-107.00	4.62	0.13	
00040	0.0	22.0	0.	0.	0.	-160.	14.4	0.50	
00050	22.0	5.0	0.	0.	0.	-90.0	7.66	0.26	
00060	123.0	5.50	0.	0.	0.	-24.	0.4	0.	
00070	123.0	0.	0.	0.	0.	-90.0	7.66	0.26	
00080	328.9	5.50	0.	0.	0.	-24.	0.4	0.	
00090	328.9	0.	0.	0.	0.	-24.	0.4	0.	
00100	533.4	0.	0.	0.	0.	-24.	0.4	0.	
00110	730.4	0.	0.	0.	0.	-24.	0.4	0.	
00120	1011.4	0.	0.	0.	0.	585.6	8.4	0.	
00130	1011.4	18.	0.	0.	0.	-155.	10.65	0.34	
00140	1529.9	0.	0.	0.	0.	-24.	0.4	0.	
00150	2009.9	0.	0.	0.	0.	-24.	0.4	0.	
00160	2443.4	0.	0.	0.	0.	488.	7.0	0.	
00170	2493.4	13.	0.	0.	0.	-131.	9.5	0.31	
00180	2508.4	0.	0.	0.	0.	-24.	0.4	0.	
00190	2993.9	0.	0.	0.	0.	-20.	0.4	0.	
00200	3498.9	0.	0.	0.	0.	244.	3.5	0.	
00210	3498.9	8.	0.	0.	0.	-79.	5.76	0.15	
00220	3508.9	0.	0.	0.	0.	-24.	0.41	0.	
00230	3885.9	0.	0.	0.	0.	-24.	0.4	0.	
00240	4791.9	2.5	0.	0.	0.	-53.	4.6	0.12	
00250	4796.4	0.	0.	0.	0.	-24.	0.4	0.	
00260	4860.9	0.	0.	0.	0.	732.	10.5	0.	
00270	4860.9	18.	0.	0.	0.	-152.	7.15	0.2	
00280	4898.9	4.5	0.	0.	0.	-30.	0.93	0.03	
00290	0.269	96.	0.	0.	0.	0.154	10000000.		
00300	0.269	200.40	0.	0.	0.	0.154	10000000.		
00310	0.269	199.00	0.	0.	0.	0.154	10000000.		

Table 5.7 Input Data for the Subsurface Model System

00320	0.269	197.00	0.239	0.154	10000000.
00330	0.269	281.	0.239	0.154	10000000.
00340	0.269	500.50	0.239	0.154	10000000.
00350	0.375	480.00	0.148	0.0375	1123.
00360	0.375	483.50	0.148	0.0375	1110.
00370	0.5	2.0	0.262	0.0667	1578.
00380	0.375	485.50	0.148	0.0375	1558.
00390	0.375	505.00	0.148	0.0375	1544.
00400	0.50	2.0	0.262	0.0667	1765.
00410	0.375	377.0	0.148	0.0375	1749.
00420	0.375	906.00	0.148	0.0375	1736.
00430	0.5	2.0	0.262	0.0667	1690.
00440	0.375	64.5	0.148	0.0375	1672.
00450	0.75	20.	0.476	0.0457	2407.
00460	0.064	0.	0.	0.	1.4
00470	0.064	0.	0.	0.	0.028
00480	0.064	0.	0.	0.	0.028
00490	0.064	0.	0.	0.	0.028
00500	0.064	0.	0.	0.	0.028
00510	0.064	0.	0.	0.	0.028
00520	1250.	1.8	1350.	1.6	1.4
00530	1250.	1.8	1350.	1.6	1.4
00540	1250.	1.8	1350.	1.6	1.4
00550	1250.	1.8	1350.	1.6	1.4
00560	1250.	1.8	1350.	1.6	1.4
00570	1250.	1.8	1350.	1.6	1.4
00580	1250.	1.8	1350.	1.6	1.4
00590	1250.	1.8	1350.	1.6	1.4
00600	1250.	1.8	1350.	1.6	1.4
00610	1250.	1.8	1350.	1.6	0.028
00620	88.	1.94	74.8	1.87	1.4
00630	392.75	443.5	596.5	1048.5	3450.5
					4664.

Table 5.7 (cont.) Input Data for the Subsurface Model System

SSD3.DATA	27	17	50	100	7	5462.	365.	3.
00010	0.	0.	2.02	1.01	45.	1.75	0.	
00020	0.	0.	18.76	9.38	976.	14.0	0.	
00030	0.0	0.	3.70	3.70	-107.00	4.62	0.13	
00040	0.0	22.0	10.25	10.25	-160.	14.4	0.50	
00050	22.0	5.0	5.43	5.43	-90.0	7.66	0.26	
00060	123.0	5.50	2.02	1.01	-24.	0.4	0.	
00070	123.0	0.	2.02	1.01	-24.	0.4	0.	
00080	328.9	5.50	5.43	5.43	-90.0	7.66	0.26	
00090	328.9	0.	2.02	1.01	-24.	0.4	0.	
00100	533.4	0.	2.02	1.01	-24.	0.4	0.	
00110	730.4	0.	2.02	1.01	-24.	0.4	0.	
00120	1011.4	0.	11.25	5.63	585.6	8.4	0.	
00130	1011.4	18.	7.61	7.61	-155.	10.65	0.34	
00140	1529.9	0.	2.02	1.01	-24.	0.4	0.	
00150	2009.9	0.	2.02	1.01	-24.	0.4	0.	
00160	2493.4	0.	9.38	4.69	488.	7.0	0.	
00170	2493.4	13.	6.83	6.83	-131.	9.5	0.31	
00180	2508.4	0.	2.02	1.01	-24.	0.4	0.	
00190	2973.9	0.	2.02	1.01	-20.	0.4	0.	
00200	3498.9	0.	4.69	2.35	244.	3.5	0.	
00210	3498.9	8.	5.06	5.06	-79.	5.76	0.15	
00220	3508.9	0.	2.02	1.01	-24.	0.41	0.	
00230	3885.9	0.	2.02	1.01	-24.	0.4	0.	
00240	4791.9	2.5	3.50	3.50	-53.	4.6	0.12	
00250	4796.4	0.	2.02	1.01	-24.	0.4	0.	
00260	4860.9	0.	14.07	7.03	732.	10.5	0.	
00270	4860.9	18.	8.54	8.54	-152.	7.15	0.2	
00280	4898.9	4.5	1.60	1.60	-30.	0.93	0.03	
00290	0.269	96.	0.239	0.239	0.154	10000000.		
00300	0.269	200.40	0.239	0.239	0.154	10000000.		
00310	0.269	199.00	0.239	0.239	0.154	10000000.		

Table 5.8 Input Data for the Subsurface Moored System

00320	0.269	197.00	0.239	0.154	10000000.
00330	0.269	281.	0.239	0.154	10000000.
00340	0.269	500.50	0.239	0.154	10000000.
00350	0.375	480.00	0.148	0.0375	1123.
00360	0.375	483.50	0.148	0.0375	1110.
00370	0.5	2.0	0.262	0.0667	1578.
00380	0.375	485.50	0.148	0.0375	1558.
00390	0.375	505.00	0.148	0.0375	1544.
00400	0.50	2.0	0.262	0.0667	1765.
00410	0.375	377.0	0.148	0.0375	1749.
00420	0.375	906.00	0.148	0.0375	1736.
00430	0.5	2.0	0.262	0.0667	1690.
00440	0.375	64.5	0.148	0.0375	1672.
00450	0.75	20.	0.476	0.0457	2407.
00460	0.064	0.	0.	0.	1.4
00470	0.064	0.	0.	0.	1.4
00480	0.064	0.	0.	0.	1.4
00490	0.064	0.	0.	0.	1.4
00500	0.064	0.	0.	0.	1.4
00510	0.064	0.	0.	0.	1.4
00520	1250.	1.8	1350.	1.6	1.0
00530	1250.	1.8	1350.	1.6	1.0
00540	1250.	1.8	1350.	1.6	1.0
00550	1250.	1.8	1350.	1.6	1.0
00560	1250.	1.8	1350.	1.6	1.0
00570	1250.	1.8	1350.	1.6	1.0
00580	1250.	1.8	1350.	1.6	1.0
00590	1250.	1.8	1350.	1.6	1.0
00600	1250.	1.8	1350.	1.6	1.0
00610	1250.	1.8	1350.	1.6	1.0
00620	88.	1.94	74.8	1.87	1.0
00630	392.75	443.5	596.5	1048.5	1400.
					3450.5
					4664.

Table 5.8 (cont.) Input Data for the Subsurface Moored System

VACM-EAST COMPONENTS

-169-

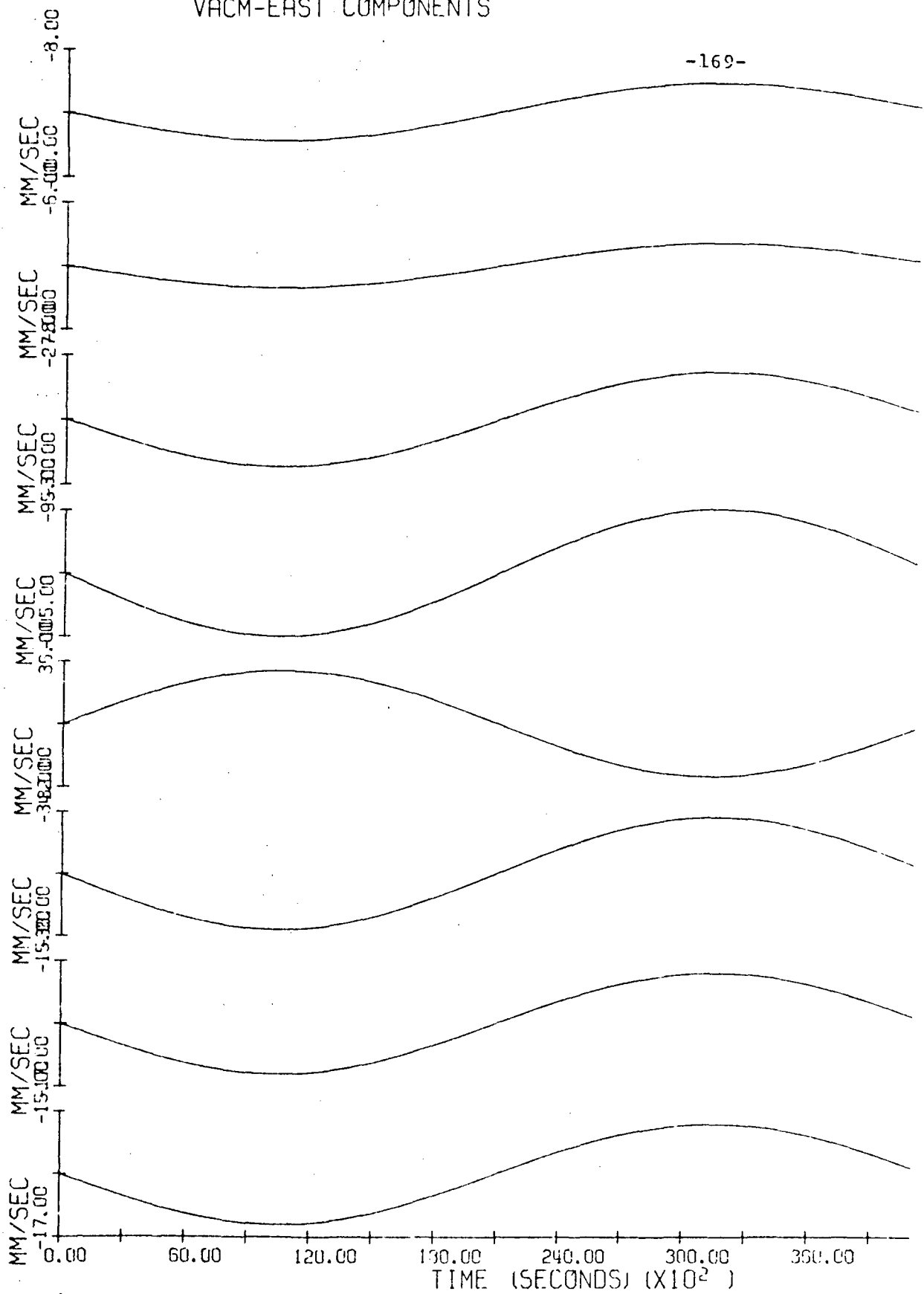


Figure 5.54 Absolute Velocity Data for the Subsurface Moored System

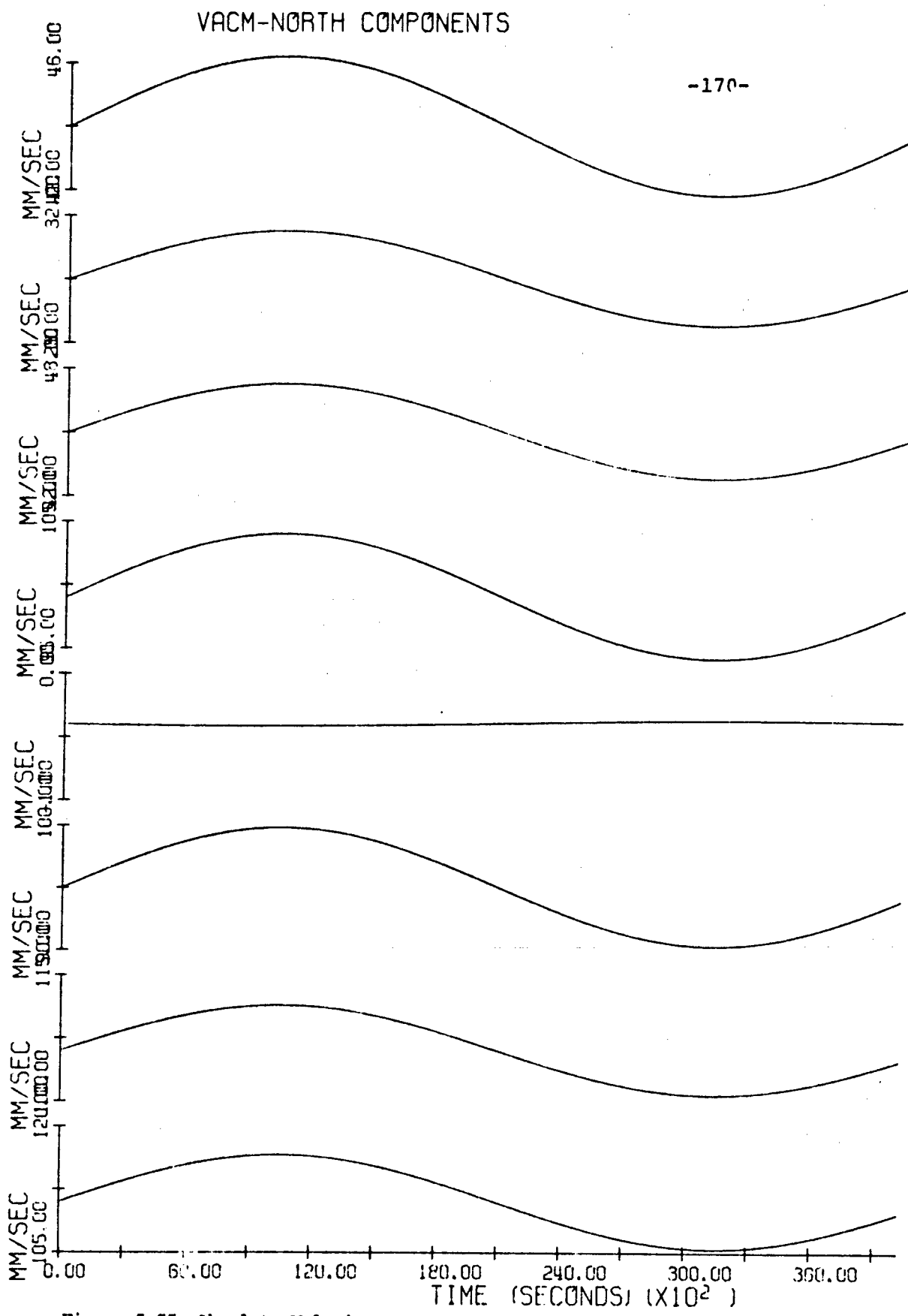


Figure 5.55 Absolute Velocity Data for the Subsurface Moored System

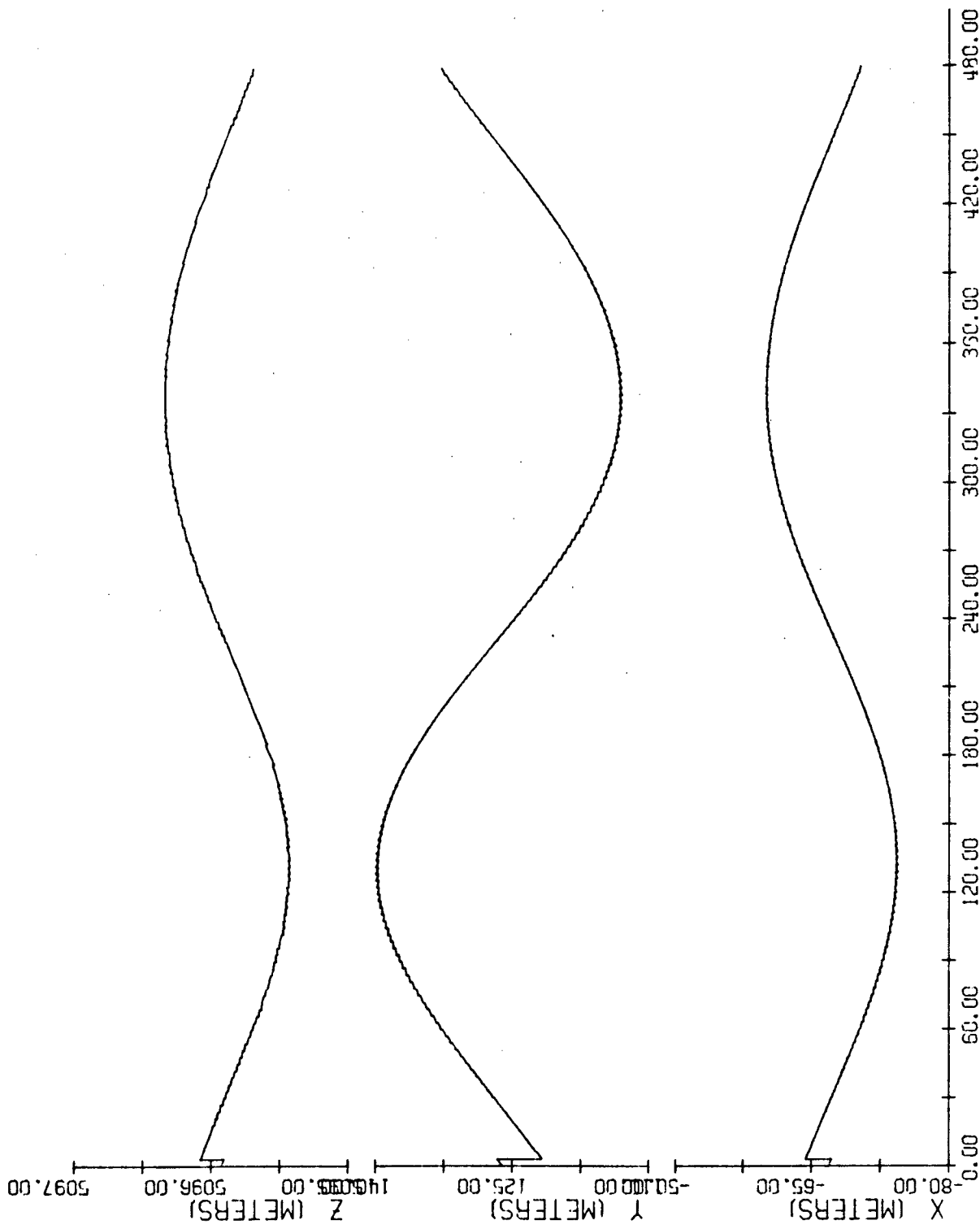


Figure 5.56 Motion of the Subsurface Mounted System Top

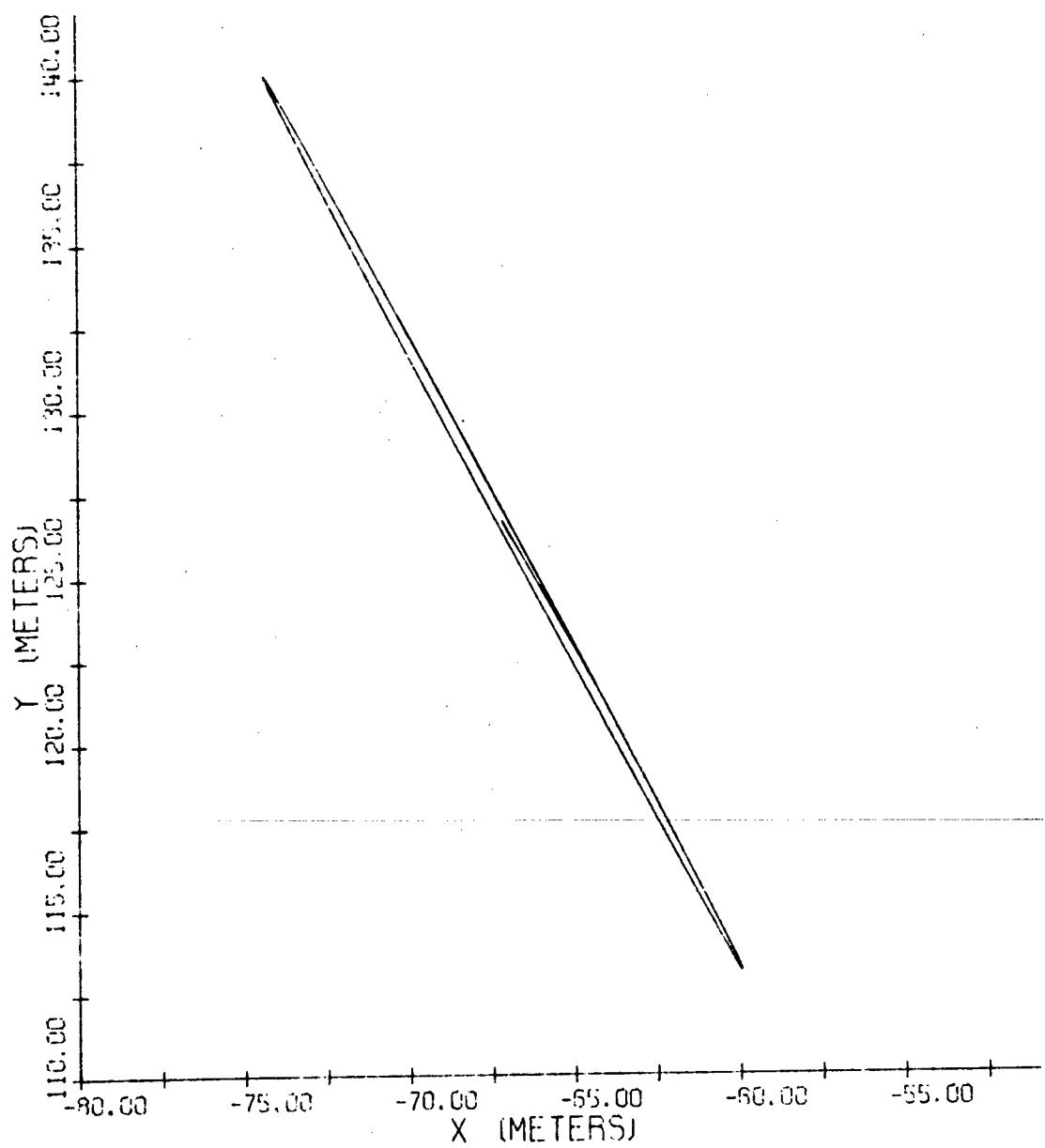


Figure 5.57 Trajectory of the Subsurface Moored System Top

SSD31.DATA		17	125	7	5462.	365.	3.	0.1
00010	27	0.	0.	2.02	1.01	45.	1.75	0.
00020	0.	0.	0.	18.76	9.38	976.	14.0	0.
00030	0.0	0.	0.	3.70	3.70	-107.00	4.62	0.13
00040	0.0	22.0	5.0	10.25	10.25	-160.	14.4	0.50
00050	22.0	5.50	5.43	5.43	5.43	-90.0	7.66	0.26
00060	123.0	0.	2.02	1.01	24.	0.4	0.	
00070	123.0	0.	5.50	5.43	5.43	-90.0	7.66	0.26
00080	328.9	0.	2.02	1.01	24.	0.4	0.	
00090	328.9	0.	2.02	1.01	24.	0.4	0.	
00100	533.4	0.	2.02	1.01	24.	0.4	0.	
00110	730.4	0.	2.02	1.01	24.	0.4	0.	
00120	1011.4	0.	11.25	5.63	585.6	8.4	0.	
00130	1011.4	18.	7.61	7.61	-155.	10.65	0.34	
00140	1529.9	0.	2.02	1.01	24.	0.4	0.	
00150	2009.9	0.	2.02	1.01	24.	0.4	0.	
00160	2493.4	0.	9.38	4.69	488.	7.0	0.	
00170	2493.4	13.	6.83	6.83	-131.	9.5	0.31	
00180	2508.4	0.	2.02	1.01	24.	0.4	0.	
00190	2993.9	0.	2.02	1.01	20.	0.4	0.	
00200	3496.9	0.	4.69	2.35	244.	3.5	0.	
00210	3498.9	8.	5.06	5.06	-79.	5.76	0.15	
00220	3508.9	0.	2.02	1.01	24.	0.41	0.	
00230	3885.9	0.	2.02	1.01	24.	0.4	0.	
00240	4791.9	2.5	3.50	3.50	-53.	4.6	0.12	
00250	4796.4	0.	2.02	1.01	24.	0.4	0.	
00260	4860.9	0.	14.07	7.03	732.	10.5	0.	
00270	4860.9	18.	8.54	8.54	-152.	7.15	0.2	
00280	4898.9	4.5	1.60	1.60	-30.	0.93	0.03	
00290	0.269	96.	0.239	0.239	0.154	1000000.		
00300	0.269	200.40	0.239	0.239	0.154	1000000.		
00310	0.269	199.00	0.239	0.239	0.154	1000000.		
00320	0.269	197.00	0.239	0.239	0.154	1000000.		
00330	0.269	281.	0.239	0.239	0.154	1000000.		
00340	0.269	500.50	0.239	0.239	0.154	1000000.		

Table 5.9 Input Data for the Subsurface Moored System

00350	0.375	480.00	0.148	0.0375	1123.
00360	0.375	483.50	0.148	0.0375	1110.
00370	0.5	2.0	0.262	0.0667	1578.
00380	0.375	485.50	0.148	0.0375	1558.
00390	0.375	505.00	0.148	0.0375	1544.
00400	0.50	2.0	0.262	0.0667	1765.
00410	0.375	377.0	0.148	0.0375	1749.
00420	0.375	906.00	0.148	0.0375	1736.
00430	0.5	2.0	0.262	0.0667	1690.
00440	0.375	64.5	0.148	0.0375	1672.
00450	0.75	20.	0.476	0.0457	2407.
00460	0.064	0.	0.	0.	1.0
00470	0.064	0.	0.	0.	1.0
00480	0.064	0.	0.	0.	1.0
00490	0.064	0.	0.	0.	1.0
00500	0.064	0.	0.	0.	1.0
00510	0.064	0.	0.	0.	1.0
00520	1250.	1.8	1350.	1.6	1.0
00530	1250.	1.8	1350.	1.6	1.0
00540	1250.	1.8	1350.	1.6	1.0
00550	1250.	1.8	1350.	1.6	1.0
00560	1250.	1.8	1350.	1.6	1.0
00570	1250.	1.8	1350.	1.6	1.0
00580	1250.	1.8	1350.	1.6	1.0
00590	1250.	1.8	1350.	1.6	1.0
00600	1250.	1.8	1350.	1.6	1.0
00610	1250.	1.8	1350.	1.6	1.0
00620	88.	1.94	74.8	1.87	1.0
00630	392.75	443.5	596.5	1048.5	1400.
00640	-15.	111.	0.	-16.	106.
00650	95.	0.	34.	-0.4	0.
00660	0.	-29.	45.	0.	-100.
00670	-9.	44.	0.	-7.	30.
00680	0.000150	300.	300.	50000.	0.
00690	1.0	0.0	0.0	0.0	0.0

Table 5.9 (cont.) Input Data for the Subsurface Moored System

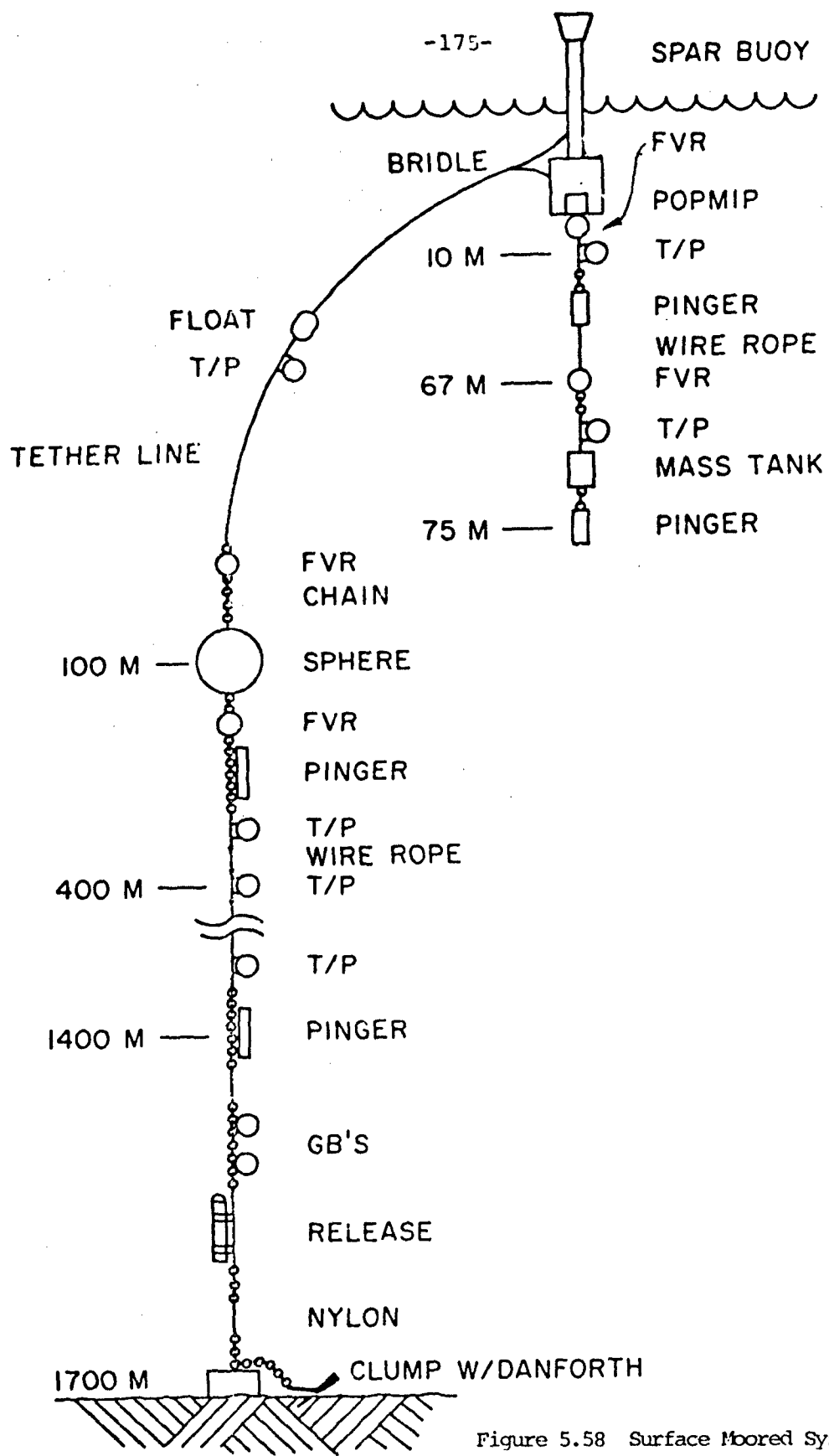


Figure 5.58 Surface Moored System

bouy/buoyant tether/subsurface mooring line with an instrument line hanging beneath the spar was deployed as part of the ONR/NDBO Mooring Dynamics Experiment during October 1976. The system is reduced to seven nodes for this simulation. These nodes are shown in Figure 5.59. Figure 5.59 shows the mean configuration of these nodes in the x-z plane. This configuration is the result of the static solution calculated by SD3.FORT using the equivalent velocity profile described in Section 4.1. The equivalent velocity profile and the actual velocity profile in the x-z plane is also shown in Figure 5.59. Figures 5.60 through 5.64 display time responses of these seven nodes to the input data presented in Table 5.10 which describes the moored system and the environment forcing this system. Forcing the system is a constant current profile and a surface wave of amplitude 1 foot, a frequency of 1 radian per second, and having a wave direction inclined at 0.1 radians with the x-axis of the earth fixed frame. Figures 5.60 through 5.62 are the plots of surge, sway and heave responses of the seven nodes. Figure 5.63 displays the roll, pitch and yaw of the tuned spar buoy (node 6), and Figure 5.64 displays tensions in the seven segments of mooring lines preceding the seven nodes.

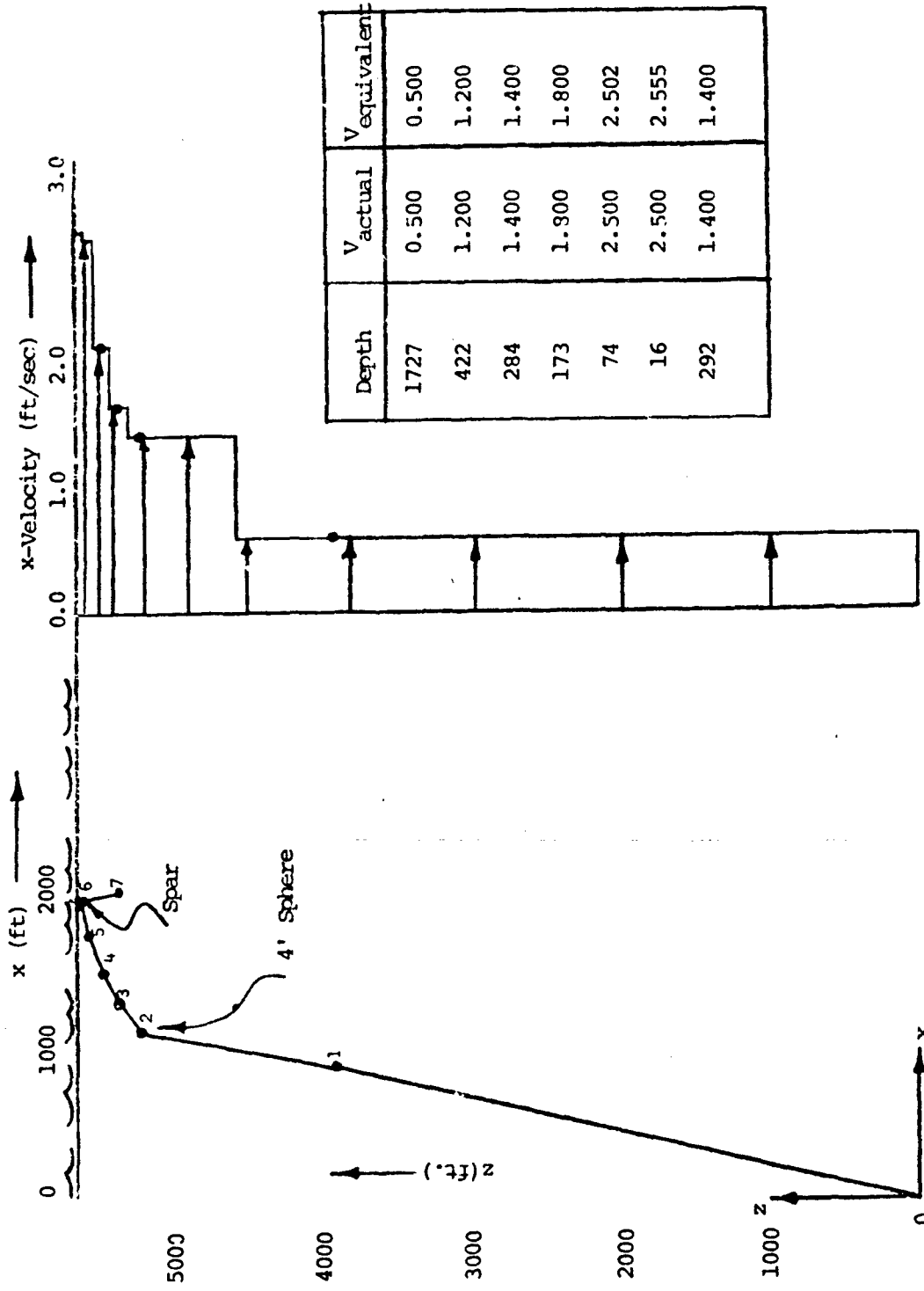


Figure 5.59 Static (Mean) Configuration of Surface Moored System

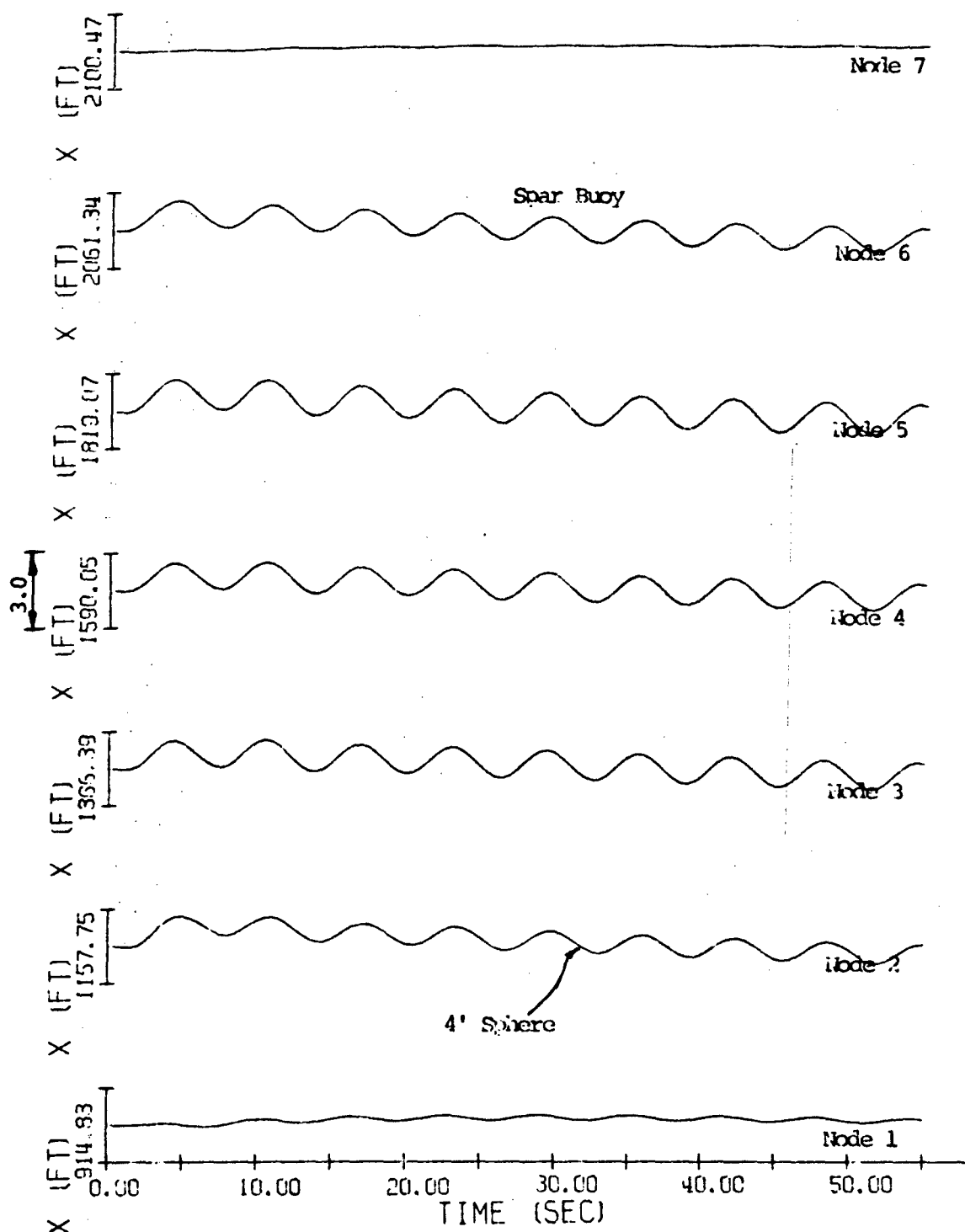


Figure 5.60 Surge Motions of a Surface Moored System

BEST AVAILABLE COPY

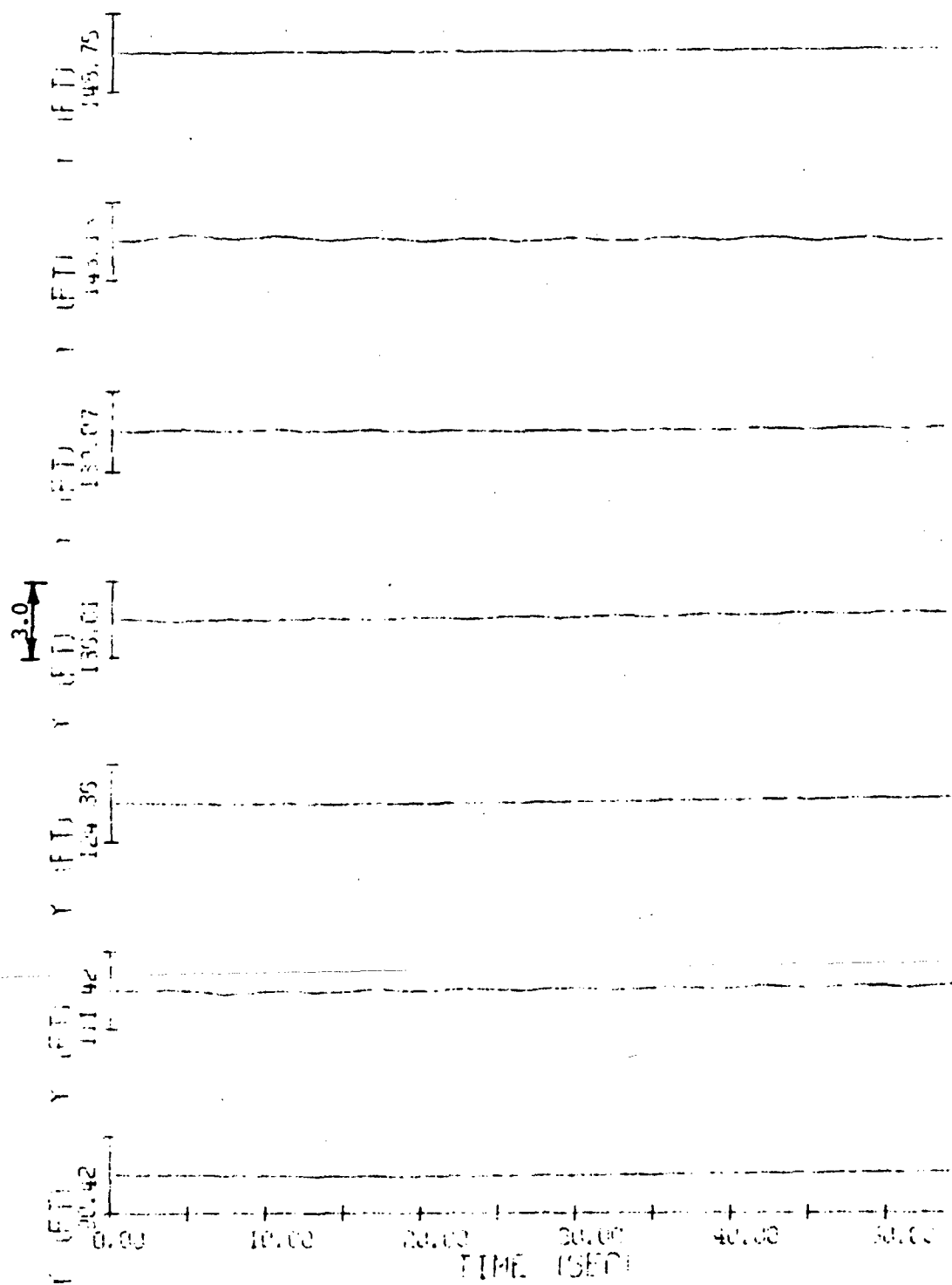


Figure 5.61 Sway Motions of a Surface Moored System

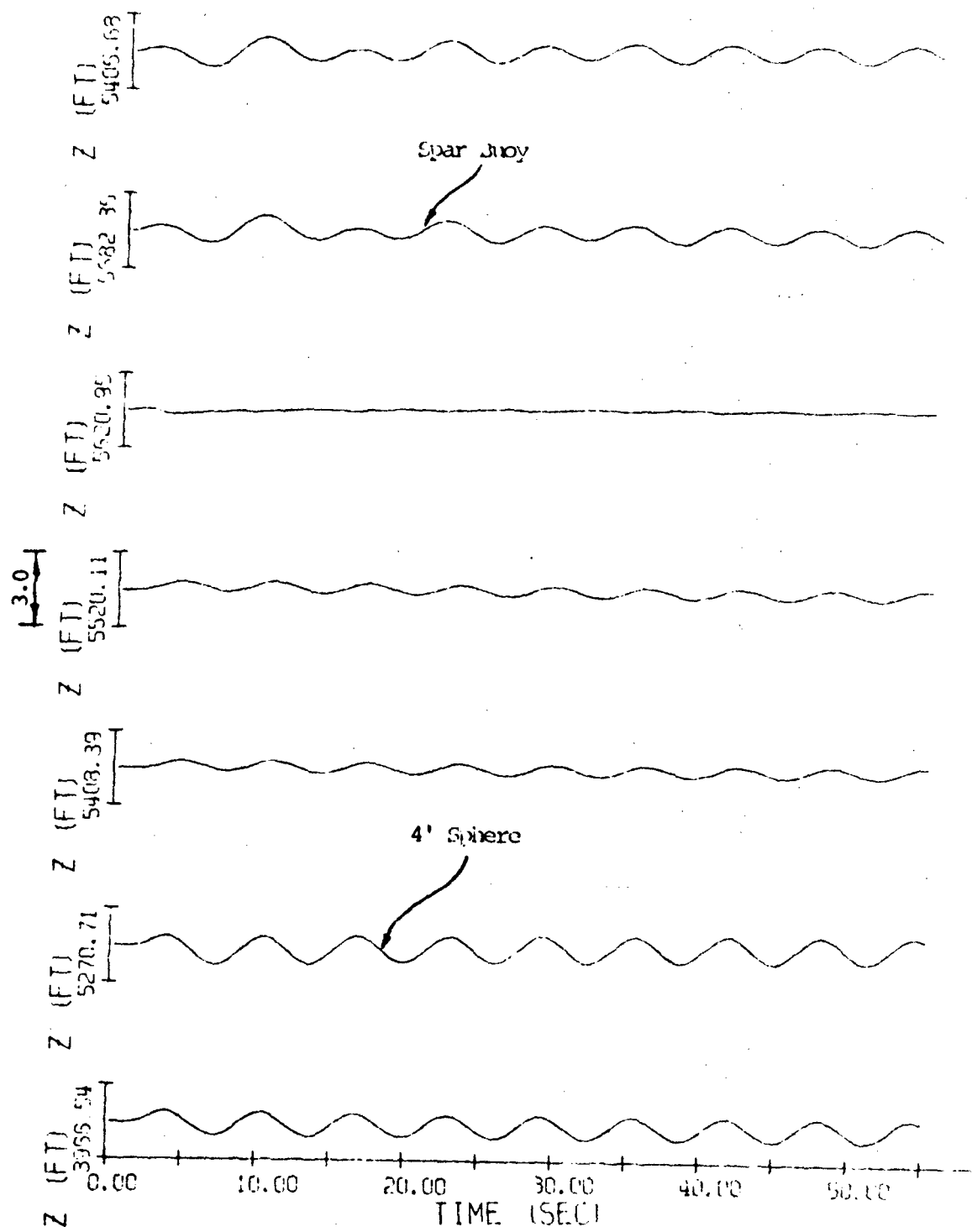


Figure 5.62 Heave Motions of a Surface Moored System

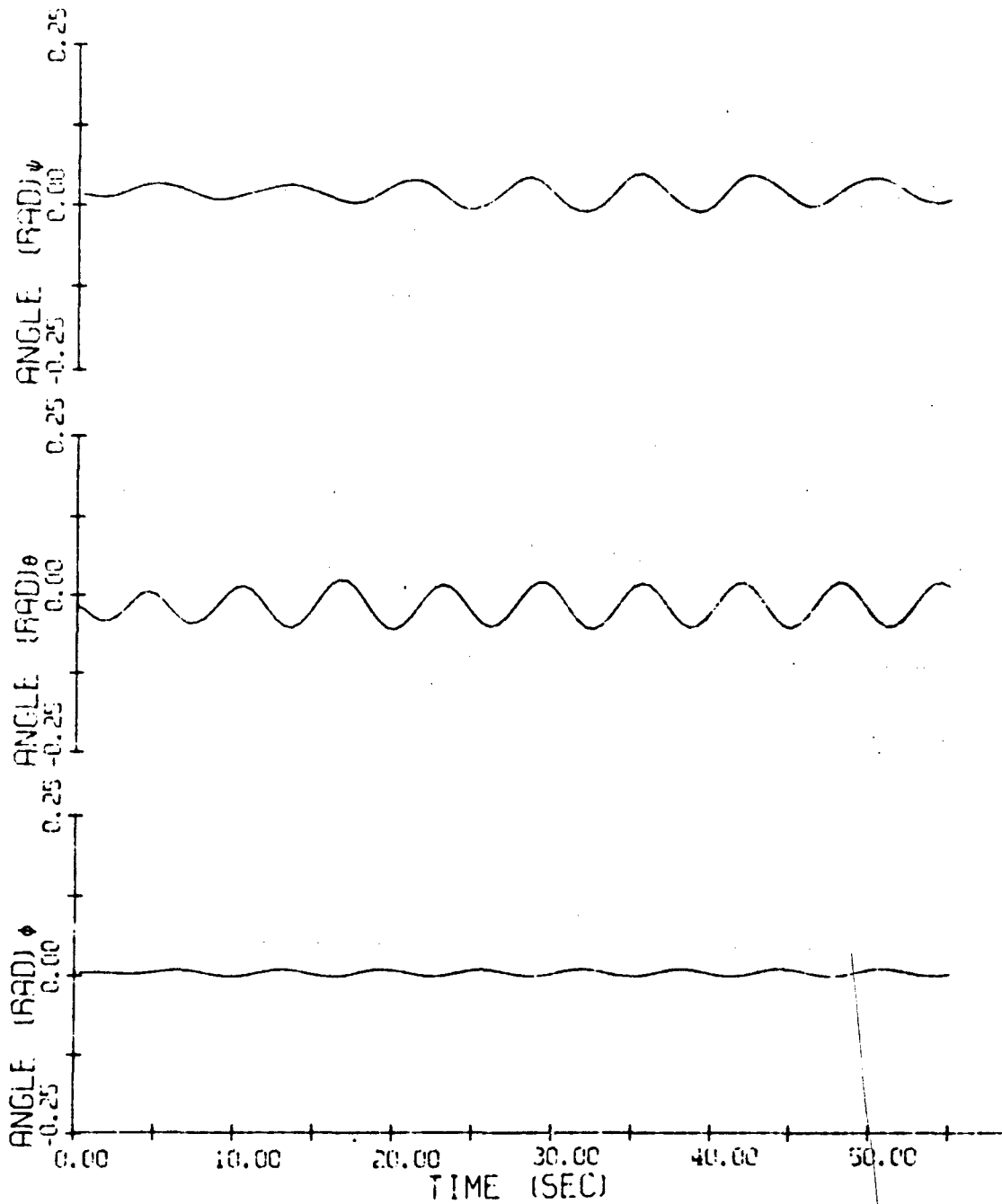


Figure 5.63 Roll, Pitch, and Yaw Motion of the Moored Spar Buoy

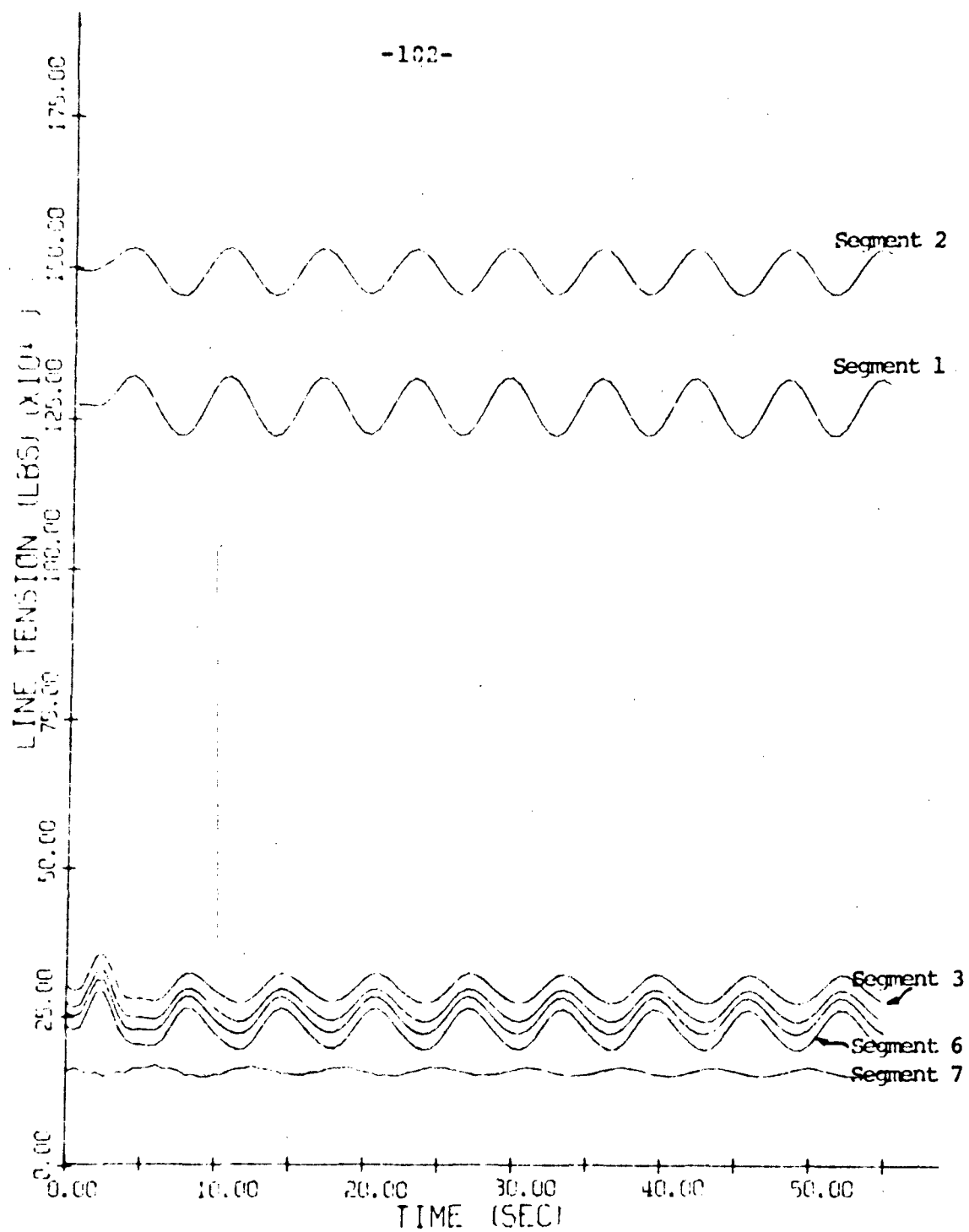


Figure 5.64 Tension Magnitudes in Different Segments of the Surface Moored System

SMDE	DATA	7	6	0	25	1	5700.	0.02	55.0	0.5
00010		1.7	0.5	1.0	3.35	5.11	30.	1.0	5.27	
00020										
00021										
00025										
00030										
00035										
00040										
00050										
00055										
00056										
00060										
00070										
00075										
00080										
00085										
00090										
00100										
00105										
00110										
00111										
00112										
00120										
READY										

Table 5.10 Input Data for the Surface Moored Buoy System

5.4 Drifting Drogued Buoy System

A submerged window shade drogue attached to a cylindrical spar buoy by means of an elastic nylon line is simulated on the computer by the three dimensional computer program SD3.FORT. The system is subjected to simple harmonic surface waves without any current profile. A 47 feet long 3/8" nylon line is attached to the center of the bottom of the buoy. The spar buoy is 30 feet long and 0.66 foot in diameter. Its static draft with no lines attached is 19.43 feet and weighs 426 pounds in air. The distance between the center of gravity and the bottom end of the buoy is 8.69 feet. The window shade drogue is made of nylon cloth ($9 \frac{1}{4}$ oz/yd²) and has the dimensions of 7.5' x 32'. Its approximate thickness is 0.02". The drogue has two metallic bars, one at each end. The bottom bar also acts as the dead weight, keeping the drogue in tension. For computer simulation the drogue was divided into four strips and the parameters of each strip lumped at a node. Tensions in three links between these four nodes and the tension in the nylon tether line were simulated on the computer. Figure 5.65 shows the system. Figures 5.66 through 5.70 show the time histories of the response of the system in a surface wave of amplitude 1 foot and circular frequency of 1 radian per second, and having a wave direction inclined at 0.25 radians with the x-axis. No current profile is present. Figures 5.66

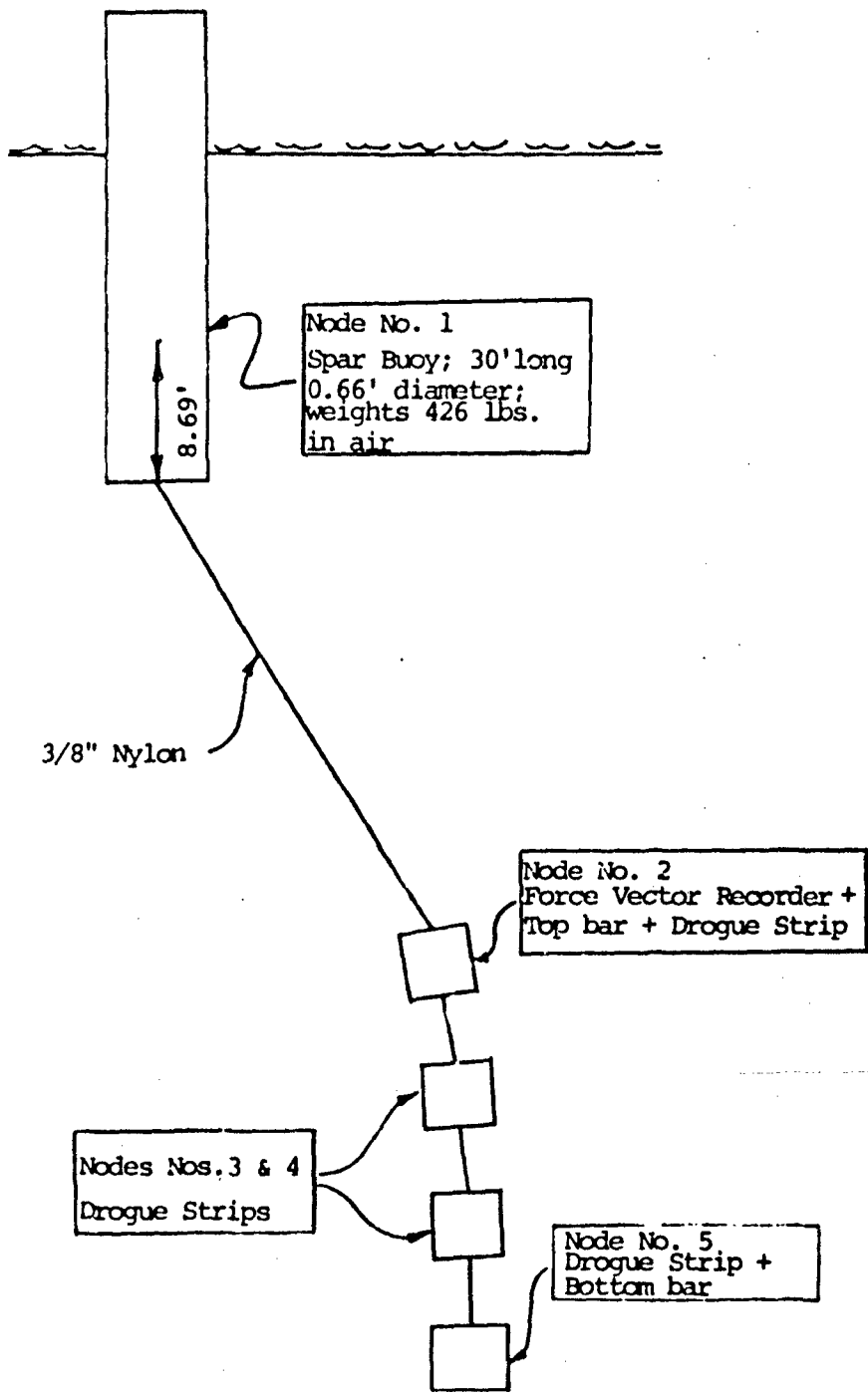


Figure 5.65 Drifting Drogued Buoy System

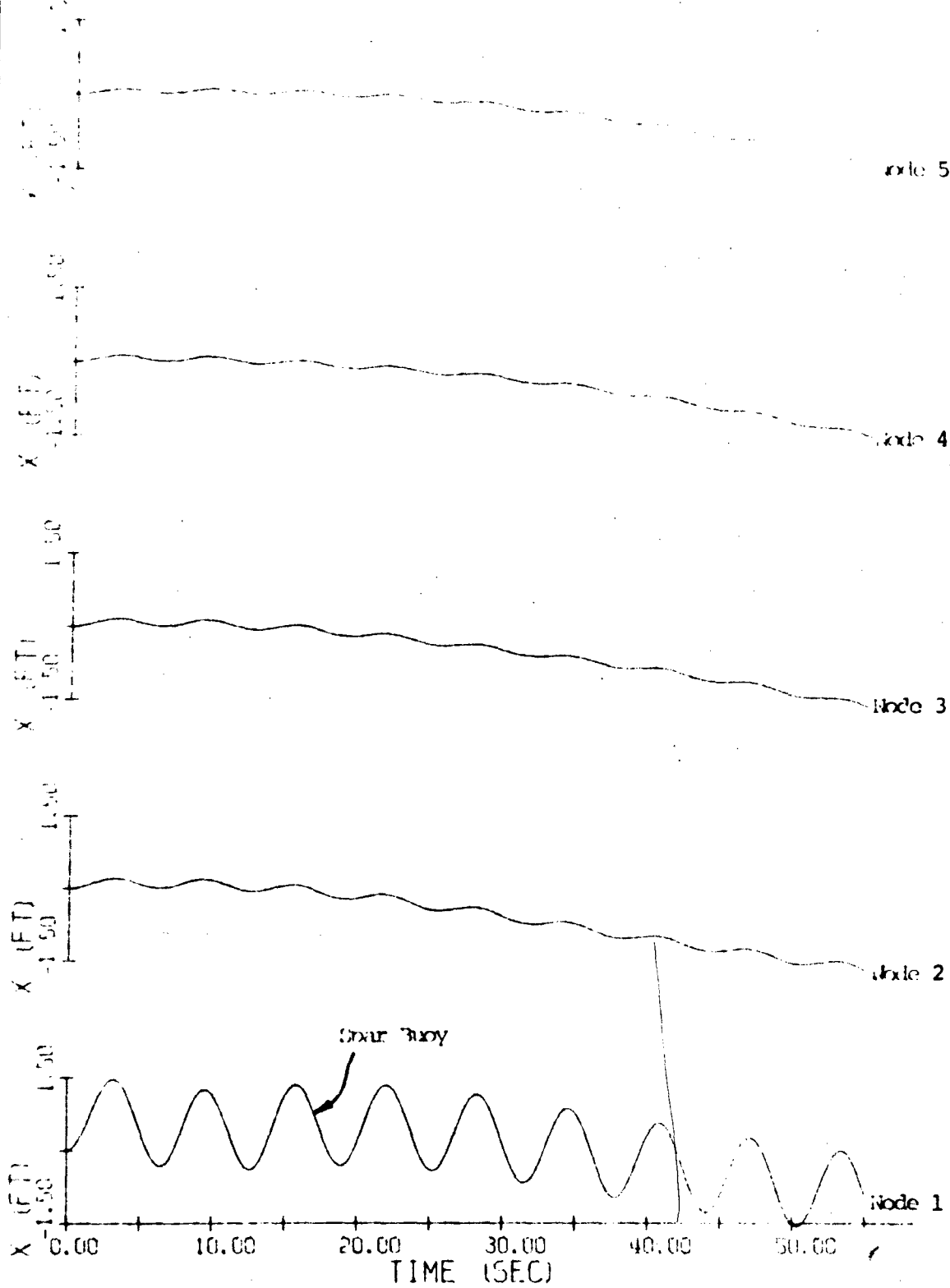


Figure 5.66 Surge Motions of the Drifting Drogued System

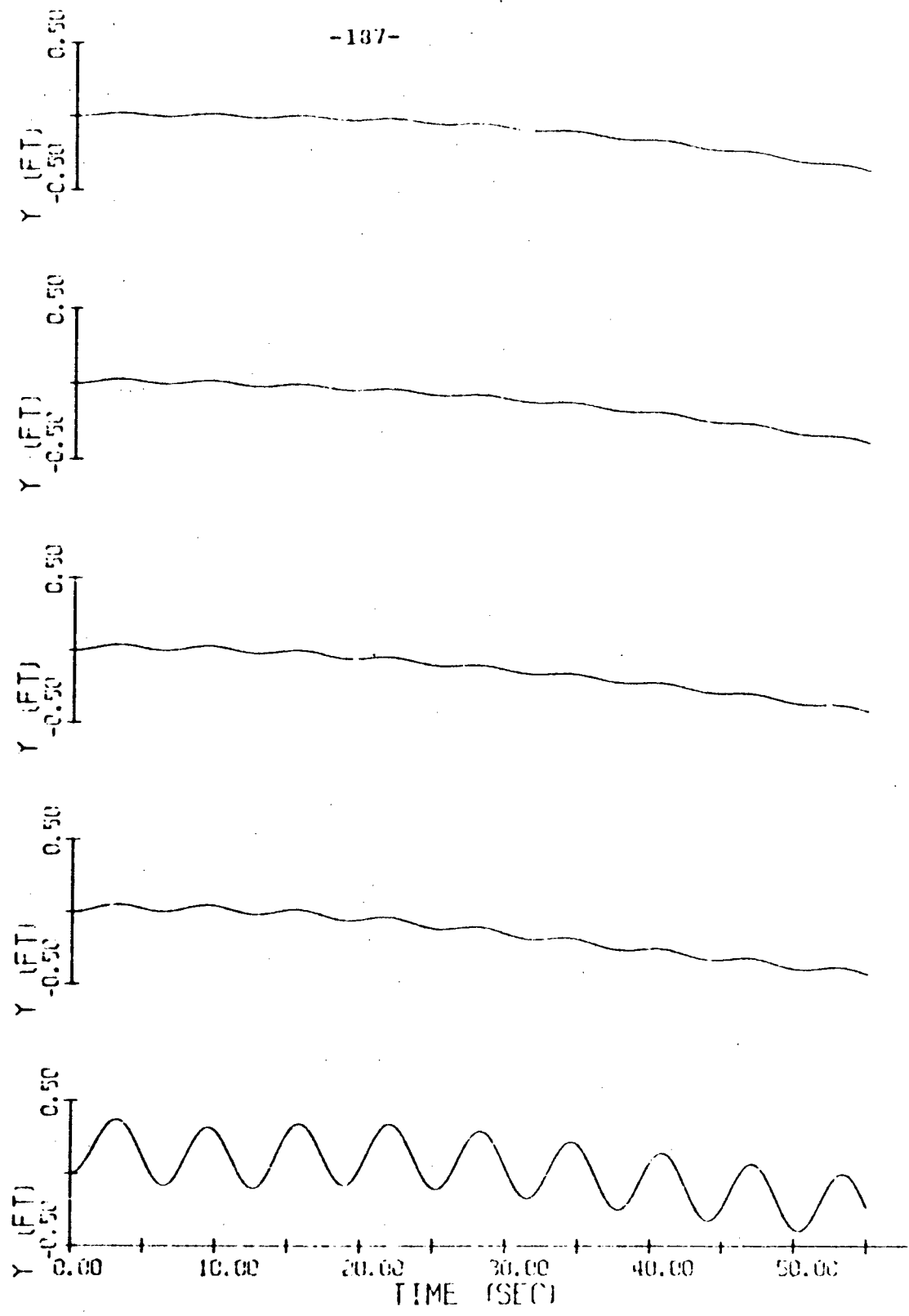


Figure 5.67 Sway Motions of the Drifting Drogued System

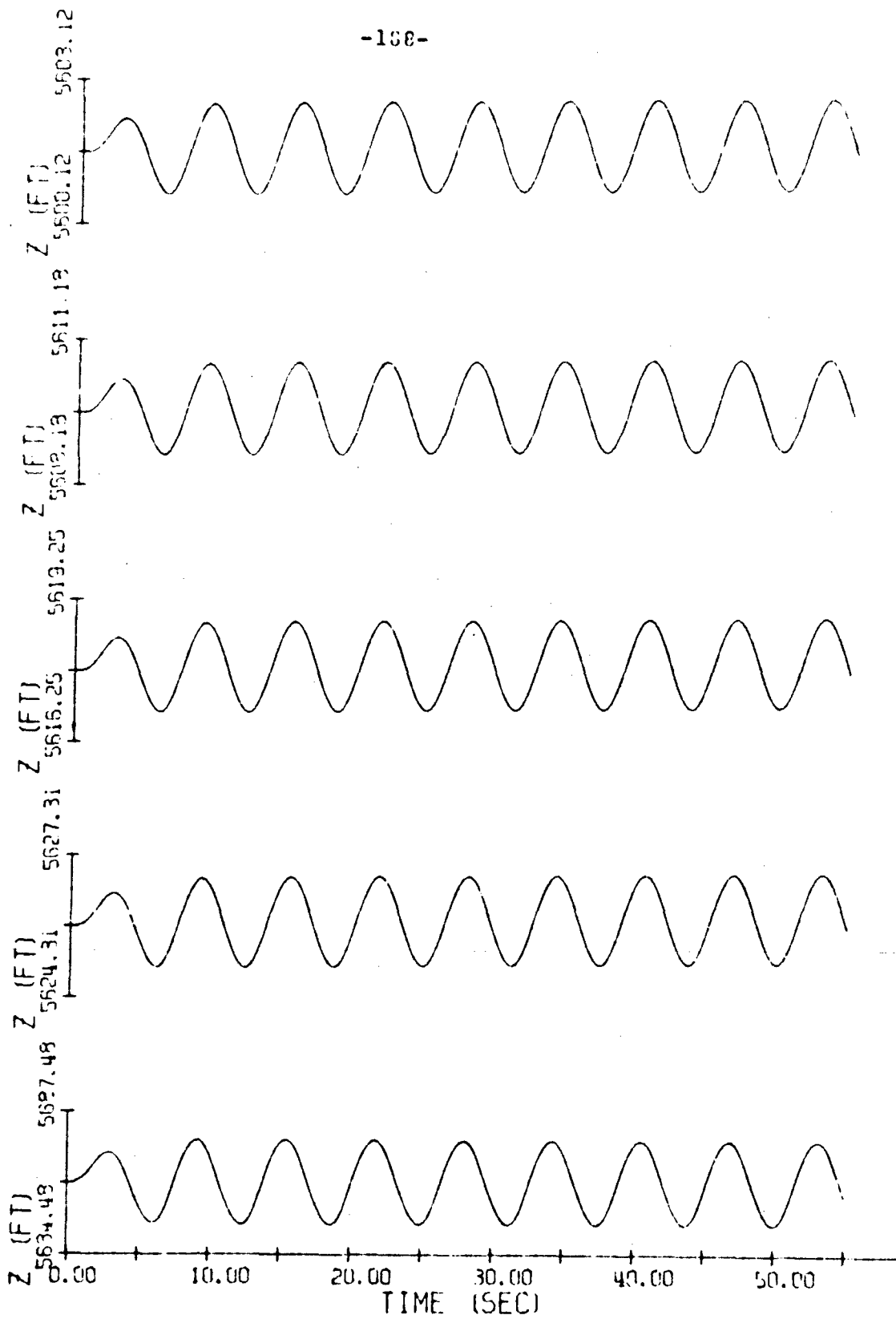


Figure 5.68 Heave Motions of the Drifting Propugnoid System

-102-

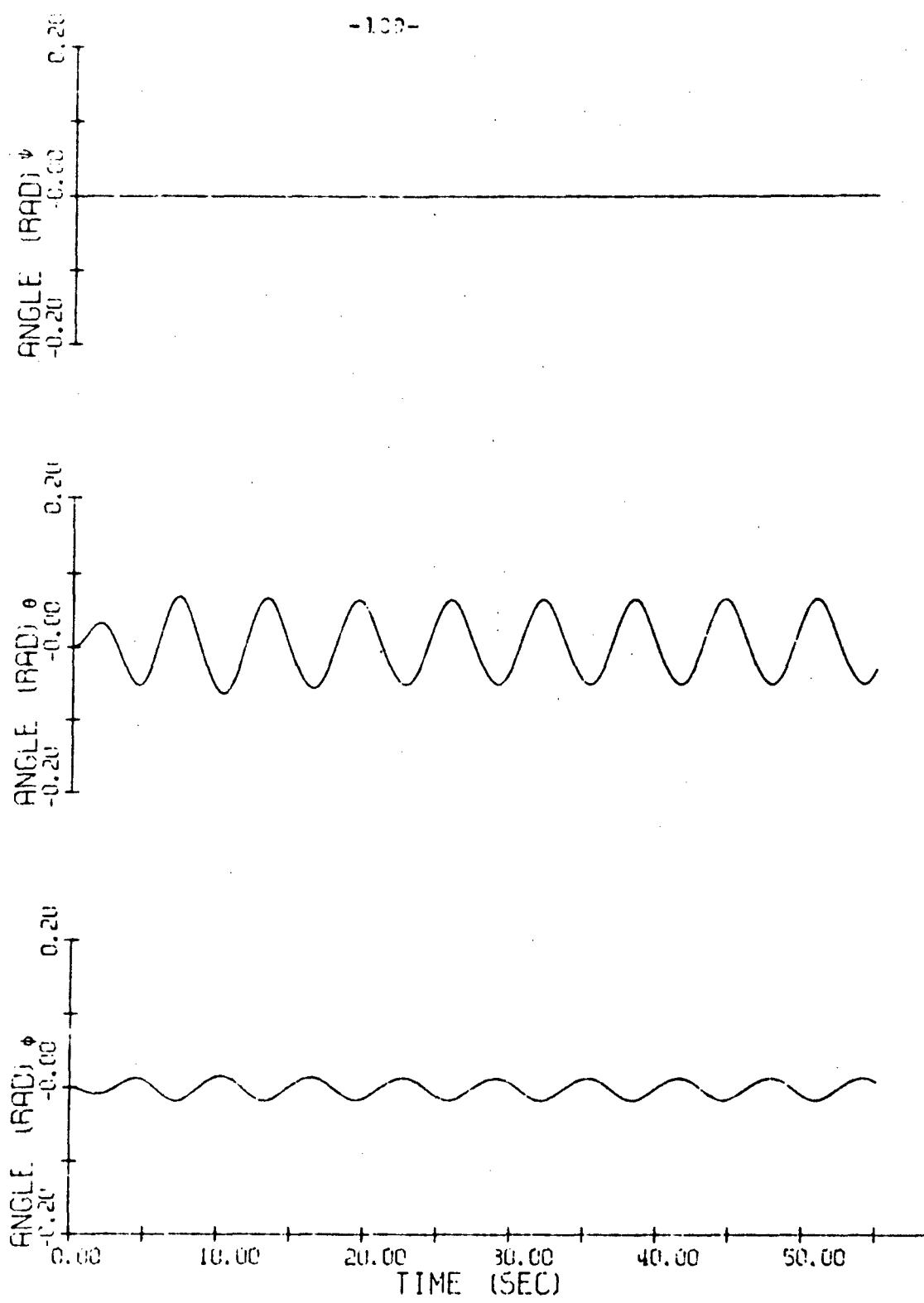


Figure 5.09 Roll, Pitch, and Yaw Motion of the Drifting Drogued Spar Buoy

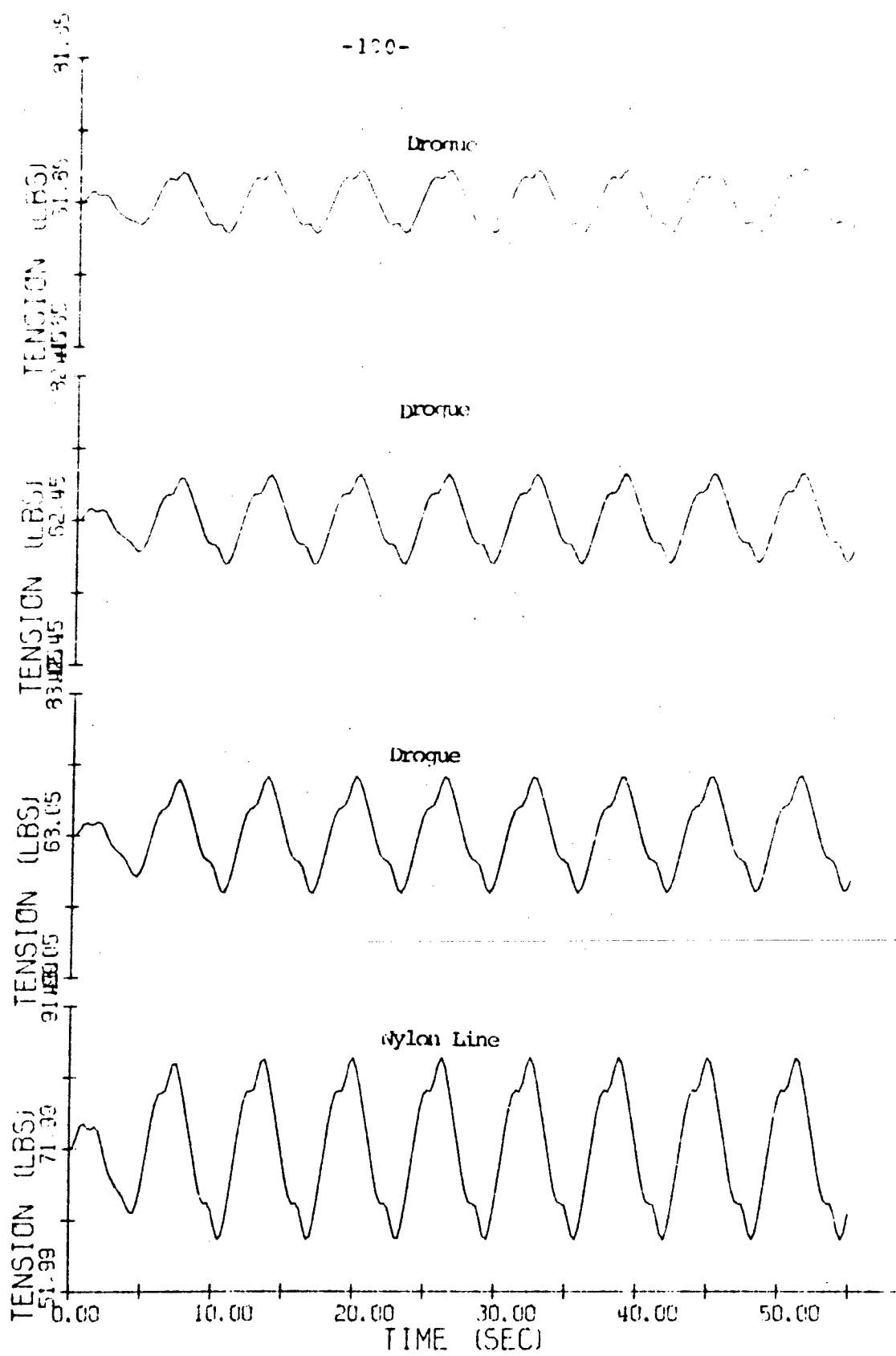


Figure 5.70 Tension Magnitude in Different Segments of the Drifting Drogued Buoy System

through 5.68 show the surge, sway and heave coordinates of the spar buoy C.G. and the four nodes on the drogue. Figure 5.69 shows the roll, pitch, and yaw angles of the buoy and Figure 5.70 shows the tension magnitudes in the nylon line below the buoy and the three segments of the drogue. The input data used for this simulation is presented in Table 5.11.

SNDR. DATA	5	1	2	25	1	2	5700.	0.010	55.0	0.25
00010	0.33	0.33	8.69		6.46		30.		1.0	5.27
00020	1.0	1.0								
00021										
00030	426.									
00031	8.94	3.0		1.1		705.1		704.		0.
00032	0.6	0.1		0.		704.		704.		0.
00033	0.6	0.1		0.		704.		704.		0.
00034	61.85	2.6		0.5		704.5		704.		0.
00060	5500.	0.0								-14.
00062	51.	150.		114.5		2.3		2.		-74.
00064	8.	1000.0		114.5		2.3		0.		-82.
00066	8.	1000.0		114.5		2.3		0.		-90.
00100	8.	1000.0		114.5		2.3		1.5		-98.
00105	0.0	0.0		0.0		0.0		0.0		-8.69
00112	0.0	0.0		0.0		0.0		0.0		0.00
00113	0.0	0.0		0.00		0.0		0.0		0.00
00114	0.0									0.0
00120	1.	1.0		0.25						
READY										

Table 5.11 Input Data for the Drifting Drogued Buoy System

6.0 SUMMARY

Dynamics of moored and drifting buoy systems in a three-dimensional space has been presented in this report. Formulation of mathematical models, which are programmed on the inhouse computer AMDAHL 470 V6, along with time-domain computer simulations of these systems are presented. Four case studies (freely floating spar buoy; a single point subsurface moored system; a spar buoy plus instrument line/buoyant tether/subsurface mooring; a freely drifting spar buoy attached to a window shade drogue) are simulated with forcing being supplied by a velocity profile and a fully developed surface wave field. One (a single point subsurface moored system) of these four case studies was evaluated with full scale ocean test data (CHHABRA, DAHLEN and FROIDEVAUX, 1974; CHHAERA, 1976). Simulations of other three case studies can now be readily evaluated with full scale ocean test data.

For the two-dimensional analysis of a freely floating spar buoy, where the assumption of small motions is not made, three sets of computer simulations are compared with the undamped linear analytical solution. This comparison is presented in Figures 5.8 through 5.11 for a cylindrical spar and Figures 5.31 through 5.34 for a tuned spar buoy. This comparison shows the effects of viscous drag and varying wave amplitude on the response

of a freely floating spar buoy. Plots for the undamped linear analytical solution and the computer simulation where wave amplitude is small and viscous drag is neglected are almost identical. For the case of a cylindrical spar, when viscous drag is added, the surge magnification vs K_h plots show a scatter near the heave and pitch natural frequencies (Figure 5.8). This emphasizes the coupling effects. Surge drift vs. K_h plots in Figure 5.9 show a markedly different responses near these same frequencies and viscous damping is evident in heave and pitch magnification plots (Figures 5.10 and 5.11). The non-linearity in the response with respect to wave amplitude is also evident. These plots also show a heave-pitch coupling near their resonance frequencies. Similar observations can be made for the case of the tuned spar.

For the three-dimensional analysis of a freely floating spar buoy, comparison is made with the two-dimensional analysis for the same input data. The only appreciable difference is observed in the surge drift, which can be attributed directly to the small motion assumption of the three-dimensional analysis.

Simulation of the spar buoy plus instrument line tethered to a subsurface mooring line shows a noteworthy transmittal of motion from the surface buoy to the subsurface line, by the tether. The tether line seems to

move mainly in the tangential direction due to the high viscous drag force in the transverse direction. As a result the combined surge, sway, and heave motions of the spar are transmitted to the subsurface line. Hence, the surge/sway motions of the spar (even if heave was negligible) could be transmitted to the subsurface line as heave. Therefore some modifications of the system may be necessary to minimize longitudinal motions of the subsurface line.

Simulation of the freely drifting spar buoy attached to a window shade drogue shows drift of the buoy and the drogue even though no current (except surface wave) is present. This drift is due to the same reasons as postulated for the freely floating spar buoy.

Full scale ocean test data for the spar buoy plus instrument line/buoyant tether/subsurface mooring is now available (October 1976 ONR/NDBO Mooring Dynamics Experiment). Using this and other data which might be available in the future; the next logical step is the evaluation of the mathematical models of the remaining three case studies.

APPENDIX A

Computer Program Listings	Page
SD3.FORT	197
SD2.FORT	222
SSD31.FORT	245
SSS3.FORT	255
SSD3.FORT	262

```
SD3.FORT
00010 C
00020 C
00030 C
00040 C
00050 C
00060 C
00070 C
00080 C
00090 C
00100 C
00110 C
00120 C
00130 C
00140 C
00150 C
00160 C
00170 C
00180 C
00190 C
00200 C
00210 C
00220 C
00230 C
00240 C
00250 C
00260 C
00270 C
00280 C
00290 C
00300 C
00310 C

      3 D DYNAMIC ANALYSIS OF A SPAR BUOY, A SURFACE MOORED SYSTEM,
      AND A DRIFTING DROGUED SPAR BUOY.

      THE UNITS USED IN THIS ANALYSIS ARE FEET/POUNDS/SECONDS.

      CASE STUDY 1---MOOR=0---SPAR BUOY FREELY FLOATING IN A SURFACE WAVE.
      CASE STUDY 2---MOOR=1---SPAR BUOY ANCHORED WITH A LUMPED MASS
      MOORING LINE; NM=NB.

      CASE STUDY 3---MOOR=1---SPAR BUOY ANCHORED WITH A LUMPED MASS
      MOORING LINE AND A LUMPED MASS INSTRUMENT LINE HANGING FROM THE
      BUOY; NM NOT EQUAL TO NB. THIS CASE STUDY SIMULATES THE MOORING
      DYNAMICS EXPERIMENT ALTERNATE MOORING SYSTEM CONFIGURATION.

      CASE STUDY 4---MOOR=2---SPAR BUOY ATTACHED TO A WINDOW SHADE DROGUE
      NB=1.

C*****START OF THE MAIN PROGRAM*****
IMPLICIT REAL*8(A-H,O-Z)
COMMON W(8),CM(8),CMS(8),CMD(8),CMN(8),CMT(8),SL(8),EK(8),CDIN(8),
1CDIT(8),CDIA(8),DEF(8),TN(8),TN(8),TL(8),YD(27),YD(27),Y(27),
17),F(27),DD(27),TC(30),CS(30),VN(3),V(3,8),UV(3,8),GM(27),
127),WWD1,WWD2,HMAX,HO,HI,HST,HOD,XC1,YC1,ZC1,XC2,YC2,ZC2,RRH01,RRH
00240 102,XJ1,YJ1,ZJ1,XJ2,YJ2,ZJ2,RD1,RD2,S01,S02,BB1,BB2,CSB,SNB,TMASS,Y
1NERT1,YNERT2,VVO,ZCG,SNK,Csk,DEPTH,CDL,CDP,PI,RHO,GR,OEXP,AW,AWX,A
1WY,AMF,WE,T,DT,P1,P2,QO,Q1,NST,NM,NM2,NDF,NB,NB1,NB2>NN,MOOR,N
1D
100 FORMAT(12F10.2)
101 FORMAT(7F10.0)
102 FORMAT(6I5,4F10.0)
103 FORMAT(6F10.0)
```

```
00320 C****GENERAL DATA*****NM,NB,ND,NST,NC,MOOR,DEPTH,DT,TMAX,T2
00330          READ(5,102)NM,NB,ND,NST,NC,MOOR,DEPTH,DT,TMAX,T2
00340 C****BUOY DATA*****RD1,SD2,ZCG,RGYR,HMAX,CDL,HST,CDF,ALPHA
00350          READ(-,101)RD1,SD2,ZCG,RGYR,HMAX,CDL,HST,CDF,ALPHA
00360 C****MOORING LINE DATA*****CMT,I,CMN(I),CMN(I),CMT(I),I=1,NM
00370          READ(5,103)(W(I),CM(I),CMS(I),CMD(I),CMT(I),CMT(I),I=1,NM)
00380          READ(5,103)(SL(I),EK(I),CDIN(I),CDIT(I),CDIA(I),DEP(I),I=1,NM)
00390 C****ATTACHMENT DATA*****CMT,I,CDIN(I),CDIT(I),CDIA(I),DEP(I),I=1,NM
00400          READ(5,101)XC1,YC1,ZC1,XC2,YC2,ZC2
00410 C****CURRENT PROFILE DATA*****V(I,J,I),IJ=1,3),I=1,NM
00420          READ(5,101)((V(I,J,I),IJ=1,3),I=1,NM)
00430 NM1=NM-NB
00440 NN=3*NB
00450 NB1=NB-1
00460 NB2=NB+1
00470 NM2=NM+1
00480 NDF=3*NM+3
00490 C****INITIALIZE PHYSICAL CONSTANTS*****
00500 PI=4.*DATAN(1.0D0)
00510 S01=PI*RD1*RD1
00520 S02=PI*RD2*RD2
00530 RHO=1.9905
00540 GR=32.2
00550 TMASS=W(NB)/GR
00560 YNERT1=TMASS*RGYR*RGYR
00570 RRH01=RHO*CDL*RD1*HST
00580 RRH02=RHO*CDL*RD2
00590 BB1=RHO*S01
00600 BB2=RHO*S02
00610 YNERT2=(BB1*RD1*RD1*HST+BB2*RD2*RD2*HST)/2.
00620 WWD1=BB1*GR*HST
00630 WWD2=BB2*GR
```

```
00640 VVO=1.33*RHO*ALPHA*(RD1**3+(RD1-RD2)**3)
00650 C*****START LOOP FOR DYNAMIC RESPONSE TO DIFFERENT SURFACE WAVES*****
00660 DO 12 ICC=1,NC
00670 C*****SURFACE WAVE DATA*****
00680 READ(5,101)WE,AMP,BETA
00690 CSB=DCOS(BETA)
00700 SNB=DSIN(BETA)
00710 C****INITIALIZE DYNAMIC VARIABLES*****
00720 DO 1 I=1,NDF
00730 F(I)=0.
00740 YD(I)=0.
00750 Y(I)=0.
00760 TC(I)=0.
00770 DD(I)=0.
00780 DO 1 J=1,NM
00790 1 GK(J,I)=0.
00800 AW=WE*WE/GR
00810 AWX=AW*CSB
00820 AWY=AW*SNB
00830 T3=0.
00840 C****FIND THE CURRENT PROFILE FOR STATIC SOLUTION*****
00850 DO 4 I=1,NM
00860 DO 2 IS=1,3
00870 2 UV(IS,I)=0.
00880 ZX1=WE*AMP*DEXP(AW*DEP(I))
00890 DO 3 J=1,12
00900 UN(1)=V(1,I)+ZX1*CSB*DSIN(PI*I/6.)
00910 UN(2)=V(2,I)+ZX1*SNB*DSIN(PI*I/6.)
00920 UN(3)=V(3,I)+ZX1*DCOS(PI*I/6.)
00930 VEM=DSQRT(VN(1)**2+VN(2)**2+VN(3)**2)
00940 DO 3 JK=1,3
00950 3 UV(IJK,I)=VV(IJK,I)+VEM*VN(IJK)
```

```
00960 VEM1=(UU(1,I)**2+UU(2,I)**2+UU(3,I)**2)*0.25
00970 DO 4 IKJ=1,3
00980   UU(IKJ,I)=UU(IKJ,I)/(VEM1*12.*0.5)
00990   4 IF(DABS(UU(IKJ,I)).LE.0.000001)UU(IKJ,I)=0.
01000   WRITE(6,100)((UU(IJ,I),IJ=1,3),I=1,NM)
01010   TC(NDFF+1)=0.
01020   TC(NDFF+2)=0.
01030   TC(NDFF+3)=0.
01040   IF(NM.EQ.NB)GO TO 8
01050   CS(NDFF+1)=0.
01060   CS(NDFF+2)=0.
01070   CS(NDFF+3)=-1.
01080   IF(MOOR.EQ.1)GO TO 8
01090 C*****STATIC SOLUTION OF THE LUMPED MASSES (INSTRUMENT LINE)*****
01100   DO 7 I=1,NM1
01110   J=NM2-I
01120   K=J+1
01130   II=3*K+1
01140   VN(1)=UU(1,J)*(1.-CS(II))*CS(II)-UU(2,J)*CS(II)*CS(II+1)
01150   VN(2)=UU(3,J)*CS(II)*CS(II+2)
01160   VN(3)=UU(2,J)*(1.-CS(II+1))*CS(II+1)-UU(3,J)*CS(II+1)*CS(II+2)
01170   1-UU(1,J)*CS(II+1)*CS(II)
01180   VN(3)=UU(3,J)*(1.-CS(II+2))*CS(II+2)-UU(1,J)*CS(II+2)*CS(II)
01190   1-UU(2,J)*CS(II+2)*CS(II+1)
01200   VT=UU(1,J)*CS(II)+UU(2,J)*CS(II+1)+UU(3,J)*CS(II+2)
01210   VNH=DSQRT(VN(1)*VN(1)+VN(2)*VN(2)+VN(3)*VN(3))
01220   VNMI=DSQRT(UU(1,J)*UU(1,J)+UU(2,J)*UU(2,J)+UU(3,J)*UU(3,J))
01230   DDTT=CDIT(J)*UT*DABS(VI)
01240   DO 5 IC=1,3
01250   KK=II+IC-4
01260   TC(KK)=TC(KK+3)+CDIA(J)*VNMI*UU(IC,J)+DDTT*CS(KK+3)+CDIN(J)*VNMI*VN
1(IC)
```

```
01280      5  CONTINUE
          01290      TC(II-1)=TC(II-1)-W(J)
          01300      TNN(J)=DSORT(TC(II-3)*#2+TC(II-2)*#2+TC(II-1)*#2)
          01310      DO 6 IC=1,3
          01320      KK=II-4+IC
          01330      6   CS(KK)=TC(KK)/TNN(J)
          01340      7   TL(J)=SL(J)+TNN(J)/EK(J)
          01350      8   CALL STATIC
          01360      IF(MOOR.GT.0)GO TO 9
          01370      CALL BUOYS
          01380      CALL MINVER(NDF,GM)
          01390      ?   T=0.
          01400      10  SS=AUX*X(NN-2)+AWY*X(NN-1)-WE*T
          01410      SNK=DSIN(SS)
          01420      CSK=DCOS(SS)
          01430      OEXP=IEXP(-HO*AW)
          01440      HI=HO-AMP*SNK
          01450      IF(CDL.NE.0.0)CALL DBDRG
          01460      IF(MOOR.GT.0)CALL BUOYS
          01470      CALL MATRIX
          01480      IF(T.LT.T3)GO TO 11
          01490      WRITE(6,100)T
          01500      WRITE(6,100)(X(I),I=1,NDF)
          01510      IF(MOOR.EQ.1)WRITE(6,100)(TN(K),K=1,NM)
          01520      IF(MOOR.EQ.2)WRITE(6,100)(TN(K),K=2,NM)
          01530      IF(T.GT.TMAX)GO TO 12
          01540      T3=T3+T2
          01550      11  T=T+DT
          01560      IF(MOOR.GT.0)CALL NEXT
          01570      GO TO 10
          01580      12  CONTINUE
          01590      CALL EXIT
```

```
01600 END
01610 IMPLICIT REAL*8(A-H,O-Z)
01620 SUBROUTINE STATIC
01630 C THIS SUBROUTINE CALCULATES THE STATIC SOLUTION TO THE FOUR CASE
01640 C STUDIES OUTLINED IN THE MAIN PROGRAM.
01650 C
01660 C
01670 COMMON W(8),CM(8),CMS(8),CMT(8),CMN(8),SL(8),EK(8),CDIN(8),
01680 ICDIT(8),CDIA(8),DEP(8),TN(8),TNN(8),TL(8),YD(27),Y(27),X(2
01690 17),F(27),DD(27),TC(30),CS(30),VN(3),U(3,8),VU(3,8),GN(8,27),GM(27,
01700 127),WWD1,WHD2,HMAX,HD,HI,HST,HOU,XC1,YC1,ZC1,XC2,YC2,ZC2,RKH01,RRH
01710 102,XJ1,YJ1,ZJ1,XJ2,YJ2,ZJ2,RD1,RD2,S01,S02,BR1,BR2,CSB,SNB,TMASS,Y
01720 INERT1,YNER12,UVO,ZCG,SNK,CSK,DEPTH,CPL,CDF,P1,RHO,GR,DXF,AU,AUX,A
01730 LWY,AMP,WE,T,DT,F1,P2,QO,Q1,NST,NM,NM1,F42,NDF,NB,NB1,NB2,NN,MOOR,N
01740 LD
01750 100 FORMAT(12F10.2)
01760 102 FORMAT(//10X,65HSTATIC CALCULATION TERMINATED -- BUOY HAS EXCEEDED
01770 1ED MAXIMUM DRAFT )
01780 103 FORMAT(//10X,100HSTATIC CALCULATION TERMINATED -- NUMBER OF ITER
01790 1ATIONS TO FIND SYSTEM SOLUTION HAS EXCEEDED MAXIMUM ( 13,1H) ,
01800 IF(MOOR.EQ.0) GO TO 26
01810 ITMAX=100
01820 IT=0
01830 IF(MOOR.EQ.1) GO TO 7
01840 C
01850 C*****CASE STUDY 4 *****
01860 C
01870 C*****INITIALIZE VARIABLES*****
01880 IS2=0
01890 DC3=0.
01900 VE=0.
01910 FXE=0.02*HMAX*RD2*U(1,1)*U(1,1)+0.01
```

```

01920      DVE=DABS(V(1,NM))/2.
01930  C*****START STATIC VELOCITY ITERATION LOOP*****
01940      IT=IT+1
01950      IF(IT.GT.ITMAX)GO TO 27
01960      DO 3 I=1,NM1
01970      J=NM2-I
01980      K=J+1
01990      II=3*K+1
02000      U1=VV(1,J)-VE
02010      U2=VV(2,J)
02020      U3=VV(3,J)
02030      VN(1)=U1*(1.-CS(II)*CS(II))-U2*CS(II)*CS(II+1)-U3*CS(II)*CS(II+2)
02040      VN(2)=U2*(1.-CS(II+1)*CS(II+1))-U3*CS(II+1)*CS(II+2)-U1*CS(II+1)*CS(II+2)
02050      IS(JI)
02060      VN(3)=U3*(1.-CS(II+2)*CS(II+2))-U1*CS(II+2)*CS(II)-U2*CS(II+2)*CS(II+3)
02070      III+;
0208C      VT=U1*CS(II)+U2*CS(II+1)+U3*CS(II+2)
02090      UNM=DSORT(VN(1)*VN(1)+VN(2)*VN(3))
02100      UNM1=DSORT(U1*U1+U2*U2+U3*U3)
02110      DDTT=CDIT(J)*VT*DABS(VT)
02120      TC(II-3)=TC(II)+CDIA(J)*VNMI*U1+DDTT*CS(II)+CDIN(J)*VNMM*VN(1)
02130      TC(II-2)=TC(II+1)+CDIA(J)*VNMI*U2+DDTT*CS(II+1)+CDIN(J)*VNMM*VN(2)
02140      TC(II-1)=TC(II+2)-W(J)+CDIA(J)*VNMI*U3+DDTT*CS(II+2)+CDIN(J)*VNMM*U
02150      1N(3)
02160      TNN(J)=DSORT(TC(II-3)**2+TC(II-2)**2+TC(II-1)**2)
02170      DO 2 IC=1,3
02180      KK=II-4+IC
02190      2 CS(KK)=TC(KK)/TNN(J)
02200      3 TL(J)=SL(J)+TNN(J)/EK(J)
02210      HO=HST+(W(1)-TC(9)-DC3-WUD1)/WWD2
02220      IF(HO.GT.0.99*HMAX)GO TO 28
02230      HOD=HO-HST

```

```
UNH1=LN(SQRT((VV(1,1)-VE)**2+VV(2,1)**2)
02240 RRHO=RRHO1+RRHO2*XHOD
02250 DC1=RRHO*UNM1*(VV(1,1)-VE)
02260 DC2=RRHO*UNM1*VV(2,1)
02270 DC3=(0.02*RRHO+0.5*RRHO*CDP*(2.*S01-S02))*DARS(VV(3,1))*VV(3,1)
02280 FX=DC1+TC(7)
02290 WRITE(6,100)VE,HO,FX
02300 IF(DARS(FX).LE.FXE)GO TO 4
02310 IS3=DSIGN(1.0D0,FX)
02320 IF(IS2+IS3.EQ.0)DVE=DVE/2.
02330 VE=VE+J53*DVE
02340 IS2=IS3
02350 GO TO 1
02360 4 YD(1)=VE
02370 DO 5 I=2,NM
02380 II=3*I+1
02390 5 YD(II)=VE
02400 X(1)=0.
02410 X(2)=0.
02420 X(3)=ZCG-HO+DEPTH
02430 B=WWDD1+WWDD2*XHOD
02440 TNN(1)=0.
02450 DO 6 IC=1,3
02460 CS(IC)=0.
02470 6 GO TO 18
02480
02490 C
02500 C*****CASE STUDIES 2 AND 3 *****
02510 C
02520 7 INDEX=1
02530 NBB=NB-1
02540 HO=HST+(W(NB)-TC(NN+6)-WWDD1)/WWDD2
02550 DH=0.
```

```
02560      WADD=W(NRB)/10.
02570      UNM1=DSQRT(UV(1,NB)*UV(1,NB)+UV(2,NB)*UV(2,NB))
02580      C*****INITIALIZE ERROR TOLERANCE*****
02590      ER= 0.0010*DEPTH
02600      C*****START CABLE (BUOY DRAFT) ITERATION LOOP*****
02610      8   IT=IT+1
02620      DH=DH/2.
02630      IF (IT.GT.ITMAX) GO TO 27
02640      IF (HO.GT.0.99*HMAX)GO TO 28
02650      HOD=HO-HST
02660      B=WWD1+WWN2*HOD
02670      RRHO=KRHO1+RRHO2*HOD
02680      DC1=RRHO*UNM1*UV(1,NB)
02690      DC2=RRHO*UNM1*UV(2,NB)
02700      DC3=(0.02*RRHO*CDP*(2.*S01-S02))*DABS(UV(3,NB))*UV(3,NB)
02710      TC(NN-2)=DC1+TC(NN+4)
02720      TC(NN-1)=DC2+TC(NN+5)
02730      TC(NN)=DC3+B-W(NB)+TC(NN+6)
02740      TNN(NB)=DSQRT(TC(NN-2)*TC(NN-2)+TC(NN-1)*TC(NN-1)+TC(NN)*TC(NN))
02750      TL(NB)=SL(NB)+TNN(NB)/EK(NB)
02760      DO 9 IC=1,3
02770      KK=NN+IC-3
02780      9   CS(KK)=IC(KK)/TNN(NB)
02790      IF(NB.EQ.1)GO TO 14
02800      10  DO 13 I=1,NB1
02810      J=NB-I
02820      K=J+1
02830      II=J*3
02840      VN(1)=UV(1,J)*(1.-CS(II+1))*CS(II+1))-UV(2,J)*CS(II+1)*CS(II+2)
02850      1-VV(3,J)*CS(II+1)*CS(II+3)
02860      VN(2)=UV(2,J)*(1.-CS(II+2))*CS(II+2)-UV(3,J)*CS(II+2)*CS(II+3)
02870      1-VV(1,J)*CS(II+2)*CS(II+1)
```

```
02880 UN(3)=VV(3,J)*(1.-CS(II+3))*CS(II+3))-VV(1,J)*CS(II+3)*CS(II+1)
02890 1-VV(2,J)*CS(II+3)*CS(II+2)
02900 VT=VV(1,J)*CS(II+1)+VV(2,J)*CS(II+2)+VV(3,J)*CS(II+3)
02910 VNM=DSQRT(VN(1)*VN(1)+VN(2)*VN(2)+VN(3)*VN(3))
02920 VN2=DSQRT(VV(1,J)*VV(1,J)+VV(2,J)*VV(2,J)+VV(3,J)*VV(3,J))
02930 DDTT=CDIT(J)*UT*DABS(UT)
02940 DO 11 IC=1,3
02950 KK=II+IC-3
02960 TC(KK)=TC(KK+3)+CDIA(J)*VN2*VV(IC,J)+DDTT*CS(KK+3)+CIN(J)*VN
02970 1(IC)
11 CONTINUE
02980
02990 TC(II)=TC(II)-W(J)
03000 TNN(J)=DSQRT(TC(II)**2+TC(II-2)**2+TC(II-1)**2)
03010 DO 12 IC=1,3
03020 KK=II-3+IC
03030 12 CS(KK)=TC(KK)/TNN(J)
03040 13 TL(J)=SL(J)+TNN(J)/EK(J)
03050 14 ZJ1=C.
03060 DO 15 I=1,NB
03070 II=I*3
03080 15 ZJ1=ZJ1+TL(I)*CS(II)
03090 DEPTH1=ZJ1+(HO-ZCG-ZC1)
03100 EE=DEPTH-DEPTH1
03110 WRITE(6,100)HO,EE,(W(NCC),NCC=1,NB)
03120 EEE=DABS(EE)
03130 IF(EEE.LE.ER)GO TO 17
03140 IF(INDEX.EQ.1.AND.EE.LT.0.)GO TO 25
03150 IF(INDEX.EQ.2)GO TO 16
03160 INDEX=2
03170 DH=(HMAX-HO)/2.
03180 *****ITERATION ON BUOY DRAFT*****
03190 HO=HO+DH
```

```
03200      60 TO 8
03210      16   HO=HO+EEE*DH/EE
03220      60 TO 8
03230      17   DEPTH=DEPTH1
03240      WRITE(6,100)DEPTH1
03250 C*****STATIC SOLUTION HAS CONVERGED--COMPUTE ALL ANGLES AND COORDINATES
03260      18   AL1=(S01*HST*(HST/2.-ZCG)+S02*HOD*((HO+HST)/2.-ZCG))/((S01*HST+S02*1HOD))
03270
03280      AL2=(HST/2.-ZCG)+RD2*HOD*HO/(2.*((RD1*HST+RD2*HOD)))
03290      GM(1,1)=B*AL1+DC3*AL2-TC(NN-1)*YC1-TC((NN-1)*ZC1+TC(NN+5)*YC2+TC(NN+6
03300      1)*ZC2)
03310      GM(1,2)=TC(NN-1)*XC1-TC(NN+5)*XC2
03320      GM(1,3)=TC(NN)*XC1-TC(NN+6)*XC2
03330      GM(2,1)=TC(NN-2)*YC1-TC(NN+4)*YC2
03340      GM(2,2)=B*AL1+DC3*AL2-TC(NN-2)*XC1-TC(NN)*ZC1+TC(NN+4)*XC2
03350      1+TC(NN+6)*ZC2
03360      GM(2,3)=TC(NN)*YC1-TC(NN+6)*YC2
03370      GM(3,1)=-DC1*AL2+TC(NN-2)*ZC1-TC(NN+4)*ZC2
03380      GM(3,2)=-DC2*AL2+TC(NN-1)*ZC1-TC(NN+5)*ZC2
03390      GM(3,3)=-TC(NN-2)*XC1-TC(NN-1)*YC1+TC(NN+4)*XC2+TC(NN+5)*YC2
03400      IF(GM(3,3).EQ.0.)GM(3,3)=0.00001
03410      UN(1)=-DC2*AL2+TC(NN-1)*ZC1-TC(NN+5)*ZC2
03420      UN(2)=DC1*AL2-TC(NN-2)*ZC1+TC(NN)*XC1+TC(NN+4)*ZC2-TC(NN+6)*XC2
03430      UN(3)=TC(NN-2)*YC1-TC(NN-1)*XC1-TC(NN+4)*YC2+TC(NN+5)*XC2
03440      CALL MINVER(3,GM)
03450      DO 19 IC=1,3
03460      X(NN+IC)=0.
03470      DO 19 IC1=1,3
03480      19   X(NN+IC)=X(NN+IC)+GM(IC,IC1)*UN(IC1)
03490      IF(MOOR.EQ.2)GO TO 22
03500      X(1)=TL(1)*CS(1)
03510      X(2)=TL(1)*CS(2)
```

```
03520 X(3)=TL(1)*CS(3)
03530 IF(NB.EQ.1)GO TO 21
03540 DO 20 I=2,NB
03550 II=3*I
03560 X(II-2)=X(II-5)+TL(I)*CS(II-2)
03570 X(II-1)=X(II-4)+TL(I)*CS(II-1)
03580 20 X(II)=X(II-3)+TL(I)*CS(II)
03590 21 XJ1=X(NN-2)
03600 X(NN-2)=XJ1-XC1
03610 YJ1=X(NN-1)
03620 X(NN-1)=YJ1-YC1
03630 X(NN)=ZJ1-ZC1
03640 IF(NM.EQ.NB)GO TO 24
03650 22 XJ2=X(NN-2)+XC2
03660 YJ2=X(NN-1)+YC2
03670 ZJ2=X(NN)+ZC2
03680 X(NN+4)=XJ2+TL(NB2)*CS(NN+4)
03690 X(NN+5)=YJ2+TL(NB2)*CS(NN+5)
03700 X(NN+6)=ZJ2+TL(NB2)*CS(NN+6)
03710 IF(NB2.EQ.NM)GO TO 24
03720 NB3=NB2+1
03730 DO 23 I=NB3,NM
03740 II=3*I+1
03750 X(II)=X(II-3)+TL(I)*CS(II)
03760 X(II+1)=X(II-2)+TL(I)*CS(II+1)
03770 23 X(II+2)=X(II-1)+TL(I)*CS(II+2)
03780 24 WRITE(6,100)HQ,X(NN+1),X(NN+2),X(NN+3)
03790 WRITE(6,100)(X(I),I=1,NDF)
03800 RETURN
03810 C****IF PART OF THE MOORING LINE IS FLOATING ON THE SURFACE FIND IT*****
03820 25 W(NBB)=W(NBB)-ADD
03830 IF(W(NBB).LT.0.)GO TO 10
```

03840 W(NBB)=0.
03850 NBB=NBB-1
03860 GO TO 25
03870 C
03880 C*****CASE STUDY 1 *****
03890 C*****
03900 C 26 HO=HST+((W(1)-WWD1)/WWD2
03910 WAW=AW*HO
03920 OEXP=DEXP(-WAU)
03930 HOD=HO-HST
03940 BK1=(BB1-BB2)*HST
03950 BK2=BB2*HO
03960 P1=BK2*(0.5*HO-ZCG)+BK1*(0.5*HST-ZCG)
03970 F2=BK2*((HO*HO/3.-HO*ZCG+ZCG*ZCG)+BK1*(HST*HST/3.-HST*ZCG+ZCG*ZCG))
03980 Q02=DEXF(-HOD*AW)
03990 Q0=(BB1*(Q02-0EXP)+BB2*(1.-Q02))/AW
04000 Q1=(BB1*(Q02*(HST-1./AW-ZCG))+OEXP*(1./AW+ZCG))+BB2*(HO-1./AW-ZCG-Q
04010 1Q2*(HST-1./AW-ZCG))/AW
04020 X(1)=-AMP*CSB*Q0/TMASS
04030 X(2)=-AMP*SNB*Q0/TMASS
04040 X(3)=ZCG-H0+DEPTH
04050 X(4)=-WE*WE*AMP*SNB*(2.*Q1-P1*Q0/TMASS)/(P1*GR-WE*WE*(YNERT1+P2-P1*
04060 1*P1/(2.*TMASS)))
04070 X(5)=WE*WE*AMP*CSB*(2.*Q1-P1*Q0/TMASS)/(P1*GR-WE*WE*(YNERT1+P2-P1*
04080 1*P1/(2.*TMASS)))
04090 X(6)=0.
04100 YD(1)=UU(1,1)
04110 YD(2)=VV(2,1)
04120 YD(3)=WE*AMP*(RH0*SO2*GR-WE*WE*Q0)/(RHO*SO2*GR-WE*WE*(TMASS+VVO))
04130 XAW=X(1)/AMP
04140 YAW=X(2)/AMP
04150 ZAW=YD(3)/(WE*AMP)

```
PAW=X(5)/(AW*XAMP)
RAW=X(4)/(AW*XAMP)
WRITE(6,100)WAU,XAU,YAU,ZAU,RAW,PAW
RETURN
04160
04170
04180
04190
04200    WRITE(6,103)ITMAX
04210    CALL EXIT
04220    WRITE(6,102)
04230    CALL EXIT
04240
04250    IMPLICIT REAL*8(A-H,O-Z)
04260    SUBROUTINE DBDRG
04270 C   THIS SUBROUTINE CALCULATES THE VISCOUS DRAG FORCE ON THE
04280 C   SPAR BUOY DURING ITS DYNAMIC MOTIONS. INTEGRATION OF FORCES
04290 C   IS DONE ALONG THE AXIS OF THE SPAR.
04300 C
04310 C
04320 COMMON W(8),CM(8),CMS(8),CMD(8),CMN(8),CMT(8),SL(8),EK(8),CDIN(8),
04330 1CDIT(8),CDIA(8),DEP(8),TN(8),TNN(8),TL(8),YDD(27),YD(27),Y(27),X(2
04340 17),F(27),DD(27),TC(30),CS(30),VN(30),V(3,8),UU(3,8),GM(8,27),GM(27,
04350 127),WWD1,WWD2,HMAX,HO,HI,HST,HOD,XC1,YC1,ZC1,XC2,YC2,ZC2,RRHO1,RRH
04360 102,XJ1,YJ1,ZJ1,XJ2,YJ2,ZJ2,RD1,RD2,S01,S02,BB1,BB2,CSB,SNB,THASS,Y
04370 INERT1,YNERT2,UVO,ZCG,SNK,CSK,DEPTH,CPL,CDF,PI,RHO,GR,DEXP,AU,AWX,A
04380 IWY,AMP,WE,T,DT,F1,F2,QO,Q1,NST,NM,NM2,NDF,NB,NB1,NB2,NN,HOOR,N
04390 1D
04400 C*****COEFFICIENTS OF THE VELOCITY EQUATION ARE CALCULATED BELOW*****
04410 V1=V(1,NB)-YD(NN-2)+X(NN+3)*(V(2,NB)-YD(NN-1))-X(NN+2)*(V(3,NB)-YD
04420 1(NN))
04430 V2=WE*XAMP*CSB*SNK
04440 V3=-X(NN+3)*(V(1,NB)-YD(NN-2))+V(2,NB)-YD(NN-1)+X(NN+1)
04450 1*(V(3,NB)-YD(NN))
04460 V4=WE*XAMP*SNB*SNK
04470 V5=X(NN+2)*(V(1,NB)-YD(NN-2))-X(NN+1)*(V(2,NB)-YD(NN-1))
```

04480 1+U(3,NB)-YD(NN)
04490 V6=-WE*AMP*CCK
04500 VTB=V5-V6*OEXP
04510 VTS=V5-V6*OEXP*DEXP(AW*HST)
04520 C****PRESSURE DRAG DUE TO BOTTOM END AND STEP OF THE SPAR IS CALCULATED
04530 DF=0.5*RHO*CDP*(S01*DABS(VTB)*VTB+(S01-S02)*DABS(VTS))
04540 DNT1=0.
04550 DNT2=0.
04560 DDTT=0.
04570 DM1=0.
04580 DM2=0.
04590 C*****THE VISCOUS DRAG FORCE AND MOMENT ON THE SPAR IS CALCULATED****
04600 RD=RDI
04610 NDS1=NST*HST/HI
04620 NDS2=NST-NDS1
04630 NDS=NDS1
04640 DZ=HST/NDS
04650 ZZ=DZ/2.-ZCG
04660 RH00=RHO*CDL
04670 DO 2 INZ=1,2
04680 DO 1 IZ=1,NDS
04690 XXE=DEXP(AW*(ZCG+ZZ))
04700 UN1=V1-V2*OEXP*XXE-ZZ*YD(NN+2)
04710 UN2=V3-V4*OEXP*XXE+ZZ*YD(NN+1)
04720 UNM=ISQRT(UN1*UN1+UN2*UN2),
04730 DN1=UNM*UN1*RD*DZ
04740 DN2=UNM*UN2*RD*DZ
04750 DNT1=DNT1+DN1
04760 DNT2=DNT2+DN2
04770 VTT=V5-V6*OEXP*XXE
04780 DDTT=DDTT+VTT*DABS(VTT)*RD*DZ
04790 DM1=DM1-ZZ*DN2

```
04800      DM2=DM2+ZZ*DN1
04810      1      ZZ=ZZ+DZ
04820      RD=RD2
04830      NDS=NDS2
04840      DZ=(HI-HST)/NDS
04850      ZZ=HST+DZ/2.-ZCG
04860      2      CONTINUE
04870      DD(NN-2)=RHOO*(INT1-X*(NN+3)*INT2+X*(NN+2)*(DDT*0.02+DP/RHOO))
04880      DD(NN-1)=RHOO*(INT1*X*(NN+3)+INT2-X*(NN+1)*(DDT*0.02+DP/RHOO))
04890      DD(NN)=RHOO*(-INT1*X*(NN+2)+INT2*X*(NN+1)+DDT*0.02+DP/RHOO)
04900      DB(INT1)=RHOU*(UM1-DM2*X*(NN+3))
04910      DD(NN+2)=RHOO*(UM1*X*(NN+3)+DM2)
04920      DD(NN+3)=RHOO*(-UM1*X*(NN+2)+DM2*X*(NN+1))
04930      RETURN
04940      END
04950      IMPLICIT REAL*8(A-H,O-Z)
04960      SUBROUTINE BUYS
04970      C THIS SUBROUTINE CALCULATES THE MASS MATRIX FOR THE SPAR BUOY
04980      C
04990      C
05000      COMMON W(8),CM(8),CMS(8),CMD(8),CMT(8),SL(8),EK(8),CDIN(B),
05010      CDIT(8),CDIA(B),DEP(8),TN(8),TNN(8),TL(8),YD(27),Y(27),X(2
05020      17),F(27),DD(27),TC(30),CS(30),VN(3),V(3,8),VV(3,8),GM(27,
05030      127),WWD1,WWD2,HMAX,HO,HI,HST,HOD,XC1,YC1,ZC1,XC2,YC2,ZC2,RRH01,FRH
05040      1Q2,XJ1,YJ1,ZJ1,XJ2,YJ2,ZJ2,RD1,RO2,S01,S02,BB1,BB2,CSB,SNB,TMASS,Y
05050      INERT1,YNERT2,VVO,ZCG,SNK,CSK,DEPTH,CBL,CDP,P1,RHD,GS,DEXP,AW,AWX,A
05060      1WY,AMP,WE,T,DT,P1,P2,QO,Q1,NST,NM,NM1,NM2,NDF,NB,NR1,NB2>NN,MOOR,N
05070      ID
05080      DO 1 I=1,NDF
05090      DO 1 J=1,NDF
05100      1      GM(I,J)=0.
05110      BK1=(BB1-BB2)*HST
```

```
05120 BK2=BB2*HO
05130 P0=BB1*HST+BB2*(HO-HST,
05140 P1=BK2*(0.5*HO-ZCG)+BK1*(0.5*HST-ZCG)
05150 P2=BK2*(HO*HO/3.-HO*ZCG+ZCG*ZCG)+BK1*(HST*HST/3.-HST*ZCG+ZCG*ZCG)
05160 QQ2=DEXP(-HOD*AW)
05170 Q0=(BB1*(QQ2-OEXP)+BB2*(1.-QQ2))/AW
05180 Q1=(BB1*(QQ2*(HST-1./AW-ZCG)+OEXP*(1./AW+ZCG))+BB2*(HO-1./AW-ZCG-Q
05190 1Q2*(HST-1./AW-ZCG))/AW
05200 C*****CODEFFICIENTS IN EQUATIONS OF BUOY MOTION*****
05210 GM(NN-2,NN-2)=TMASS+F0
05220 GM(NN-2,NN)=X(NN+2)*(VVD-PO)
05230 GM(NN-2,NN+2)=F1
05240 GM(NN-1,NN-1)=GM(NN-2,NN-2)
05250 GM(NN-1,NN)=X(NN+1)*(F0-VVO)
05260 GM(NN-1,NN+1)=-GM(NN-2,NN+2)
05270 GM(NN,NN-2)=GM(NN-2,NN)
05280 GM(NN,NN-1)=GM(NN-1,NN)
05290 GM(NN,NN)=TMASS+VVO
05300 GM(NN+1,NN)=-F1*X(NN+1)
05310 GM(NN+1,NN-1)=GM(NN-1,NN+1)
05320 GM(NN+1,NN+1)=YNERT1+P2
05330 GM(NN+2,NN-2)=GM(NN-2,NN+2)
05340 GM(NN+2,NN)=-P1*X(NN+2)
05350 GM(NN+2,NN+2)=GM(NN+1,NN+1)
05360 GM(NN+3,NN-2)=-GM(NN+1,NN)
05370 GM(NN+3,NN-1)=-GM(NN+2,NN)
05380 GM(NN+3,NN+3)=YNERT2
05390 RETURN
05400 END
05410 IMPLICIT REAL*8(A-H,O-Z)
05420 SUBROUTINE NEXT
05430 C THIS SUBROUTINE UPDATES THE GEOMETRY OF THE SYSTEM DURING
```

05440 C ITS DYNAMIC MOTIONS.

```
05450 C
05460 C
05470      COMMON W(8),CM(8),CM2(8),CMD(8),CMT(8),SL(8),EK(8),CDIN(8),
1CDIT(8),CDIA(8),DEP(8),TN(8),TNN(8),TL(8),YDD(27),YD(27),Y(27),
05480      F(27),DD(27),TC(30),CS(30),VN(3),V(3,8),UU(3,8),GK(8,27),GM(27,
05490      17),WWD1,WWD2,HMAX,HO,HI,HST,HOD,XC1,ZC1,YC1,ZC2,RC2,RRH01,RRH
05500      102,XJ1,YJ1,ZJ1,XJ2,YJ2,RD1,RD2,S01,S02,BB1,BB2,CSB,SNB,TMASS,Y
05510      INERT1,YNERT2,VV0,ZCG,SNK,CSK,DEPTH,CDL,CDP,PI,RHO,GR,OEXP,AW,AWX,A
05520      IW,AMP,WE,T,DT,P1,P2,Q0,Q1,NST,NM,NM1,NM2,NDF,NB,NB1,NB2,NN,MOOR,N
05530
05540      1D
05550      IF(MOOR.EQ.2)GO TO 3
05560      XJ1=X(NN-2)+XC1
05570      YJ1=X(NN-1)+YC1
05580      ZJ1=X(NN)+ZC1
05590      IF(NB.EQ.1)GO TO 1
05600      TL(1)=DSQRT(X(1)**2+X(2)**2+X(3)**2)
05610      CS(1)=X(1)/TL(1)
05620      CS(2)=X(2)/TL(1)
05630      CS(3)=X(3)/TL(1)
05640      TL(NB)=DSQRT((XJ1-X(NN-5))**2+(YJ1-X(NN-4))**2+(ZJ1-X(NN-3))**2)
05650      CS(NN-2)=(XJ1-X(NN-5))/TL(NB)
05660      CS(NN-1)=(YJ1-X(NN-4))/TL(NB)
05670      CS(NN)=(ZJ1-X(NN-3))/TL(NB)
05680      GO TO 2
05690      1      TL(1)=DSQRT(XJ1**2+YJ1**2+ZJ1**2)
05700      2      CS(1)=XJ1/TL(1)
05710      3      CS(2)=YJ1/TL(1)
05720      CS(3)=ZJ1/TL(1)
05730      2      IF(NM.EQ.NB)GO TO 4
05740      3      XJ2=X(NN-2)+XC2
05750      YJ2=X(NN-1)+YC2
```

```
05760 ZJ2=X(NN)+ZC2
05770 TL(NB2)=DSQRT((X(NN+4)-XJ2)**2+(X(NN+5)-YJ2)**2+(X(NN+6)-ZJ2)**2)
05780 CS(NN+4)=(X(NN+4)-XJ2)/TL(NB2)
05790 CS(NN+5)=(X(NN+5)-YJ2)/TL(NB2)
05800 CS(NN+6)=(X(NN+6)-ZJ2)/TL(NB2)
05810 4 DO 5 I=2,NN
05820 IF(I.EQ.NB.OR.I.EQ.NB2)GO TO 5
05830 II=3*I+1
05840 IF(I.LT.NB)II=II-3
05850 TL(I)=DSQRT((X(II)-X(II-3))*2+(X(II+1)-X(II-2))*2+(X(II+2)-X(II-
11))**2)
05860 5 CONTINUE
05870 CS(II)=(X(II)-X(II-3))/TL(I)
05880 CS(II+1)=(X(II+1)-X(II-2))/TL(I)
05890 CS(II+2)=(X(II+2)-X(II-1))/TL(I)
05900 5 CONTINUE
05910 RETURN
05920 END
05930 IMPLICIT REAL*8(A-H,O-Z)
05940 SUBROUTINE MINUER(N,C)
05950 C THIS SUBROUTINE CALCULATES THE INVERSE OF A MATRIX 'C'
05960 C OF ORDER 'N'
05970 C -----
05980 C
05990 DIMENSION C(27,27),H(27),G(27)
06000 NN=N-1
06010 C(1,1)=1.0/C(1,1)
06020 DO 6 M=1,NN
06030 K=M+1
06040 DO 1 I=1,M
06050 G(I)=0.
06060 DO 1 J=1,M
06070 1 G(I)=G(I)+C(I,J)*C(J,K)
```

```
06080      D=0.
06090      DO 2 I=1,M
06100      2   D=D+C(K,I)*G(I)
06110      E=C(K,K)-D
06120      C(K,K)=1.0/E
06130      DO 3 I=1,M
06140      3   C(I,K)=-G(I)*C(K,K)
06150      DO 4 J=1,M
06160      H(J)=0.
06170      DO 4 I=1,M
06180      4   H(J)=H(J)+C(K,I)*C(I,J)
06190      DO 5 J=1,M
06200      5   C(K,J)=-H(J)*C(K,K)
06210      DO 6 I=1,M
06220      DO 6 J=1,M
06230      6   C(I,J)=C(I,J)-G(I)*C(K,J)
06240      RETURN
06250      END
06260      IMPLICIT REAL*8(A-H,O-Z)
06270      SUBROUTINE MATRIX
06280      C THIS SUBROUTINE CALCULATES THE REMAINING ELEMENTS OF THE GLOBAL
06290      C MATRICES AND INTEGRATES THE 'NDF' SIMULTANEOUS DIFFERENTIAL
06300      C EQUATIONS OF MOTION BY THE METHOD OF RECTANGULAR RULE.
06310      C
06320      C
06330      COMMON W(8),CM(8),CMS(8),CMD(8),CMN(8),CMT(8),SL(8),EK(8),CDIN(8),
06340      1CDIT(8),CDIA(8),DEP(8),TN(8),TNN(8),TL(8),YD(27),YD(27),Y(27),X(2
06350      17),F(27),DD(27),TC(30),CS(30),VN(3),V(3,8),VV(3,8),GK(8,27),GM(27,
06360      127),WWD1,WWD2,WMAX,HO,HI,HST,HOD,XC1,YC1,ZC1,XC2,YC2,ZC2,RRHO1,RRH
06370      102,XJ1,YJ1,ZJ1,XJ2,YJ2,ZJ2,RD1,RD2,S01,S02,BB1,BB2,CSB,SNB,TMASS,Y
06380      1NERT1,YNERT2,VV0,ZCG,SNK,CSK,DEPTH,CDL,CDP,PI,RHO,GR,OEXP,AU,AWX,A
06390      1WY,AMP,WE,T,DT,P1,P2,Q0,Q1,NM1,NM2,NDF,NB,NB1,NB2,NN,MDR,N
```

06400 1D
06410 C*****WAVE EXCITING PLUS HYDROSTATIC FORCES ON THE SPAR BUOY*****
06420 F(NN-2)=2.*WE*WE*AMP*CSB*D0*CSK
06430 F(NN-1)=2.*WE*WE*AMP*SNB*Q0*CSK
06440 F(NN)=WE*WE*AMP*Q0*SNK+GR*(KB1*HST+BB2*(HI-HST)-THASS)
06450 F(NN+1)=-WE*WE*2.*AMP*SNB*Q1*CSK-GR*P1*X(NN+1)
06460 F(NN+2)=WE*WE*2.*AMP*CSB*Q1*CSK-GR*P1*X(NN+2)
06470 IF(MOOR.EQ.0)GO TO 11
06480 C****STIFFNESS MATRIX FOR THE MOORING LINES*****
06490 AA1=XC1-YC1*X(NN+3)+ZC1*X(NN+2)
06500 AA2=XC2-YC2*X(NN+3)+ZC2*X(NN+2)
0510 AB1=XC1**X(NN+3)+YC1-ZC1*X(NN+1)
06520 AB2=XC2**X(NN+3)+YC2-ZC2*X(NN+1)
06530 AC1=-XC1*X(NN+2)+YC1*X(NN+1)+ZC1
06540 AC2=-XC2*X(NN+2)+YC2*X(NN+1)+ZC2
06550 GK(1,1)=EK(1)*CS(1)
06560 GK(1,2)=EK(1)*CS(2)
06570 GK(1,3)=EK(1)*CS(3)
06580 GK(NB,NN+1)=EK(NB)*(-AC1*CS(NN-1)+AB1*CS(NN))
06590 GK(NB,NN+2)=EK(NB)*(AC1*CS(NN-2)-AA1*CS(NN))
06600 GK(NB,NN+3)=EK(NB)*(-AB1*CS(NN-2)+AA1*CS(NN-1))
06610 IF(NM.EQ.1)GO TO 5
06620 IF(NM.EQ.NB)GO TO 1
06630 GK(NB2,NN-2)=-EK(NB2)*CS(NN+4)
06640 GK(NB2,NN-1)=-EK(NB2)*CS(NN+5)
06650 GK(NB2,NN)=-EK(NB2)*CS(NN+6)
06660 GK(NB2,NN+1)=-EK(NB2)*(-AC2*CS(NN+5)+AB2*CS(NN+6))
06670 GK(NB2,NN+2)=-EK(NB2)*(AC2*CS(NN+4)-AA2*CS(NN+6))
06680 GK(NB2,NN+3)=-EK(NB2)*(-AB2*CS(NN+4)+AA2*CS(NN+5))
06690 GK(NB2,NN+4)=-GK(NB2,NN-2)
06700 GK(NB2,NN+5)=-GK(NB2,NN-1)
06710 GK(NB2,NN+6)=-GK(NB2,NN)

```
06720   1 DO 2 I=2,NM
06730     IF(I.EQ.NB2)GO TO 2
06740     II=3*I
06750     IF(I.GT.NB)II=II+3
06760     GK(I,II-5)=-EK(I)*CS(II-2)
06770     GK(I,II-4)=-EK(I)*CS(II-1)
06780     GK(I,II-3)=-EK(I)*CS(II)
06790     GK(I,II)=-GK(I,II-3)
06800     GK(I,II-1)=-GK(I,II-4)
06810     GK(I,II-2)=-GK(I,II-5)
06820   2 CONTINUE
06830 C*****A MATRIX FOR THE MOORING LINES*****
06840   DO 4 I=1,NM
06850     IF(I.EQ.NB)GO TO 4
06860     II=3*I+1
06870     IF(I.LT.NB)II=II-3
06880     GM(II,II)=CM(I)+CMS(I)*(1.-CS(II+3)**2)+CMT(I)*CS(II+3)**2
06890     GM(II+1,II+1)=CM(I)+CMS(I)+CMN(I)*(1.-CS(II+4)**2)+CMT(I)*CS(II+4)
1***2
06900     GM(II+2,II+2)=CM(I)+CMS(I)+CMN(I)*(1.-CS(II+5)**2)+CMT(I)*CS(II+5)
1***2
06910     GM(II,II+1)=(CMT(I)-CMN(I))*CS(II+4)*CS(II+3)
06920     GM(II+1,II)=GM(II,II+1)
06930     GM(II,II+2)=(CMT(I)-CMN(I))*CS(II+3)
06940     GM(II+1,II+2)=(CMT(I)-CMN(I))*CS(II+3)
06950     GM(II+1,II+3)=(CMT(I)-CMN(I))*CS(II+3)
06960     GM(II+2,II)=(CMT(I)-CMN(I))*CS(II+4)
06970     GM(II+2,II+1)=GM(II,II+2)
06980     GM(II+2,II+1)=GM(II+1,II+2)
06990     UWE=GR*AMF*DEXP(AU*(X(II+2)-DEPTH))
07000     SUE=AUX*X(II)+AUY*X(II+1)-WE*T
07010     SNK1=DSIN(SUE)
07020     CSK1=DCOS(SUE)
07030     PHX=UWE*AUX*CSK1
```

07040 PHY=WWE*AWY*CSK1
07050 PHZ=WWE*AW*SNK;
07060 C*****VISCOUS DRAG FORCE ARRAY FOR THE MOORING LINES*****
07070 U1=U(1,I)-YD(I,I)-AUX*SNK1*WWE/WE
07080 U2=U(2,I)-YD(I,I+1)-AWY*SNK1*WWE/WE
07090 U3=U(3,I)-YD(I,I+2)+AW*CSK1*WWE/WE
07100 UT1=U1*CS(I,I+3)+U2*CS(I,I+4)+U3*CS(I,I+5)
07110 VN(1)=U1*(1.-CS(I,I+3))*CS(I,I+3)*CS(I,I+4)-U3*CS(I,I+3)*
1CS(I,I+5)
07120 VN(2)=U2*(1.-CS(I,I+4))*CS(I,I+4)-U3*CS(I,I+5)-U1*CS(I,I+4)*
1CS(I,I+3)
07130 VN(3)=U3*(1.-CS(I,I+5))*CS(I,I+5)-U1*CS(I,I+3)-U2*CS(I,I+5)*
1CS(I,I+4)
07140 DDTT=CDIT(I)*UT1*ABS(UT1)
07150 VNM=DSQRT(VN(1)*VN(1)+VN(2)*VN(2)+VN(3)*VN(3))
07160 VNM1=DSQRT(U1*U1+U2*U2+U3*U3)*CDIA(I)
07170 DD(I,I)=CDIN(I)*VNM*VN(1)+DDTT*CS(I,I+3)+VN1*U1
07180 DD(I,I+1)=CDIN(I)*VNM1*VN(2)+DDTT*CS(I,I+4)+VN1*U2
07190 DD(I,I+2)=CDIN(I)*VNM1*VN(3)+DDTT*CS(I,I+5)+VN1*U3
07200 IF(MOOR.EQ.2.AND.I.GE.ND) GO TO 3
07210 C*****FROUDE KRYLOV FORCE ARRAY FOR THE MOORING LINES*****
07220 F(I,I)=CMD(I)*PHX
07230 F(I,I+1)=CMD(I)*PHY
07240 F(I,I+2)=-W(I)+CMD(I)*PHZ
07250 GO TO 4
07260 3 F(I,I)=CMD(I)*(PHX*(1.-CS(I,I+3))*CS(I,I+3)-PHY*CS(I,I+4)-PHZ
07270 1*CS(I,I+3)*CS(I,I+5),
07280 F(I,I+1)=CMD(I)*(PHY*(1.-CS(I,I+4))*CS(I,I+4)-PHZ*CS(I,I+4)*CS(I,I+5)-P
07290 1HX*CS(I,I+4)*CS(I,I+3),
07300 F(I,I+2)=CMD(I)*(PHZ*(1.-CS(I,I+5))*CS(I,I+5)-PHX*CS(I,I+4)*CS(I,I+3)-P
07310 1HY*CS(I,I+5)*CS(I,I+4)-W(I)
07320 4 CONTINUE

```
07360 C*****TENSION FORCE ARRAY FOR THE MOORING LINES*****
07370      5 DO 7 K=1,NM
07380      TG=0.
07390      DO 6 IK=1,NDF
07400      6 TG=.3+GK(K,IK)*Y(IK)
07410      TNN(K)=TG+TNN(K)
07420      TN(K)=TNN(K)
07430      IF(TN(K).LE.0.)TN(K)=0.
07440      KK=3*K+1
07450      IF(K.LE.NB)KK=KK-3
07460      TC(KK)=TN(K)*CS(KK)
07470      TC(KK+2)=TN(K)*CS(KK+2)
07480      7 TC(KK+1)=TN(K)*CS(KK+1)
07490      TC(NN+1)=-AC1*TC(NN-1)+AB1*TC(NN)+AC2*TC(NN+5)-AB2*TC(NN+6)
07500      TC(NN+2)=AC1*TC(NN-2)-AA1*TC(NN)-AC2*TC(NN+4)+AA2*TC(NN+6)
07510      TC(NN+3)=-AP1*TC(NN-2)+AA1*TC(NN-1)+AB2*TC(NN+5)
07520      IF(NM.EQ.1)GO TO 11
07530      IF(MOOR.EQ.2)GO TO 9
07540      NZ=NN-3
07550      DO 8 N=1,NZ
07560      8 TC(M)=TC(M)-TC(M+3)
07570      9 TC(NN-2)=TC(NN-2)-TC(NN+4)
07580      TC(NN-1)=TC(NN-1)-TC(NN+5)
07590      TC(NN)=TC(NN)-TC(NN+6)
07600      IF(NM.EQ.NB)GO TO 11
07610      NZ=NN+4
07620      DO 10 M=NZ,NDF
07630      10 TC(M)=TC(M)-TC(M+3)
07640      C****SOLUTION OF THE DIFFERENTIAL EQUATIONS*****
07650      CALL MINVER(NDF,GM)
07660      11 DO 13 M=1,NDF
07670      YDD(M)=0.
```

```
07680      DO 12 K=1,NDF
07690      12      YDD(M)=YDD(M)+GM(M,K)*(DD(K)-TC(K)+F(K))
07700      YD(M)=YD(M)+YDD(M)*DT
07710      Y(M)=YD(M)*DT
07720      X(M)=X(M)+Y(M)
07730      HO=HO-Y(NN),
07740      HOD=HO-HST
07750      RETURN
07760      END
READY
```

SD2.FORT

```
00010 C
00020 C 2 D DYNAMIC ANALYSIS OF A SPAR BUOY, A SURFACE MOORED SYSTEM,
00030 C AND A DRIFTING DROGUE SPAR BUOY.
00040 C
00050 C THE UNITS USED IN THIS ANALYSIS ARE FEET/POUNDS/SECONDS.
00060 C
00070 C CASE STUDY 1--MOOR=0--SPAR BUOY FREELY FLOATING IN A SURFACE WAVE.
00080 C CASE STUDY 2--MOOR=1--SPAR BUOY ANCHORED WITH A LUMPED MASS
00090 C MOORING LINE; NM=NB.
00100 C CASE STUDY 3--MOOR=1--SPAR BUOY ANCHORED WITH A LUMPED MASS
00110 C MOORING LINE AND A LUMPED MASS INSTRUMENT LINE HANGING FROM
00120 C THE BUOY; NM NOT EQUAL TO NB.
00130 C CASE STUDY 4--MOOR=2--SPAR BUOY ATTACHED TO A WINDOW SHADE
00140 C DROGUE; NB=1.
00150 C
00160 C
00170 C*****START OF THE MAIN PROGRAM*****
00176 C*****IMPLICIT REAL*(A-H,0-Z)
00180 IMPLICIT REAL*(A-H,0-Z)
00190 COMMON W(8),CM(8),CMS(8),CMD(8),CMT(8),SL(8),EK(8),CDIN(8),
00200 1CDIT(8),CDIA(8),DEF(8),V(8),UU(8),TN(8),TL(8),CS(9),SN(9),Y
00210 1D(17),YD(17),Y(17),X(17),F(17),DD(17),TC(19),GK(8,17),GM(17,17),D
00220 1C1,DC2,DC3,XC1,ZC1,XC2,ZC2,WWD1,WWD2,S01,S02,CS1,SN1,RD1,RD2,XJ1,Y
00230 1J1,XJ2,YJ2,BB1,BB2,HMAX,HD,HST,RRH01,RRH02,TMASS,YNERT,ZCG,HI,
00240 1TH0,CMF,CDL,CON,COT,ALPHA,PI,RHO,GR,AW,T,DT,AMP,WE,SNK,CSK,DEPTH,O
00250 1K,UUV(8),QEXP,UVD,UW1,XW,ZW,EMW,MOOR,NST,NM,NM1,NM2,NDF,NB,NB1,NB2
00260 1,NN,ND
00270 100 FORMAT(12F10.2)
00280 101 FORMAT(7F10.0)
00290 102 FORMAT(6I5,4F10.0)
00300 103 FORMAT(6F10.0)
00310 C*****GENERAL DATA*****
```

```
00320 READ(5,102)NM,NF,ND,NST,NC,MOOR,DEPTH,DT,TMAX,T2
00330 C*****BUOY DATA*****HMAX,CDF,HST,CON,COT,CDF,ALPHA
00340 READ(5,101)RD1,RD2,ZCG,RGYR,HMAX,CDF,HST,CON,COT,CDF,ALPHA
00350 C*****MOORING LINE DATA*****HMAX,CDF,HST,CON,COT,CDF,ALPHA
00360 READ(5,103)(W(I),CM(I),CMS(I),CMT(I),CMN(I),I=1,NM)
00370 READ(5,103)(SL(I),EK(I),CDIN(I),CDIT(I),CDIA(I),I=1,NM)
00380 C*****ATTACHMENT DATA*****HMAX,CDF,HST,CON,COT,CDF,ALPHA
00390 READ(5,101)XC1,ZC1,XC2,ZC2
00400 C*****CURRENT PROFILE DATA*****HMAX,CDF,HST,CON,COT,CDF,ALPHA
00410 READ(5,101)(V(I),I=1,NM)
00420 NM1=NM-NB
00430 NN=NB+NB
00440 NB1=NB-1
00450 NB2=NB+1
00460 NM2=NM+1
00470 NDF=2*NM+1
00480 C*****INITIALIZE PHYSICAL CONSTANTS*****HMAX,CDF,HST,CON,COT,CDF,ALPHA
00490 PI=4.*PI*DATA(1,DO)
00500 S01=PI*RD1*RD1
00510 S02=PI*RD2*RD2
00520 RHO=1.9905
00530 GR=32.2
00540 TMASS=W(NB)/GR
00550 YNERT=TMASS*RGYR*RGYR
00560 RRHO1=RHO*CDL*RD1*HST
00570 RRHO2=RHO*CDL*RD2
00580 BB1=RHO*S01
00590 BB2=RHO*S02
00600 WWD1=BB1*GR*HST
00610 WWD2=BB2*GR
00620 VVD=1.33*RHO*ALPHA*RD1**3
00630 VV1=1.33*RHO*ALPHA*(RD1-RD2)**3
```

```
00640 C*****START LOOP FOR DYNAMIC RESPONSE TO DIFFERENT SURFACE WAVES*****
00650      DO 8 ICC=1,NC
00660      READ(5,101)WE,AMP
00670 C*****INITIALIZE DYNAMIC VARIABLES*****
00680      DC1=0.
00690      DC2=0.
00700      DC3=0.
00710      DO 1 I=1,NDF
00720      YD(I)=0.
00730      TC(I)=0.
00740      Y(I)=0.
00750      DO 1 J=1,NM
00760      1 GK(J,I)=0,
00770      AW=WE*WE/GR
00780      T3=0.
00790 C****FIND THE CURRENT PROFILE FOR STATIC SOLUTION*****
00800      DO 3 I=1,NM
00810      VV(I)=0.
00820      ZX4=0.
00830      ZX1=WE*AMP*DEXP(AW*DEP(I))
00840      DO 2 J=1,12
00850      ZX3=ZX1*DCOS(PI*j/6.)
00860      ZX2=V(I)+ZX1*DSIN(PI*j/6.)
00870      VEM=DSQRT((ZX2**2+ZX3**2),
00880      ZX4=ZX4+ZX3*UEM
00890      2 VU(I)=UU(I)+ZX2*UEM
00900      UEM=(ZX4**2+UU(I)**2)**0.25
00910      UU(I)=UU(I)/(UEM1*12.***0.5)
00920      3 IF(DABS(UU(I)).LE.0.000001)UU(I)=0.
00930      WRITE(6,100)(UU(I),I=1,NM)
00940      TC(NDF+1)=0.
00950      TC(NDF+2)=0.
```

```
00960 IF(NM,ER,NR)GO TO 5
00970 CS(NM2)=0.
00980 SN(NM2)=-1.
00990 IF(MODR,ER,2)GO TO 5
01000 C*****STATIC SOLUTION OF THE LUMPED MASSES (INSTRUMENT LINE)*****
01010 DO 4 I=1,NM1
01020 J=NM2-I
01030 N=J+1
01040 II=J+J
01050 VN=UU(J)*SN(K)
01060 VT=UU(J)*CS(K)
01070 DI=CDIA(J)*UU(J)*DABS(UV(J))
01080 DTTT=CDIT(J)*UT*DABSC(UT)
01090 DN=CDIN(J)*VN*DABSC(VN)
01100 TC(I,I)=TC(I,I+2)+DI+DTTT*CS(K)+DN*SN(K)
01110 TC(I,I+1)=TC(I,I+3)+DTTT*SN(K)-DN*CS(K)-W(J)
01120 TN(N,J)=DSQRT(TC(I,I)*X2+TC(I,I+1)**2)
01130 CS(J)=TC(I,I)/TNN(J)
01140 SN(J)=TC(I,I+1)/TNN(J)
01150 4 TL(J)=SL(J)+TNN(J)/EK(J)
01160 5 CALL STATIC
01170 T=0.
01180 6 SS=AUX(X(NN-1)-WE*T
01190 SNK=DSIN(SS)
01200 CSK=DCOS(SS)
01210 OK=AUX*CS1
01220 OEXP=DEXP(-HO*XCK)
01230 HI=HO-AMP*SNK/CS1
01240 IF(CDL.NE.0.0)CALL DBDRG
01250 CALL BUOYS
01260 CALL MATRIX
01270 IF(T.LT.T3)GO TO 7
```

```
01280      WRITE(6,100)T
01290      WRITE(6,100)(X(I),I=1,NDF)
01300      IF(MODR.EQ.1)WRITE(6,100)(TN(K),K=1,NM)
01310      IF(MODR.EQ.2)WRITE(6,100)(TN(K),K=2,NM)
01320      IF(T.GT.TMAX)GO TO 8
01330      T3=Y3+T2
01340      7   T=T+DT
01350      IF(MODR.GT.0)CALL NEXT
01360      GO TO 6
01370      8   CONTINUE
01380      CALL EXIT
01390      END
01400      IMPLICIT REAL*8(A-H,D-Z)
01410      SUBROUTINE STATIC
01420      THIS SUBROUTINE CALCULATES THE STATIC SOLUTION OF THE FOUR CASE
01430      STUDIES OUTLINED IN THE MAIN PROGRAM
01440      C
01450      C
01460      COMMON W(8),CM(8),CMS(8),CND(8),CMN(8),CMT(8),SL(8),EK(8),CDIN(8),
01470      CDIT(8),CDIA(8),DEP(8),V(8),VV(8),TN(8),TNN(8),TL(8),CS(9),SN(9),Y
01480      1D(17),YD(17),Y(17),X(17),F(17),DD(17),TC(17),GK(8,17),GM(17,17),D
01490      1C1,DC2,DC3,XC1,XC2,ZC1,ZC2,WWD1,WWD2,SQ1,SQ2,CS1,SN1,RD1,RD2,XJ1,Y
01500      1J1,XJ2,YJ2,BR1,BB2,HMAX,HQ,HST,HOD,RRHO1,RRHO2,TMASS,YNERT,ZCG,HI,
01510      THO,CDF,CDL,CON,COT,ALPHA,PI,RHQ,GR,AW,T,DT,AMF,WE,SNK,CSK,DEPTH,O
01520      1K,VUU(8),OEXP,VVD,VV1,XW,ZW,EMW,MDR,NST,NM,NM1,NM2,NDF,NB,NB1,NB2
01530      1,NN,ND
01540      100   FORMAT(9F12.3)
01550      101   FORMAT(//9X11HSTATIC CALCULATION TERMINATED -- NUMBER OF ITERATI
01560      1ONS TO DETERMINE BUOY EQUILIBRIUM CONDITION EXCEEDS MAXIMUM ( 13,
01570      1 1H),
01580      102   FORMAT(//10X,6SHSTATIC CALCULATION TERMINATED -- BUOY HAS EXCEEDED
01590      1ED MAXIMUM DRAFT )
```

```
01600 103 FORMAT (//10X,100HSTATIC CALCULATION TERMINATED -- NUMBER OF ITER
01610 IATIONS TO FIND STATIC SOLUTION HAS EXCEEDED MAXIMUM ( 13,1H))
01620 IF(MDOR.EQ.0)GO TO 33
01630 DATA ITMAX,ITIMAX/100,100/
01640 IT1=0
01650 INDEX=1
01660 EMAX=.01*XW(NB)*(RD1+RD2)
01670 IF(MDOR.EQ.1)GO TO 8
01680 C
01690 C*****CASE STUDY 4 ****
01700 C*****
01710 C*****INITIALIZE VARIABLES*****
01720 IS2=0
01730 DC2=0.
01740 VE=0.
01750 FXE=0.02*XMAX*RD2*V(1)*V(1)+0.01
01760 TUE=DABS(V(NM))/2.
01770 X(3)=0.
01780 CS1=1.
01790 SN1=0.
01800 DTTHI=0.05
01810 C*****START STATIC VELOCITY ITERATION LOOP*****
01820 1 INDEX=INDEX+1
01830 2 IT1=IT1+1
01840 IF(IT1.GT.ITIMAX)GO TO 30
01850 ITTH=DTTHI
01860 IT=0
01870 IS=0
01880 DO 3 IC=1,NM
01890 3 UVV(IC)=UV(IC)-VE
01900 DO 4 IC=2,NM
01910 K=NM-JC+3
```

```
J=K-1
01920
01930
01940
01950
01960
01970
01980
01990
02000
02010
02020
02030
02040
02050
02060
02070
02080
02090
02100
02110
02120
02130
02140
02150
02160
02170
02180
02190
02200
02210
02220
02230

    UN=UUU(J)*SN(K)
    UT=UUU(J)*CS(K)
    DN=CDIN(J)*VN*DABS(VN)
    DDTT=CDIT(J)*UT*DABS(UT)
    DI=CDIA(J)*UUU(J)*DABS(UUU(J))
    TC(II)=TC(II+2)+DI+DDTT*CS(K)+DN*SN(K)
    TC(II+1)=TC(II+3)+DDTT*SN(K)-DN*CS(K)-W(J)
    TNN(J)=DSQRT(TC(II)*TC(II)+TC(II+1)*TC(II+1))
    CS(J)=TC(II)/TNN(J)
    SN(J)=TC(II+1)/TNN(J)
    TL(J)=SL(J)+TNN(J)/EK(J)
    IF(INDEX.EQ.3)GO TO 11
    HO=HST+`W(1)-TC(5)-DC2-WWD1)/WWD2
    RRHO=RRHO1+RRHO2*(HO-HST)
    VN=UUU(1)*CS1
    VT=UUU(1)*SN1
    DDTT=(0.02*RRHO+0.5*RHO*CDP*(2.*S01-S02))*DABS(UT)*VT
    DN=RRHO*VN*DABS(VN)
    DC1=DN*CS1+DDTT*SN1
    FX=DC1+TC(4)
    WRITE(6,100)VE,HO,FX
    IF(DABS(FX).LE.FXE)GO TO 6
    IS3=DSIGN(1.0D0,FX)
    IF(IS2+IS3.EQ.0)DVE=DVE/2.
    VE=VE+IS3*DVE
    IS2=IS3
    GO TO 2
    IF(INDEX.EQ.2)GO TO 1
    WRITE(6,100)VE,HO,E
    YD(1)=VE
```

```
02240      DO 7 I=2,NM
02250      II=I+I
02260      7 YD(I)=VE
02270      X(1)=0.
02280      X(2)=(ZCG-H0)*CS1+DEPTH
02290      TN(1)=0.
02300      CS(1)=0.
02310      SN(1)=0.
02320      GO TO 25
02330      C
02340      C*****CASE STUDIES 2 AND 3 *****
02350      C
02360      8 NBB=NB-1
02370      VV(NB)=VV(NB)
02380      HD=HST+(W(NB)-TC(NN+3)-WD1)/WD2
02390      DH=0.
02400      WADD=W(NBB)/10.
02410      C*****INITILIZE ERROR TOLERANCES*****
02420      ER= 0.0010*DEPTH
02430      9 HD=HO+DH
02440      X(NN+1)=0.0
02450      DTHI=0.05
02460      IT1=0
02470      C*****START CABLE (BUOY DRAFT) ITERATION LOOP*****
02480      10 IT1=IT1+1
02490      IF(IT1.GT.IT1MAX)GO TO 30
02500      DTH=DTHI
02510      IT=0
02520      IS=0
02530      11 E=1.D25
02540      C*****START BUOY ITERATION*****
02550      12 IF(MOOR.EQ.2)HO=HST+(W(1)-TC(5)-DC2-WD1)/WD2
```

```
02560 IF(HO.GT.0.99*HMAX)GO TO 31
02570 HOD=HO-HST
02580 B=WWD1+WWD2*HOD
02590 E1=E
02600 IT=IT+1
02610 IF(IT.GT.ITMAX)GO TO 32
02620 RRHO=RRHO1+RRHO2*HOD
02630 CS1=DCOS(X(NN+1))
SN1=DSIN(X(NN+1))
VN=UV(NB)*CS1
VT=UV(NB)*SN1
02640 DDTT=(J.C2*RRHO+0.5*RRHO*CDP*(2.*S01-S02))*DARS(VT)*VT
DN=RRHO*VN*DARS(VN)
DC1=DN*CS1+DDTT*SN1
DC2=DDTT*CS1-DN*SN1
DC3=DN*(HST/2.-ZCG)+RRHO2*HO*HO*VN*DARS(VN)/2.
02650 IF(MODR.EQ.2)GO TO 13
02660 TC(NN-1)=DC1+TC(NN+2)
02670 TC(NN)=DC2+B-W(NB)+TC(NN+3)
02680 DC1=DN*CS1+DDTT*SN1
02690 DC2=DDTT*CS1-DN*SN1
02700 DC3=DN*(HST/2.-ZCG)+RRHO2*HO*HO*VN*DARS(VN)/2.
02710 IF(MODR.EQ.2)GO TO 13
02720 TC(NN-1)=DC1+TC(NN+2)
02730 TC(NN)=DC2+B-W(NB)+TC(NN+3)
02740 13 ARMX1=ZC1*SN1+XC1*CS1
02750 ARMZ1=ZC1*CS1-XC1*SN1
02760 ARMX2=ZC2*SN1+XC2*CS1
02770 ARMZ2=ZC2*CS1-XC2*SN1
02780 C*****CALCULATE UNBALANCED MOMENT ON BUOY*****
02790 BGZ=SN1*(WWD1*(HST/2.-ZCG)+WWD2*HGD*(HO+HST)/2.-ZCG))
E=DC3-BGZ-TC>NN-1)*ARMZ1+TC>NN)*ARMX1+TC>NN+3)*ARMX
12
02800 IF(MODR.EQ.1)WRITE(6,100)HO,X(NN+1),DH,E
02810 IF(MODR.EQ.2)WRITE(6,100)VE,HO,X(3),E
02820 C****TEST FOR CONVERGENCE*****
02830 IF(DABS(E).LT.EMA) GO TO 16
IS1=DSIGN(1.D0,E)
02840
02850
02860
02870
```

```
02880 C*****TEST FOR CHANGE IN SIGN OF UNBALANCED MOMENT (ERROR)*****
02890   IF((IS1+IS).EQ.0) GO TO 14
02900   IF(DABS(E).GT.DABS(E1)) GO TO 15
02910 C****NO CHANGE IN SIGN - CONTINUE IN SAME DIRECTION*****
02920   X(NN+1)=X(NN+1)+IS1*DTH
02930   IS=IS1
02940   GO TO 12
02950 C****CHANGE IN SIGN - GO BACK HALF A STEP*****
02960   14  DTH=DTH/2.
02970   X(NN+1)=X(NN+1)+IS1*DTH
02980   IS=IS1
02990   GO TO 12
03000 C****ERROR IS GROWING - ITERATE IN OPPOSITE DIRECTION*****
03010   15  DTH=-DTH
03020   X(NN+1)=X(NN+1)+IS1*DTH*X2.
03030   IS=IS1
03040   GO TO 12
03050   16  IF(MODR.EQ.2)GO TO 5
03060 C****BUOY-CABLE SOLUTION HAS CONVERGED - START INTEGRATION DOWN CABLE
03070   DTH=DTH/2.
03080   DH=DH/2.
03090   TNN(NB)=DSQRT(TC(NN-1)*TC(NN-1)+TC(NN)*TC(NN))
03100   TL(NB)=SL(NB)+TNN(NB)/EK(NB)
03110   CS(K)=TC(NN-1)/TNN(NB)
03120   SN(NB)=TC(NN)/TNN(NB)
03130   IF(NB.EQ.1) GO TO 19
03140   DO 18 I=1,NB1
03150   J=NB-I
03160   K=J+1
03170   I=J+J
03180   UN=UU(J)*SN(K)
03190   UT=UU(J)*CS(K)
```

```
03200      DZ=CDIA(J)*VV(J)*DABS(VV(J))
03210      DDTT=CDIT(J)*UT*DABS(UT)
03220      DN=CDIN(J)*VN*DABS(VN)
03230      TC(II-1)=TC(II+1)+DI+DDTT*CS(K)+DN*SN(K)
03240      TC(II)=TC(II+2)+DDTT*SN(K)-DN*CS(K)-N(J)
03250      TNN(J)=DSQRT(TC(II-1)**2+TC(II)**2)
03260      CS(J)=TC(II-1)/TNN(J)
03270      SN(J)=TC(II)/TNN(J)
03280      TL(J)=SL(J)+TNN(J)/EK(J)
03290      YJ1=0.
03300      DO 20 I=1,NB
03310      20   YJ1=YJ1+TL(I)*SN(I)
03320      DEPTH1=YJ1+(HO-ZCG-ZC1)*CS1+XC1*SN1
03330      EE=DEPTH-DEPTH1
03340      WRITE(6,100,HO,X(NN+1),EE,(W(NCC),NCC=1,NB))
03350      EEE=DABS(EE)
03360      *****TEST FOR CONVERGENCE*****
03370      IF(EEE.LE.ER)GO TO 22
03380      IF(INDEX.EQ.1.AND.EE.LT.0.)GO TO 29
03390      IF(INDEX.EQ.2)GO TO 21
03400      INDEX=2
03410      DH=(HMAX-HO)/2.
03420      GO TO 9
03430      21   HO=HO+EEE*Dn/EE
03440      GO TO 10
03450      *****STATIC SOLUTION HAS CONVERGED- COMPUTE ALL COORDINATES*****
03460      22   DEPTH=DEPTH1
03470      WRITE(6,100)DEPTH
03480      X(1)=TL(1)*CS(1)
03490      X(2)=TL(1)*SN(1)
03500      IF(NB.EQ.1)GO TO 24
03510      DO 23 I=2,NB
```

```
03520      II=I+1
03530      X(II-1)=X(II-3)+TL(I)*CS(I)
03540      23      X(II)=X(II-2)+TL(I)*SN(I)
03550      24      XJ1=X(NN-1)
03560      X(NN-1)=XJ1-XC1*CS1-ZC1*SN1
03570      X(NN)=YJ1-ZC1*CS1+XC1*SN1
03580      IF (NM.EQ.NR) GO TO 27
03590      25      XJ2=X(NN-1)+XC2*CS1+ZC2*SN1
03600      YJ2=X(NN)+ZC2*CS1-XC2*SN1
03610      X(NN+2)=XJ2+TL(NB2)*CS(NB2)
03620      X(NN+3)=YJ2+TL(NB2)*SN(NB2)
03630      IF (NB2.EQ.NM) GO TO 27
03640      NB3=NB2+1
03650      DO 26 I=NB3,NM
03660      II=I+1
03670      X(II)=X(II-2)+TL(I)*CS(I)
03680      26      X(II+1)=X(II-1)+TL(I)*SN(I)
03690      27      WRITE(6,100)HO,X(NN+1),TC(NN-1),TC(NN),E
03700      WRITE(6,100)(X(I),I=1,NDF)
03710      28      RETURN
03720      C*****PART OF THE MOORING LINE IS FLOATING ON THE SURFACE(FIND IT)*****
03730      29      W(NBB)=W(NBB)-WADD
03740      IF (W(NBB).LT.0.)GO TO 17
03750      _____W(NBB)=C,
03760      NBB=NBB-1
03770      GO TO 29
03780      30      WRITE(6,103)ITIMAX
03790      CALL EXIT
03800      31      WRITE(6,1C2)
03810      CALL EXIT
03820      32      WRITE(6,101)ITMAX
03830      CALL EXIT
```

```
03840 C
03850 C*****CASE STUDY 1 ****
03860 C*****
03870 33 HO=HST+(W(1)-WWD1)/WWD2
03880 WAU=AW*HO
03890 OEXP=DEXP(-WAU)
03900 HOD=HO-HST
03910 BK1=(BB1-BB2)*HST
03920 BK2=BB2*HO
03930 P1=BK2*(0.5*HO-ZCG)+BK1*(0.5*HST-ZCG)
03940 P2=BK2*(HO*HO/3.*HO*ZCG+ZCG*ZCG)+BK1*(HST*HST/3.*HST*ZCG+ZCG*ZCG)
03950 Q02=DEXP(-HOD*AW)
03960 Q0=(BB1*(QQ2-OEXP)+BB2*(1.-QQ2))/AW
03970 Q1=(BB1*(QQ2*(HST-1./AW-ZCG))+BB2*(HO-1./AW-ZCG-Q
03980 1Q2*(HST-1./AW-ZCG))/AW
03990 YD(1)=VV(1)
04000 YD(2)=WE*AMP*(RHO*SD2*GR-WE*WE*(TMASS+VVO+VV
04010 11))
04020 X(1)=-AMP*Q0/TMASS
04030 X(2)=ZCG-HO+DEPTH
04040 X(3)=WE*WE*AMP*(2.*Q1-P1*Q0/TMASS)/(P1*GR-WE*WE*(YNERT+P2-P1*P1/(2
04050 1.*TMASS))
04060 XAW=X(1)/AMP
04070 ZAW=YD(2)/(WE*AMP)
04080 TAW=X(3)/(AW*AMP)
04090 SN1=DSIN(X(3))
04100 CS1=DCOS(X(3))
04110 WRITE(6,100)WAU,XAW,ZAW,TAU
04120 RETURN
04130 END
04140 IMPLICIT REAL*8(A-H,O-Z)
04150 SUBROUTINE DBDRG
```

04160 C THIS SUBROUTINE CALCULATES THE VISCOUS DRAG FORCE ON THE
04170 C SPAR BUOY DURING ITS DYNAMIC MOTIONS. INTEGRATION OF FORCES
04180 C IS DONE ALONG THE AXIS OF THE SPAR.

```
04190 C
04200 C
04210 COMMON W(8),CM(8),CMS(8),CMD(8),CMN(8),CMT(8),SL(8),EK(8),CDIN(8),
04220 1CDIT(8),CDIA(8),DEP(8),V(8),UU(8),TN(8),TL(8),CS(9),SN(9),Y
04230 1DD(17),YD(17),Y(17),X(17),F(17),DD(17),TC(17),GK(8,17),GM(17,17),D
04240 1C1,DC2,DC3,XC1,ZC1,XC2,ZC2,WWD1,WWD2,S01,S02,CS1,SN1,RD1,RD2,XJ1,Y
04250 1J1,XJ2,YJ2,BB1,BB2,HMAX,HO,HST,HOD,RRHO1,RRHO2,TMASS,YNERT,ZCG,HI,
04260 1TH0,CDF,CDF,CON,COT,ALPHA,PI,RHO,GR,AW,T,DT,AMP,WE,SNK,CSK,DEFTH,O
04270 1K,UUU(8),OEXP,UVO,UU1,XW,ZW,EMW,MOOR,NST,NM,NM1,NM2,NDF,NB,NB1,NB2
04280 1,NN,ND
04290 C*****COEFFICIENTS OF THE VELOCITY EQUATION ARE CALCULATED BELOW*****
04300 V1=(V(NB)-YD(NN-1))*CS1+YD(NN)*SN1
04310 V2=WE*XAMP*(SNK*CS1+CSK*SN1)
04320 V3=(V(NB)-YD(NN-1))*SN1-YD(NN)*CS1
04330 V4=WE*XAMP*(SNK*SN1-CSK*CS1)
04340 UTB=U3-U4*XEXP
04350 UTS=U3-U4*XEXP*XEXP*(OK*XHST)
04360 C****PRESSURE DRAG DUE TO BOTTOM END AND STEP OF THE SPAR IS CALCULATED
04370 DP=0.5*RRHO*CDP*(S01*DABS(UTB)*UTS)*DABS(UTS)*UTS)
04380 DN=0.
04390 DDTT=0.
04400 DM=0.
04410 C*****THE VISCOUS DRAG FORCE AND MOMENT ON THE SPAR BUOY ARE CALCULATED
04420 RD=RD1
04430 NDS1=NST*XHST/HI
04440 NDS2=NST-NDS1
04450 NDS=NDS1
04460 DZ=HST/NDS
04470 ZZ=DZ/2.-ZCG
```

```
04480      RHOO=RHO*CDL
04490      DO 2 INZ=1,2
04500      DO 1 IZ=1,NDS
04510      XXE=DEXP(OK*(ZZ+ZCG))
UNN=U1-V2*OEXP**XXE-ZZ*YD(NN+1)
DNN=UNN*DABS(UNN)*RD*DZ
DN=DN+DNN
04520      VTT=V3-U4*OEXP***XE
DDTT=DDTT+VTT*DARS(VTT)*RD*DZ
04530      DM=DM+DNN*ZZ
04540
04550      ZZ=ZZ+DZ
04560      RD=RD2
NDS=NDS2
04610      DZ=(HI-HST)/NDS
04620      ZZ=HST+DZ/2.-ZCG
CONTINUE
04630      DN=RHO0*DN
04640      DDTT=0.02*RHO0*DDTT
04650      DC3=RHO0*DM
04660      C*****DC1&DC2 ARE THE VISCOUS DRAG FORCES IN SURGE AND HEAVE DIRECTIONS*
04670      DC1=DN*CS1+(DDTT+DF)*SN1
04680      DC2=(DDTT+DP)*CS1-DN*SN1
04690      RETURN
04700
04710      END
04720      IMPLICIT REAL*8(A-H,0-Z)
04730      SUBROUTINE BUOYS
04740      C THIS SUBROUTINE CALCULATES THE MASS MATRIX FOR THE SPAR BUOY,
04750      C PART (EXCEPT VISCOUS) OF THE (FA) MATRIX AS DD, AND (FD+FG)
04760      C ARRAYS AS XW,ZW, AND EMW.
04770      C
04780      C
04790      COMMON W(8),CM(8),CMS(8),CMD(8),CMN(8),CMT(8),SL(8),EK(8),CDIN(8),
```

```
1CDIT(8),CDIA(8),DEP(8),V(8),VV(8),TN(8),TL(8),CS(9),SN(9),Y  
04800 1DD(17),YD(17),Y(17),X(17),F(17),DD(17),TC(19),GK(8,17),GM(17,17),D  
04810 IC1,DC2,DC3,XC1,ZC1,XC2,ZC2,WWD2,S01,S02,CS1,SN1,RD1,RD2,XJ1,Y  
04820 1J1,XJ2,YJ2,BB1,BR2,HMAX,HO,HST,HOD,RRH01,RRH02,TMASS,YNERT,ZCG,HI,  
04830 1THO,CDF,CNL,CON,COT,ALPHA,PI,RHO,GR,AW,T,D,AMF,WE,SNK,CSK,DEPTH!,O  
04840 1K,VV(8)*EXP,VV0,VV1,XW,ZW,EMW,MOOR,NST,NM,NM1,NM2,NDF,NB,NB1,NB2  
04850 1,AN,NG  
04860 DO 1 I=1,NDF  
04870 DO 1 J=1,NDF  
04880 1 GM(I,J)=0.  
04890 BK1=(BB1-BB2)*HST  
04900 BK2=BB2*HO  
04910 P0=BB1*HST+BB2*(HO-HST)  
04920 P1=BK2*(0.5*HO-ZCG)+BK1*(0.5*XHST-ZCG)  
04930 P2=BK2*(HO*HO/3.-HO*ZCG+ZCG*ZCG)+BK1*(HST*XHST/3.-HST*ZCG+ZCG*ZCG)  
04940 Q02=DEXP(-HOD*OK)  
04950 Q0=(BB1*(Q02-0EXP)+BB2*(1.-Q02))/OK  
04960 Q1=(BB1*(Q02*(HST-1./OK-ZCG)+0EXP*(1./OK+ZCG))+BB2*(HO-1./OK-  
04970 1ZCG-QQ2*(HST-1./OK-ZCG))/OK  
04980 C*****COEFFICIENTS IN EQUATIONS OF BUOY MOTION(MASS MATRIX)*****  
04990 GM(NN-1,NN-1)=TMASS+F0*(CON*CS1*CS1+COT*SN1*SN1)+(UU0+VV1)*SN1*SN  
05000 1  
05010 GM(NN-1,NN)=FO*SN1*CS1*(COT-CON)+(UU0+VV1)*SN1*CS1  
05020 GM(NN-1,NN+1)=F1*CS1*CON  
05030 GM(NN,NN-1)=GM(NN-1,NN)  
05040 GM(NN,NN)=TMASS+F0*(CON*SN1*SN1+COT*CS1*CS1)+(UU0+VV1)*CS1*CS1  
05050 GM(NN+1,NN+1)=-F1*SN1*CON  
05060 GM(NN+1,NN-1)=GM(NN,NN+1)  
05070 GM(NN+1,NN)=GM(NN,NN+1)  
05080 GM(NN+1,NN+1)=YNERT+P2*CON  
05090 GM(NN+1,NN+1)=YNERT+P2*CON  
05100 C*****PART OF THE (FA) ARRAY*****  
05110 DD(NN-1)=(COT*P1*SN1-VV0*SN1*ZCG+VV1*SN1*(HST-ZCG))*YD(NN+1)*YD(NN
```

```
05120      1+1)
05130      DD(NN)=(COT*P1*CS1-VV0*CS1*ZCG+VV1*CS1*(HST-ZCG))*YD(NN+1)*YD(NN+1)
05140      DD(NN+1)=0.
05150
05160 C*****WAVE EXCITATION AND HYDROSTATICS FORCES ON THE SPAR*****
05170      XW=WE*WE*AMP*Q0*(CSK*(1.+CON*CS1*CS1+COT*SN1*SN1)+SNK*SN1*CS1*(COT
05180      1-CON))
05190      ZW=WE*WE*AMP*Q0*(SNK*(1.+CON*SN1*SN1+COT*CS1*CS1)+CSK*SN1*CS1*(COT
05200      1-CON))+GR*(BE1*HST+BB2*(HI-HST)-TMASS)
05210      EMW=WE*WE*AMP*Q1*(1.+CON)*(CSK*CS1-SNK*SN1)-GR*P1*SN1
05220      RETURN
05230
05240      IMPLICIT REAL*8(A-H,O-Z)
05250      SUBROUTINE NEXT
05260      C THIS SUBROUTINE UPDATES THE GEOMETRY OF THE MOORING SYSTEM
05270      C DURING ITS DYNAMIC MOTIONS.
05280      C
05290      C
05300      COMMON W(8),CM(8),CMS(8),CMD(8),CMT(8),SL(8),EK(8),CDIN(8),
05310      CDIT(8),CDIA(8),DEP(8),U(8),VU(8),TN(8),TL(8),CS(9),SN(9),Y
05320      LD(17),YD(17),Y(17),X(17),F(17),DC(17),TC(17),GK(17),GM(17),D
05330      1C1,DC2,DC3,XC1,XC2,ZC2,WW1,WW2,SO1,SO2,CS1,SN1,RD1,RD2,XJ1,Y
05340      1J1,XJ2,YJ2,EB1,BB2,HMAX,HO,HST,HOD,RRHO1,RRHO2,TMASS,YNERT,ZCG,HI,
05350      THO,CDP,CNL,CON,COT,ALPHA,PI,RHO,GR,AW,T,DT,AMP,WE,SNK,CSK,DEPTH,O
05360      1K,VVU(8),QEXP,VV0,VV1,XW,ZW,EMW,MOOR,NST,NM,NM1,NM2,NDF,NB,NB1,NB2
05370      1,NN,ND
05380      IF(MOOR.EQ.2)GO TO 3
05390      XJ1=X(NN-1)+ZC1*SN1+XC1*CS1
05400      YJ1=X(NN)+ZC1*CS1-XC1*SN1
05410      IF(NB.EQ.1)GO TO 1
05420      TL(1)=DSQR(X(1)**2+X(2)**2)
05430      CS(1)=X(1)/TL(1)
```

```
05440 SN(1)=X(2)/TL(1)
05450 TL(NB)=DSQRT((XJ1-X(NN-3))*2+(YJ1-X(NN-2))*2)
05460 CS(NB)=(XJ1-X(NN-3))/TL(NB)
05470 SN(NB)=(YJ1-X(NN-2))/TL(NB)
05480 GO TO 2
05490 1  TL(1)=DSQRT(XJ1*X2+YJ1*Y2)
05500 CS(1)=XJ1/TL(1)
05510 SN(1)=YJ1/TL(1)
05520 2  IF(NM.EQ.NB)GO TO 4
05530 3  XJ2=X(NN-1)+ZC2*SN1+XC2*CS1
05540 YJ2=X(NN)+ZC2*CS1-XC2*SN1
05550 TL(NB2)=DSQRT((X(NN+2)-XJ2)*2+(X(NN+3)-YJ2))*2)
05560 CS(NB2)=(X(NN+2)-XJ2)/TL(NB2)
05570 SN(NB2)=(X(NN+3)-YJ2)/TL(NB2)
05580 DO 5 I=2,N
05590 4  IF(I.EQ.NB.OR.I.EQ.NB2)GO TO 5
05600 II=I+1
05610 IF(I.LT.NB)II=II-1
05620 TL(1)=DSQRT((X(II)-X(II-2))*2+(X(II+1)-X(II-1))*2)
05630 CS(1)=(X(II)-X(II-2))/TL(1)
05640 SN(1)=(X(II+1)-X(II-1))/TL(1)
05650 5  CONTINUE
05660 DO 6 I=1,NN
05670 6  IF(SN(I).LT.-1.)SN(I)=-1.0
05680 RETURN
05690 END
05700 IMPLICIT REAL*8(A-H,O-Z)
05710 SUBROUTINE MINVER(N,C)
05720 C THIS SUBROUTINE CALCULATES THE INVERSE OF MATRIX 'C' OF ORDER 'N'
05730 C -----
05740 C
05750 DIMENSION C(17,17),H(17),G(17)
```

```
NN=N-1
C(1,1)=1.0/C(1,1)
DO 6 M=1,NN
K=M+1
05800      DO 1 I=1,M
05810      G(I)=0.
05820      DO 1 J=1,M
05830      1   G(I)=G(I)+C(I,J)*C(J,K)
05840      D=0.
05850      DO 2 I=1,M
05860      2   D=D+C(K,I)*G(I)
E=C(K,K)-D
C(K,K)=1.0/E
05870      DO 3 I=1,M
05880      3   C(I,K)=-G(I)*C(K,K)
05890      DO 4 J=1,M
05900      4   H(J)=H(J)+C(K,I)*C(I,J)
05910      DO 5 J=1,M
05920      5   C(K,J)=-H(J)*C(K,K)
05930      DO 6 I=1,M
05940      6   C(I,J)=C(I,J)-G(I)*C(K,J)
05950      RETURN
END
IMPLICIT REAL*8(A-H,O-Z)
06020      SUBROUTINE MATRIX
06030      THIS SUBROUTINE CALCULATES ALL THE REMAINING ELEMENTS OF THE
06040      GLOBAL MATRICES AND INTEGRATES THE 'NDF' SIMULTANEOUS DIFFERENTIAL
06050      EQUATIONS OF MOTION BY THE METHOD OF RECTANGULAR RULE.
06060
06070
```

```
06080 C
06090 COMMON W(8),CM(8),CMS(8),CMD(8),CMT(8),SL(8),EK(8),CDIN(8),
06100 ICDIT(8),CDIA(8),DEP(8),V(8),UV(8),TN(8),TL(8),SN(9),CS(9),Y
06110 IND(17),YD(17),Y(17),X(17),F(17),ID(17),TC(19),GK(8,17),GM(17,17),D
06120 IC1,DC2,DC3,XC1,XC2,ZC1,ZC2,WWD2,SC1,SC2,S1,RD1,RD2,YJ1,
06130 1J1,XJ2,YJ2,BR1,BR2,HMAX,HO,HST,HOD,KRH01,RF402,TMASS,YNERT,ZG6,HT
06140 ITHO,CDF,CDL,CON,COT,ALPHA,PI,RHO,GR,AU,T,DT,AN,WE,SN,CSN,DEPTH,L
06150 1K,UVU(8),EXP,VV0,UV1,XW,ZW,EMW,MOOR,NST,NM,NM1,NM2,NDF,NB,NB1,NB2
06160 1,NN,ND
06170 C*****WAVE EXCITING + HYDROSTATIC + VISCOUS DRAG FORCES ON THE SPAR*****
06180 F(NN-1)=DC1+XW
06190 F(NN)=ZW+DC2
06200 F(NN+1)=DC3+EMW
06210 IF(MOOR.EQ.0)GO TO 11
06220 C*****STIFFNESS MATRIX FOR THE MOORING LINES*****
06230 AA1=XC1*CS1+ZC1*SN1
06240 AA2=XC2*CS1+ZC2*SN1
06250 AB1=-XC1*SN1+ZC1*CS1
06260 AB2=-XC2*SN1+ZC2*CS1
06270 GK(1,1)=EK(1)*CS(1)
06280 GK(1,2)=EK(1)*SN(1)
06290 GK(NB,NN+1)=EK(NB)*(AB1*CS(NB)-AA1*SN(NB))
06300 IF(NM.EQ.1)GO TO 5
06311 IF(NM.EQ.NB)GO TO 1
06320 GK(NB2,NN-1)=-EK(NB2)*CS(NB2)
06330 GK(NB2,NN)=-EK(NB2)*SN(NB2)
06340 GK(NB2,NN+1)=-EK(NB2)*(AB2*CS(NB2)-AA2*SN(NB2))
06350 GK(NB2,NN+2)=-EK(NB2,NN-1)
06360 GK(NB2,NN+3)=-EK(NB2,NN)
06370 1 DO 2 I=2,NM
06380 IF(I.EQ.NB2)GO TO 2
06390 I=I+1
```

```
06400 IF(I.GT.NB)II=II+1
      GK(I,II-3)=-EK(I)*CS(I)
      GK(I,II-2)=-EK(I)*SN(I)
      GK(I,II)=-3K(I,II-2)
      GK(I,II-1)=-GK(I,II-3)
06410      2 CONTINUE
06420      DO 4 I=1,NM
06430      C*****MASS MATRIX FOR THE MOORING LINES*****
06440      IF(I.EQ.NB)GO TO 4
06450      II=I+1
06460      IF(I.LT.NB)II=II-1
06470      GM(II,II)=CM(I)+CMN(I)+CMT(I)*SN(I)**2+CM(I)*CS(I)**2
06480      GM(II+1,II+1)=CM(I)+CMS(I)+CMN(I)*CS(I)**2+CM(I)*SN(I)**2
06490      GM(II,II+1)=(CMT(I)-CMN(I))*2+CM(I)*SN(I)**2
06500      GM(II+1,II)=GM(II,II) '
06510      WWE=W*AMF*DEXP(AW*(X((II+1)-DEPTH))
06520      SWE=AW*X(II)-WE*T
06530      SNK1=ISIN(SWE)
06540      CSK1=DCOS(SWE)
06550      C*****VISCOUS DRAG FORCES ON THE MOORING LINES*****
06560      U1=V(I)-YD(II)-WWE*SNK1
06570      U2=-YD(II+1)+WWE*CSK1
06580      UT1=U1*CS(I+1)+U2*SN(I+1)
06590      UN1=U1*SN(I+1)-U2*CS(I+1)
06600      DN=CDIN(I)*UN1*DARS(UN1)
06610      DDTT=CDIT(I)*UT1*DABS(UT1)
06620      U3=DSQRT(U1**2+U2**2)*CDIA(I)
06630      DD(II)=DN*SN(I+1)+DDTT*CS(I+1)+U3*U1
06640      DD(II+1)=DDTT*SN(I+1)-DN*CS(I+1)+U3*U2
06650      IF(MOOR.EQ.2.AND.I.GE.ND)GO TO 3
06660      F(II)=CMD(I)*WE*WWE*CSK1
06670      F(II+1)=CMD(I)*WE*WWE*SNK1-W(I)
```

```
06720      GO TO 4
06730      3   F(I)=WE*WE*CMD(I)*SN(I)*(CSK1*SN(I)-SNK1*CS(I))
06740      4   F(I+1)=WE*WE*CMD(I)*CS(I)*(SNK1*CS(I)-CSK1*SN(I))-W(I)
06750      4   CONTINUE
06760      5   DO 7 K=1,NM
06770      5   TG=0.
06780      6   DO 6 IK=1,NDF
06790      6   TG=TG+GK(K,IK)*Y(IK)
06800      6   TNN(K)=TG+TNN(K)
06810      7   TN(K)=TNN(K)
06820      7   IF(TN(K).LE.0.)TN(K)=0.
06830      7   KK=K+K
06840      7   IF(K.LE.NR)KK=KK-1
06850      7   TC(KK)=TN(K)*CS(K)
06860      7   TC(KK+1)=TN(K)*SN(K)
06870      7   TC(NN+1)=-(TC(NN-1)*(-ZC1*CS1+XC1*SN1)+TC(NN)*(-XC1*CS1-ZC1*
1SN1)+TC(NN+2)*(-ZC2*CS1+XC2*SN1)-TC(NN+3)*(-XC2*CS1-ZC2*SN1))
06880      8   IF(NM.EQ.1)GO TO 11
06890      8   IF(MODR.EQ.2)GO TO 9
06900      8   NZ=NN-2
06910      8   DO 8 M=1,NZ
06920      8   DO 8 M=1,NZ
06930      8   TC(M)=TC(M)-TC(M+2)
06940      9   TC(NN-1)=TC(NN-1)-TC(NN+2)
06950      9   TC(NN)=TC(NN)-TC(NN+3)
06960      10  IF(NM.EQ.NB)GO TO 11
06970      10  NZ=NN+2
06980      10  DO 10 M=NZ,NDF
06990      10  TC(M)=TC(M)-TC(M+2)
07000      11  CALL MINVER(NDF,GM)
07010      11  DO 13 M=1,NDF
07020      11  YDD(M)=0.
07030      12  DO 12 K=1,NDF
```

```
07040 12 YDD(M)=YDD(M)+GM(M,K)*(DD(K)-TC(K)+F(K))  
07050 YD(M)=YD(M)+YDD(M)*DT  
07060 Y(M)=YD(M)  
07070 13 X(M)=X(M)+Y(M)  
07080 CS1=DCOS(X(NN+1))  
07090 SN1=DSIN(X(NN+1))  
07100 H0=ZCG+(DEPTH-X(NN))/CS1  
07110 HOD=H0-HST  
07120 RETURN  
07130 END  
READY
```

SSD31.FORT

00010 C PROGRAM TO COMPUTE LOW FREQ. MOTION OF SUBSURFACE MOORED SYSTEMS.
00020 C THIS ANALYSIS IS DONE IN THREE DIMENSIONS, AND INERTIA FORCES ARE
00030 C INCLUDED. ABSOLUTE VELOCITY PROFILE IS INPUTTED AS AMPLITUDE AND
00040 C FREQUENCY. A SINUSOIDAL SURFACE WAVE IS ALSO INPUTTED.

00060 C

00070 C IMPLICIT REAL*8(A-H,O-Z)

00080 C*****BEGINING OF THE MAIN PROGRAM*****
00090 C*****COMMON PI(30),SI(30),F(3,30),CDIN(30),CDIT(30),DIAL(20),SLL(20),AW
00100 COMMON PI(30),SI(30),F(3,30),CDIN(30),CDIT(30),DIAL(20),SLL(20),AW
00110 1L(20),CDN(20),CDT(20),TFL(20),CD1(20),CD2(20),CDI(20),C01(20),F01(20),
00120 1(20),U(3,10),NM(20),SL(20),SWA(20),CDIA(20),U(3),X(3),THETA(3),AWX
00130 1,DN(3),WN(3),CS(3),SN(3),ID(3),UN(3),UT(3),FSTRA(20),AO(20),D(10),
00140 1WVL(20),SWW(20),SWD(20),YDL(150,3),YDL(2,150,3),YL(2,150,3),YDDI(1
00150 130,3),YDI(2,30,3),YI(2,30,3),YDDT(3),YDDN(3),ZM(30),ZMU(30),DEPTH,
00160 1VS(3),S2,TE,H2,IK,NI,J,NC,WS,AMP,NS,NP,DDT,E,ER,PII,T,SINT,AU,AWY,
00170 IDIA,ER1,XOLD(3),GR,WE,DT,T2,TMAX,INK,I
00180 C*****BEGINING OF FORMAT STATEMENTS*****
00190 101 FORMAT(4I15,5F10.0)
00200 132 FORMAT(7F8.0)
00210 103 FORMAT(5F10.0)
00220 104 FORMAT(10F7.0)
00230 105 FORMAT(7F10.0)
00240 106 FORMAT(16F7.2)
00250 107 FORMAT(10F8.2)
00260 C*****GENERAL DATA*****
00270 C DEPTH, DUT, ER, AND ER1 ARE IN METERS.
00280 READ(5,101)NI,np,ns,ink,depth,ddt,er,er1
00290 C*****READ IN THE INSERTED INSTRUMENTS AND FLOATS SPECIFICATIONS*****
00300 C PI AND SI ARE IN METERS; ZM AND ZMU IN SLUGS; F IN POUNDS; AND
00310 C CDIN, CDIT ARE IN F.P.S. UNITS.

```
00320 READ(5,102)(PI(J),SI(J),ZHU(J),ZHV(J),F(3,J),CDIN(J),CDIT(J)
00330 1,J=1,NI;
00340 DO 1 I1=1,2
00350 DO 1 I2=1,NI
00360 1 F(I1,I2)=0.
00370 C*****READ IN THE PARAMETERS FOR DIFFERENT MOORING PARTS*****
00380 C DIAL IS IN INCHES; SLL IN METERS; AWL AND WWL IN LBS/M; TPL IN
00390 C POUNDS OR LBS/(SQ.IN.); C01 IS IN INCHES FOR JACKETED WIRE ROPE
00400 READ(5,103)(DIAL(I),SLL(I),AWL(I),WWL(I),TPL(I),I=1,NF)
00410 READ(5,105)(C01(I),PO1(I),PO2(I),C02(I),AO(I),CDN(I),CDT(I)
00420 1,I=1,NP)
00430 C*****READ THE FORCING CURRENT PROFILE*****
00440 C D ARE IN METERS; V IN MM/SEC; AND WE IN RAD/SEC.
00450 READ(5,105)(D(I),I=1,IKK)
00460 READ(5,105)((V(I,J),I=1,3),J=1,8)
00470 READ(5,105)WE,DT,T2,TMAX
00480 C*****READ IN THE SINUSOIDAL SURFACE WAVE.*****
00490 C WS IS IN RAD/SEC; AMP IN MM.
00500 READ(5,105)WS,AMP,BETA
00510 CSB=DCCS(BETA)
00520 SNB=DSIN(BETA)
00530 PI=4.*DATAN(1.D0)
00540 RHO=1.9905
00550 GR=32.2
00560 CONS1=RHO*GR*PII*0.0057
00570 AW=WS*WS/GR
00580 AWX=AW*CSB
00590 AWY=AW*SNB
00600 SLT=0.
00610 DO 2 I=1,NP
00620 IF(P01(I).EQ.0.0)GO TO 2
00630 C*****PERMANENT STRETCH FOR SYNTHETIC ROPES.*****
```

```
00640      PSTR(A,I)=((TPL(I)/(DIAL(I)**2)-200.0)/CD1(I))**(1.0/F01(I))
00650      2      SLT=SLL+SLL(I)
00660      C*****SEGMENTATION OF THE MOORING LINE IN NPTS SEGMENTS*****
00670      DO 3 I=1,NP
00680      NM(I)=(SLL(I)/SLT)*NS+0.5
00690      IF(NM(I).EQ.0)NM(I)=1
00700      SL(I)=SLL(I)/NM(I)
00710      SWA(I)=AWL(I)*SL(I)
00720      SWW(I)=WWL(I)*SL(I)
00730      SWD(I)=SWA(I)-SWW(I)
00740      CDIA(I)=SL(I)*(DIAL(I)**2)
00750      3      CONS(I)=CDIA(I)*CONS1
00760      NS1=NS+NP
00770      C*****INITIALIZE DYNAMIC VARIABLES*****
00780      DO 5 I1=1,3
00790      DO 4 I2=1,NS1
00800      YDDL(I2,I1)=0.
00810      DO 4 I3=1,2
00820      YDL(I3,I2,I1)=0.
00830      4      YL(I3,I2,I1)=0.
00840      DO 5 I4=1,30
00850      YDDI(I4,I1)=0.
00860      DO 5 I5=1,2
00870      YDI(I5,I4,I1)=0.
00880      5      YI(I5,I4,I1)=0.
00890      CALL MOTION
00900      CALL EXIT
00910      END
00920      IMPLICIT REAL*8(A-H,O-Z)
00930      SUBROUTINE MOTION
J0940      C      THIS SUBROUTINE CALCULATES THE DYNAMIC EQUILIBRIUM OF THE MOORING
00950      C      LINE FOR TMAX SECONDS.
```

```
00960 C
00970 C
00980      COMMON PI(30),SI(30),F(3,30),CDIN(30),CDIT(30),DIAL(20),SLL(20),AW
00990     IL(20),CDN(20),CDT(20),TPL(20),CN1(20),CN2(20),P01(20),P02(20),CDNS
01000     1(20),U(3,10),NM(20),SL(20),SWA(20),CNA(20),U(3),X(3),THETA(3),AWX
01010     1,DN(3),WN(3),CS(3),SN(3),DN(3),UN(3),UT(3),PSTRA(20),AO(20),D(10),
01020     1WWL(20),SWW(20),SWD(20),YDUL(150,3),YDL(2,150,3),YDI(2,150,3),YDDI(
01030     130,3),YDI(2,30,3),YD(3),YD(2,30,3),YIDN(3),ZM(30),ZMV(30),DEPTH,
01040     1VS(3),S2,TE,H2,IK,NI,J,NC,WS,AMF,NS,NP,DDT,E,ER,PII,T,SINT,AW,AWY,
01050     1DIA,ER1,XOLD(3),GR,WE,DT,T2,THAX,IKK,I
01060   101  FORMAT(5F10.2)
01070   102  FORMAT('1X,' SOLUTION IS TERMINATING AS THE ERROR IN MOORING LINE V
01080     1ELocity AND ACCELERATION CALCULATIONS IS EXCESSIVE'/'1X,' ER1 IS EX
01090     1CEEDED BY= ',F5.3)
01100     T=0.
01110     T3=0.
01120     UTRY=GR*AAMP/WS
01130 C*****BEGINNING OF MOORING LINE CALCULATIONS*****
01140   1  SINT=DSIN(W*T)
01150     SINTW=DSIN(WS*T)
01160     VS(1)=-UTRY*AWX*SINTW
01170     VS(2)=-UTRY*AWY*SINTW
01180     VS(3)=UTRY*AWX*COS(WS*T)
01190     INDEX=0
01200   2  INDEX=INDEX+1
01210     S2=0.0
01220     X(3)=DDT
01230     K=1
01240     X(1)=0.
01250     X(2)=0.
01260     J=1
01270     TE=0.0
```

```
01280      THETA(1)=PI/2.
01290      THETA(2)=THETA(1)
01300      THETA(3)=0.
01310      DO 13 I=1,NP
01320      NK=NM(I)+K-1
01330      DO 12 N=K,NK
01340 C*****CHECK FOR ANY INSERTED INSTRUMENTS OR FLOATS*****
01350      IF(J.GT.NI)GO TO 4
01360      3   IF((S2+SL(I)*0.5).GE.PI(J))CALL FORCES
01370      IF(J.GT.NI)GO TO 4
01380      IF((S2+SL(I)*0.5).GE.PI(J))GO TO 3
01390 C****STRESS-STRAIN CALCULATIONS FOR A MOORING SEGMENT*****
01400      4   IF(F01(I).EQ.0.0)GO TO 6
01410 C****SYNTHETIC ROPE*****
01420      STR=TE/(DIAL(I)**2)
01430      IF(STR.LE.200.0)GO TO 5
01440      TSTRA=PSTRA(I)+((STR-200.0)/CO2(I))**(1.0/PO2(I))
01450      S1=AQ(I)*SL(I)*(1.0+TSTRA/100.0)
01460      GO TO 7
01470      5   S1=SL(I)
01480      GO TO 7
01490 C****WIRE ROPES-TPL IS ELASTIC MODULUS AND CO1 IS JACKET DIAM*****
01500      6   TSTRA=TE/(*.7854*TFL(I)*(DIAL(I)-CO1(I))*2)
01510      S1=SL(I)*(1.+TSTRA)
01520 C****BEGINNING OF THE NUMERICAL INTEGRATION PROCEDURE*****
01530      7   DIA=DSQRT(CDIA(I)/S1)
01540      S2=S2+SL(I)
01550      DO 8 IC=1,3
01560      SN(IC)=DSIN(THETA(IC))
01570      CS(IC)=DCOS(THETA(IC))
01580      X(IC)=X(IC)+S1*CS(IC)
01590      8   YL(2,N,IC)=X(IC)
```

```
01600 H2=X(3)-S1*CS(3)/2.
01610 CALL 3PEED
01620 DO 9 IC=1,3
01630 U(IC)=U(IC)/304.8-YDL(2,N,IC)
01640 UT(IC)=U(IC)*CS(IC)
01650 YDDT(IC)=YDDL(N,IC)*CS(IC)
01660 9 WN(IC)=SWW(I)*CS(IC)*CS(3)
01670 WN(3)=WN(3)-SWW(I)
01680 UTT=UT(1)+UT(2)+UT(3)
01690 YDDT=YDDT(1)+YDDT(2)+YDDT(3)
01700 DTT=3.28*CDT(I)*S1*DIA*DABS(UTT)*UTT/12.
01710 TE=TE-SWW(I)*CS(3)+DTT-SWA(I)*YDDT/GR
01720 TN=TE-H2*SWD(I)/S1
01730 DO 10 IC=1,3
01740 YDDN(IC)=YDDL(N,IC)-YDDDT*CS(IC)
01750 10 UN(IC)=U(IC)-UTT*CS(IC)
01760 VN=DSQRT(UN(1)*X2+UN(2)*X2+UN(3)**2)
01770 DO 11 IC=1,3
01780 DN(IC)=3.28*CDN(I)*S1*DIA*UNM*UN(IC)/12.+WN(IC)-((2.*SWA(I))-SWW(I)
01790 1)/GR)*YDDN(IC)
01800 IF(SN(3).EQ.0.)GO TO 11
01810 THETA(IC)=THETA(IC)-DN(IC)/(TE*SN(IC))
01820 11 CONTINUE
01830 12 CONTINUE
01840 K=NK+1
01850 13 CONTINUE
01860 C*****CHECK FOR ANY INSERTED INSTRUMENTS OR FLOATS BEFORE THE ANCHOR****
01870 14 IF(J.GT.N)GO TO 15
01880 CALL FORCES
01890 GO TO 14
01900 15 E=DEPTH-X(3)
01910 IF(T.EQ.0.)GO TO 21
```

```
01920 IF (INDEX.EQ.1) GO TO 17
01930 IF (T.EQ.DT) GO TO 21
01940 DO 16 IE=1,2
01950 TRY=DARS((X(IE)-XOLD(IE))/X(IE))
01960 IF (TRY.GT.ER1) GO TO 25
01970 16 CONTINUE
01980 GO TO 21
01990 17 DO 18 IC=1,3
02000 18 XOLD(IC)=X(IC)
02010 DO 20 IC=1,3
02020 DO 19 I1=1,N
02030 YDL(2,I1,IC)=(X(IC)-YL(2,I1,IC)-YL(1,I1,IC))*3.28/DT
02040 19 YDIL(11,IC)=(YDI(2,I1,IC)-YDL(1,I1,IC))/DT
02050 DO 20 I2=1,NI
02060 YDI(2,I2,IC)=(X(IC)-YI(2,I2,IC)-YI(1,I2,IC))*3.28/DT
02070 20 YDDI(12,IC)=(YDI(2,I2,IC)-YDI(1,I2,IC))/DT
02080 WRITE(6,101)T,(X(KJ),KJ=1,3),E
02090 GO TO 2
02100 21 DO 23 IC=1,3
02110 DO 22 I1=1,N
02120 YL(1,I1,IC)=X(IC)-YL(2,I1,IC)
02130 22 YDL(1,I1,IC)=YDL(2,I1,IC)
02140 DO 23 I2=1,NI
02150 YI(1,I2,IC)=X(IC)-YI(2,I2,IC)
02160 23 YDI(1,I2,IC)=YDI(2,I2,IC)
02170 IF (T.LT.T3) GO TO 24
02180 X(3)=X(3)-DDT
02190 WRITE(6,101)T,(X(KJ),KJ=1,3),E
02200 IF (T.GT.TMAX) GO TO 26
02210 T3=T3+T2
02220 24 T=T+DT
02230 GO TO 1
```

```
02240    25   EE1=TRY-ER1
02250      WRITE(6,102)EE1
02260    26   RETURN
02270      END
02280      IMPLICIT REAL*8(A-H,O-Z)
02290      SUBROUTINE FORCES
02300      C THIS SUBROUTINE CALCULATES THE FORCE EQUILIBRIUM FOR INSERTED
02310      C INSTRUMENTS OR FLOATS.
02320      C
02330      C
02340      COMMON PI(30),SI(30),F(3,30),CDIN(30),CDIT(30),DIAL(20),SLL(20),AW
02350      1L(20),CDN(20),CDIT(20),TPL(20),CO1(20),CO2(20),FO1(20),FO2(20),CONS
02360      1(20),U(3,10),NM(20),SL(20),SMA(20),CDIA(20),U(3),X(3),THETA(3),AWX
02370      1,DN(3),WN(3),CS(3)*SN(3),DD(3),UN(3),UT(3),FSTRA(20),AO(20),D(10),
02380      1WWL(20),SWD(20),YDL(2,150,3),YL(2,150,3),YDDI(
02390      130,3),YDI(2,30,3),YI(2,30,3),YDDT(3)*YDNN(3),ZMU(30),DEPTH,
02400      1VS(3),S2,TE,H2,IK,NI,J,NC,WS,AMP,NS,NF,DIT,E,ER,FII,T,SINT,AW,AWY,
02410      1DIA,ER1,XOLD(3),GR,WE,DT,T2,TMAX,INK,I
02420      C*****NUMERICAL INTEGRATION PROCEDURE*****
02430      S2=S2+SI(J)
02440      DO 1 IC=1,3
02450      SN(IC)=DSIN(THETA(IC))
02460      CS(IC)=DCOS(THETA(IC))
02470      X(IC)=X(IC)+SI(J)*CS(IC)
02480      1 YI(2,J,IC)=X(IC)
02490      H2=X(3)-SI(J)*CS(3)/2.
02500      CALL SPEED
02510      DO 2 IC=1,3
02520      U(IC)=U(IC)/304.8-YDI(2,J,IC)
02530      2 CONTINUE
02540      IF(SI(J).NE.0.)GO TO 4
02550      UNM=DEQRT(U(1)**2+U(2)**2+U(3)**2)
```

```
02560      DO 3 IC=1,3
02570      3 DD(IC)=TE*CS(IC)+CDIN(J)*VNM*U(IC)+F(IC,J)-(ZM(J)+ZMV(J))
02580      1*YDDI(J,IC)
02590      60 TO 8
02590      4 DO 5 IC=1,3
02600      4 YDDT(IC)=YDDI(J,IC)*CS(IC)
02610      5 UT(IC)=U(IC)*CS(IC)
02620      5 UT=UT(1)+UT(2)+UT(3)
02630      6 YDDTT=YDDT(1)+YDDT(2)+YDDT(3)
02640      DTT=CDIT(J)*DABS(UTT)*UTT
02650      DO 6 IC=1,3
02660      6 YDDN(IC)=YDDI(J,IC)-YDDTT*CS(IC)
02670      6 UN(IC)=U(IC)-UTT*CS(IC)
02680      6 VNM=DSQRT(UN(1)**2+UN(2)**2+UN(3)**2)
02690      DO 7 IC=1,3
02700      7 DD(IC)=(TE+NTT)*CS(IC)+CDIN(J)*VNM*UN(IC)+F(IC,J)
02710      1-ZM(J)*YDDI(J,IC)-ZMV(J)*YDDN(IC)
02720      7 CONTINUE
02730      7
02740      8 TE=DSQRT(DD(1)**2+DD(2)**2+DU(3)**2)
02750      8 DO 9 IC=1,3
02760      9 THETA(IC)=DARCOS(DD(IC)/TE)
02770      9 J=J+1
02780      RETURN
02790      END
02800      IMPLICIT REAL*8(A-H,O-Z)
02810      SUBROUTINE SFEED
02820      C THIS SUBROUTINE CALCULATES THE TOTAL PROFILE+SURFACE WAVE VEL.+
02830      C ABSOLUTE VELOCITY FIELD; GIVEN VELOCITY AT FEW DEPTHS AND A SIN.
02840      C SURFACE WAVE. STEPPED PROFILE (#2 OF VOLUME 1 CHHABRA(1973)) IS
02850      C USED.
02860      C
02870      C
```

```
COMMON PI(30),SI(30),F(3,30),CDIN(30),CDIT(30),DIAL(20),SLL(20),AW
1L(20),CDN(20),CDT(20),TPL(20),CO1(20),CO2(20),PO1(20),PO2(20),CONS
1(20),V(3,10),NM(20),SL(20),SWA(20),CDIA(20),U(3),X(3),THE TA(3),AWX
1,DN(3),WN(3),CS(3),SN(3),DD(3),UN(3),UT(3),PSTRA(20),AO(20),D(10),
1WWL(20),SWW(20),SWD(20),YDDL(150,3),YDL(2,150,3),YDDI(
130,3),YDI(2,30,3),YI(2,30,3),YDDN(3),ZM(30),ZMV(30),DEPTH,
1VS(3),S2,TE,H2,IK,NI,J,NC,WS,AMP,NS,NP,DDT,E,ER,PII,T,SINT,AW,AWY,
1DIA,ER1,XOLD(3),GR,WE,DT,T2,THAX,IKK,I
0EXP=DEXP(-AW*XH2)
02950
02960
02970
02980      DO 5 JN=1,3
02990      IF(H2.LE.D(1))GO TO 3
03000      IF(H2.GE.D(IKK))GO TO 4
03010      1 IF(H2.GT.D(M).AND.H2.LE.D(M+1))GO TO 2
          M=M+1
          GO TO 1
03020      2 U(JN)=V(JN,M+1)*(1.+0.05*SINT)+VS(JN)*0EXP
03030      3 U(JN)=V(JN,1)*(1.+0.05*SINT)+VS(JN)*0EXP
03040      4 U(JN)=V(JN,IKK+1)*(1.+0.05*SINT)+VS(JN)*0EXP
03050      5 CONTINUE
03060      RETURN
03070      END
03080      READY
```

```
SSS3.FORT
00010 C
00020 C
00030 C
00040 C
00050 C
00060 C
00070 C
00080 C*****BEGINNING OF THE MAIN PROGRAM*****
00090- COMMON PI(30),SI(30),F(3,30),CDIN(30),CDIT(30),DIAL(20),
00100 1L(20),CDN(20),CDT(20),TPL(20),CO1(20),CO2(20),SLL(20),AW
00110 1(20),V(850,2,10),NM(20),SL(20),SWA(20),CJIA(20),U(3),
00120 1,DN(3),WN(3),CS(3),SN(3),DD(3),UN(3),UT(3),X(3),THETA(3)
00130 1WWL(20),SWW(20),SWD(20),PSTRA(20),AO(20),D(10),
00140 1,NFT,NS,NP,DDT,E,ER,PII,CONS1,DIA,IKK
00150 C*****BEGINNING OF FORMAT STATEMENTS*****
00160 101 FORMAT(5I5,5F10.0)
00170 102 FORMAT(7F8.0)
00180 103 FORMAT(5F10.0)
00190 104 FORMAT(10F7.0)
00200 105 FORMAT(7F10.0)
00210 106 FORMAT(16F7.2)
00220 107 FORMAT(10F8.2)
00230 C*****GENERAL DATA*****
00240 C DEPTH,DDT, AND ER ARE IN METERS.
00250 READ(5,101)NI,NP,NS,NFT,IKK,DEPTH,DDT,ER
00260 C*****READ IN THE INSERTED INSTRUMENT OR FLOAT SPECIFICATIONS*****
00270 C PI,SI ARE IN METERS; F IN POUNDS; AND CDIN,CDIT IN F.F.S. UNITS.
00280 READ(5,102)(PI(J),SI(J),F(2,J),F(1,J),CDIN(J),CDIT(J)
00290 1,J=1,NI)
00300 C*****READ IN THE PARAMETERS FOR DIFFERENT MOORING PARTS*****
00310 C DIAL IN INCHES, SLL IN METERS, AWL AND WWL IN POUNDS/M; TFL IN
```

```
00320 C FOUNDS/(SQ,IN.) OR FOUND(S,C01 IS JACKET HIA.(IN.) FOR WIRE ROPE.
00330 READ(5,103)(DIAL(I),SLL(I),AWL(I),WWL(I),TFL(I),I=1,NF)
00340 READ(5,105)(C01(I),F01(I),C02(I),F02(I),C03(I),AO(I),CIN(I),CDT(I),I=1,NF
1)
00350
00360 C*****READ THE FORCING CURRENT PROFILE*****C
00370 C D ARE IN METERS, AND U IN MM/SEC.
00380 READ(5,105)(D(I),I=1,IKK)
00390 I(3)=0.
00400 READ(10,106) (((U(L,I,J),I=1,8),J=1,8),L=1,NFT)
00410 FII=4.*ATAN(1.)
00420 RHO=1.9905
00430 GR=32.2
00440 CONS1=RHO*GR*FII*0.0057
00450 SLT=0.
00460 DO 1 I=1,NF
00470 IF(F01(I).EQ.0.0)GO TO 1
00480 C*****PERMANENT STRETCH FOR SYNTHETIC LINES*****
00490 PSTRAC(I)=((TFL(I)/(DIAL(I)**2)-200.0)/C01(I))**(.1,0/F01(I))
00500 1 SLT=SLL+SLL(I)
00510 C*****SEGMENTATION OF THE MOORING LINE IN NS SEGMENTS*****
00520 DO 2 I=1,NF
00530 NM(I)=(SLL(I)/SLT)*NS+0.5
00540 IF(NM(I).EQ.0)NM(I)=1
00550 SL(I)=SLL(I)/NM(I)
00560 SWA(I)=AWL(I)*SL(I)
00570 SWW(I)=WWL(I)*SL(I)
00580 SWP(I)=SWA(I)-SWW(I)
00590 CDIA(I)=SL(I)*(DIAL(I)**2)
00600 2 CONS(I)=CDIA(I)*CONS1
00610 CALL MOTION
00620 CALL EXIT
00630 END
```

00640 SUBROUTINE MOTION
00650 C THIS SUBROUTINE CALCULATES THE DYNAMIC EQUILIBRIUM OF THE MOORING
00660 C LINE AT NFT INSTANTS OF TIMES.
00670 C
00680
00690 COMMON PI(30),SI(30),F(3,30),CDIN(30),CDIT(30),DIAL(20),SLL(20),AW
00700 1L(20),CDN(20),CDT(20),TPL(20),CD1(20),CD2(20),CO1(20),CO2(20),CONS
00710 1(20),V(850,2,10),NM(20),SL(20),U(3),X(3),THETA(3)
00720 1,DN(3),WN(3),CS(3),SN(3),DD(3),UN(3),UT(3),PSTRA(20),AO(20),D(10),
00730 1WL(20),SWW(20),SWD(20),DEPTH,TSTRA,I,S2,TE,H2,IK,NI,J,NC,INDEX,JJ
00740 1,NFT,NS,NF,IND,ER,PII,CONS1,DIA,INK
00750 101 FORMAT(3F8.2)
00760 C*****BEGINNING OF MOORING LINE CALCULATIONS*****
00770 DO 14 IK=1,NFT
00780 S2=0.0
00790 X(3)=DDT
00800 K=1
00810 X(1)=0.
00820 X(2)=0.
00830 J=1
00840 TE=0.0
00850 DIA=0.
00860 THETA(1)=PI/2.
00870 THETA(2)=THETA(1)
00880 THETA(3)=0.
00890 DO i1 I=1,NF
00900 NK=NM(I)+K-1
00910 DO 10 N=NK,NK
00920 INDEX=1
00930 C*****CHECK FOR ANY INSERTED INSTRUMENT OR FLOAT*****
00940 IF(J.GT.NI) GO TO 2
00950 1 IF((S2+SL(I)*0.5).GE.FI(J))CALL FORCES

```
00960 IF(J.GT.NI)GO TO 2
00970 IF((S2+SL(I))*0.5).GE.PI(J)GO TO 1
00970 2 CONTINUE
00990 C*****STRESS-STRAIN CALCULATIONS FOR MOORING SEGMENT*****
01000 IF(FO1(I).EQ.0.0)GO TO 4
01010 C*****SYNTHETIC ROPE*****
01020 STR=TE/(DIAL(I)*X2)
01030 IF(STR.LE.200.0)GO TO 3
01040 TSTRA=FSTRA(I)+((STR-200.0)/CO2(I))**((1.0/F02(I)))
01050 S1=A0(I)*SL(I)*(1.0+TSTRA/100.0)
01060 GO TO 5
01070 3 S1=SL(I)
01080 GO TO 5
01090 C*****WIRE ROPES-TPL IS ELASTIC MODULUS AND CO1 IS JACKET DIA*****
01100 4 TSTRA=TFL(I)*(DIAL(I)-CO1(I))*X2
01110 S1=SL(I)*(1.+TSTRA)
01120 C*****BEGINNING OF THE NUMERICAL INTEGRATION PROCEDURE*****
01130 5 DIA=SQRT(CDIA(I)/S1)
01140 S2=S2+SL(I)
01150 DC 6 IC=1,3
01160 SN(IC)=SIN(THETA(IC))
01170 CS(IC)=COS(THETA(IC))
01180 6 X(IC)=X(IC)+S1*CS(IC)
01190 IF(SN(3).EQ.0.)SN(3)=0.000001
01200 H2=X(3)-S1*CS(3)/2.
01210 CALL SPEED
01220 DO 7 IC=1,3
01230 UT(IC)=U(IC)*CS(IC)
01240 7 WN(IC)=SWW(I)*CS(IC)*CS(3)
01250 WN(3)=WN(3)-SWW(I)
01260 UTT=UT(1)+UT(2)+UT(3)
01270 DTT=(2.94E-6)*CDT(I)*S1*DIA*ABS(UTT)*UTT
```

```
01280      TE=TE-SWW(1)*CS(3)+DTT
01290      T=TE-H2*SWD(1)/S1
01300      DO 8 IC=1,3
01310      8      UN(IC)=U(IC)-UTT*CS(IC)
01320      VNM=SDRT(UN(1)**2+UN(2)**2+UN(3)**2)
01330      DO 9 IC=1,3
01340      DN(IC)=(2.94E-6)*CDN(I)*S1*DIA*UNM*UN(IC)+WN(IC)
01350      ?      THETA(IC)=THETA(IC)-DN(IC)/(TEXSN(IC))
01360      10     CONTINUE
01370      K=NK+1
01380      11     CONTINUE
01390 C*****CHECK FOR ANY INSTRUMENT OR FLOAT BEFORE ANCHOR*****
01400      INDEX=1
01410      12     IF(J.GT.NI)GO TO 13
01420      CALL FORCES
01430      GO TO 12
01440      13     E=DEPTH-X(3),
01450      X(3)=X(3)-DOT
01460      WRITE(6,101)(X(KJ),KJ=1,3)
01470      14     CONTINUE
01480      RETURN
01490      END
01500      SUBROUTINE FORCES
01510      C      THIS SUBROUTINE CALCULATES THE FORCE EQUILIBRIUM FOR INSERTED
01520      C      INSTRUMENTS OR FLOATS.
01530      C
01540      C
01550      COMMON PI(30),SI(30),F(3,30),CDIN(30),CDIT(30),DIAL(20),SLL(20),AW
01560      1L(20),CDN(20),CDT(20),TFL(20),C01(20),C02(20),F01(20),F02(20),CONS
01570      1(20),V(850,2,10),NM(20),SL(20),SWA(20),CDIA(20),U(3),X(3),THETA(3)
01580      1,IN(3),WN(3),CS(3),SN(3),DD(3),UN(3),UT(3),PSTRA(20),AO(20),D(10),
01590      1WWL(20),SWW(20),SWD(20),DEPTH,TSTRA,I,S2,TE,H2,IK,NI,J,NC,INDEX,J
```

```
01600 1,NFT,NS,NP,DD,E,ER,PII,CONS1,DIA,INK
01610 C*****NUMERICAL INTEGRATION PROCEDURE*****
01620 S2=S2+SI(J)
01630 DO 1 IC=1,3
01640 SN(IC)=SIN(THETA(IC))
01650 CS(IC)=COS(THETA(IC))
01660 1 X(IC)=X(IC)+SI(J)*CS(IC)
01670 IF(SN(3).EQ.0.)SN(3)=0.000001
01680 H2=X(3)-SI(J)*CS(3)/2.
01690 CALL SPEED
01700 IF(SI(J).NE.0.)GO TO 3
01710 UNM=SQRT(U(1)**2+U(2)**2+U(3)**2)
01720 DO 2 IC=1,3
01730 2 DD(IC)=TE*CS(IC)+CDIN(J)*UNM*U(IC)/92903.+F(IC,J)
01740 60 TO 7
01750 3 DO 4 IC=1,3
01760 4 UT(IC)=U(IC)*CS(IC)
01770 UTT=UT(1)+UT(2)+UT(3)
01780 DT(I)=CDIT(J)*ABS(UTT)*UTT/92903.
01790 5 DO 5 IC=1,3
01800 UN(IC)=U(IC)-UTT*CS(IC)
01810 UNM=SQRT(UN(1)**2+UN(2)**2+UN(3)**2)
01820 DO 6 IC=1,3
01830 6 DD(IC)=(TE+DTT)*CS(IC)+CDIN(J)*UNM*UN(IC)/92903.+F(IC,J)
01840 7 TE=SQRT(DD(1)**2+DD(2)**2+DD(3)**2)
01850 DO 8 IC=1,3
01860 8 THETA(IC)=ARCCOS(DD(IC)/TE)
01870 J=J+1
01880 INDEX=2
01890 RETURN
01900 END
01910 SUBROUTINE SPEED
```

01920 C THIS SUBROUTINE CALCULATES THE VELOCITY PROFILE GIVEN THE VELOCITY
01930 C AT A FEW DEPTHS. HERE THE STEPPED PROFILE (#2 IN VOLUME 1
01940 C (CHHABRA,1973)), IS USED.
01950 C

```
01960 C
01970 COMMON PI(30),SI(30),F(3,30),CDIN(30),CDIT(30),DIAL(20),SLL(20),AW
01980 1L(20),CDN(20),CDT(20),TFL(20),C01(20),C02(20),P01(20),P02(20),CONS
01990 1(20),V(850,2,10),NM(20),SWA(20),CDIA(20),U(3),X(3),THETA(3)
02000 1,DN(3),WN(3),CS(3),SN(3),E(3),UN(3),UT(3),PSTRA(20),AD(20),D(10),
02010 1,WL(20),SWW(20),SWD(20),DEPTH,TSTRA,I,S2,TE,H2,IK,NI,J,NC,INDEX,JJ
02020 1,NFT,NS,NP,DDT,E,ER,P11,CONS1,DIA,IKK
02030 M=1
02040 DO 5 JN=1,2
02050 IF(H2.LE.D(1))GO TO 3
02060 IF(H2.GE.D(IKK))GO TO 4
02070 1 IF(H2.GT.D(M).AND.H2.LE.D(M+1))GO TO 2
02080 M=M+1
02090 GO TO 1
02100 2 U(JN)=V(IK,JN,X+1)
02110 3 GO TO 5
02120 3 U(JN)=V(IK,JN,1)
02130 3 GO TO 5
02140 4 U(JN)=V(IK,JN,IKK+1)
02150 5 CONTINUE
02160 RETURN
02170 END
READY
```

SSD3.FORT

00010 C
00020 C PROGRAM TO COMPUTE LOW FREQ. MOTION OF SUBSURFACE MOORED SYSTEMS.
00030 C THIS ANALYSIS IS DONE IN THREE DIMENSIONS, AND INCLUDES INERTIA
00040 C FORCES. INPUT VELOCITY PROFILE RELATIVE TO THE MOORING SYSTEM IS
00050 C READ AT EACH TIME STEP.

00060 C
00070 C
00080 C*****BEGINNING OF THE MAIN PROGRAM*****
00090 COMMON PI(30),SI(30),CDIN(30),CDIT(30),DIAL(20),SLL(20),AW
00100 1L(20),CDIN(20),CDT(20),TPL(20),CO1(20),CO2(20),FO1(20),FO2(20),CONS
00110 1(20),V(B50,2,10),NM(20),SL(20),SWA(20),CDIA(20),U(3),X(3),THETA(3)
00120 1,DN(3),WN(3),CS(3),SN(3),DD(3),UN(3),UT(3),FSTRA(20),AO(20),D(10),
00130 1WWL(20),SWW(20),SWD(20),YDOL(150,3),YDL(2,150,3),YL(2,150,3),YDDI(30),
00140 130,3),YDI(2,30,3),YI(2,30,3),YDDT(3),YDN(3),ZM(30),ZMU(30),DEPTH,
00150 ITSTRA,I,S2,TE,H2,IK,NI,J,NFT,NS,NP,DDR,E,ER,FII,CONS1,DIA,GR,IKK
00160 C*****BEGINNING OF FORMAT STATEMENTS*****
00170 101 FORMAT(S15.5F10.0)
00180 102 FORMAT(7F8.0)
00190 103 FORMAT(5F10.0)
00200 104 FORMAT(10F7.0)
00210 105 FORMAT(7F10.0)
00220 106 FORMAT(16F7.2)
00230 107 FORMAT(10F8.2)
00240 C*****GENERAL DATA*****
00250 C DEPTH, DDt, AND ER ARE IN METERS.
00260 READ(5,101)NI,np,ns,nft,ikk,depth,ddt,er
00270 C*****READ IN THE INSERTED INSTRUMENT OR FLOAT SPECIFICATIONS*****
00280 C PI, SI ARE IN METERS; ZM, ZMU IN SLUGS; F IN POUNDS; AND CDIN,
00290 C CDIT IN F.F.S. UNITS.
00300 READ(5,102)(PI(J),SI(J),ZM(J),ZMU(J),F(3,J),CDIN(J),CDIT(J))
00310 1,J=1,NI)

```
00320      DO 1 I1=1,2
00330      DO 1 I2=1,NI
00340      1  F(I1,I2)=0.
00350 C*****READ IN THE PARAMETERS FOR DIFFERENT MOORING PARTS*****
00360 C      DIAL IN INCHES, SLL IN METERS; AWL AND WWL IN LBS/M; AND TPL IN
00370 C      POUNDS OR POUNDS/SQ.IN.). CO1 IS IN INCHES FOR JACKETED WIRE ROPE
00380      READ(5,103)(DIAL(I),SLL(I),AWL(I),WWL(I),TPL(I),I=1,NP)
00390      READ(5,105)(CO1(I),P01(I),CDN(I),CDT(I),I=1,NF
1)
00400      C*****READ THE FORCING CURRENT PROFILE*****
00410      C      D ARE IN METERS; AND V ARE IN MM/SEC.
00420      C      D ARE IN METERS; AND V ARE IN MM/SEC.
00430      READ(5,105)(D(I),I=1,IKK)
00440      U(3)=0.
00450      READ(10,106)((V(L,I,J),I=1,8),J=1,8),L=1,NFT
00460      PII=4.*ATAN(1.)
00470      RHO=1.9905
00480      GR=32.2
00490      CONS1=RHO*GR*PII*0.0057
00500      SLT=0.
00510      DO 2 I=1,NP
00520      IF(P01(I).EQ.0.0)GO TO 2
00530 C*****PERMANENT STRETCH FOR SYNTHETIC LINES.*****
00540      PSTR(A)=(TPL(I)/(DIAL(I)*(DIAL(I)**2)-200.0)/CO1(I))**((1.0/F01(I))
00550      2  SLT=SLT+SLL(I)
00560 C*****SEGMENTATION OF THE MOORING LINE IN NS SEGMENTS*****
00570      DO 3 I=1,NP
00580      NM(I)=(SLL(I)/SLT)*NS+0.5
00590      IF(NM(I).EQ.0)NM(I)=1
00600      SL(I)=SLL(I)/NM(I)
00610      SWA(I)=AWL(I)*SL(I)
00620      SWW(I)=WWL(I)*SL(I)
00630      SWD(I)=SWA(I)-SWW(I)
```

```
00640      CDIA(I)=SL(I)*(DIAL(I)**2)
00650      3      CONS(I)=CDIA(I)*CONS1
00660      NS1=NS+NP
00670      C*****INITIALIZE ALL DYNAMIC VARIABLES.*****
00680      DO 5 I1=1,3
00690      DO 4 I2=1,NS1
00700      YDDL(I2,I1)=0.
00710      DO 4 I3=1,2
00720      YDL(I3,I2,I1)=0.
00730      4      YL(I3,I2,I1)=0.
00740      DO 5 I4=1,30
00750      YDNI(I4,I1)=0.
00760      DO 5 I5=1,2
00770      YDI(I5,I4,I1)=0.
00780      5      YI(I5,I4,I1)=0.
00790      CALL MOTION
00800      CALL EXIT
00810      END
00820      SUBROUTINE MOTION
00830      C      THIS SUBROUTINE CALCULATES THE DYNAMIC EQUILIBRIUM OF THE MOORING
00840      C      LINE AT NFT INSTANTS OF TIMES.
00850      C
00860      C
00870      COMMON PI(30),SI(30),F(3,30),CDIN(30),CDIT(30),DIAL(20),SLL(20),AW
00880      1L(20),CDN(20),CDT(20),TPL(20),CO1(20),CO2(20),PO1(20),PO2(20),CONS
00890      1(20),V(B50,2,10),NM(20),SL(20),SWA(20),CDIA(20),U(3),X(3),THETA(3)
00900      1,DN(3),WN(3),CS(3),SN(3),DD(3),UN(3),UT(3),PSTRA(20),AO(20),D(10),
00910      1WWL(20),SWW(20),SWD(20),YDDL(150,3),YL(2,150,3),YDNI(
00920      130,3),YDI(2,30,3),YI(2,30,3),YDIT(3),YDNN(3),ZM(30),ZMV(30),DEPTH,
00930      1TSTRA,1,S2,TE,H2,IK,NI,J,NFT,NS,NF,DOIT,E,ER,PII,CONS1,DIA,GR,IKK
00940      101     FORMAT(3FB.2)
00950      DO 16 IK=1,NFT
```

```
00960 C*****BEGINNING OF MOORING LINE CALCULATIONS*****
00970      S2=0.0
00980      X(3)=DDT
00990      K=1
01000      X(1)=0.
01010      X(2)=0.
01020      J=1
01030      TE=0.0
01040      THETA(1)=PII/2.
01050      THETA(2)=THETA(1)
01060      THETA(3)=0.
01070      DO 11 I=1,NF
01080      NK=NM(I)+K-1
01090      DO 10 N=N,NK
01100      C****CHECK FOR ANY INSERTED INSTRUMENT OR FLOAT ****
01110      IF(J.GT.N)GO TO 2
01120      1  IF((S2+SL(I)*0.5).GE.PI(J))CALL FORCES
01130      IF((J.GT.N)GO TO 2
01140      IF((S2+SL(I)*0.5).GE.PI(J))GO TO 1
01150      C****STRESS-STRAIN CALCULATIONS FOR MOORING SEGMENT*****
01160      2  IF(F01(I).EQ.0.0)GO TU 4
01170      C****SYNTHETIC ROPE***** ****
01180      STR=TE/(DIAL(I)**2)
01190      IF(STR.LE.200.0)GO TO 3
01200      TSTRA=PSTRA(I)+((STR-200.0)/CO2(I))*(1.0/F02(I))
01210      S1=A0(I)*SL(I)*(1.0+TSTRA/100.0)
01220      GO TO 5
01230      3  S1=SL(I)
01240      GO TO 5
01250      C****WIRE ROPE-TFL IS ELASTIC MONOLUS AND CO1 IS JACKET DIA*****
01260      4  TSTRA=TE/(.7854*TFL(I)*(DIAL(I)-CO1(I))*2)
01270      S1=SL(I)*(1.+TSTRA)
```

```
01280 C****BEGINNING OF THE NUMERICAL INTEGRATION PROCEDURE*****  
01290      S   DIA=SQRT(CDIA(I)/S1)  
01300      S2=S2+SL(I)  
01310      DO 6 IC=1,3  
01320      SN(IC)=SIN(THETA(IC))  
          CS(IC)=COS(THETA(IC))  
01330      X(IC)=X(IC)+S1*CS(IC)  
01340      YDL(1,N,IC)=X(IC)  
01350      6   IF(SN(3).EQ.0.)SN(3)=0.000001  
01360      H2=X(3)-S1*CS(3)/2.  
01370      CALL SPEED  
01380      DO 7 IC=1,3  
01390      U(IC)=U(IC)*CS(IC)  
01400      YDNT(IC)=YDDL(N,IC)*CS(IC)  
01410      7   WN(IC)=SWW(I)*CS(IC)*CS(3)  
01420      WN(3)=WN(3)-SWW(I)  
01430      UTT=UT(1)+UT(2)+UT(3)  
01440      YDNT=YDNT(1)+YDNT(2)+YDNT(3)  
01450      DTT=(2.94E-6)*CDT(I)*S1*DIA*ABS(UTT)*UTT  
01460      TE=TE-SWW(I)*CS(3)+DTT-SWA(I)*YDNTT/GR  
01470      T=TE-H2*SWD(I)/S1  
01480      DO 8 IC=1,3  
01490      YDDN(IC)=YDDL(N,IC)-YDNTT*CS(IC)  
01500      UN(IC)=U(IC)-UTT*CS(IC)  
01510      8   UN(IC)=U(IC)**2+UN(2)**2+UN(3)**2  
01520      VNM=SQRT(UN(1)**2+UN(2)**2+UN(3)**2)  
01530      DO 9 IC=1,3  
01540      DN(IC)=(2.94E-6)*CDN(I)*S1*DIA*VNM*UN(IC)+WN(IC)-((2.*SWA(I)-SWW(I)  
01550      1.)/GR)*YDNN(IC)  
01560      9   THETA(IC)=THETA(IC)-DN(IC)/(TE*SN(IC))  
01570      10  CONTINUE  
01580      K=NK+1  
01590      11  CONTINUE
```

01600 C*****CHECK FOR ANY INSERTED INSTRUMENT OR FLOAT BEFORE ANCHOR*****
01610 12 IF(J.GT.NI)GO TO 13
01620 CALL FORCES
01630 GO TO 12
01640 13 E=DEPTH-X(3)
01650 X(3)=X(3)-DDT
01660 WRITE(6,101)(X(KJ),KJ=1,3)
01670 C*****CALCULATIONS FOR VELOCITIES AND ACCELERATIONS OF THE MOORING.
01680 DO 15 IC=1,3
01690 DO 14 I1=1,N
01700 YL(1,I1,IC)=YL(2,I1,IC)
01710 YL(2,I1,IC)=X(IC)-YDL(1,I1,IC)
01720 YDL(1,I1,IC)=YDL(2,I1,IC)
01730 YDL(2,I1,IC)=(YL(2,I1,IC)-YL(1,I1,IC))*0.003645
01740 YDDL(1,I1,IC)=(YDL(2,I1,IC)-YDL(1,I1,IC))/900.
01750 14 IF(IK.LE.2)YDDL(1,I1,IC)=0.
01760 DO 15 I2=1,NI
01770 YI(1,I2,IC)=YI(2,I2,IC)
01780 YI(2,I2,IC)=X(IC)-YDI(1,I2,IC)
01790 YDI(1,I2,IC)=YDI(2,I2,IC)
01800 YDI(2,I2,IC)=(YI(2,I2,IC)-YI(1,I2,IC))*0.003645
01810 YDDI(1,I2,IC)=(YDI(2,I2,IC)-YDI(1,I2,IC))/900.
01820 15 IF(IK.LE.2)YDDI(1,I2,IC)=0.
01830 16 CONTINUE
01840 RETURN
01850 END
01860 SUBROUTINE FORCES
01870 C THIS SUBROUTINE CALCULATES THE FORCE EQUILIBRIUM FOR INSERTED
01880 C INSTRUMENTS OR FLOATS.
01890 C-----
01900 C
01910 COMMON PI(30),SI(30),F(3,30),CDIN(30),CDIT(30),DIAL(20),SLL(20),AW

```
01920 1L(20),CDN(20),CDT(20),TFL(20),CO1(20),CO2(20),P01(20),P02(20),CONS
01930 1(20),V(B50,2,10),NM(20),SL(20),SWA(20),CDIA(20),U(3),X(3),THETA(3)
01940 1,DN(3),WN(3),CS(3),SN(3),DD(3),UN(3),UT(3),PSTRA(20),AO(20),D(10),
01950 1WNL(20),SWW(20),SWD(20),YDL(150,3),YL(2,150,3),YDDI(1
01960 130,3),YDI(2,30,3),YI(2,30,3),YDT(3),YDN(3),ZMU(30),DEPTH,
01970 1ITRA,I,S2,TE,H2,IN,NI,J,NFT,NS,NF,DUT,E,ER,PII,CONS1,DIA,GR,IKK
01980 C*****NUMERICAL INTEGRATION PROCEDURE*****  
S2=S2+SI(J)
01990
02000 DO 1 IC=1,3
02010 SN(IC)=SIN(THETA(IC))
02020 CS(IC)=COS(THETA(IC))
02030 X(IC)=X(IC)+SI(J)*CS(IC)
02040 1 YDI(1,J,IC)=X(IC)
02050 IF(SN(3).EQ.0.)SN(3)=0.000001
02060 H2=X(3)-SI(J)*CS(3)/2.
02070 CALL SPEED
02080 IF(SI(J).NE.0.)GO TO 3
02090 VNM=SQRT(U(1)**2+U(2)**2+U(3)**2)
02100 DO 2 IC=1,3
02110 2 DD(IC)=TE*CS(IC)+CDIN(J)*VNM*U(IC)/92903.4F(IC,J)-(ZM(J)+ZMV(J))*Y
02120 1DDI(J,IC)
02130 60 TO 7
02140 3 DO 4 IC=1,3
02150 4 YDDI(IC)=YDDI(J,IC)*CS(IC)
02160 4 UT(IC)=U(IC)*CS(IC)
02170 UTT=UT(1)+UT(2)+UT(3)
02180 YDDIT=YDDI(1)+YDT(2)+YDT(3)
02190 DTT=CDIT(J)*ABS(UTT)*UTT/92903.
02200 DO 5 IC=1,3
02210 5 YDIN(IC)=YDNI(J,IC)-YDDIT*CS(IC)
02220 5 UN(IC)=U(IC)-UTT*CS(IC)
02230 5 UNM=SQRT(UN(1)**2+UN(2)**2+UN(3)**2)
```

```
02240      DO 6 IC=1,3
02250      6 DD(IC)=(TE+DTT)*CS(IC)+CDIN(J)*VNMM*UN(IC)/92903.+F(IC,J)
02260      1-ZM(J)*YDDI(J,IC)-ZMV(J)*YDDN(IC)
02270      7 TE=SQRT(DD(1)**2+DD(2)**2+DD(3)**2)
02280      DO 8 IC=1,3
02290      8 THETA(IC)=ACOS(DD(IC)/TE)
02300      J=J+1
02310      RETURN
02320      END
02330      C SUBROUTINE SPEED
02340      C THIS SUBROUTINE CALCULATES THE VELOCITY PROFILE, GIVEN THE
02350      C VELOCITY AT A FEW DEPTHS. HERE THE STEPPED PROFILE (#2 IN
02360      C VOLUME 1 CHHABRA(1973) IS USED.
02370      C
02380      C
02390      COMMON PI(30),SI(30),F(3,30),CDIN(30),CINI(30),DIAL(20),SLL(20),AW
02400      1L(20),CDN(20),CDT(20),TFL(20),CO1(20),CO2(20),FO2(20),CONS
02410      1(20),U(850,2,10),NM(20),SL(20),SWA(20),CDIA(20),U(3),X(3),THETA(3)
02420      1,DN(3),WN(3),CS(3),SN(3),DD(3),UN(3),UT(3),FSTRA(20),AO(20),D(10),
02430      1WUL(20),SWU(20),SWD(20),YDDL(150,3),YDL(2,150,3),YL(2,150,3),YDDI(
02440      130,3),YDI(2,30,3),YI(2,30,3),YDDT(3),YDDN(3),ZM(30),ZMV(30),DEPTH,
02450      1TSTRA,I,S2,TE,H2,IK,NI,J,NFT,NS,NP,DDT,E,ER,PII,CONS1,DIA,GR,IKK
02460      M=1
02470      DO 5 JN=1,2
02480      5 IF(H2.LE.D(1))GO TO 3
02490      6 IF(H2.GE.D(IKK))GO TO 4
02500      1 IF(H2.GT.D(M).AND.H2.LE.D(M+1))GO TO 2
02510      M=M+1
02520      GO TO 1
02530      2 U(JN)=V(IK,JN,M+1)
02540      3 U(JN)=V(IK,JN,1)
```

02560 GO TO 5
02570 4 U(JN)=V(IK,JN,IKK+1)
02580 5 CONTINUE
02590 RETURN
02600 END
READY

REFERENCES

- CHHABRA, N. K. (1973) Mooring Mechanics a Comprehensive Computer Study, Vol. 1, C. S. Draper Laboratory, Inc., Report R-775.
- CHHABRA, N. K., J. M. DAHLEN and M. R. FROIDEVAUX (1974) Mooring Dynamics Experiment-Determination of a Verified Dynamic Model of the WHOI Intermediate Mooring, C. S. Draper Laboratory, Inc., Report R-823.
- CHHABRA, N. K. (1976) Correction of Vector Averaging Current Meter Records from the MODE-1 Central Mooring for the Effects of Low-Frequency Mooring Line Motion, Accepted Deep-Sea Research.
- CHUNG, J. S. (1976) Motion of a Floating Structure in Water of Uniform Depth, Journal of Hydronautics, Vol. 10, 65-73.
- GOODMAN, T. R., and J. P. BRESLIN (1976) Statics and Dynamics of Anchoring Cables in Waves, Journal of Hydronautics, Vol. 10, 113-120.
- LAMB, H. (1945) Hydrodynamics, Sixth edition, Dover Publications, New York, N.Y., Article 68.
- NEWMAN, J. N. (1963) The Motions of a Spar Buoy in Regular Waves, David Taylor Model Basin, Washington, D.C., Report 1499.
- RUDNICK, P. (1967) Motion of a Large Spar Buoy in Sea Waves, Journal of Ship Research, December 1967, 257-267.
- VACHON, W. A. (1973) Scale Model Testing of Drogues for Free Drifting Buoys, C. S. Draper Laboratory, Inc., Report R-769.
- VACHON, W. A. (1975) Instrumented Full-Scale Tests of a Drifting Buoy and Drogue, C.S. Draper Lab., Inc., Report R-947.
- WUNSCH, C. and J. M. DAHLEN (1974) A Moored Temperature and Pressure Recorder, Deep-Sea Research, 21, 145-154.

MANDATORY DISTRIBUTION LIST

FOR UNCLASSIFIED TECHNICAL REPORTS, REPRINTS, & FINAL REPORTS PUBLISHED BY
OCEANOGRAPHIC CONTRACTORS OF THE OCEAN SCIENCE AND TECHNOLOGY DIVISION OF
THE OFFICE OF NAVAL RESEARCH

1 Director of Defense Research
and Engineering
Office of the Secretary of Defense
Washington, DC 20301
ATTN: Office, Assistant Director
(Research)

Office of Naval Research
Arlington, Virginia 22217
1 ATTN: (Code 460)
1 ATTN: (Code 102-OS)
1 ATTN: (Code 200)
6 ATTN: (Code 102IP)

1 ONR Resident Representative
M.I.T. Room E19-628

National Space Technology Laboratories
Bay St. Louis, Miss. 39520
3 ATTN: (Code 400)*

Director
Naval Research Laboratory
Washington, DC 20375
6 ATTN: Library, Code 2620

12** Defense Documentation Center
Cameron Station
Alexandria, VA 22314

Commander
Naval Oceanographic Office
Washington, DC 20390
1 ATTN: Code 1640
1 ATTN: Code 70

1 NODC/NOAA
Rockville, MD 20882

Total Required - 35 Copies

*Add one separate copy of Form DD-1473

**Send with these 12 copies 2 completed forms DDC-50, one self-addressed
back to contractor, the other addressed to NSTL, Code 400.

DISTRIBUTION

C.S. DRAPER LABORATORY, INC.

10	Library	1	Prusze' ski, Anthony S.
1	Araujo, Richard K.	1	Reid, Robert W.
1	Bowditch, Philip N.	1	Scholten, James
35	Chhabra, Narendra K.	1	Shepard, G. Dudley
1	Cummings, Damon E.	1	Shillingford, John
6	Dahlen, John M.	1	Toth, William E.
1	Lozow, Jeffery	1	Vachon, William
1	Morey, Ronald L.		

MASSACHUSETTS INSTITUTE OF TECHNOLOGY

1	Abkowitz, Martin A.		
1	Milgram, J. H.		Dept. of Ocean Engineering
1	Newman, J. N.		

1	Wunsch, Carl I.		Dept. of Earth & Planetary Sciences
---	-----------------	--	-------------------------------------

1	Heinmiller, Robert		
1	Mollo-Christensen, Erik L.		Dept. of Meteorology
1	Stommel, Henry M.		

EXTERNAL

1	Christensen, Thomas, Code 450		
1	Gregory, John B., Code 450		
1	Lange, Edward, Code 410		
1	Wilson, Stanley, Code 410		
	NORDA,		
	National Space Technology Laboratories		
	Bay St. Louis, Miss. 39520		

1	Director		
1	Canada, Raymond		
1	DeBok, Donald		
1	Kerut, Edmund G.		
	NOAA Data Buoy Office		
	National Space Technology Laboratories		
	Bay St. Louis, Miss. 39520		

1	Brooks, David		
	Sperry Support Services		
	National Space Technology Laboratories		
	Bay St. Louis, Miss. 39520		

DISTRIBUTION (Cont.)

1 Silva, Eugene A.
Ocean Engr. & Constr. Project Office
Navy Facilities Engineering Command
Chesapeake Division
Washington Navy Yard, Bldg. 200
Washington, DC 20374

1 Beardsley, Robert
1 Berteaux, Henri
1 Briscoe, Melbourne A.
1 Eriksen, Charles C.
1 Fofonoff, Nicolas P.
1 McCullough, James
1 Moller, Donald
1 Saunders, Peter
1 Schmitz, William
1 Walden, Robert
1 Webster, Ferris
Woods Hole Oceanographic Institution
Woods Hole, Mass. 02543

1 Collins, Curtis
1 Jennings, Feenan D.
IDOE Office
National Science Foundation
Washington, DC 20550

1 Swensen, Richard
USN Undersea Center
Code 2212
New London, CT 06320

1 Baker, D. James
School of Oceanography
University of Washington
Seattle, WA 98195

1 Halpern, David
Pacific Marine Environmental Laboratory/NOAA
Seattle, WA 98195

DISTRIBUTION (Cont.)

1 Wenstrand, David
John Hopkins University
Applied Physics Laboratory
John Hopkins Road
Laurel, MD 20810

1 Mesecar, Rod
1 Nath, John H.
1 Niiler, Peter
1 Smith, R. L.
School of Oceanography
Oregon State University
Corvallis, OR 97331

1 Savage, Godfrey H.
Professor and Director
Engineering Design & Analysis Lab
University of New Hampshire
Durham, NH 03824

1 Kirwan, A. D., Jr.
1 Nowlin, Worth D., Jr.
1 Cochrane, J.
Texas A&M University
College of Geosciences
College Station, TX 77843

1 Bonde, Les
Washington Analytical Services Center, Inc.
Hydrospace-Challenger Group
2150 Fields Road
Rockville, MD 20850

1 Bernstein, Robert L.
1 Cox, Charles
1 Davis, Russ
1 Sessions, Meredith
Scripps Institution of Oceanography
University of California, San Diego
La Jolla, CA 92037

DISTRIBUTION (Cont.)

- 1 Albertsen, Norman D.
Code L44
U.S. Civil Engineering Lab
Port Hueneme, CA 93093
- 1 Kalvaitis, A.
NOAA/OMT
Test and Evaluation Lab
Rockville, MD 20852
- 1 Harvey, R. t
Department of Oceanography
University of Hawaii
Hawaii
- 1 McGorman, Robert E.
Bedford Institute, Room 602
Dartmouth, Nova Scotia
CANADA
- 1 Bourgault, Thomas
NUSC,
Newport, RI USA 02840
- 1 Earle, Marshall
USN Oceanographic Office
Code 6110
Washington, DC 20373
-
- 1 Bedard, Philip P.
Oceanography Lab
Nova University
8000 North Ocean Drive
Dania, FL 33004
- 1 Coudeville, J. M.
Centre Oceanologique de Bretagne
Boite Postale 337
29.273 Brest CEDEX
FRANCE

DISTRIBUTION (Cont.)

1 **Froidevaux, Michel**
 Aerospatiale
 Subdivision Systemes, SYX/E
 78130, Les Mureaux
 FRANCE

1 **J. E. Bowker Associates, Inc.**
 Statler Office Building
 Boston, Mass. 02116

1 **Evans-Hamilton, Inc.**
 8100 Kirkwood, Suite 130
 Houston, TX 77072

1 **Leedham, Clive D.**
 General Motors Corporation
 6767 Hollister Avenue
 Goleta, CA 93017